

# Scattering in $\mathcal{N} = 4$ super Yang–Mills and $\mathcal{N} = 8$ supergravity

Thesis by  
Enrico Herrmann

In Partial Fulfillment of the Requirements for the  
degree of  
Doctor of Philosophy

The logo for the California Institute of Technology (Caltech), featuring the word "Caltech" in a bold, orange, sans-serif font.

CALIFORNIA INSTITUTE OF TECHNOLOGY  
Pasadena, California

2017  
Defended May 15, 2017

© 2017

Enrico Herrmann

ORCID: 0000-0002-3983-2993

All rights reserved

# Acknowledgments

During my time as a graduate student at Caltech I had the pleasure to interact with a number of remarkable scientists.

First and foremost I would like to thank my advisor, Mark Wise, for taking me on as a graduate student during my first year at Caltech. Even more so, I am thankful that he gave me the opportunity to follow my own research interests and for all his support along the way. Mark always had an open ear and good advice concerning practical matters like organizing travel funding or navigating the academic life in general. I am grateful that he also nominated me for a Dominic Orr Fellowship, which allowed me a one year break from all teaching duties.

Along with Mark, I would like to thank my co-advisor, Jaroslav Trnka, from whom I learned an enormous amount about scattering amplitudes and physics in general. I very much appreciate all his invaluable support and encouragement throughout my graduate studies. Without him and his generous help, many of my conference visits and trips would not have been possible. In all the workshops he co-organized, Jaroslav enabled young scientists to present their research. In many respects, Jaroslav is my scientific role model.

In addition to the mentorship I have received by Mark and Jaroslav, I have benefited significantly from the interaction with my collaborators Zvi Bern, Jacob Bourjaily, Sean Litsey, James Stankowicz, and Jaroslav Trnka. Without them, much of this thesis research would not have been possible. Especially Zvi has been an important academic mentor and like a third advisor to me. I enjoyed the hospitality and many great discussions during my numerous trips to UCLA, and I would like to take this opportunity to congratulate Zvi on the establishment of the Bhaumik Institute for Theoretical Physics at UCLA.

Special thanks also go to Nima Arkani-Hamed, Livia Ferro, Johannes Henn, Yu-tin Huang, Henrik Johansson, Marcus Spradlin, Mathias Staudacher, and Anastasia Volovich for inviting me to various workshops and extended research visits. I have greatly benefited from many interesting conversations.

I would also like to thank the remaining members of my thesis committee, Clifford Cheung, Ryan Patterson and Maria Spiropulu, for their time and input.

Furthermore, I would like to thank Anders Andreassen, John Joseph Carrasco, Wei-Ming Chen, Scott Davies, Lance Dixon, Alexander Edison, Michael Enciso, David Kosower, Lionel Mason, Andrew McLeod, David Meidinger, Josh Nohle, Julio Parra-Martinez, Jan Plefka, Gregor Richter, Oliver Schlotterer, John Schwarz, Congkao Wen, Ellis Ye Yuan, and Mao Zeng for stimulating discussions around physics in general and scattering amplitudes in particular.

I would also say thank you to all the people who, through their friendship, made my five years at Caltech an overwhelmingly positive experience: David Aasen, Michael Beverland, Thom Bohdanovicz, Aidan Chatwin-Davies, Chia-Hsien Shen, Murat Kologlu, Noah Olsman, Paul Plucinsky, Jason Pollack, Ingmar Saberi, and Christoph Uhlemann.

Of course, my family deserves special credit for all their support throughout my entire life. Without them, I would not be the person who I am now. My girlfriend, Ellen Dooley, also deserves extra thanks for putting up with all my little quirks as well as my persistent lack of punctuality when coming home from work.

My work was supported in part by the Walter Burke Institute for Theoretical Physics, by a Dominic Orr Fellowship and by the United States Department of Energy under Grant DE-SC0011632.

# Abstract

The scattering amplitudes of *planar*  $\mathcal{N} = 4$  super-Yang-Mills theory (sYM) exhibit a number of remarkable analytic structures, including dual conformal symmetry, logarithmic singularities of integrands, and the absence of poles at infinite loop momentum. None of these properties are apparent from our usual formulation of quantum field theory in terms of Lagrangians and Feynman rules. In the past years, the hidden features inspired a *dual formulation* for scattering amplitudes that is not built on the two pillars of locality and unitarity. Instead, a new geometric formulation in terms of Grassmannians and the amplituhedron emerged, which is based on the key analytic properties of scattering amplitudes in the planar sector of  $\mathcal{N} = 4$  super-Yang-Mills theory. Starting from geometric concepts, the amplituhedron geometry derives all properties of scattering amplitudes in said theory, including locality and factorization. From a practical perspective, expanding the amplitude in terms of a local diagrams, the amplituhedron construction implies that scattering amplitudes in planar  $\mathcal{N} = 4$  super-Yang-Mills are fully specified by a surprisingly simple subset of all unitarity cuts. Concretely, integrands are uniquely (up to an overall constant) fixed by demanding their vanishing on all spurious singularities.

Extending an initial proposal by Arkani-Hamed, Bourjaily, Cachazo, and Trnka, we conjecture that the same analytic structures extend beyond the planar limit of  $\mathcal{N} = 4$  super-Yang-Mills. Furthermore we show that the  $d\log$  and *no pole at infinity* constraints give the key integrand level analytic information contained in *dual conformal symmetry* in the planar sector. While it is presently unclear how to extend either dual conformal symmetry or the amplituhedron picture beyond the planar sector, our results suggest that related concepts might exist and await discovery.

In order to support our conjectures, we have analyzed several nontrivial multi-loop multi-leg amplitudes. For the nonplanar three-loop four-point and two-loop five point  $\mathcal{N} = 4$  super-Yang-Mills amplitudes, we explicitly construct a complete basis of diagram integrands that has only logarithmic singularities and no poles at infinity. We also give examples at three loops showing how to make the logarithmic singularity properties manifest by writing explicit  $d\log$  forms. We give additional evidence at four and five loops supporting the nonplanar logarithmic singularity conjecture. Our investigations show that the singularity structures of planar and nonplanar integrands in  $\mathcal{N} = 4$  super-Yang-Mills are strikingly similar. Finally, we express the complete amplitude in

terms of our special basis diagrams, with the coefficients determined by the vanishing conditions on the amplitude. By successfully carrying out this procedure, we provide nontrivial evidence that the zero conditions also carry over into the nonplanar sector. Our analysis suggests that the concept of the amplituhedron can be extended to the nonplanar sector of  $\mathcal{N} = 4$  super-Yang-Mills theory and one might hope to ultimately reformulate more general quantum field theories in a geometric language.

Using the marvelous squaring relation between Yang-Mills and gravity theories discovered by Bern, Carrasco, and Johansson (BCJ), we relate our newly gained knowledge on the Yang-Mills side to properties of gravity. We conjecture that to all loop orders, while  $\mathcal{N} = 8$  supergravity has poles at infinity, at least at four points it has only logarithmic singularities at finite locations. We provide nontrivial evidence for these conjectures. We describe the singularity structure of  $\mathcal{N} = 8$  supergravity at three loops and beyond.

In order to approach a geometric formulation for scattering in gravitational theories, we retrace the initial steps taken in planar  $\mathcal{N} = 4$  super-Yang-Mills in the gravitational setting. In particular, we study on-shell diagrams for gravity theories with any number of supersymmetries and find a compact Grassmannian formula in terms of edge variables of the graphs. Unlike in gauge theory where the analogous form involves only  $d\log$ -factors, in gravity we find a non-trivial numerator as well as higher degree poles in the edge variables. Based on the structure of the Grassmannian formula for  $\mathcal{N} = 8$  supergravity we conjecture that gravity loop amplitudes also possess similar properties. In particular, we find that there are only logarithmic singularities on cuts with finite loop momentum and that poles at infinity are present.

# Published Content and Contributions

Much of this thesis is adapted from articles that originally appeared in other forms. All are available as arXiv preprints as well as published journal articles. References [1, 2] serve as chapters 1 and 2 in this thesis respectively; The last chapter is taken from reference [3];

- Z. Bern, E. Herrmann, S. Litsey, J. Stankowicz, and J. Trnka, *Logarithmic Singularities and Maximally Supersymmetric Amplitudes*, JHEP **06** (2015) 202. doi: [10.1007/JHEP06\(2015\)202](https://doi.org/10.1007/JHEP06(2015)202), [[arXiv:1412.8584](https://arxiv.org/abs/1412.8584)]

All authors contributed equally. I was mostly involved in the construction of the  $d\log$  bases and constructing explicit  $d\log$  forms.

- Z. Bern, E. Herrmann, S. Litsey, J. Stankowicz, and J. Trnka, *Evidence for a Nonplanar Amplituhedron* JHEP **06** (2016) 098. doi: [10.1007/JHEP06\(2016\)098](https://doi.org/10.1007/JHEP06(2016)098), [[arXiv:1512.08591](https://arxiv.org/abs/1512.08591)]

All authors contributed equally. I was involved in the basis construction and checking the unitarity cuts.

- E. Herrmann, and J. Trnka, *Gravity On-shell Diagrams* JHEP **11** (2016) 136. doi: [10.1007/JHEP11\(2016\)136](https://doi.org/10.1007/JHEP11(2016)136), [[arXiv:1604.03479](https://arxiv.org/abs/1604.03479)]

Both authors contributed equally.

# Contents

<b>Acknowledgments</b>	<b>iii</b>
<b>Abstract</b>	<b>v</b>
<b>Published Content and Contributions</b>	<b>vii</b>
<b>Introduction</b>	<b>1</b>
<b>Logarithmic singularities and maximally supersymmetric amplitudes</b>	<b>6</b>
1.1 Introduction	7
1.2 Singularities of the integrand	9
1.2.1 Dual formulation of planar theory	10
1.2.2 Logarithmic singularities	12
1.2.3 Loop integrands and poles at infinity	14
1.2.4 Singularities and maximum transcendental weight	18
1.3 Strategy for nonplanar amplitudes	20
1.3.1 Constructing a basis	21
1.3.2 Expansion of the amplitude	26
1.3.3 Amplitudes and sums of $d\log$ forms	28
1.4 Three-loop amplitude	29
1.4.1 Diagram numerators	29
1.4.2 Determining the coefficients	35
1.4.3 Relation to rung rule	40
1.5 Finding $d\log$ forms	44
1.5.1 One loop	45
1.5.2 Two loops	48
1.5.3 Three loops	51
1.6 Logarithmic singularities at higher loops	55
1.7 Back to the planar integrand	59
1.7.1 Brief review of dual conformal invariance	60
1.7.2 Dual conformal invariance at three and four loops	61
1.7.3 Simple rules for eliminating double poles	63



1.7.4	Applications of three types of rules	67
1.8	From gauge theory to gravity	71
1.9	Conclusion	75
<b>Evidence for a nonplanar amplituhedron</b>		<b>77</b>
2.1	Introduction	78
2.2	Dual picture for planar integrands	80
2.2.1	Dual conformal symmetry	82
2.2.2	On-shell diagrams	85
2.2.3	Zero conditions from the amplituhedron	88
2.3	Nonplanar amplitudes	91
2.3.1	Nonplanar conjectures	92
2.3.2	Two-loop four-point amplitude	95
2.3.3	Three-loop four-point amplitude	97
2.3.4	Two-loop five-point amplitude	101
2.4	Zeros of the integrand	105
2.5	Conclusion	111
<b>Gravity on-shell diagrams</b>		<b>115</b>
3.1	Introduction	116
3.1.1	On-shell diagrams	117
3.1.2	Grassmannian formulation	121
3.1.3	Hidden properties of $\mathcal{N} = 4$ sYM amplitudes	126
3.2	Non-planar on-shell diagrams	127
3.2.1	First look: MHV leading singularities	129
3.2.2	Three point amplitudes with spin $s$	131
3.2.3	Grassmannian formula	134
3.3	Properties of gravity on-shell diagrams	136
3.3.1	Calculating on-shell diagrams	136
3.3.2	More examples	139
3.3.3	Structure of singularities	141
3.4	From on-shell diagrams to scattering amplitudes	144
3.4.1	Non-planar $\mathcal{N} = 4$ sYM amplitudes	145
3.4.2	Gravity from Yang-Mills	146
3.4.3	Collinear behavior	148
3.5	Conclusion	154
<b>References</b>		<b>156</b>

# Introduction

Unifying quantum mechanics and special relativity, quantum field theory (QFT) is our central theoretical framework to describe the microscopic world. One of the most prominent instances of a QFT is the Standard Model, which summarizes our current understanding of the realm of elementary particles, successfully describing electromagnetism, the weak and strong force. The relevance of QFT for our understanding of nature makes studying its physical and mathematical properties one of the most exciting research directions in the field of theoretical physics. Within QFT, primary objects of interest are scattering amplitudes. These are required to compute cross sections which describe the probabilities of elementary particles interacting with one another. In this regard, experimentalists at particle accelerators like the Large Hadron Collider (LHC) measure scattering amplitudes. Traditionally, scattering amplitudes have been calculated using Feynman diagrams derived from an underlying Lagrangian written in terms of quantum fields. Together with the path integral formulation, this framework encodes two of the main pillars of twentieth century physics: *locality* and *unitarity* (for a textbook introduction to QFT, see e.g. [4, 5]). However, in the past two decades we have learned from multiple directions that this standard formulation of QFT should not be the final answer.

On one hand, we now know of remarkable theories at strong coupling that defy a Lagrangian description altogether; see e.g. [6–11]. On the other hand, even at weak coupling, explicit computations revealed significant surprises in the past three decades starting with the seminal work of Parke and Taylor, who computed the gluonic  $2 \mapsto 4$  scattering amplitude at tree-level in 1985 [12]. This was one of the first instances where people noticed the tension between the apparent complexity of the intermediate calculation using standard *off-shell* Feynman diagram techniques and the simplicity of the final answer. Even for relatively simple interaction processes, the calculation can involve thousands of Feynman diagrams, leading to hundreds of pages of algebra. In contrast to this apparent complexity, Parke and Taylor’s final result, after summing all diagrams, fits on a single line (for a specific, color-stripped helicity amplitude with two negative helicity gluons MHV in terms of spinor-helicity variables),

$$A_{\text{MHV}}^{\text{tree}}(1^-2^-3^+4^+5^+6^+) = \frac{\langle 12 \rangle^4}{\langle 12 \rangle \langle 23 \rangle \langle 34 \rangle \langle 45 \rangle \langle 56 \rangle \langle 61 \rangle}.$$

For a detailed account of the notation and definitions commonly used in the amplitudes community, such as color-organization and spinor-helicity variables, see e.g. the excellent review articles [13–16]. Shortly thereafter, they were able to generalize their formula to an arbitrary number of particles  $2 \mapsto n$  [17],

$$A_{\text{MHV}}^{\text{tree}}(1^- 2^- 3^+ 4^+ \dots n^+) = \frac{\langle 12 \rangle^4}{\langle 12 \rangle \langle 23 \rangle \langle 34 \rangle \dots \langle n-1n \rangle \langle n1 \rangle}.$$

The absence of simplicity in the traditional computations points towards a more natural formulation of QFT.

A third major motivation to look for a reformulation of QFT is rooted in the problem of unifying gravity and quantum mechanics, which has puzzled theoretical physicists for decades. Amongst others, it is required for a detailed understanding of the Big Bang and various questions about black hole physics. Applying the standard quantization prescription to the variables describing spacetime geometry leads to immediate problems. There are underlying reasons to believe that the correct route to a quantum theory of gravity should not start from the fundamental principles of locality and unitarity, the major players in the traditional formulation of QFT. In the context of planar  $\mathcal{N} = 4$  super-Yang-Mills theory, a simplified theory which shares several features of the Standard Model, such a reformulation has been achieved, leading to the *amplituhedron* [18]. In this construction, scattering amplitudes are calculated geometrically as volume forms in an auxiliary space. In the planar limit,  $\mathcal{N} = 4$  sYM is believed to be completely solvable, which makes it an interesting laboratory to test new ideas in QFT and –via the AdS/CFT correspondence [19]– in gravity.

In this thesis, we are primarily interested in exploring new mathematical structures in perturbative QFT by exploiting and extending modern on-shell techniques for scattering amplitudes. In any such endeavor, it is essential to have a good toy model which is simple enough to calculate sufficiently many interesting quantities and still shares several features of more general quantum field theories. In the context of this work, our drosophilae are going to be the maximally supersymmetric gauge- and gravity- theories in four spacetime dimensions,  $\mathcal{N} = 4$  super-Yang-Mills and  $\mathcal{N} = 8$  supergravity respectively [20–22]. As parenthetical side note, we would like to mention that a number of advances originally developed in these toy models eventually found their way into practical computational tools employed for real world collider calculations. One of these tools, which also plays a prominent role in this thesis, is the generalized unitarity method developed by Bern, Dixon, Dunbar, and Kosower [23]. Their key insight is to factorize scattering amplitudes into simpler tree objects in order to determine the loop amplitudes. In the context of Standard Model processes, this has been incorporated in computational tools like BlackHat [24].

Arguably, the most amount of progress in our understanding of the structure of scattering amplitudes has been achieved in planar  $\mathcal{N} = 4$  super-Yang-Mills theory [20, 21]. (See reviews, e.g. Refs. [13, 14, 25–28].) Discoveries of new structures and symmetries have led to the development of deep theoretical frameworks which greatly aid new computations while also connecting to new areas of mathematics. Along with the conceptual progress have come significant computational advances, including new explicit results for amplitudes after integration up to high loop orders (see e.g. Refs. [29–34]), as well as some all-loop order predictions [35]. Among the theoretical advances are connections to twistor string theory [36, 37], on-shell recursion relations [38–40], unveiling of hidden dual conformal symmetry [41–43], Yangian symmetry [44], integrability [45, 46], momentum twistors [47], a dual interpretation of scattering amplitudes as supersymmetric Wilson loops [48–53], a duality to correlation functions [54, 55], amplitudes at finite coupling in special kinematic regimes using OPE [56–58], the hexagon function bootstrap [29, 31, 59–62] and its extension to higher points [30, 63], and the use of symbols and cluster polylogarithmics [63–66], as well as a variety of other structures. More recently, four-dimensional planar integrands in  $\mathcal{N} = 4$  sYM were reformulated using on-shell diagrams and the positive Grassmannian [40, 67–72] (see related work in Ref. [73–77]). This reformulation fits nicely into the concept of the amplituhedron [18, 78–84], and makes an extremely interesting connection to active areas of research in algebraic geometry and combinatorics (see e.g. [85–90]). This picture also makes certain properties of amplitudes completely manifest, including properties like Yangian invariance [44] that are obscure in standard field-theory descriptions.

A special feature of  $\mathcal{N} = 4$  sYM scattering amplitudes that appears after integration is uniform transcendentality [46, 91, 92], a property closely related to the  $d$ log-structure of the integrand in the dual formulation [67] (for recent discussion on integrating  $d$ log forms see Ref. [93]). For a mathematical account of Feynman integrals and an introduction to the required function space related to the transcendentality properties, see e.g. [94–96] and references therein. The dual formulation can perhaps also be extended to integrated results via special functions that are motivated by the positive Grassmannian [64, 65, 97, 98]. For a recent connection between positivity inside the amplituhedron at integrand level and certain positivity properties of integrated results, see [99]. Ultimately, such an extension might naturally incorporate the integrability of planar  $\mathcal{N} = 4$  sYM theory [45]. So far this has not played a major role in the dual formulation, but is very useful in the flux tube  $S$ -matrix approach [56, 100–103], leading to some predictions at finite coupling. Integrability should be present in the dual formulation of the planar theory through Yangian symmetry. Therefore, it is natural to attempt to search for either a Yangian-preserving regulator of infrared di-

vergenences of amplitudes [104–107], or directly for Yangian-preserving deformations of the Grassmannian integral [108, 109]. For a recent attempt to extend Yangian symmetry and integrability beyond S-Matrix elements and on-shell functions to the level of the classical equations of motion, see [110].

The general structure of this thesis is as follows: Following this more general introduction to scattering amplitudes, we briefly outline each of the three main chapters here, hoping that the reader gets a glimpse of the most important results. In addition, to set this thesis in context with the existing literature and to give additional motivation for the main questions addressed in the individual chapters, we have prepended a separate introduction to each.

In this thesis, we are motivated to explore if any of the aforementioned analytic features of scattering amplitudes ( $d\log$ -form of integrands and the absence of poles at infinity) persist outside of planar  $\mathcal{N} = 4$  super-Yang-Mills theory. In collaboration with Zvi Bern, Sean Litsey, James Stankowicz, and Jaroslav Trnka, we investigated the analytic properties of multi-loop scattering amplitudes in  $\mathcal{N} = 4$  sYM without resorting to the planar limit, which first appeared as a research article in [1]. This work constitutes Chapter 1 of this thesis in a slightly adapted form. In this study we extended several properties of planar amplitudes that were originally believed to be intimately tied to the special symmetries and the integrable nature of the planar sector to the full non-planar theory. We clarified the link between *dual conformal invariance*, a hidden symmetry of planar  $\mathcal{N} = 4$  sYM not visible from Feynman diagrams, to the absence of certain residues of the loop-integrand for infinite loop-momentum. Following the planar example one step further, we analyzed the implications of the *on-shell diagram* formulation of scattering amplitudes in planar  $\mathcal{N} = 4$  sYM. On-shell diagrams can be viewed either as residues of loop amplitudes or as a product of on-shell three-point amplitudes. In planar  $\mathcal{N} = 4$  sYM, on-shell diagrams possess special analytic properties ( $d\log$  singularities) derived from a dual formulation using a geometric object known as the *positive Grassmannian*. In our work we were able to show that the same structure is present in amplitudes of the full  $\mathcal{N} = 4$  sYM theory, suggesting the existence of a dual formulation for the full theory.

In a subsequent work [2] with the same collaborators, which appears as Chapter 2, we were able to give evidence that the amplituhedron construction of planar  $\mathcal{N} = 4$  sYM theory extends to the full theory as well. The amplituhedron is the first instance of the desired reformulation of QFT where locality and unitarity are derived from deeper mathematical properties of scattering amplitudes in planar  $\mathcal{N} = 4$  sYM. In broad terms, the amplituhedron posits that scattering amplitudes are calculated as differential forms with logarithmic singularities on the boundary of the amplituhedron space. In

this picture, the geometry of the space –generalizing the positive Grassmannian of individual on-shell diagrams– dictates the properties of amplitudes. Building on this work, it would be interesting to find the actual construction of an amplituhedron-like object in the future. Currently we are limited by the fact that global variables defining a unique integrand are not known.

In recent years, Bern, Carrasco, and Johansson (BCJ) elucidated the squaring relation between gauge theories and gravity via the celebrated color-kinematics duality in conjunction with the double-copy property of gravity amplitudes. This novel construction implies a tight link between the properties of scattering amplitudes in both theories which led us to the study of the analytic properties of scattering amplitudes in  $\mathcal{N} = 8$  supergravity (sugra). It has been a long-standing question, whether  $\mathcal{N} = 8$  sugra is perturbatively finite. In our work (c.f. Sec. 1.8 here), we found that unlike in gauge theory, poles at infinity are present in gravity amplitudes. However, the direct connection between such poles and a potential UV-divergence is not presently clear. It is an open question left to future work to understand this relation in more detail, which requires a combination of integrand as well as integration techniques to identify naively divergent terms that ultimately integrate to zero. These cancellations cause the UV-finiteness of certain supersymmetric gravity theories where no known symmetry explanation exists; see e.g. [111]. Understanding the underlying reason behind the cancellations should ultimately shed light on the structure of quantum gravity itself.

In order to extend our understanding of gravity theories, in collaboration with Jaroslav Trnka, we found a new formula to express gravity on-shell diagrams in terms of an auxiliary Grassmannian space, which was published in [3] and appears as Chapter 3 here. Guided by the work on planar  $\mathcal{N} = 4$  sYM, where on-shell diagrams serve directly as building blocks for scattering amplitudes via the BCFW-recursion relation, we were motivated to investigate the properties of the on-shell functions in gravity. In planar  $\mathcal{N} = 4$  sYM it was the reformulation of on-shell diagrams in terms of the geometric structure of the Grassmannian, which finally led to a complete reformulation of perturbation theory and culminated in the amplituhedron construction. Taking this analogy seriously, our Grassmannian formula can be seen as a first step to a similar reformulation in gravity. This has not been worked out so far, and it is one of my future research projects. Similarly to nonplanar Yang–Mills theory, it is the lack of good variables that currently hampers direct progress in this direction. Starting from gravity on-shell diagrams, it is tempting to write scattering amplitudes in terms of these objects. Partial progress has been achieved by Heslop and Lipstein, who wrote the one-loop four-point integrand for gravity in terms of on-shell functions. It is an open problem how to extend this construction to more general integrands.

# Logarithmic singularities and maximally supersymmetric amplitudes

The dual formulation of planar  $\mathcal{N} = 4$  super-Yang-Mills scattering amplitudes makes manifest that the integrand has only logarithmic singularities and no poles at infinity. Recently, Arkani-Hamed, Bourjaily, Cachazo, and Trnka conjectured that the same singularity properties hold to all loop orders in the nonplanar sector as well. Here we conjecture that to all loop orders these constraints give us the key integrand level analytic information contained in dual conformal symmetry. We also conjecture that to all loop orders, while  $\mathcal{N} = 8$  supergravity has poles at infinity, and at least at four points it has only logarithmic singularities at finite locations. We provide nontrivial evidence for these conjectures. For the three-loop four-point  $\mathcal{N} = 4$  super-Yang-Mills amplitude, we explicitly construct a complete basis of diagram integrands that has only logarithmic singularities and no poles at infinity. We then express the complete amplitude in terms of the basis diagrams, with the coefficients determined by unitarity. We also give examples at three loops showing how to make the logarithmic singularity properties manifest via  $d\log$  forms. We give additional evidence at four and five loops, supporting the nonplanar logarithmic singularity conjecture. Furthermore, we present a variety of examples illustrating that these constraints are more restrictive than dual conformal symmetry. Our investigations show that the singularity structures of planar and nonplanar integrands in  $\mathcal{N} = 4$  super-Yang-Mills are strikingly similar. While it is not clear how to extend either dual conformal symmetry or a dual formulation to the nonplanar sector, these results suggest that related concepts might exist and await discovery. Finally, we describe the singularity structure of  $\mathcal{N} = 8$  supergravity at three loops and beyond.

## 1.1 Introduction

In this paper we are interested in understanding how to carry these many advances and promising directions over to the nonplanar sector of  $\mathcal{N} = 4$  sYM theory. Unfortunately much less is known about nonplanar  $\mathcal{N} = 4$ , in part because of the difficulty of carrying out loop integrations. In addition, lore suggests that we lose integrability and thereby many nice features of planar amplitudes believed to be associated with it. (We do not use a  $1/N$  expansion.) Even at the integrand level, the absence of a unique integrand makes it difficult to study nonplanar amplitudes globally, rather than in some particular expansion. One approach to extending planar properties to the nonplanar sector is to search for the dual formulation of the theory using on-shell diagrams. Despite the fact that these are well-defined objects beyond the planar limit with many interesting properties [112], yet it is still not known how to expand scattering amplitudes in terms of these objects.

Nevertheless, there are strong hints that at least some of the properties of the planar theory survive the extension to the nonplanar sector. In particular, the Bern–Carrasco–Johansson (BCJ) duality between color and kinematics [113, 114] shows that the nonplanar sector of  $\mathcal{N} = 4$  sYM theory is intimately linked to the planar one, so we should expect that some of the properties carry over. BCJ duality can be used to derive  $\mathcal{N} = 8$  supergravity integrands starting from  $\mathcal{N} = 4$  sYM ones, suggesting that some properties of the gauge theory should extend to  $\mathcal{N} = 8$  supergravity as well. An encouraging observation is that the two-loop four-point amplitude of both  $\mathcal{N} = 4$  sYM theory and  $\mathcal{N} = 8$  supergravity has a uniform transcendental weight [91, 115–119]. Related to the leading transcendentality properties is the recent conjecture by Arkani-Hamed, Bourjaily, Cachazo, and Trnka [119] that, to all loop orders, the full  $\mathcal{N} = 4$  sYM amplitudes, including the nonplanar sector, have only logarithmic singularities and no poles at infinity. This is motivated by the possibility of dual formulation that would make these properties manifest [67]. As evidence for their conjecture, they rewrote the two-loop four-point amplitude [120] in a format that makes these properties hold term by term. In this paper we follow this line of reasoning, showing that key features of planar  $\mathcal{N} = 4$  sYM amplitudes carry over to the nonplanar sector. In particular, we demonstrate that the three-loop four-point amplitude of  $\mathcal{N} = 4$  sYM theory has only logarithmic singularities and no poles at infinity. We find a diagrammatic representation of the amplitude, using standard Feynman propagators, where these properties hold diagram by diagram. While we do not expect that these properties can be made manifest in each diagram to all loop orders, for the amplitudes studied in this paper this strategy works well. We proceed here by analyzing all singularities of the integrand; this includes singularities both from propagators and from Jacobians of cuts. We then construct



numerators to cancel unwanted singularities, where we take “unwanted singularities” to mean double or higher poles and poles at infinity. In the planar case, subsets of these types of constraints have been used in Refs. [48, 121]. As a shorthand, we call numerators with the desired properties “ $d\log$  numerators” (and analogously for “ $d\log$  integrands” and “ $d\log$  forms”). Once we have found all such objects, we use unitarity constraints to determine the coefficients in front of each contribution. To verify that the amplitude so deduced is complete and correct we evaluate a complete set of unitarity cuts. The representation of the three-loop four-point amplitude that we find in this way differs from the previously found ones [114, 122] by contact terms that have been nontrivially rearranged via the color Jacobi identity. While all forms of this amplitude have only logarithmic singularities, it is not at all obvious in earlier representations that this is true, because of nontrivial cancellations between different diagrams.

After constructing the three-loop basis of  $d\log$  integrands, we address some interesting questions. One is whether there is a simple pattern dictating the coefficients with which the basis integrands appear in the amplitude. Indeed, we show that many of the coefficients follow the rung rule [120], suggesting that a new structure remains to be uncovered. Another question is whether it is possible to explicitly write the integrands we construct as  $d\log$  forms. In general, this requires a nontrivial change of variables, but we have succeeded in writing all but one type of basis integrand form as  $d\log$  forms. We present three explicit examples at three loops showing how this is done. These  $d\log$  forms make manifest that the integrand basis elements have only logarithmic singularities, although the singularity structure at infinity is not manifest. The requirement of only logarithmic singularities and no poles at infinity strongly restricts the integrands. In fact, we conjecture that in the planar sector logarithmic singularities and absence of poles at infinity imply dual conformal invariance in the integrand. We check this for all contributions at four loops and give a five-loop example illustrating that these singularity conditions impose even stronger constraints on the integrand than dual conformal symmetry.

Related to the  $d\log$  forms, the results presented in this paper offer a useful bridge between integrands and integrated results. The objects we construct here are a subset of the uniform transcendental integrals needed in the Henn and Smirnov procedure [123–126] to find a relatively simple set of differential equations for them. The importance of uniform transcendental weight was first realized in Ref. [115]. It was noted that through three loops the  $\mathcal{N} = 4$  sYM anomalous dimensions of Wilson twist 2 operator match the terms in the corresponding QCD anomalous dimension that have maximal transcendental weight. The ideas of uniform transcendental weight were expanded on in a variety of subsequent papers and include examples with nonplanar contributions [91, 116–119]. In this paper we focus mainly on integrands relevant to  $\mathcal{N} = 4$  sYM theory,

which correspond to the subset of integrands with no poles at infinity. In any case, a side benefit of the methods described here is that it should offer an efficient means for identifying integrals of uniform transcendental weight. Ref. [119] noted a simple relation between the singularity structure of the two-loop four-point amplitude of  $\mathcal{N} = 8$  supergravity and the one of  $\mathcal{N} = 4$  sYM. How much of this continues at higher loops? Starting at three loops, the situation is more complicated because the integrals appearing in the two theories are different. Nevertheless, by making use of the BCJ construction [113, 114], we can obtain the corresponding  $\mathcal{N} = 8$  amplitude in a way that makes its analytic properties relatively transparent. In particular, it allows us to immediately demonstrate that away from infinity,  $\mathcal{N} = 8$  supergravity has only logarithmic singularities. We also find that starting at three loops,  $\mathcal{N} = 8$  supergravity amplitudes have poles at infinity whose degree grow with the number of loops.

This paper is organized as follows: In Sect. 1.2 we will briefly discuss logarithmic singularities and poles at infinity in loop integrands. In Sect. 1.3 we outline our strategy for studying nonplanar amplitudes and illustrate it using the two-loop four-point amplitude. In Sect. 1.4 we construct a basis of three-loop four-point integrands that have only logarithmic singularities and no poles at infinity. We then express the three-loop four-point amplitude in this basis and show that the rung rule determines a large subset of the coefficients. Then in Sect. 1.5 we discuss  $d\log$  forms in some detail. In Sect. 1.6, we give a variety of multiloop examples corroborating that only logarithmic singularities are present in  $\mathcal{N} = 4$  sYM theory. In Sect. 1.7, we present evidence that the constraints of only logarithmic singularities and no poles at infinity incorporate the constraints from dual conformal symmetry. In Sect. 1.8, we comment on the singularity structure of the  $\mathcal{N} = 8$  supergravity four-point amplitude. In Sect. 1.9, we present our conclusions and future directions.

## 1.2 Singularities of the integrand

Integrands offer enormous insight into the structure of scattering amplitudes. This includes the discovery of dual conformal symmetry [41], the Grassmannian structure [67–70], the geometric structures [18], and ultraviolet properties [127–129]. The singularity structure of integrands, along with the integration contours, determine the properties of integrated expressions. In particular, the uniform transcendentality property is determined by the singularity structure of the integrand. The nonplanar sector of  $\mathcal{N} = 4$  sYM theory is much less developed than the planar one. Studying integrands offers a means of making progress in this direction, especially at high loop orders where it is difficult to obtain integrated expressions.

It would be ideal to study the amplitude as a single object and not to rely on an expansion using diagrams as building blocks which carry their own labels. In the planar sector, we can avoid such an expansion by using globally defined dual variables to obtain a unique rational function called the *integrand* of the amplitude. Unfortunately, it is unclear how to define such a unique object in the nonplanar case. In this paper we sidestep the lack of global variables by focusing on smaller pieces of the amplitude, organized through covariant, local diagrams with only three-point vertices and Feynman propagators. Such diagrams have also proved useful in the generalized unitarity method. Diagrams with only cubic vertices are sufficient in gauge and gravity theories, because it is possible to express diagrams containing higher point vertices in terms of ones with only cubic vertices by multiplying and dividing by appropriate Feynman propagators. For future reference, when not stated otherwise, this is what we mean by a “diagrammatic representation” or an “expansion in terms of diagrams”.

For a given diagram, there is no difficulty in having a well-defined notion of an integrand, at least for a given set of momentum labels. For this to be useful, we need to be able to expose the desired singularity properties one diagram at a time, or at worst for a collection of a small subset of diagrams at a time. In general, there is no guarantee that this can be done, but in cases where it can be, it offers a useful guiding principle for making progress in the nonplanar sector. A similar strategy proved successful for BCJ duality. In that case, at most three diagrams at a time need to share common labels in order to define the duality, bypassing the need for global labels.

At three loops we will explicitly construct a basis of integrands that have only logarithmic singularities and no poles at infinity. We also discuss some higher-loop examples. Before doing so, we summarize the dual formulation of planar amplitudes, in order to point out the properties that we wish to carry over to the nonplanar case.

### 1.2.1 Dual formulation of planar theory

Here we summarize the dual formulation of planar  $\mathcal{N} = 4$  sYM theory, with a focus on our approach to extending this formulation to the nonplanar sector. For details beyond what appear here, we refer the reader to Refs. [67–69].

As mentioned in the previous subsection, for planar amplitudes we can define an *integrand* based on a global set of variables valid for all terms in the amplitude [40]. Up to terms that vanish under integration, the integrand of a planar amplitude is a unique rational function constrained by the requirement that all unitarity cuts of the function are correct. Methods based on unitarity and factorization construct the integrand using only on-shell input information. On-shell diagrams capitalize on this efficiency by representing integrands as graphs where all internal lines are implicitly on shell, and all vertices are three-point amplitudes.

An important further step is to promote on-shell diagrams from being only reference data to being actual building blocks for the amplitude. This idea was exploited in Ref. [68], where loop-level [40] recursion relations for integrands were interpreted directly in terms of higher-loop on-shell diagrams. A preliminary version of this notion is already visible in the early version of the BCFW recursion relations [38], where the tree-level amplitudes are expressed in terms of leading singularities of one-loop amplitudes.

More recently, the construction of amplitudes from on-shell diagrams has been connected [67] to modern developments in algebraic geometry and combinatorics [85–90] where the same type of diagrams appeared in a very different context. Each on-shell diagram can be labeled using variables associated with edges  $e_i$  or faces  $f_j$ , from which one can build a  $k \times n$  matrix  $C$ , where  $n$  is the number of external particles, and  $k$  is related to the number of negative helicity particles. This matrix has a  $\text{GL}(k)$  symmetry and therefore belongs to a Grassmannian  $C \in G(k, n)$ . If the edge and face variables are taken to be real and to have fixed sign based on certain rules, all the maximal minors of the matrix  $C$  are positive and produce cells in the positive Grassmannian  $G_+(k, n)$ . This is more than just a mathematical curiosity, as this viewpoint can be used to evaluate on-shell diagrams independently of the notion of the notion of gluing together three-point on-shell amplitudes.

After parametrizing the on-shell diagram as described, the diagram takes the value [68]

$$\Omega = \frac{df_1}{f_1} \wedge \frac{df_2}{f_2} \wedge \cdots \wedge \frac{df_m}{f_m} \delta(C(f_j) \cdot \mathcal{W}), \quad (1.2.1)$$

where we collectively encode all external data, both bosonic and fermionic, in  $\mathcal{W}$ . The delta function implies a set of equations that can be solved for the  $f_j$  in terms of external data. Any on-shell diagrams that have an interpretation as building blocks for tree-level amplitudes exactly determine all variables  $f_j$  so that  $\Omega$  becomes a function of external data only, and  $\Omega$  gives exactly the tree amplitude. Likewise, any on-shell diagrams that have an interpretation as building blocks of an  $L$ -loop integrand leave  $4L$  variables  $f_j$  unfixed, and  $\Omega$  is the  $4L$ -form giving exactly the unique  $L$ -loop integrand. Even on-shell diagrams that do not directly correspond to tree amplitudes or loop integrands have some meaning as cuts or factorizations of the amplitude. This construction is often referred to as the *dual formulation* of planar amplitudes. One of our motivations is to look for possible extensions of this formulation to the nonplanar sector.

A crucial feature of  $\Omega$  is that it has only logarithmic singularities in  $f_j$ , inherited from the structure of Eq. (1.2.1). As written there, these singularities are in the abstract Grassmannian space, or equivalently in the extended bosonic variables within the amplituhedron construction of the integrand. When translated back to momen-

tum (or twistor or momentum twistor) space, the logarithmic property is lost due to the supersymmetric-part of the delta function in Eq. (1.2.1). However, for both MHV ( $k = 2$ ) and NMHV ( $k = 3$ ) on-shell diagrams, the supersymmetric-part of delta functions can be separated from the bosonic parts, resulting in a logarithmic form in momentum space [18, 78]. The other property that is completely manifest when forms are written in momentum twistor space is the absence of poles at infinity. Both these properties are preserved for all on-shell diagrams and so are true for all tree-level amplitudes and integrands for planar loop amplitudes.

We can also compute nonplanar on-shell diagrams, either by gluing together three-point on-shell amplitudes or by using the relation to the Grassmannian. The relation to the positive part of the Grassmannian is naively lost, but reappears under more careful scrutiny [112]. We can still associate a logarithmic form to diagrams as in Eq. (1.2.1). Using the same arguments as in the planar sector, all MHV and NMHV on-shell diagrams have logarithmic singularities in momentum space. However, it is not known at present how to construct complete  $\mathcal{N} = 4$  sYM amplitudes, including the nonplanar parts, using recursion relations of these nonplanar on-shell diagrams. Unlike in the planar sector, a major obstacle in the nonplanar sector is the absence of a unique integrand. If this problem can be solved so that the amplitude is expressible in terms of on-shell diagrams, then the same arguments as used in the planar sector would prove that the full nonplanar  $\mathcal{N} = 4$  sYM amplitudes have logarithmic singularities. In any case, even if the existence of a dual formulation for the nonplanar sector cannot be straightforwardly established, we can still test the key consequences: only logarithmic singularities and no poles at infinity. This is what we turn to now.

## 1.2.2 Logarithmic singularities

Before discussing the basis of integrands for  $\mathcal{N} = 4$  sYM amplitudes, we consider some simple toy cases that display the properties relevant for subsequent sections. It is natural to define an integrand form  $\Omega(x_1, \dots, x_m)$  of the integral  $F$  by stripping off the integration symbol

$$F = \int \Omega(x_1, \dots, x_m), \quad (1.2.2)$$

and to study its singularity structure. There is a special class of forms that we are interested in here: those that have only *logarithmic singularities*. A form has only logarithmic singularities if near any pole  $x_i \rightarrow a$  it behaves as

$$\Omega(x_1, \dots, x_m) \rightarrow \frac{dx_i}{x_i - a} \wedge \hat{\Omega}(x_1, \dots, \hat{x}_i, \dots, x_m), \quad (1.2.3)$$

where  $\hat{\Omega}(x_1, \dots, \hat{x}_i, \dots, x_m)$  is an  $(m-1)$ -form<sup>1</sup> in all variables except  $\hat{x}_i$ . An equivalent terminology is that there are only simple poles. That is, we are interested in integrands where we can change variables  $x_i \rightarrow g_i(x_j)$  such that the form becomes

$$\Omega = d\log g_1 \wedge d\log g_2 \wedge \cdots \wedge d\log g_m, \quad (1.2.4)$$

where we denote

$$d\log x \equiv \frac{dx}{x}. \quad (1.2.5)$$

We refer to this representation as a “ $d\log$  form”.

A simple example of such a form is  $\Omega(x) = dx/x \equiv d\log x$ , while  $\Omega(x) = dx$  or  $\Omega(x) = dx/x^2$  are examples of forms which do not have this property. A trivial two-form with logarithmic singularities is  $\Omega(x, y) = dx \wedge dy/(xy) = d\log x \wedge d\log y$ . A less trivial example of a  $d\log$  form is

$$\Omega(x, y) = \frac{dx \wedge dy}{xy(x+y+1)} = d\log \frac{x}{x+y+1} \wedge d\log \frac{y}{x+y+1}. \quad (1.2.6)$$

In this case, the property of only logarithmic singularities is not obvious from the first expression, but a change of variables resulting in the second expression makes the fact that  $\Omega$  is a  $d\log$  form manifest. This may be contrasted with the form

$$\Omega(x, y) = \frac{dx \wedge dy}{xy(x+y)}, \quad (1.2.7)$$

which is not logarithmic because near the pole  $x = 0$  it behaves as  $dy/y^2$ ; this form cannot be written as a  $d\log$  form. In general, the nontrivial changes of variables required can make it difficult to find the explicit  $d\log$  forms even where they exist.

In a bit more detail, consider the behavior of a form near  $x = 0$ . If the integrand scales as  $dx/x^m$  for integer  $m$ , we consider two different regimes where integrands can fail to have logarithmic singularities. The first is when  $m \geq 2$ , which results in double or higher poles at  $x = 0$ . The second is when  $m \leq 0$ , which results in a pole at infinity. Avoiding unwanted singularities, either at finite or infinite values of  $x$ , leads to tight constraints on the integrand of each diagram. Since we take the denominators to be the standard Feynman propagators associated to a given diagram, in our expansion of the amplitude the only available freedom is to adjust the kinematic numerators. As a simple toy example, consider the form

$$\Omega(x, y) = \frac{dx \wedge dy N(x, y)}{xy(x+y)}. \quad (1.2.8)$$

---

<sup>1</sup>The signs from the wedge products will not play a role because at the end we will construct basis elements whose normalization in the amplitude is fixed from unitarity cuts.

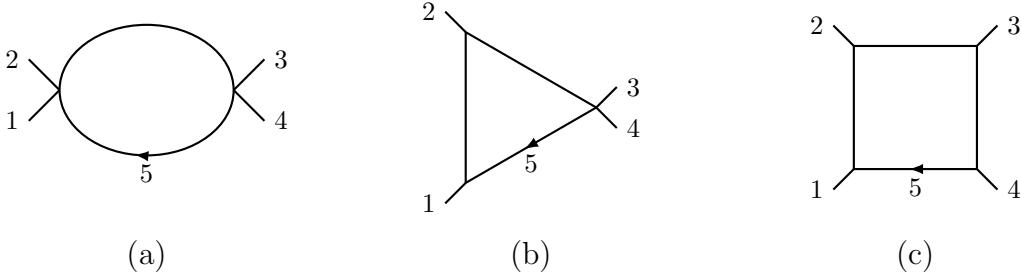


**Figure 1.1.** The (a) bubble, (b) triangle, and (c) box one-loop diagrams.

As noted above, for a constant numerator  $N(x, y) = 1$  the form develops a double pole at  $x = 0$ . Similarly, for  $N(x, y) = x^2 + y^2$  the form behaves like  $dy$  for  $x = 0$  and again it is not logarithmic. There is only one class of numerators that make the form logarithmic near  $x = 0$  and  $y = 0$ :  $N(x, y) = a_1x + a_2y$  for arbitrary  $a_1$  and  $a_2$ .

Our discussion of loop integrands will be similar: constant numerators (i.e. those independent of loop momenta) are dangerous, for they may allow double or higher poles located at finite values of loop momenta, while a numerator with too many powers of loop momentum can develop higher poles at infinity. It turns out that the first case is generally the problem in gauge theory, whereas the second case usually arises for gravity amplitudes, because the power counting of numerators is boosted relative to the gauge-theory case. For sYM integrands, we will carefully tune numerators so that only logarithmic singularities are present. The desired numerators live exactly on the boundary between too many and too few powers of loop momenta.

### 1.2.3 Loop integrands and poles at infinity

Now consider the special class of four-forms that correspond to one-loop integrands. Standard integral reduction methods [130, 131] reduce any massless one-loop amplitude to a linear combination of box, triangle, and bubble integrals. In nonsupersymmetric theories there are additional rational terms arising from loop momenta outside of  $D = 4$ ; these are not relevant for our discussion of  $\mathcal{N} = 4$  sYM theory. While it will eventually be necessary to include the  $(-2\epsilon)$  dimensional components of loop momenta, since these are in general required by dimensional regularization, for the purposes of studying the singularities of the integrand we simply put this matter aside. In any case, direct checks reveal that these  $(-2\epsilon)$  dimensional pieces do not lead to extra contributions through at least six loops in  $\mathcal{N} = 4$  sYM four-point amplitudes [132]. That is, the naive continuation of the four-dimensional integrand into  $D$  dimensions yields the correct results. As usual, infrared singularities are regularized using dimensional regularization. (See for example, Refs. [122, 129, 133].) We focus here on the four-point case, but a

similar analysis can be performed for larger numbers of external legs as well, although in this case we expect nontrivial corrections from  $(-2\epsilon)$  components of the loop momenta. Consider the bubble, triangle, and box integrals in Fig. 1.1. In these and all following diagrams, we take all external legs as outgoing. The explicit forms in  $D = 4$  are

$$\begin{aligned} d\mathcal{I}_2 &= d^4\ell_5 \frac{1}{\ell_5^2(\ell_5 - k_1 - k_2)^2}, \\ d\mathcal{I}_3 &= d^4\ell_5 \frac{s}{\ell_5^2(\ell_5 - k_1)^2(\ell_5 - k_1 - k_2)^2}, \\ d\mathcal{I}_4 &= d^4\ell_5 \frac{st}{\ell_5^2(\ell_5 - k_1)^2(\ell_5 - k_1 - k_2)^2(\ell_5 + k_4)^2}, \end{aligned} \tag{1.2.9}$$

where we have chosen a convenient normalization. The variables  $s = (k_1 + k_2)^2$  and  $t = (k_2 + k_3)^2$  are the usual Mandelstam invariants, depending only on external momenta. Under integration, these forms are infrared or ultraviolet divergent and need to be regularized, but as mentioned before we set this aside and work directly in four dimensions.

In  $D = 4$ , we can parametrize the loop momentum in terms of four independent vectors constructed from the spinor-helicity variables associated with the external momenta  $k_1 = \lambda_1 \tilde{\lambda}_1$  and  $k_2 = \lambda_2 \tilde{\lambda}_2$ . A clean choice for the four degrees of freedom of the loop momentum is

$$\ell_5 = \alpha_1 \lambda_1 \tilde{\lambda}_1 + \alpha_2 \lambda_2 \tilde{\lambda}_2 + \alpha_3 \lambda_1 \tilde{\lambda}_2 + \alpha_4 \lambda_2 \tilde{\lambda}_1, \tag{1.2.10}$$

where the  $\alpha_i$  are now the independent variables. Writing  $d\mathcal{I}_2$  in this parametrization we obtain

$$d\mathcal{I}_2 = \frac{d\alpha_1 \wedge d\alpha_2 \wedge d\alpha_3 \wedge d\alpha_4}{(\alpha_1\alpha_2 - \alpha_3\alpha_4)(\alpha_1\alpha_2 - \alpha_3\alpha_4 - \alpha_1 - \alpha_2 + 1)}. \tag{1.2.11}$$

In general, since we are not integrating the expressions, we ignore Feynman's  $i\epsilon$  prescription and any factors of  $i$  from Wick rotation.

To study the singularity structure, we can focus on subregions of the integrand by imposing on-shell or cut conditions. As an example, the cut condition  $\ell_5^2 = 0$  can be computed in these variables by setting

$$0 = \ell_5^2 = (\alpha_1\alpha_2 - \alpha_3\alpha_4)s. \tag{1.2.12}$$

We can then eliminate one of the  $\alpha_i$ , say  $\alpha_4$ , by computing the residue on the pole located at  $\alpha_4 = \alpha_1\alpha_2/\alpha_3$ . This results in a residue,

$$\text{Res}_{\ell_5^2=0} d\mathcal{I}_2 = \frac{d\alpha_3}{\alpha_3} \wedge \frac{d\alpha_2}{(\alpha_2 + \alpha_1 - 1)} \wedge d\alpha_1. \tag{1.2.13}$$



Changing variables to  $\alpha_{\pm} = \alpha_1 \pm \alpha_2$ , this becomes

$$\text{Res}_{\ell_5^2=0} d\mathcal{I}_2 = \frac{d\alpha_3}{\alpha_3} \wedge \frac{d\alpha_+}{(\alpha_+ - 1)} \wedge d\alpha_- . \quad (1.2.14)$$

We can immediately see that the form  $d\mathcal{I}_2$  is non-logarithmic in  $\alpha_-$ , and thus the bubble integrand has a nonlogarithmic singularity in this region.

Carrying out a similar exercise for the triangle  $d\mathcal{I}_3$  using the parametrization in Eq. (1.2.10), we obtain

$$d\mathcal{I}_3 = \frac{d\alpha_1 \wedge d\alpha_2 \wedge d\alpha_3 \wedge d\alpha_4}{(\alpha_1\alpha_2 - \alpha_3\alpha_4)(\alpha_1\alpha_2 - \alpha_3\alpha_4 - \alpha_2)(\alpha_1\alpha_2 - \alpha_3\alpha_4 - \alpha_1 - \alpha_2 + 1)} . \quad (1.2.15)$$

We can make a change of variables and rewrite it in the manifest  $d\log$  form,

$$d\mathcal{I}_3 = d\log(\alpha_1\alpha_2 - \alpha_3\alpha_4) \wedge d\log(\alpha_1\alpha_2 - \alpha_3\alpha_4 - \alpha_2) \wedge d\log(\alpha_1\alpha_2 - \alpha_3\alpha_4 - \alpha_1 - \alpha_2 + 1) \wedge d\log \alpha_3 . \quad (1.2.16)$$

Translating this back into momentum space:

$$d\mathcal{I}_3 = d\log \ell_5^2 \wedge d\log(\ell_5 - k_1)^2 \wedge d\log(\ell_5 - k_1 - k_2)^2 \wedge d\log(\ell_5 - k_1) \cdot (\ell_5^* - k_1) , \quad (1.2.17)$$

where  $\ell_5^* \equiv \beta\lambda_2\tilde{\lambda}_1 + \lambda_1\tilde{\lambda}_1$  is one of the two solutions to the triple cut. The parameter  $\beta$  is arbitrary in the triple cut solution, and the  $d\log$  form is independent of it. For the box integral, a similar process followed in Ref. [67] results in

$$d\mathcal{I}_4 = d\log \frac{\ell_5^2}{(\ell_5 - \ell_5^*)^2} \wedge d\log \frac{(\ell_5 - k_1)^2}{(\ell_5 - \ell_5^*)^2} \wedge d\log \frac{(\ell_5 - k_1 - k_2)^2}{(\ell_5 - \ell_5^*)^2} \wedge d\log \frac{(\ell_5 + k_4)^2}{(\ell_5 - \ell_5^*)^2} , \quad (1.2.18)$$

where  $\ell_5^* \equiv -\frac{\langle 14 \rangle}{\langle 24 \rangle} \lambda_2 \tilde{\lambda}_1 + \lambda_1 \tilde{\lambda}_1$ ; see also our discussion in subsection 1.5.1.

While both triangle and box integrands can be written in  $d\log$  form, there is an important distinction between the triangle form  $d\mathcal{I}_3$  and the box form  $d\mathcal{I}_4$ . On the cut  $\alpha_4 = \alpha_1\alpha_2/\alpha_3$ , only one  $d\log$ -factor in  $d\mathcal{I}_3$  depends on  $\alpha_3$  and develops a singularity in the limit  $\alpha_3 \rightarrow \infty$  (which implies  $\ell_5 \rightarrow \infty$ ), while  $d\mathcal{I}_4$  does not. We refer to any singularity that develops as a loop momentum approaches infinity (in our example,  $\ell_5 \rightarrow \infty$ ) at any step in the cut structure as a *pole at infinity*. To be more specific, even if a  $d\log$  form has no pole at infinity before imposing any cut conditions, it is possible to generate such poles upon taking residues, as we saw in the example of the triangle integrand above. In this sense, the pole at infinity property is more refined than simple power counting, which only considers the overall scaling of an integrand before taking any cuts.

The issue of poles at infinity will be important for our discussion of  $\mathcal{N} = 4$  sYM theory as well as  $\mathcal{N} = 8$  supergravity amplitudes. While a lack of poles at infinity implies

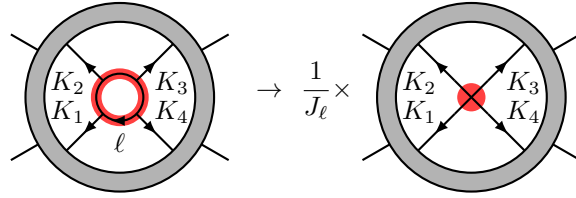


**Figure 1.2.** The left diagram is a generic  $L$ -loop contribution to the four-point  $\mathcal{N} = 4$  sYM amplitude. The thick (red) highlighting indicates propagators replaced by on-shell conditions. After this replacement, the highlighted propagators leave behind the simplified diagram on the right multiplied by an inverse Jacobian, Eq. (1.2.21). The four momenta  $K_1, \dots, K_4$  can correspond either to external legs or propagators of the higher-loop diagram.

ultraviolet finiteness, having poles at infinity does not necessarily mean that there are divergences. For example, the triangle integral contains such a pole in the cut structure but is ultraviolet finite. In principle, there can also be nontrivial cancellations between different contributions.

To find numerators that do not allow these poles at infinity and also ensure only logarithmic singularities, it is not necessary to compute every residue of the integrand. This is because cutting box subdiagrams from a higher loop diagram, as on the left in Fig. 1.2, can only increase the order of remaining poles in the integrand. To see this, consider computing the four residues that correspond to cutting the four highlighted propagators in Fig. 1.2,

$$\ell^2 = (\ell - K_1)^2 = (\ell - K_1 - K_2)^2 = (\ell + K_4)^2 = 0. \quad (1.2.19)$$

This residue is equivalent to computing the Jacobian obtained by replacing the box propagator with on-shell delta functions. This Jacobian is then

$$J_\ell = |\partial P_i / \partial \ell^\mu|, \quad (1.2.20)$$

where the  $P_i$  correspond to the four inverse propagators placed on shell in Eq. (1.2.19). See, for example, Ref. [134] for more details. Another way to obtain this Jacobian is by reading off the rational factors appearing in front of the box integrals—see appendix I of Ref. [131].

For the generic case  $J_\ell$  contains square roots, making it difficult to work with. In special cases it simplifies. For example, for  $K_1 = k_1$  massless, the three-mass normalization is

$$J_\ell = (k_1 + K_2)^2 (K_4 + k_1)^2 - K_2^2 K_4^2. \quad (1.2.21)$$

If in addition  $K_3 = k_3$  is massless (the so called “two-mass-easy” case) then the numerator factorizes into a product of two factors, a feature that is important in many

calculations. This gives,

$$J_\ell = (K_2 + k_1)^2(K_4 + k_1)^2 - K_2^2 K_4^2 = (K_2 \cdot q)(K_2 \cdot \bar{q}), \quad (1.2.22)$$

where  $q = \lambda_1 \tilde{\lambda}_3$  and  $\bar{q} = \lambda_3 \tilde{\lambda}_1$ . If instead both  $K_1 = k_1$  and  $K_2 = k_2$  are massless, we get so called two-mass-hard normalization:

$$J_\ell = (k_1 + k_2)^2(K_3 + k_2)^2. \quad (1.2.23)$$

These formula are useful at higher loops, where the  $K_j$  depend on other loop momenta. These Jacobians go into the denominator of the integrand after a box-cut is applied. It therefore can only raise the order of the remaining poles in the integrand. Our basic approach utilizes this fact: we cut embedded box subdiagrams from diagrams of interest and update the integrand by dividing by the obtained Jacobian (1.2.20). Then we identify all kinematic regions that can result in a double pole in the integrand. It would be cumbersome to write out all cut equations for every such sequence of cuts, so we introduce a compact notation:

$$\text{cut} = \{\dots, (\ell - K_i)^2, \dots, B(\ell), \dots, B(\ell', (\ell' - Q)), \dots\}. \quad (1.2.24)$$

Here:

- Cuts are applied in the order listed.
- A propagator listed by itself, as  $(\ell - K_i)^2$  is, means “Cut just this propagator.”
- $B(\ell)$  means “Cut the four propagators that depend on  $\ell$ .” This exactly corresponds to cutting the box propagators as in Eq. (1.2.19) and Fig. 1.2.
- $B(\ell', (\ell' - Q))$  means “Cut the three standard propagators depending on  $\ell'$ , as well as a fourth  $1/(\ell' - Q)^2$  resulting from a previously obtained Jacobian.” The momentum  $Q$  depends on other momenta besides  $\ell'$ . The four cut propagators form a box.

We use this notation in subsequent sections.

#### 1.2.4 Singularities and maximum transcendental weight

There is an important link between the singularity structure of the integrand and the transcendental weight of an integral, as straightforwardly seen at one loop. If we evaluate the bubble, triangle, and box integrals displayed in Fig. 1.1 in dimensional

regularization [135], through  $\mathcal{O}(\epsilon^0)$  in the dimensional regularization parameter  $\epsilon$ , we have [131, 136]

$$\begin{aligned} I_2 &= \frac{1}{\epsilon} + \log(-s/\mu^2) + 2, \\ I_3 &= \frac{1}{\epsilon^2} - \frac{\log(-s/\mu^2)}{\epsilon} + \frac{\log^2(-s/\mu^2) - \zeta_2}{2}, \\ I_4 &= \frac{4}{\epsilon^2} - 2 \frac{\log(-s/\mu^2) + \log(-t/\mu^2)}{\epsilon} + \log^2(-s/\mu^2) + \log^2(-t/\mu^2) - \log^2(s/t) - 8\zeta_2. \end{aligned} \tag{1.2.25}$$

Here  $\mu$  is the dimensional regularization scale parameter, and the integrals are normalized by an overall multiplicative factor of

$$-i \frac{e^{\gamma\epsilon} (4\pi)^{2-\epsilon}}{(2\pi)^{4-2\epsilon}}, \tag{1.2.26}$$

where  $s, t < 0$ . In the bubble integral the  $1/\epsilon$  singularity originates from the ultraviolet, while in the triangle and box integrals all  $1/\epsilon$  singularities originate from the infrared. Following the usual rules for counting transcendental weight in the normalized expressions of Eq. (1.2.25), we count logarithms and factors of  $1/\epsilon$  to have weight 1 and  $\zeta_2 = \pi^2/6$  to have weight 2. Integers have weight 0. With this counting we see that the bubble integral, which has nonlogarithmic singularities as explained in the previous subsection 1.2.3, is not of uniform transcendental weight, and has maximum weight 1. On the other hand the triangle and box, which both have only logarithmic singularities, are of uniform weight 2.

Building on the one-loop examples, a natural conjecture is that the uniform transcendentality property of integrated expressions noted by Kotikov and Lipatov [91] is directly linked to the appearance of only logarithmic singularities. In fact, experience shows that after integration the  $L$ -loop planar  $\mathcal{N} = 4$  sYM amplitudes have transcendental weight  $2L$ . Various examples are found in Refs. [32, 33, 35, 137]. One of our motivations is to make the connection between logarithmic forms and transcendental functions more precise. It is clearly an important connection that deserves further study.

Recently, Henn et al. observed [123–126] that integrals with uniform transcendental weight lead to simple differential equations. An interesting connection is that the integrands we construct do appear to correspond to integrals of uniform transcendental weight.<sup>2</sup> Here we mainly focus on the particular subset with no poles at infinity, since they are the ones relevant for  $\mathcal{N} = 4$  sYM theory.

---

<sup>2</sup>We thank Johannes Henn for comparisons with his available results showing that after integration our integrands are of uniform transcendental weight.

### 1.3 Strategy for nonplanar amplitudes

As introduced in Sect. 1.2, instead of trying to define a nonplanar global integrand, we subdivide the amplitude into diagrams with their own momentum labels and analyze them one by one. In Ref. [119], the  $\mathcal{N} = 4$  sYM four-point two-loop amplitude was rewritten in a form with no logarithmic singularities and no poles at infinity. In this section, we develop a strategy for doing the same at higher loop orders. We emphasize that we are working at the level of the amplitude integrand prior to integration. In particular we do not allow for any manipulations that involve the integration symbol (e.g. integration-by-parts identities) to shuffle singularities between contributions. Our general procedure has four steps:

1. Define a set of parent diagrams whose propagators are the standard Feynman ones. The parent diagrams are defined to have only cubic vertices and loop momentum flowing through all propagators.
2. Construct *dlog numerators*. These are a basis set of numerators constructed so that each diagram has only logarithmic singularities and no poles at infinity. These numerators also respect diagram symmetries, including color signs. Each *dlog* numerator, together with the diagram propagators, forms a basis diagram.
3. Use simple unitarity cuts to determine the linear combination of basis diagrams that gives the amplitude.
4. Confirm that the amplitude so constructed is correct and complete. We use the method of maximal cuts [138] for this task.

There is no a priori guarantee that this will succeed. In principle, requiring *dlog* numerators could make it impossible to expand the amplitude in terms of independent diagrams with Feynman propagators. Indeed, at a sufficiently high loop order we expect that even in the planar sector it may not be possible to find a covariant diagrammatic representation manifesting the desired properties; in such circumstances we would expect that unwanted singularities cancel between diagrams. This may happen even earlier in the nonplanar sector. As in many amplitude calculations, we simply assume that we can construct a basis with the desired properties, and then, once we have an ansatz, we check that it is correct by computing a complete set of cuts.

In this section, we illustrate the process of finding diagram integrands with the desired properties and explain the steps in some detail. For simplicity, we focus on the four-point amplitude, but we expect that a similar strategy is applicable for higher-point amplitudes in the MHV and NMHV sectors as well.

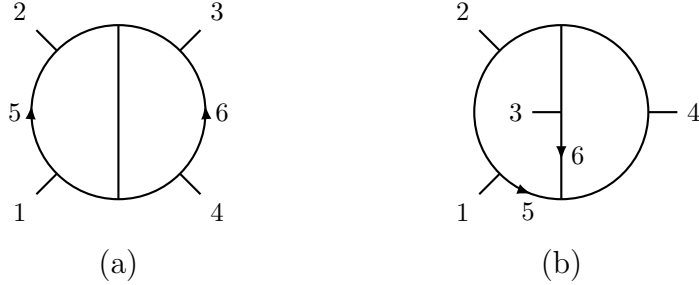


**Figure 1.3.** Two-loop four-point parent diagrams for  $\mathcal{N} = 4$  sYM theory.

We use the one- and two-loop contributions to the four-point amplitudes to illustrate the procedure, before turning to three loops in Sect. 1.4. We find that the canonical one-loop numerator is already a  $d\log$  numerator, while the two-loop result illustrates the issues that we face at higher loops. The two-loop amplitude was first obtained in [120], but in a form that does not make clear the singularity structure. In Ref. [119], the two-loop amplitude was rewritten in a form that makes these properties manifest by rearranging contact terms in the amplitude by using the color-Jacobi identity. In this section we replicate this result by following our strategy of systematically constructing a basis of integrands with the desired properties. In subsequent sections we apply our strategy to higher loops.

### 1.3.1 Constructing a basis

The construction of a basis of integrands starts from a set of parent diagrams. As mentioned in the introduction to Sect. 1.2, we focus on graphs with only cubic vertices. Furthermore we restrict to diagrams that do not have triangle or bubble subdiagrams, since these are not necessary for  $\mathcal{N} = 4$  amplitudes that we study. We also exclude any diagrams in which a propagator does not carry loop momentum, because such contributions can be absorbed into diagrams in which all propagators contain loop momenta. At the end, we confirm this basis of diagrams is sufficient by verifying a set of unitarity cuts that fully determine the amplitude.

At one loop the parent diagrams are the three independent box integrals, one of which is displayed in Fig. 1.1(c), and the other two of which are cyclic permutations of the external legs  $k_2$ ,  $k_3$  and  $k_4$  of this one. At two loops the four-point amplitude of  $\mathcal{N} = 4$  sYM theory has twelve parent diagrams, two of which are displayed in Fig. 1.3; the others are again just given by relabelings of external legs.

Unlike the planar case, there is no global, canonical way to label loop momenta in all diagrams. In each parent diagram, we label  $L$  independent loop momenta as  $\ell_5, \dots, \ell_{4+L}$ .

By conserving momentum at each vertex, all other propagators have sums of the loop and external momenta flowing in them. We define the  $L$ -loop *integrand*,  $\mathcal{I}^{(x)}$ , of a diagram labeled by  $(x)$  by combining the kinematic part of the numerator with the Feynman propagators of the diagram as

$$\mathcal{I}^{(x)} \equiv \frac{N^{(x)}}{\prod_{\alpha(x)} p_{\alpha(x)}^2}. \quad (1.3.1)$$

The product in the denominator in Eq. (1.3.1) runs over all propagators  $p_{\alpha(x)}^2$  of diagram  $(x)$ , and the kinematic numerator  $N^{(x)}$  generally depends on loop momenta. From this we define an *integrand form*

$$d\mathcal{I}^{(x)} \equiv \prod_{l=5}^{4+L} d^4 \ell_l \mathcal{I}^{(x)}. \quad (1.3.2)$$

This integrand form is a  $4L$  form in the  $L$  independent loop momenta  $\ell_5, \dots, \ell_{4+L}$ . We have passed factors of  $i$ ,  $2\pi$ , and coupling constants into the definition of the amplitude, Eq. (1.3.21). As mentioned previously, we focus on  $D = 4$ .

We define an expansion of the numerator

$$N^{(x)} = \sum_i a_i^{(x)} N_i^{(x)}, \quad (1.3.3)$$

where the  $N_i^{(x)}$  are the  $d\log$  numerators we aim to construct, and the  $a_i^{(x)}$  are coefficients. We put off a detailed discussion of how to fix these coefficients until subsection 1.3.2, and here just mention that the coefficients can be obtained by matching an expansion of the amplitude in  $d\log$  numerators to unitarity cuts or other physical constraints, such as leading singularities.

Starting from a generic numerator  $N_i^{(x)}$ , we impose the following constraints:

- *Overall dimensionality.*  $N_i^{(x)}$  must be a local polynomial of momentum invariants (i.e.  $k_a \cdot k_b$ ,  $k_a \cdot \ell_b$ , or  $\ell_a \cdot \ell_b$ ) with dimensionality  $N_i^{(x)} \sim (p^2)^K$ , where  $K = P - 2L - 2$ , and  $P$  is the number of propagators in the integrand. We forbid numerators with  $K < 0$ .
- *Asymptotic scaling.* For each loop momentum  $\ell_l$ , the integrand  $\mathcal{I}^{(x)}$  must not scale less than  $1/(\ell_l^2)^4$  for  $\ell_l \rightarrow \infty$  in all possible labellings.
- *No double/higher poles.* The integrand  $\mathcal{I}^{(x)}$  must be free of poles of order two or more in all kinematic regions.
- *No poles at infinity.* The integrand  $\mathcal{I}^{(x)}$  must be free of poles of any order at infinity in all kinematic regions.

The overall dimensionality and asymptotic scaling give us power counting constraints on the subdiagrams. In practice, these two constraints dictate the initial form of an ansatz for the numerator, while the last two conditions of no higher degree poles and no poles at infinity constrain that ansatz to select “ $d\log$  numerators”. The constraint on overall dimensionality is the requirement that the overall mass dimension of the integrand is  $-4L - 4$ ;<sup>3</sup> in  $D = 4$  this matches the dimensionality of gauge-theory integrands. The asymptotic scaling constraint includes a generalization of the absence of bubble and triangle integrals at one-loop order in  $\mathcal{N} = 4$  sYM theory and  $\mathcal{N} = 8$  supergravity [139, 140]. This constraint is a necessary, but not a sufficient, condition for having only logarithmic singularities and no poles at infinity.

At one loop, the asymptotic scaling constraint implies that only the box diagram, Fig. 1.1(c), appears; coupling that with the overall dimensionality constraint implies that the numerator is independent of loop momentum. The box numerator must then be a single basis element which we can normalize to be unity:

$$N_1^{(\text{B})} = 1. \quad (1.3.4)$$

In the one-loop integrand, neither higher degree poles nor poles at infinity arise. Thus everything at one loop is consistent and manifestly exhibits only logarithmic singularities. A more thorough treatment of the one-loop box, including the sense in which logarithmic singularities are manifest in a box, is found in the context of  $d\log$  forms in subsection 1.5.1

Next consider two loops. Here the asymptotic scaling constraint implies that only the planar and nonplanar double box diagrams in Fig. 1.3 appear, since the constraint forbids triangle or bubble subdiagrams. We now wish to construct the numerators  $N^{(\text{P})}$  and  $N^{(\text{NP})}$  for the planar (Fig. 1.3(a)) and nonplanar (Fig. 1.3(b)) diagrams, respectively. There are different ways of labeling the two graphs. As already mentioned, we prefer labels in Fig. 1.3, where the individual loop momenta appear in the fewest possible number of propagators. This leads to the tightest power counting constraints in the sense of our general strategy outlined above. We consider the planar and nonplanar diagrams separately.

For the planar diagram in Fig. 1.3, only four propagators contain either loop momentum  $\ell_5$  or  $\ell_6$ . By the asymptotic scaling constraint, the numerator must be independent of both loop momenta:  $N^{(\text{P})} \sim \mathcal{O}((\ell_5)^0, (\ell_6)^0)$ . Since overall dimensionality restricts  $N^{(\text{P})}$  to be quadratic in momentum, we can write down two independent numerator basis elements:

$$N_1^{(\text{P})} = s, \quad N_2^{(\text{P})} = t. \quad (1.3.5)$$

---

<sup>3</sup> The  $-4$  in the mass dimension originates from factoring out a dimensionful quantity from the final amplitude in Eq. (1.3.21).



The resulting numerator is then a linear combination of these two basis elements:

$$N^{(\text{P})} = a_1^{(\text{P})} s + a_2^{(\text{P})} t, \quad (1.3.6)$$

where the  $a_j^{(\text{P})}$  are constants, labeled as discussed after Eq. (1.3.3). Again, as in the one-loop case, there are no hidden double poles or poles at infinity from which nontrivial constraints could arise.

The nonplanar two-loop integrand  $\mathcal{I}^{(\text{NP})}$  is the first instance where nontrivial constraints result from requiring logarithmic singularities and the absence of poles at infinity, so we discuss this example in more detail. The choice of labels in Fig. 1.3(b) results in five propagators with momentum  $\ell_5$  but only four with momentum  $\ell_6$ , so  $N^{(\text{NP})}$  is at most quadratic in  $\ell_5$  and independent of  $\ell_6$ :  $N^{(\text{NP})} \sim \mathcal{O}((\ell_5)^2, (\ell_6)^0)$ . Overall dimensionality again restricts  $N^{(\text{NP})}$  to be quadratic in momentum. This dictates the form of the numerator to be

$$N^{(\text{NP})} = c_1 \ell_5^2 + c_2 (\ell_5 \cdot Q) + c_3 s + c_4 t, \quad (1.3.7)$$

where  $Q$  is some vector and the  $c_i$  are coefficients independent of loop momenta.

Now we search the integrand

$$\mathcal{I}^{(\text{NP})} = \frac{c_1 \ell_5^2 + c_2 (\ell_5 \cdot Q) + c_3 s + c_4 t}{\ell_5^2 (\ell_5 + k_1)^2 (\ell_5 - k_3 - k_4)^2 \ell_6^2 (\ell_5 + \ell_6)^2 (\ell_5 + \ell_6 - k_4)^2 (\ell_6 + k_3)^2} \quad (1.3.8)$$

for double poles as well as poles at infinity, and impose conditions on the  $c_i$  and  $Q$  such that any such poles vanish. For the nonplanar double box, we apply this cut on the four propagators carrying momentum  $\ell_6$ ,

$$\ell_6^2 = (\ell_5 + \ell_6)^2 = (\ell_5 + \ell_6 - k_4)^2 = (\ell_6 + k_3)^2 = 0. \quad (1.3.9)$$

The Jacobian for this cut is

$$J_6 = (\ell_5 - k_3)^2 (\ell_5 - k_4)^2 - (\ell_5 - k_3 - k_4)^2 \ell_5^2 = (\ell_5 \cdot q) (\ell_5 \cdot \bar{q}), \quad (1.3.10)$$

where  $q = \lambda_3 \tilde{\lambda}_4$ ,  $\bar{q} = \lambda_4 \tilde{\lambda}_3$ .

After imposing the quadruple cut conditions in Eq. (1.3.9) the remaining integrand, including the Jacobian (1.3.10), is

$$\text{Res}_{\ell_6\text{-cut}} [\mathcal{I}^{(\text{NP})}] \equiv \tilde{\mathcal{I}}^{(\text{NP})} = \frac{c_1 \ell_5^2 + c_2 (\ell_5 \cdot Q) + c_3 s + c_4 t}{\ell_5^2 (\ell_5 + k_1)^2 (\ell_5 - k_3 - k_4)^2 (\ell_5 \cdot q) (\ell_5 \cdot \bar{q})}, \quad (1.3.11)$$

where the integrand evaluated on the cut is denoted by a new symbol  $\tilde{\mathcal{I}}^{(\text{NP})}$  for brevity. To make the potentially problematic singularities visible, we parametrize the four-dimensional part of the remaining loop momentum as

$$\ell_5 = \alpha \lambda_3 \tilde{\lambda}_3 + \beta \lambda_4 \tilde{\lambda}_4 + \gamma \lambda_3 \tilde{\lambda}_4 + \delta \lambda_4 \tilde{\lambda}_3. \quad (1.3.12)$$

This gives us

$$\begin{aligned} \tilde{\mathcal{I}}^{(\text{NP})} = & \left( c_1(\alpha\beta - \gamma\delta)s + c_2 [\alpha(Q \cdot k_3) + \beta(Q \cdot k_4) + \gamma\langle 3|Q|4\rangle + \delta\langle 4|Q|3\rangle] + c_3s + c_4t \right) \\ & \times \left[ s^2(\alpha\beta - \gamma\delta)(\alpha\beta - \gamma\delta - \alpha - \beta + 1) \right. \\ & \left. \times \left( (\alpha\beta - \gamma\delta)s + \alpha u + \beta t - \gamma\langle 13\rangle[14] - \delta\langle 14\rangle[13] \right) \gamma\delta \right]^{-1}, \end{aligned} \quad (1.3.13)$$

where we use the convention  $2k_i \cdot k_j = \langle ij\rangle[ij]$  and  $\langle i|k_m|j\rangle \equiv \langle im\rangle[mj]$ . Our goal is to identify double- or higher-order poles. To expose these, we take residues in a certain order. For example, taking consecutive residues at  $\gamma = 0$  and  $\delta = 0$  followed by  $\beta = 0$  gives

$$\text{Res}_{\substack{\gamma=\delta=0 \\ \beta=0}} \left[ \tilde{\mathcal{I}}^{(\text{NP})} \right] = \frac{c_2\alpha(Q \cdot k_3) + c_3s + c_4t}{s^2u\alpha^2(1-\alpha)}. \quad (1.3.14)$$

Similarly taking consecutive residues first at  $\gamma = \delta = 0$  followed by  $\beta = 1$ , we get

$$\text{Res}_{\substack{\gamma=\delta=0 \\ \beta=1}} \left[ \tilde{\mathcal{I}}^{(\text{NP})} \right] = -\frac{c_1\alpha s + c_2 [\alpha(Q \cdot k_3) + (Q \cdot k_4)] + c_3s + c_4t}{s^2t\alpha(1-\alpha)^2}. \quad (1.3.15)$$

In both cases we see that there are unwanted double poles in  $\alpha$ . The absence of double poles forces us to choose the  $c_i$  in the numerator such that the integrand reduces to at most a single pole in  $\alpha$ . Canceling the double pole at  $\alpha = 0$  in Eq. (1.3.14) requires  $c_3 = c_4 = 0$ . Similarly, the second residue in Eq. (1.3.15) enforces  $c_1s + c_2(Q \cdot (k_3 + k_4)) = 0$  to cancel the double pole at  $\alpha = 1$ . The solution that ensures  $N^{(\text{NP})}$  is a  $d\log$  numerator is

$$N^{(\text{NP})} = \frac{c_1}{s} [\ell_5^2(Q \cdot (k_3 + k_4)) - (k_3 + k_4)^2(\ell_5 \cdot Q)]. \quad (1.3.16)$$

The integrand is now free of the uncovered double poles, but requiring the absence of poles at infinity imposes further constraints on the numerator. If any of the parameters  $\alpha$ ,  $\beta$ ,  $\gamma$ , or  $\delta$  grow large, the loop momentum  $\ell_5$  Eq. (1.3.12) also becomes large. Indeed, such a pole can be accessed by first taking the residue at  $\delta = 0$ , followed by taking the residues at  $\alpha = 0$  and  $\beta = 0$ :

$$\text{Res}_{\substack{\delta=0 \\ \alpha=\beta=0}} \left[ \tilde{\mathcal{I}}^{(\text{NP})} \right] = \frac{\langle 3|Q|4\rangle}{\gamma s^2 \langle 13\rangle [14]}. \quad (1.3.17)$$

The resulting form  $d\gamma/\gamma$  has a pole for  $\gamma \rightarrow \infty$ . Similarly, taking a residue at  $\gamma = 0$ , followed by residues at  $\alpha = 0$  and  $\beta = 0$ , results in a single pole for  $\delta \rightarrow \infty$ . To prevent such poles at infinity from appearing requires  $\langle 3|Q|4\rangle = \langle 4|Q|3\rangle = 0$ , which in turn requires that  $Q = \sigma_1 k_3 + \sigma_2 k_4$  with the  $\sigma_i$  arbitrary constants. This is enough to determine the numerator up to two arbitrary coefficients.

As an exercise in the notation outlined in the beginning of the section, as well as to illustrate a second approach, we could also consider the cut sequence  $\{B(\ell_6)\}$ , following the notation defined at the end of Sect. 1.2.3. The resulting Jacobian is

$$J_6 = (\ell_5 - k_4)^2(\ell_5 - k_3)^2 - (\ell_5 + k_1 + k_2)^2\ell_5^2. \quad (1.3.18)$$

The two terms on the right already appear as propagators in the integrand, and so to avoid double poles, the  $d\log$  numerator must scale as  $N^{(\text{NP})} \sim (\ell_5 + k_1 + k_2)^2\ell_5^2$  in the kinematic regions where  $(\ell_5 - k_4)^2(\ell_5 - k_3)^2 = 0$ . This constraint is sufficient to fix the ansatz Eq. (1.3.7) for  $N^{(\text{NP})}$ .

In both approaches, the constraints of having only logarithmic singularities and no poles at infinity results in a numerator for the nonplanar double box of the form,

$$N^{(\text{NP})} = a_1^{(\text{NP})}(\ell_5 - k_3)^2 + a_2^{(\text{NP})}(\ell_5 - k_4)^2, \quad (1.3.19)$$

where  $a_1^{(\text{NP})}$  and  $a_2^{(\text{NP})}$  are numerical coefficients. Finally, we impose that the numerator should respect the symmetries of the diagram. Because the nonplanar double box is symmetric under  $k_3 \leftrightarrow k_4$  this forces  $a_2^{(\text{NP})} = a_1^{(\text{NP})}$ , resulting in a unique numerator up to an overall constant

$$N_1^{(\text{NP})} = (\ell_5 - k_3)^2 + (\ell_5 - k_4)^2. \quad (1.3.20)$$

### 1.3.2 Expansion of the amplitude

In the previous subsection we outlined a procedure to construct a basis of integrands where each element has only logarithmic singularities and no pole at infinity. The next step is to actually expand the amplitude in terms of this basis. As mentioned before, we primarily focus on the  $L$ -loop contribution to the  $\mathcal{N} = 4$  sYM theory, four-point amplitudes. Following the normalization conventions of Ref. [129], these can be written in a diagrammatic representation

$$\mathcal{A}_4^{L\text{-loop}} = g^{2+2L} \frac{i^L \mathcal{K}}{(2\pi)^{DL}} \sum_{\mathcal{S}_4} \sum_x \frac{1}{S^{(x)}} c^{(x)} \int d\mathcal{I}^{(x)}(\ell_5, \dots, \ell_{4+L}), \quad (1.3.21)$$

where  $d\mathcal{I}^{(x)}$  is the integrand form defined in Eq. (1.3.2), and we have implicitly analytically continued the expression to  $D$  dimensions to be consistent with dimensional regularization. In Eq. (1.3.21) the sum labeled by  $x$  runs over the set of distinct, non-isomorphic diagrams with only cubic vertices, and the sum over  $\mathcal{S}_4$  is over all 4! permutations of external legs. The symmetry factor  $S^{(x)}$  then removes overcounting that arises from automorphisms of the diagrams. The color factor  $c^{(x)}$  of diagram  $(x)$  is given by dressing every three-vertex with a group-theory structure constant,

$\tilde{f}^{abc} = i\sqrt{2}f^{abc}$ . In the sum over permutations in Eq. (1.3.21), any given  $d\mathcal{I}^{(x')}$  is a momentum relabeling of  $d\mathcal{I}^{(x)}$  in Eq. (1.3.2).

For the cases we consider, the prefactor is proportional to the color-ordered tree amplitude,

$$\mathcal{K} = stA_4^{\text{tree}}(1, 2, 3, 4). \quad (1.3.22)$$

Furthermore,  $\mathcal{K}$  has a crossing symmetry so it can also be expressed in terms of the tree amplitude with different color orderings,

$$\mathcal{K} = suA_4^{\text{tree}}(1, 2, 4, 3) = tuA_4^{\text{tree}}(1, 3, 2, 4). \quad (1.3.23)$$

The explicit values of the tree amplitudes are

$$A_4^{\text{tree}}(1, 2, 3, 4) = i \frac{\delta^8(\mathcal{Q})}{\langle 12 \rangle \langle 23 \rangle \langle 34 \rangle \langle 41 \rangle}, \quad (1.3.24)$$

where the other two orderings are just relabelings of the first. The factor  $\delta^8(\mathcal{Q})$  is the supermomentum conservation  $\delta$  function, as described in e.g. Ref. [13]. The details of this factor are not important for our discussion. For external gluons with helicities  $1^-, 2^-, 3^+, 4^+$  it is just  $\langle 12 \rangle^4$ , up to Grassmann parameters.

A simple method for expanding the amplitude in terms of  $d\log$  numerators is to use previously constructed representations of the amplitude as reference data, rather than sew together lower-loop amplitudes directly. Especially at higher loops, this drastically simplifies the process of determining the coefficients  $a_i^{(x)}$ . To ensure that the constructed amplitude is complete and correct, we also check a complete set of unitarity cuts via the method of maximal cuts [141].

As an illustration of the procedure for determining the coefficients, consider the two-loop amplitude. A representation of the two-loop four-point amplitude is [120] Eqs. (1.3.21) and (1.3.3) with numerators

$$N_{\text{old}}^{(\text{P})} = s, \quad N_{\text{old}}^{(\text{NP})} = s, \quad (1.3.25)$$

where we follow the normalization conventions of Ref. [129]. Following our strategy, we demand that the numerators are linear combinations of the basis elements constructed in Eqs. (1.3.6) and (1.3.19):

$$N^{(\text{P})} = a_1^{(\text{P})}s + a_2^{(\text{P})}t, \quad N^{(\text{NP})} = a^{(\text{NP})}((\ell_5 - k_3)^2 + (\ell_5 - k_4)^2), \quad (1.3.26)$$

where, for comparison to  $N_{\text{old}}^{(\text{NP})}$ , it is useful to rewrite the nonplanar numerator as

$$N^{(\text{NP})} = a^{(\text{NP})}(-s + (\ell_5 - k_3 - k_4)^2 + \ell_5^2). \quad (1.3.27)$$

We can determine the coefficients by comparing the new and old expressions on the maximal cuts. By maximal cuts we mean replacing all propagators with on-shell conditions,  $p_{\alpha(x)}^2 = 0$ , defined in Eq. (1.3.1). The planar double-box numerator is unchanged on the maximal cut, since it is independent of all loop momenta. Comparing the two expressions in Eqs. (1.3.25) and (1.3.26) gives

$$a_1^{(\text{P})} = 1, \quad a_2^{(\text{P})} = 0. \quad (1.3.28)$$

For the nonplanar numerator we note that under the maximal cut conditions  $\ell_5^2 = (\ell_5 - k_3 - k_4)^2 = 0$ . Comparing the two forms of the nonplanar numerator in Eqs. (1.3.25) and (1.3.27) after imposing these conditions means

$$a_1^{(\text{NP})} = -1, \quad (1.3.29)$$

so that the final numerators are

$$N^{(\text{P})} = s, \quad N^{(\text{NP})} = -((\ell_5 - k_3)^2 + (\ell_5 - k_4)^2). \quad (1.3.30)$$

Although this fixes all coefficients in our basis, it does not prove that our construction gives the correct sYM amplitude. At two loops this was already proven in Ref. [119], where the difference between amplitudes in the old and the new representation was shown to vanish via the color Jacobi identity. More generally, we can appeal to the method of maximal cuts since it offers a systematic and complete means of ensuring that our constructed nonplanar amplitudes are correct.

### 1.3.3 Amplitudes and sums of $d\log$ forms

At any loop order, assuming the four-point  $\mathcal{N} = 4$  sYM amplitudes have only logarithmic singularities then we can write integrand forms as a sum of  $d\log$  forms. At the relatively low loop orders that we are working, we can do this diagram by diagram, using the expansion of the diagrams given in Eq. (1.3.21). We then take each diagram form in Eq. (1.3.21) and expand it as a linear combination of  $d\log$  forms,

$$d\mathcal{I}^{(x)} = \sum_{j=1}^3 C_j d\mathcal{I}_j^{(x), d\log}, \quad (1.3.31)$$

where the  $d\mathcal{I}_j^{(x), d\log}$  are (potentially sums of)  $d\log$   $4L$  forms. As discussed in Ref. [112], for MHV amplitudes the coefficients  $C_j$  are Park-Taylor factors with different orderings. This follows from super-conformal symmetry of  $\mathcal{N} = 4$  sYM theory, which fixes the coefficients  $C_j$  to be holomorphic functions of spinor variables  $\lambda$  and normalizes  $d\mathcal{I}^{(x)}$

to be a  $d\log$  form. In the four-point nonplanar case this means that there are only three different coefficients we can get,

$$C_1 = A_4^{\text{tree}}(1, 2, 3, 4), \quad C_2 = A_4^{\text{tree}}(1, 2, 4, 3), \quad C_3 = A_4^{\text{tree}}(1, 3, 2, 4), \quad (1.3.32)$$

where the explicit form of the tree amplitudes are given in Eq. (1.3.24). The three coefficient are not independent, as they satisfy  $C_1 + C_2 + C_3 = 0$ . Suppose that the basis elements in Eq. (1.3.21) are chosen such that they have only logarithmic singularities. We will show, in Sect. 1.5, that we can indeed write the diagram as  $d\log$  forms with coefficients given by the  $C_j$ .

## 1.4 Three-loop amplitude

In this section we follow the recipe of the previous section to find a basis of three-loop diagram integrands that have only logarithmic singularities and no poles at infinity. The three-loop four-point parent diagrams are shown in Fig. 1.4. These have been classified in Ref. [122, 128], where an unintegrated representation of the three-loop four-point amplitude of  $\mathcal{N} = 4$  sYM theory including nonplanar contributions was first obtained. As mentioned in Sect. 1.3.1, we restrict to parent diagrams where no bubble or triangle diagrams appear as subdiagrams; otherwise we would find a pole at infinity that cannot be removed. Diagrams with contact terms can be incorporated into a parent diagram by including inverse propagators in the numerator that cancel propagators.

Next we assign power counting of the numerator for each parent diagram. Applying the power-counting rules in Sect. 1.3.1, we find that the maximum powers of allowed loop momenta for each parent diagram are

$$\begin{aligned} N^{(a)} &= \mathcal{O}(1), & N^{(b)} &= \mathcal{O}(\ell_6^2), & N^{(c)} &= \mathcal{O}(\ell_5^2, (\ell_5 \cdot \ell_7), \ell_7^2), \\ N^{(d)} &= \mathcal{O}(\ell_6^4), & N^{(e)} &= \mathcal{O}(\ell_5^2), & N^{(f)} &= \mathcal{O}(\ell_5^4), & N^{(g)} &= \mathcal{O}(\ell_5^2 \ell_6^2), \\ N^{(h)} &= \mathcal{O}(\ell_5^2 \ell_6^2, \ell_5^2 \ell_7^2, \ell_5^2 (\ell_6 \cdot \ell_7)), & N^{(i)} &= \mathcal{O}(\ell_5^2 \ell_6^2), \end{aligned} \quad (1.4.1)$$

where we use the labels in Fig. 1.4, since these give the most stringent power counts. For diagram (h) we need to combine restrictions from a variety of labellings to arrive at this stringent power count. Ignoring the overall prefactor of  $\mathcal{K}$ , the overall dimension of each numerator is  $\mathcal{O}(p^4)$ , including external momenta.

### 1.4.1 Diagram numerators

The next step is to write down the most general diagram numerators that are consistent with the power count in Eq. (1.4.1), respect diagram symmetry, are built only from

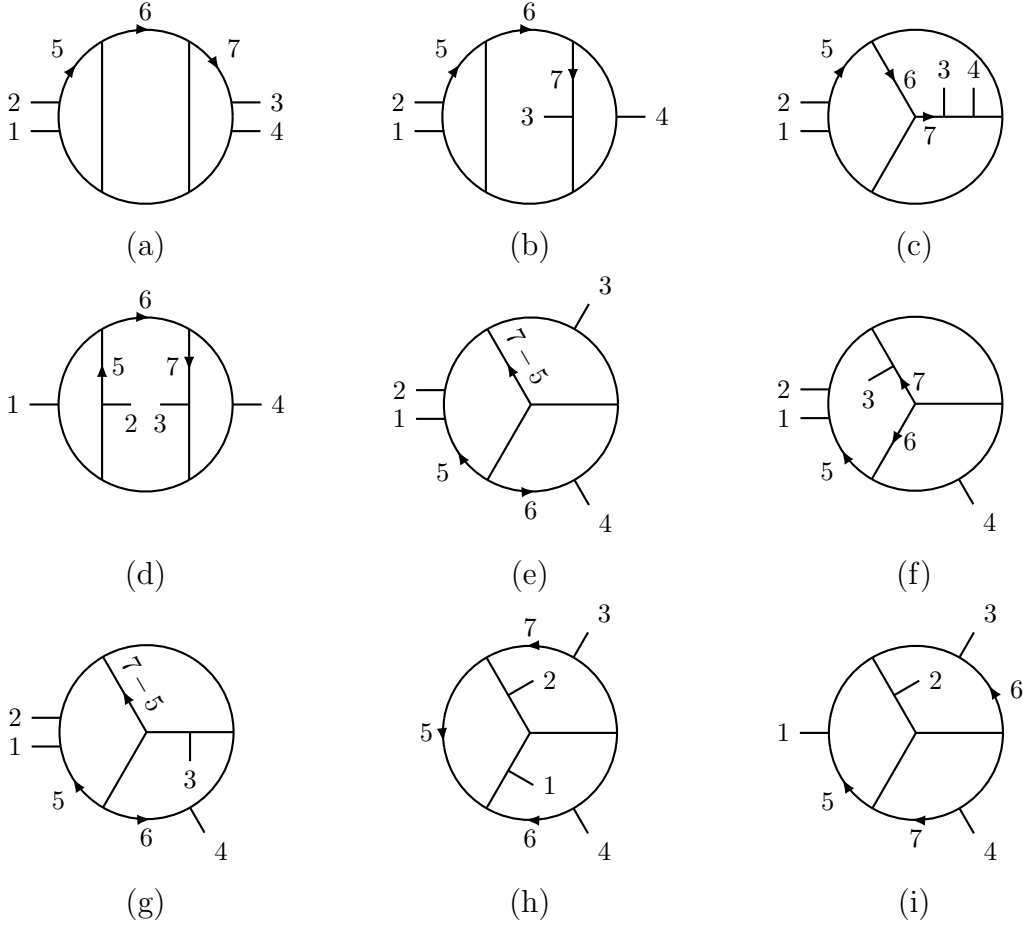


**Figure 1.4.** The distinct parent diagrams for three-loop four-point amplitudes. The remaining parent diagrams are obtained by relabeling external legs.

Lorentz dot products of the loop and external momenta, have only logarithmic singularities, and have no poles at infinity. Although the construction is straightforward, the complete list of conditions is lengthy, so here we only present a few examples and then write down a table of numerators satisfying the constraints.

We start with diagram (a) in Fig. 1.4. The required numerators are simple to write down if we follow the same logic as in the two-loop example in Sect. 1.3.1. Since the numerator of diagram (a) is independent of all loop momenta as noted in Eq. (1.4.1), we can only write numerators that depend on the Mandelstam invariants  $s$  and  $t$ . There are three numerators that are consistent with the overall dimension:

$$N_1^{(a)} = s^2, \quad N_2^{(a)} = st, \quad N_3^{(a)} = t^2. \quad (1.4.2)$$

Following similar logic as at two loops, it is straightforward to check that there are no double poles or poles at infinity.

The numerator for diagram (b) is also easy to obtain, this time by following the logic of the two-loop nonplanar diagram. From Eq. (1.4.1), we see that the only momentum dependence of the numerator must be on  $\ell_6$ . The two-loop subdiagram on the right side of diagram (b) in Fig. 1.4 containing  $\ell_6$  is just the two-loop nonplanar double box we already analyzed in Sect. 1.3.1. Repeating the earlier nonplanar box procedure for this subdiagram gives us the most general possible numerator for diagram (b):

$$N_1^{(b)} = s((\ell_6 - k_3)^2 + (\ell_6 - k_4)^2). \quad (1.4.3)$$

This is just the two-loop nonplanar numerator with an extra factor of  $s$ . A factor of  $t$  instead of  $s$  is disallowed because it violates the  $k_3 \leftrightarrow k_4$  symmetry of diagram (b).

As a somewhat more complicated example, consider diagram (e) in Fig. 1.4. Because this diagram is planar we could use dual conformal invariance to find the desired numerator. Instead, for illustrative purposes we choose to obtain it only from the requirements of having logarithmic singularities and no pole at infinity, without invoking dual conformal invariance. We discuss the relation to dual conformal symmetry further in Sect. 1.7.

From Eq. (1.4.1) we see that the numerator depends on the loop momentum  $\ell_5$  at most quadratically. Therefore we may start with the ansatz

$$N^{(e)} = (c_1 s + c_2 t)(\ell_5^2 + d_1(\ell_5 \cdot Q) + d_2 s + d_3 t), \quad (1.4.4)$$

where  $Q$  is a vector independent of all loop momenta and the  $c_i$  and  $d_i$  are numerical constants. We have included an overall factor depending on  $s$  and  $t$  so that the numerator has the correct overall dimensions, but this factor does not play a role in canceling unwanted singularities of the integrand.

In order to extract conditions on the numerator ansatz Eq. (1.4.4), we need to find any hidden double poles or poles at infinity in the integrand. The starting integrand is

$$\begin{aligned} \mathcal{I}^{(e)} &= \frac{N^{(e)}}{\ell_6^2(\ell_6 + \ell_5)^2(\ell_6 + \ell_7)^2(\ell_6 + k_4)^2(\ell_7 - \ell_5)^2(\ell_7 - k_1 - k_2)^2(\ell_7 + k_4)^2} \\ &\quad \times \frac{1}{\ell_5^2(\ell_5 - k_1)^2(\ell_5 - k_1 - k_2)^2}. \end{aligned} \quad (1.4.5)$$

Since our numerator ansatz (1.4.4) is a function of  $\ell_5$ , we seek double poles only in the regions of momentum space that we can reach by choosing convenient on-shell values for  $\ell_6$  and  $\ell_7$ . This leaves the numerator ansatz unaltered, making it straightforward to determine all coefficients.



To locate a double pole, consider the cut sequence

$$\text{cut} = \{B(\ell_6), B(\ell_7, \ell_7)\}, \quad (1.4.6)$$

where we follow the notation defined at the end of Sect. 1.2.3. Here  $B(\ell_7, \ell_7)$  indicates that we cut the  $1/\ell_7^2$  propagator produced by the  $B(\ell_6)$  cut. This produces an overall Jacobian

$$J_{6,7} = s [(\ell_5 + k_4)^2]^2. \quad (1.4.7)$$

After this sequence of cuts, the integrand of Eq. (1.4.5) becomes:

$$\text{Res}_{\substack{\ell_6\text{-cut} \\ \ell_7\text{-cut}}} [\mathcal{I}^{(e)}] = \frac{N^{(e)}}{\ell_5^2 (\ell_5 - k_1)^2 (\ell_5 - k_1 - k_2)^2 [(\ell_5 + k_4)^2]^2 s}, \quad (1.4.8)$$

exposing a double pole at  $(\ell_5 + k_4)^2 = 0$ .

To impose our desired constraints on the integrand, we need to cancel the double pole in the denominator with an appropriate numerator. We see that choosing the ansatz in Eq. (1.4.4) to have  $Q = k_4$ ,  $d_1 = 2$ ,  $d_2 = 0$ , and  $d_3 = 0$  gives us the final form of the allowed numerator,

$$N^{(e)} = (c_1 s + c_2 t) (\ell_5 + k_4)^2, \quad (1.4.9)$$

so we have two basis numerators,

$$N_1^{(e)} = s (\ell_5 + k_4)^2, \quad N_2^{(e)} = t (\ell_5 + k_4)^2. \quad (1.4.10)$$

We have also checked that this numerator passes all other double-pole constraints coming from different regions of momentum space. In addition, we have checked that it has no poles at infinity. It is interesting that, up to a factor depending only on external momenta, these are precisely the numerators consistent with dual conformal symmetry. As we discuss in Sect. 1.7, this is no accident.

Next consider diagram (d) in Fig. 1.4. From the power counting arguments summarized in Eq. (1.4.1), we see that the numerator for this diagram is a quartic function of momentum  $\ell_6$ , but that it depends on neither  $\ell_5$  nor  $\ell_7$ . When constructing numerators algorithmically we begin with a general ansatz, but to more easily illustrate the role of contact terms we start from the natural guess that diagram (d) is closely related to a product of two two-loop nonplanar double boxes. Thus our initial guess is that the desired numerator is the product of numerators corresponding to the two-loop nonplanar subdiagrams:

$$\tilde{N}^{(d)} = [(\ell_6 + k_1)^2 + (\ell_6 + k_2)^2] [(\ell_6 - k_3)^2 + (\ell_6 - k_4)^2]. \quad (1.4.11)$$

We label this numerator  $\tilde{N}^{(d)}$  because, as we see below, it is not quite the numerator  $N^{(d)}$  that satisfies our pole constraints. As always, note that we have required the numerator to satisfy the symmetries of the diagram.

Although we do not do so here, one can show that this ansatz satisfies nearly all constraints on double poles and poles at infinity. The double pole not removed by the numerator is in the kinematic region:

$$\text{cut} = \{\ell_5^2, (\ell_5 + k_2)^2, \ell_7^2, (\ell_7 - k_3)^2, B(\ell_6)\}. \quad (1.4.12)$$

Before imposing the final box cut, we solve the first four cut conditions in terms of two parameters  $\alpha$  and  $\beta$ :

$$\ell_5 = \alpha k_2, \quad \ell_7 = -\beta k_3. \quad (1.4.13)$$

The final  $B(\ell_6)$  represents a box-cut of four of the six remaining propagators that depend on  $\alpha$  and  $\beta$ :

$$(\ell_6 - \alpha k_2)^2 = (\ell_6 - \alpha k_2 + k_1)^2 = (\ell_6 + \beta k_3)^2 = (\ell_6 + \beta k_3 - k_4)^2 = 0. \quad (1.4.14)$$

Before cutting the  $B(\ell_6)$  propagators, the integrand is

$$\text{Res}_{\substack{\ell_5\text{-cut} \\ \ell_7\text{-cut}}} \tilde{\mathcal{I}}^{(d)} = \frac{\tilde{N}^{(d)}}{\ell_6^2 (\ell_6 + k_1 + k_2)^2 (\ell_6 - \alpha k_2)^2 (\ell_6 - \alpha k_2 + k_1)^2 (\ell_6 + \beta k_3)^2 (\ell_6 + \beta k_3 - k_4)^2}. \quad (1.4.15)$$

Localizing further to the  $B(\ell_6)$  cuts produces a Jacobian

$$J_6 = su(\alpha - \beta)^2, \quad (1.4.16)$$

while a solution to the box-cut conditions of Eq. (1.4.14),

$$\ell_6^* = \alpha \lambda_4 \tilde{\lambda}_2 \frac{\langle 12 \rangle}{\langle 14 \rangle} - \beta \lambda_1 \tilde{\lambda}_3 \frac{\langle 34 \rangle}{\langle 14 \rangle}, \quad (1.4.17)$$

turns the remaining uncut propagators of Eq. (1.4.15) into

$$\ell_6^2 = s\alpha\beta, \quad (\ell_6 + k_1 + k_2)^2 = s(1 + \alpha)(1 + \beta). \quad (1.4.18)$$

The result of completely localizing all momenta in this way is

$$\text{Res}_{\text{cuts}} \tilde{\mathcal{I}}^{(d)} = -\frac{s^2(\alpha(1 + \beta) + \beta(1 + \alpha))^2}{s^3 u \alpha \beta (1 + \alpha)(1 + \beta)(\alpha - \beta)^2}. \quad (1.4.19)$$

We see that there is a double pole located at  $\alpha - \beta = 0$ . To cancel this double pole, we are forced to add an extra term to the numerator. A natural choice is a term

that collapses both propagators connecting the two two-loop nonplanar subdiagrams:  $\ell_6^2(\ell_6 + k_1 + k_2)^2$ . On the support of the cut solutions Eq. (1.4.17), this becomes  $s^2\alpha\beta(\alpha + 1)(\beta + 1)$ . We can cancel the double pole at  $\alpha - \beta = 0$  in Eq. (1.4.19) by choosing the linear combination

$$N_1^{(d)} = [(\ell_6 + k_1)^2 + (\ell_6 + k_2)^2] [(\ell_6 - k_3)^2 + (\ell_6 - k_4)^2] - 4\ell_6^2(\ell_6 + k_1 + k_2)^2. \quad (1.4.20)$$

Indeed, with this numerator the diagram lacks even a single pole at  $\alpha - \beta = 0$ .

It is interesting to note that if we relax the condition that the numerator respects the diagram symmetry  $k_1 \leftrightarrow k_2$  and  $k_3 \leftrightarrow k_4$ , there are four independent numerators with no double pole. For example,

$$\tilde{N}^{(d)} = (\ell_6 + k_1)^2(\ell_6 - k_3)^2 - \ell_6^2(\ell_6 + k_1 + k_2)^2, \quad (1.4.21)$$

is a  $d\log$  numerator. When we require that  $N^{(d)}$  respect diagram symmetry, we need the first four terms in Eq. (1.4.20), each with its own ‘‘correction’’ term  $-\ell_6^2(\ell_6 + k_1 + k_2)^2$ . This accounts for the factor of four on the last term in Eq. (1.4.20).

We have carried out detailed checks of all potentially dangerous regions of the integrand of diagram (d) showing that the numerator of Eq. (1.4.20) results in a diagram with only logarithmic singularities and no poles at infinity. In fact, the numerator (1.4.20) is the only one respecting the symmetries of diagram (d) with these properties. We showed this by starting with a general ansatz subject to the power counting constraint in Eq. (1.4.1) and showing that no other solution exists other than the one in Eq. (1.4.20). We have gone through the diagrams in Fig. 1.4 in great detail, finding the numerators that respect diagram symmetry (including color signs), and that have only logarithmic singularities and no poles at infinity. This gives us a set of basis  $d\log$  numerators associated with each diagram. For the diagrams where numerator factors do not cancel any propagators, the set of numerators is collected in Table 1.1. In addition, there are also diagrams where numerators do cancel propagators. For the purpose of constructing amplitudes, it is convenient to absorb these contact contributions into the parent diagrams of Fig. 1.4 to make color assignments manifest. This allows us to treat all contributions on an equal footing, such that we can read off the color factors directly from the associated parent diagram by dressing each three vertex with an  $\tilde{f}^{abc}$ . This distributes the contact term diagrams in Table 1.3 among the parent diagrams, listed in Table 1.2. When distributing the contact terms to the parent diagrams, we change the momentum labels to those of each parent diagram and then multiply and divide by the missing propagator(s). The reason the numerators in Table 1.2 appear more complicated than those in Table 1.3 is that a single term from Table 1.3 can appear with multiple momentum relabellings in order to enforce the symmetries of the parent diagrams on the numerators.

As an example of the correspondence between the numerators in Table 1.2 and Table 1.3, consider diagram (j) and the associated numerators,  $N_1^{(j)}$  and  $N_2^{(j)}$ , in Table 1.3. To convert this into a contribution to diagram (i) in Table 1.2, we multiply and divide by the missing propagator  $1/(\ell_5 + \ell_6 + k_4)^2$ . Then we need to take the appropriate linear combination so that the diagram (i) antisymmetry (including the color sign) under  $\{k_1 \leftrightarrow k_3, \ell_5 \leftrightarrow \ell_6, \ell_7 \leftrightarrow -\ell_7\}$  is satisfied. This gives

$$N_2^{(i)} = \frac{1}{3}(\ell_5 + \ell_6 + k_4)^2 [t - s] . \quad (1.4.22)$$

In fact, there are three alternative propagators that can be inserted instead of  $1/(\ell_5 + \ell_6 + k_4)^2$ , which are all equivalent to the three relabelings of external lines for diagram (i). We have absorbed a combinatorial factor of  $\frac{1}{3}$  into the definition of the numerator because of the differing symmetries between diagram (i) in Table 1.2 and diagram (j) in Table 1.3.

As a second example, consider diagram (k) in Table 1.3, corresponding to the basis element  $N_1^{(k)}$ . If we put back the two missing propagators by multiplying and dividing by the appropriate inverse propagators, the contribution from diagram (k) in Table 1.3 corresponds to numerators  $N_2^{(c)}$ ,  $N_2^{(f)}$ ,  $N_5^{(g)}$ ,  $N_6^{(g)}$ ,  $N_2^{(h)}$ , and  $N_3^{(i)}$  in Table 1.2.

In summary, the diagrams along with the numerators in Table 1.1 and 1.2 are a complete set with the desired power counting, have only logarithmic singularities and no poles at infinity. They are also constructed to satisfy diagram symmetries, including color signs.

#### 1.4.2 Determining the coefficients

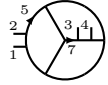
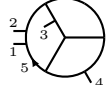
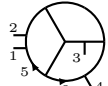
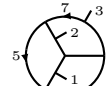
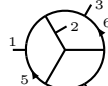
We now express the three-loop four-point  $\mathcal{N} = 4$  sYM amplitude in terms of our constructed basis. We express the numerator in Eq. (1.3.21) directly in terms of our basis via Eq. (1.3.3). Because we have required each basis numerator to reflect diagram symmetry, we need only specify one numerator of each diagram topology and can obtain the remaining ones simple by relabeling of external legs.

The coefficients in front of all basis elements are straightforward to determine using simple unitarity cuts, together with previously determined representations of the three-loop amplitude. We start from the  $\mathcal{N} = 4$  sYM numerators as originally determined in Ref. [122], since they happen to be in a particularly compact form. Rewriting these numerators using our choice of momentum labels gives

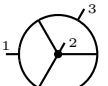
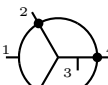
$$\begin{aligned} N_{\text{old}}^{(a)} &= N_{\text{old}}^{(b)} = N_{\text{old}}^{(c)} = N_{\text{old}}^{(d)} = s^2 , \\ N_{\text{old}}^{(e)} &= N_{\text{old}}^{(f)} = N_{\text{old}}^{(g)} = s(\ell_5 + k_4)^2 , \\ N_{\text{old}}^{(h)} &= -st + 2s(k_2 + k_3) \cdot \ell_5 + 2t(\ell_6 + \ell_7) \cdot (k_1 + k_2) , \end{aligned}$$

Diagram	Numerators
(a)	$N_1^{(a)} = s^2, \quad N_2^{(a)} = st, \quad N_3^{(a)} = t^2,$
(b)	$N_1^{(b)} = s [(\ell_6 - k_3)^2 + (\ell_6 - k_4)^2],$
(c)	$N_1^{(c)} = s [(\ell_5 - \ell_7)^2 + (\ell_5 + \ell_7 + k_1 + k_2)^2],$
(d)	$N_1^{(d)} = [(\ell_6 + k_1)^2 + (\ell_6 + k_2)^2]^2 - 4\ell_6^2(\ell_6 + k_1 + k_2)^2,$
(e)	$N_1^{(e)} = s(\ell_5 + k_4)^2, \quad N_2^{(e)} = t(\ell_5 + k_4)^2,$
(f)	$N_1^{(f)} = (\ell_5 + k_4)^2 [(\ell_5 + k_3)^2 + (\ell_5 + k_4)^2],$
(g)	$N_1^{(g)} = s(\ell_5 + \ell_6 + k_3)^2, \quad N_2^{(g)} = t(\ell_5 + \ell_6 + k_3)^2,$ $N_3^{(g)} = (\ell_5 + k_3)^2(\ell_6 + k_1 + k_2)^2, \quad N_4^{(g)} = (\ell_5 + k_4)^2(\ell_6 + k_1 + k_2)^2,$
(h)	$N_1^{(h)} = \left[ (\ell_6 + \ell_7)^2(\ell_5 + k_2 + k_3)^2 - \ell_5^2(\ell_6 + \ell_7 - k_1 - k_2)^2 \right.$ $\quad - (\ell_5 + \ell_6)^2(\ell_7 + k_2 + k_3)^2 - (\ell_5 + \ell_6 + k_2 + k_3)^2 \ell_7^2$ $\quad \left. - (\ell_6 + k_1 + k_4)^2(\ell_5 - \ell_7)^2 - (\ell_5 - \ell_7 + k_2 + k_3)^2 \ell_6^2 \right]$ $- \left[ [(\ell_5 - k_1)^2 + (\ell_5 - k_4)^2][(\ell_6 + \ell_7 - k_1)^2 + (\ell_6 + \ell_7 - k_2)^2] \right.$ $\quad - 4 \times \ell_5^2(\ell_6 + \ell_7 - k_1 - k_2)^2$ $\quad - (\ell_7 + k_4)^2(\ell_5 + \ell_6 - k_1)^2 - (\ell_7 + k_3)^2(\ell_5 + \ell_6 - k_2)^2$ $\quad \left. - (\ell_6 + k_4)^2(\ell_5 - \ell_7 + k_1)^2 - (\ell_6 + k_3)^2(\ell_5 - \ell_7 + k_2)^2 \right],$
(i)	$N_1^{(i)} = (\ell_6 + k_4)^2 [(\ell_5 - k_1 - k_2)^2 + (\ell_5 - k_1 - k_3)^2]$ $\quad - (\ell_5 + k_4)^2 [(\ell_6 + k_1 + k_4)^2 + (\ell_6 + k_2 + k_4)^2]$ $\quad - \ell_5^2(\ell_6 - k_2)^2 + \ell_6^2(\ell_5 - k_2)^2.$

**Table 1.1.** The parent numerator basis elements corresponding to the labels of the diagrams in Fig. 1.4. The basis elements respect the symmetries of the diagrams.

Diagram	Numerator
(c) 	$N_2^{(c)} = (\ell_5)^2 (\ell_7)^2 + (\ell_5 + k_1 + k_2)^2 (\ell_7)^2 + (\ell_5)^2 (\ell_7 + k_1 + k_2)^2 + (\ell_5 + k_1 + k_2)^2 (\ell_7 + k_1 + k_2)^2,$
(f) 	$N_2^{(f)} = \ell_5^2 (\ell_5 - k_1 - k_2)^2,$
(g) 	$N_5^{(g)} = (\ell_5 - k_1 - k_2)^2 (\ell_6 - k_4)^2,$ $N_6^{(g)} = \ell_5^2 (\ell_6 - k_4)^2,$
(h) 	$N_2^{(h)} = \ell_6^2 (\ell_5 - \ell_7)^2 + \ell_7^2 (\ell_5 + \ell_6)^2 + (\ell_6 + k_4)^2 (\ell_5 - \ell_7 + k_2)^2 + (\ell_5 + \ell_6 - k_1)^2 (\ell_7 + k_3)^2,$
(i) 	$N_2^{(i)} = \frac{1}{3} (\ell_5 + \ell_6 + k_4)^2 [t - s],$ $N_3^{(i)} = (\ell_6)^2 (\ell_5 - k_1)^2 - (\ell_5)^2 (\ell_6 - k_3)^2.$

**Table 1.2.** The parent diagram numerator basis elements where a numerator factor cancels a propagator. Each term in brackets does not cancel a propagator, while the remaining factors each cancel a propagator. Each basis numerator maintains the symmetries of the associated diagram, including color signs. The associated color factor can be read off from each diagram.

Diagram	Numerator
(j) 	$N_1^{(j)} = s, \quad N_2^{(j)} = t,$
(k) 	$N_1^{(k)} = 1.$

**Table 1.3.** The numerator basis elements corresponding to the contact term diagrams. Black dots indicate contact terms. Written this way, the numerators are simple, but the color factors cannot be read off from the diagrams.

$$N_{\text{old}}^{(i)} = s(k_4 + \ell_5)^2 - t(k_4 + \ell_6)^2 - \frac{1}{3}(s-t)(k_4 + \ell_5 + \ell_6)^2. \quad (1.4.23)$$

To match to our basis we start by considering the maximal cuts, where all propagators of each diagram are placed on shell. The complete set of maximal cut solutions are unique to each diagram, so we can match coefficients by considering only a single diagram at a time. We start with diagram (a) in Table 1.1. Here the numerator is a linear combination of three basis elements

$$N^{(a)} = a_1^{(a)} N_1^{(a)} + a_2^{(a)} N_2^{(a)} + a_3^{(a)} N_3^{(a)}, \quad (1.4.24)$$

corresponding to  $N_j^{(a)}$  in Table 1.1. The  $a_j^{(a)}$  are numerical parameters to be determined. This is to be compared to the old form of the numerator in Eq. (1.4.23). Here the maximal cuts have no effect because both the new and old numerators are independent of loop momentum. Matching the two numerators, the coefficients in front of the numerator basis are  $a_1^{(a)} = 1$ ,  $a_2^{(a)} = 0$ , and  $a_3^{(a)} = 0$ .

Now consider diagram (b) in Fig. 1.4. Here the basis element is of a different form compared to the old version of the numerator in Eq. (1.4.23). The new form of the numerator is

$$N^{(b)} = a_1^{(b)} N_1^{(b)} = a_1^{(b)} s [(\ell_6 - k_3)^2 + (\ell_6 - k_4)^2]. \quad (1.4.25)$$

In order to make the comparison to the old version we impose the maximal cut conditions involving only  $\ell_6$ :

$$\ell_6^2 = 0, \quad (\ell_6 - k_2 - k_3)^2 = 0. \quad (1.4.26)$$

Applying these conditions:

$$[(\ell_6 - k_3)^2 + (\ell_6 - k_4)^2] \rightarrow -s. \quad (1.4.27)$$

Comparing to  $N_{\text{old}}^{(b)}$  in Eq. (1.4.23) gives us the coefficient  $a_1^{(b)} = -1$ .

As a more complicated example, consider diagram (i). In this case the numerators depend only on  $\ell_5$  and  $\ell_6$ . The relevant cut conditions read off from Fig. 1.4(i) are

$$\ell_5^2 = \ell_6^2 = (\ell_5 - k_1)^2 = (\ell_6 - k_3)^2 = (\ell_5 + \ell_6 - k_3 - k_1)^2 = (\ell_5 + \ell_6 + k_4)^2 = 0. \quad (1.4.28)$$

With these cut conditions, the old numerator in Eq. (1.4.23) becomes

$$N_{\text{old}}^{(i)}|_{\text{cut}} = 2s(k_4 \cdot \ell_5) - 2t(k_4 \cdot \ell_6). \quad (1.4.29)$$

The full numerator for diagram (i) is a linear combination of the three basis elements for diagram (i) in Table 1.1 and 1.2,

$$N^{(i)} = a_1^{(i)} N_1^{(i)} + a_2^{(i)} N_2^{(i)} + a_3^{(i)} N_3^{(i)}. \quad (1.4.30)$$

The maximal cut conditions immediately set to zero the last two of these numerators because they contain inverse propagators. Applying the cut conditions Eq. (1.4.28) to the nonvanishing term results in

$$N^{(i)}|_{\text{cut}} = a_1^{(i)}[-2(\ell_6 \cdot k_4)t + 2(\ell_5 \cdot k_4)s]. \quad (1.4.31)$$

Comparing Eq. (1.4.29) to Eq. (1.4.31) fixes  $a_1^{(i)} = 1$ . The two other coefficients for diagram (i),  $a_2^{(i)}$  and  $a_3^{(i)}$  cannot be fixed from the maximal cuts.

In order to determine all coefficients and to prove that the answer is complete and correct, we need to evaluate next-to-maximal and next-to-next-to-maximal cuts. We need only evaluate the cuts through this level because of the especially good power counting of  $\mathcal{N} = 4$  sYM. We do not describe this procedure in detail here. Details of how this is done may be found in Ref. [138]. Using these cuts we have the solution of the numerators in terms of the basis elements as

$$\begin{aligned} N^{(a)} &= N_1^{(a)}, \\ N^{(b)} &= -N_1^{(b)}, \\ N^{(c)} &= -N_1^{(c)} + 2d_1 N_2^{(c)}, \\ N^{(d)} &= N_1^{(d)}, \\ N^{(e)} &= N_1^{(e)}, \\ N^{(f)} &= -N_1^{(f)} + 2d_2 N_2^{(f)}, \\ N^{(g)} &= -N_1^{(g)} + N_3^{(g)} + N_4^{(g)} + (d_1 + d_3 - 1)N_5^{(g)} + (d_1 - d_2)N_6^{(g)}, \\ N^{(h)} &= N_1^{(h)} + 2d_3 N_2^{(h)}, \\ N^{(i)} &= N_1^{(i)} + N_2^{(i)} + (d_3 - d_2)N_3^{(i)}, \end{aligned} \quad (1.4.32)$$

where the three  $d_i$  are free parameters not fixed by any physical constraint.

The ambiguity represented by the three free parameters,  $d_i$  in Eq. (1.4.32), derives from color factors not being independent but instead related via the color Jacobi identity. This allows us to move contact terms between different diagrams without altering the amplitude. Different choices of  $d_1, d_2, d_3$  correspond to three degrees of freedom from color Jacobi identities. These allow us to move contact contributions of diagram (k), where two propagators are collapsed, between different parent diagrams. The contact term in diagram (j) of Table 1.3 does not generate a fourth degree of freedom because the three resulting parent diagrams are all the same topology, corresponding to relabelings of the external legs of diagram (i). The potential freedom then cancels within a single diagram. We have explicitly checked that the  $d_i$  parameters in Eq. (1.4.32) drop out



of the full amplitude after using appropriate color Jacobi identities. One choice of free parameters is to take them to all vanish

$$d_1 = 0, \quad d_2 = 0, \quad d_3 = 0. \quad (1.4.33)$$

In this case every remaining nonvanishing numerical coefficient in front of a basis elements is  $\pm 1$ . (Recall that  $N_2^{(i)}$  absorbed the  $1/3$  combinatorial factor mismatch between diagram (i) and diagram (j).) Of course this is not some “best” choice of the  $d_i$ , given that the amplitude is unchanged for any other choice of  $d_i$ .

Once the coefficients in front of each basis numerator are determined, we are left with the question of whether the basis numerators properly capture all terms that are present in the amplitude. To answer this we turn to the method of maximal cuts [138]. This is a variation on the standard generalized unitarity method, but organized by starting with maximal cuts and systematically checking cuts with fewer and fewer propagators set on shell. This method has been described in considerable detail in Ref. [138], so we only mention a few points.

The overall power counting of the three-loop  $\mathcal{N} = 4$  sYM amplitude is such that it can be written with at most two powers of loop momenta in the numerator [114, 122]. This means that in principle we can fully determine the amplitude using only next-to-maximal cuts. However, here we use a higher-power counting representation with up to four powers of loop momenta in the numerator corresponding to as many as two canceled propagators. This implies that to completely determine the amplitude using our representation we need to check cuts down to the next-to-next-to-maximal level. We have explicitly checked all next-to-next-to-maximal cuts, proving that the amplitudes obtained by inserting the numerators in Eq. (1.4.32) into Eqs. (1.3.21) and (1.3.3) gives the complete amplitude, and that it is entirely equivalent to earlier representations of the amplitude [114, 122, 128]. Because each numerator basis element is constructed such that each integrand has only logarithmic singularities and no poles at infinity, this proves that the full nonplanar three-loop four-point  $\mathcal{N} = 4$  sYM amplitude has these properties, as conjectured in Ref. [119].

### 1.4.3 Relation to rung rule

Is it possible to determine the coefficients of the basis integrands as they appear in the  $\mathcal{N} = 4$  sYM amplitude from simple heuristic rules? Such rules can be useful both because they offer a simple way to cross-check derived results, and because they can often point to deeper structures. Here we show that the rung rule of Ref. [120] gives at least some of the coefficients<sup>4</sup>.

---

<sup>4</sup>We thank Lance Dixon for pointing out to us that the rung rule is helpful for identifying nonplanar integrals with uniform transcendentality, and suggesting a match to our construction as well.

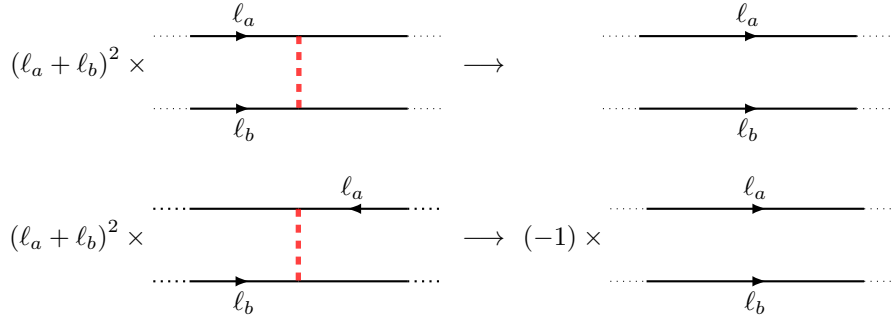


**Figure 1.5.** The rung rule gives the relative coefficient between an  $L$ -loop diagram and an  $(L - 1)$ -loop diagram. The dotted shaded (red) line represents the propagator at  $L$  loops that is removed to obtain the  $(L - 1)$ -loop diagram. As indicated on the second row, if one of the lines is twisted around, as can occur in nonplanar diagrams, there is an additional sign from the color antisymmetry.

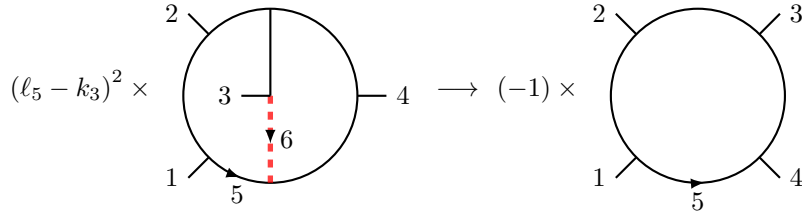


**Figure 1.6.** The rung rule determines the relative sign between the two-loop nonplanar contribution and the one-loop box to be negative.

The rung rule was first introduced as a heuristic rule for generating contributions with correct iterated-two-particle cuts in  $\mathcal{N} = 4$  sYM amplitudes [120]. It is also related to certain soft collinear cuts. Today the rung rule is understood as a means for generating contributions with simple properties under dual conformal invariance. In the planar case the rule applies even when the contributions cannot be obtained from iterated two-particle cuts [142]. However, the rung rule does not capture all contributions. It can also yield contributions that do not have the desired properties, but differ by contact terms from desired ones. For this reason, the rule is most useful once we have a basis of integrands and are interested in understanding the coefficients as they appear in amplitudes.

The rung rule was originally applied as a means for generating new  $L$ -loop contributions

from  $(L - 1)$ -loop ones. Here we use the rule in the opposite direction, going from an  $L$ -loop basis integrand to an  $(L - 1)$ -loop contribution so as to determine the coefficient of the  $L$ -loop contribution to the amplitude. As illustrated in Fig. 1.5, if we have a basis integrand containing a factor of  $(\ell_a + \ell_b)^2$  and a propagator indicated by a dotted line, we can remove these to obtain a diagram with one fewer loop. According to the rung rule, the overall coefficient of the diagram obtained by removing a rung matches that of the lower-loop diagram in the amplitude. In the nonplanar case the diagrams can be twisted around, as displayed on the second line in Fig. 1.5, leading to relative signs. These relative signs can be thought of as coming from color factors.

Because we have already determined the three-loop  $d\log$  numerators, we only need the rung rule to determine the sign of the numerator in the amplitude. This allows us to slightly generalize the rung rule beyond its original form. In the original version of the rung rule, the rung carries an independent loop momentum that becomes a new loop momentum in the diagram when the rung is added. The reverse of this means removing a rung from the diagram requires also removing an independent loop momentum. We will encounter cases where removing a rung and its loop momentum prevents the original version of the rung rule from matching the desired  $d\log$  numerators. We therefore slightly modify the rung rule by allowing the factors to be matched in any order of removing a given set of rungs or propagators. If we can match each factor in a numerator in at least one order of rung removal, then we just read off the overall sign as for other cases.

To illustrate how the rung rule determines a coefficient, consider the two-loop four-point amplitude. As discussed in Sect. 1.2, after removing the overall  $\mathcal{K}$  from the amplitude, the only allowed numerator for the nonplanar double box in Fig. 1.3(b) with the desired properties is given in Eq. (1.3.30). The first step is to determine if a given numerator can be obtained from the rung rule. The first term,  $(\ell_5 - k_3)^2$ , in the nonplanar numerator  $N^{(\text{NP})}$  (Eq. (1.3.30)) can be so determined. The rung corresponding to the  $(\ell_5 - k_3)^2$  term is displayed as the dotted (red) line on the left side of Fig. 1.6. Removing this rung gives the one-loop box diagram on the right side of Fig. 1.6, which has coefficient  $\mathcal{K}$ . However, we need to flip over leg 3 to obtain the standard box from the diagram with the rung removed, resulting in a relative minus sign between color factors. This fixes  $(\ell_5 - k_3)^2$  to enter the amplitude with a negative sign, because the box enters the amplitude with a positive sign. This precisely matches the sign in Eq. (1.3.29) obtained from the maximal cut.

At three loops the idea is the same. Consider, for example diagram (c). Examining the numerator basis element  $N_1^{(c)}$  from Table 1.1, we can identify the term  $s(\ell_5 - \ell_7)^2$  as a rung-rule factor. In Fig. 1.7, the dotted (red) line in the top part of the diagram corresponds to the factor  $(\ell_5 - \ell_7)^2$ . After removing the top rung, the bottom rung is

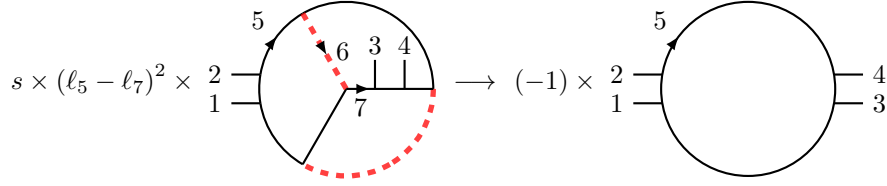


**Figure 1.7.** The rung rule determines that the basis element  $N^{(c)}$  enters the amplitude with a relative minus sign.

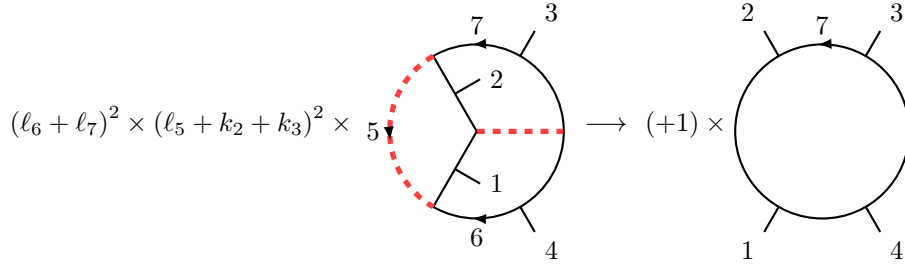


**Figure 1.8.** The rung rule determines that basis element  $N_1^{(h)}$  enters the amplitude with a relative plus sign.

just a factor of  $s = (k_1 + k_2)^2$ . An overall sign comes from the fact that the first rung was twisted as in Fig. 1.5. This determines the coefficient to be  $-1$ , and symmetry then fixes the second rung rule numerator to have the same sign. This matches the sign of the numerator in Eq. (1.4.32) found via unitarity cuts.

Now consider the more complicated case of diagram (h). In Table 1.1, the first term in  $N_1^{(h)} = (\ell_6 + \ell_7)^2(\ell_5 + k_2 + k_3)^2 + \dots$  is a more interesting example, because the original rung rule does not apply. Nevertheless, using the slightly modified rung rule described above, we can still extract the desired coefficient in front of this term. Examining Fig. 1.8, notice that if we first remove the left rung, the rung rule gives one factor of  $N_1^{(h)}$ :  $(\ell_6 + \ell_7)^2$ , while if we first remove the right rung, the rung rule gives the other factor  $(\ell_5 + k_2 + k_3)^2$ . In both cases the rung rule sign is positive. Furthermore, flipping legs 1 and 2 to get the one-loop diagram on the right side of Fig. 1.8 does not change the sign. Thus the sign is positive, in agreement with Eq. (1.4.32).

The rung rule does not fix all coefficients of  $d\log$  numerators in the amplitude. In particular, since the rule involves adding two propagators per rung, it can never generate terms proportional to propagators, such as those in Table 1.2 and 1.3. Nor is there any

guarantee that basis integrands without canceled propagators can be identified as rung rule contributions. One might be able to find various extensions of the rung rule that handle more of these cases. Such an extension was discussed in Ref. [143], but for now we do not pursue these ideas further.

## 1.5 Finding $d\log$ forms

In the previous section we performed detailed checks showing that the three-loop four-point  $\mathcal{N} = 4$  sYM amplitude has only logarithmic singularities and no poles at infinity. The first of these conditions is equivalent to being able to find  $d\log$  forms, so if we can find such forms directly then we can bypass detailed analyses of the singularity structure of integrands. There is no general procedure for how to do this, so we have to rely on a case-by-case analysis. We build up technology at one and two loops, then apply that technology to a few examples at three loops, relegating a detailed discussion to the future. As expected, exactly the same Jacobians that lead to double or higher poles in our analysis of the singularity structure block us from finding  $d\log$  forms, unless the Jacobians are appropriately canceled by numerator factors.

In this section, we use the terminology that an  $L$ -loop integrand form is a  $d\log$  form if it can be written as a linear combination,

$$d\mathcal{I} = d^4\ell_5 \dots d^4\ell_{4+L} \frac{N^{(x)}(\ell_r, k_s)}{D^{(x)}(\ell_r, k_s)} = \sum_j c_j d\log f_1^{(j)} \wedge d\log f_2^{(j)} \wedge \dots \wedge d\log f_{4L}^{(j)}, \quad (1.5.1)$$

where  $N^{(x)}(\ell_r, k_s)$  is a diagram numerator, the denominator  $D^{(x)}(\ell_r, k_s)$  is the usual product of propagators,  $f_i^{(j)} = f_i^{(j)}(\ell_r, k_s)$  is a function of loop and external momenta. The coefficients  $c_j$  are the leading singularities of  $d\mathcal{I}$  on a  $4L$  cut, where we take  $f_1^{(j)} = f_2^{(j)} = \dots = f_{4L}^{(j)} = 0$ . It is still an open question whether the smallest irreducible  $d\log$  forms may be expressed as a single form with unit leading singularity,

$$d\mathcal{I} \stackrel{?}{=} d\log f_1 \wedge d\log f_2 \wedge \dots \wedge d\log f_{4L}. \quad (1.5.2)$$

We can determine on a case by case basis if the change of variables (1.5.2) exists by checking if the integrand form has (i) only logarithmic singularities and (ii) only unit leading singularities. An integrand form has unit leading singularities if the  $4L$ -cut of the integrand form is

$$\text{Res}_{\ell_r = \ell_r^*} d\mathcal{I} = \pm 1, 0, \quad (1.5.3)$$

where  $\ell_r^*$  are positions for quadruple cuts for all loop variables. In the  $d\log$  form it is a simple matter to extract the residues via

$$\text{Res}_{f_1=0} d\mathcal{I} = d\log f_2 \wedge \dots \wedge d\log f_{4L}, \quad (1.5.4)$$

and the residues at the other  $f_j = 0$  may be obtained analogously. In doing so there are signs from the wedge products which we do not track. Clearly, it is better to find single-term  $d\log$  forms as in Eq. (1.5.2), which we do in many examples. However the multiterm  $d\log$  form (1.5.1) is sufficient for our purposes because it makes manifest that the integrand form has only logarithmic singularities.

In the previous sections, we normalized the forms such that a factor  $\mathcal{K}$ , defined in Eq. (1.3.22), was factored out. In this section, we restore this factor as

$$\mathcal{K} = stC_1, \quad (1.5.5)$$

using the definitions from Eqs. (1.3.22) and (1.3.32). In some cases it is best to use the symmetry (1.3.23) to instead write

$$\mathcal{K} = suC_2, \quad \mathcal{K} = tuC_3. \quad (1.5.6)$$

As noted in Sect. 1.3.3, in general, we write the integrand forms as linear combinations of  $d\log$  forms using the  $C_i$  as prefactors, as we find below.

### 1.5.1 One loop

At higher loops, a good starting point for finding  $d\log$  forms is to express one-loop subdiagrams in  $d\log$  forms. Following standard integral decomposition methods, any one loop integrand form with no poles at infinity can be decomposed in terms of box and pentagon forms:

$$d\mathcal{I} = \sum_j a_j^{(5)} d\mathcal{I}_5^{(j)} + \sum_k b_k^{(4)} d\mathcal{I}_4^{(k)}. \quad (1.5.7)$$

Triangle or bubble integrand forms do not appear in this decomposition because they would introduce poles at infinity.

The decomposition in Eq. (1.5.7) is valid beyond the usual one-loop integrals. We can consider any integrand form with  $m$  generalized propagators which are at most quadratic in the momenta:

$$d\mathcal{I} = \frac{d^4\ell N_m}{F_1 F_2 \dots F_m}, \quad \text{where} \quad F_j = \alpha_j \ell^2 + (\ell \cdot Q_j) + P_j. \quad (1.5.8)$$

We can then use the same expansion (1.5.7) for these objects and express it in terms of *generalized boxes* and *generalized pentagons* which are integrals with four or five generalized propagators,  $F_j$ . Unlike in the case of regular one-loop integrals, there is no simple power-counting constraint on the numerator such that  $d\mathcal{I}$  is guaranteed not to have any poles at infinity. Instead one needs to check for poles at infinity case by case.

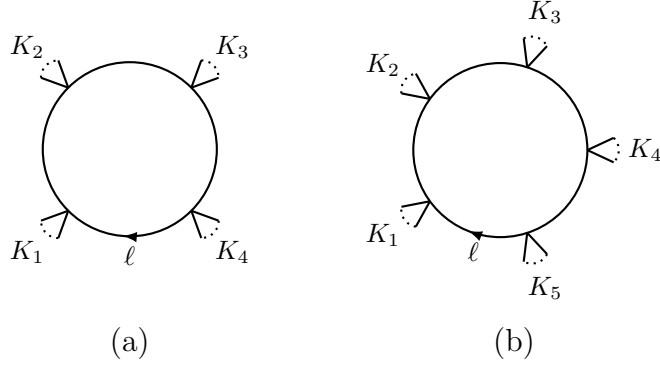


**Figure 1.9.** One-loop box and pentagon diagrams.

At one loop, Eq. (1.5.7) tells us that we need only consider boxes and pentagons, since the higher-point cases can be reduced to these. First consider the standard box form with (off-shell) external momenta  $K_1, K_2, K_3, K_4$  shown in Fig. 1.9(a):

$$d\mathcal{I}_4 \left[ \begin{array}{cc} \ell^2 & (\ell - K_1 - K_2)^2 \\ (\ell - K_1)^2 & (\ell + K_4)^2 \end{array} \right] \equiv d^4\ell \frac{N_4}{\ell^2(\ell - K_1)^2(\ell - K_1 - K_2)^2(\ell + K_4)^2}. \quad (1.5.9)$$

Here on the left hand side we introduce a compact notation for the  $d\log$  form that will be useful at higher loops. The actual positions of the arguments do not matter, since swapping the locations of arguments will only alter the overall sign of the form due to the wedge products; in amplitudes such signs are fixed using unitarity. The numerator  $N_4$  is just the Jacobian  $J_\ell$  given in Eq. (1.2.20), using the labels of the box in Fig. 1.9(a). With this numerator  $d\mathcal{I}_4$  has unit leading singularities, and we can write it as a single-term  $d\log$  form,

$$\begin{aligned} d\mathcal{I}_4 \left[ \begin{array}{cc} \ell^2 & (\ell - K_1 - K_2)^2 \\ (\ell - K_1)^2 & (\ell + K_4)^2 \end{array} \right] & \quad (1.5.10) \\ = d\log \frac{\ell^2}{(\ell - \ell^*)^2} \wedge d\log \frac{(\ell - K_1)^2}{(\ell - \ell^*)^2} \wedge d\log \frac{(\ell - K_1 - K_2)^2}{(\ell - \ell^*)^2} \wedge d\log \frac{(\ell + K_4)^2}{(\ell - \ell^*)^2}, & \end{aligned}$$

as already noted in Sect. 1.2.3. Here the  $d\log$  form depends on  $\ell^*$ , which is a solution for  $\ell$  on the quadruple cut

$$\ell^2 = (\ell - K_1)^2 = (\ell - K_1 - K_2)^2 = (\ell + K_4)^2 = 0. \quad (1.5.11)$$

There are two independent  $\ell^*$  that satisfy these equations, and we are free to choose either of them. Both give the same results when substituted into the  $d\log$  form.

An important nontrivial property of a  $d\log$  form is that the residue located at  $(\ell - \ell^*)^2 = 0$  cancels. If it were to not cancel, then there would be an unphysical singularity

which could feed into our higher-loop discussion. We illustrate the cancellation for the massless box where  $K_i = k_i$  with  $k_i^2 = 0$  for all  $i = 1, \dots, 4$ . In this case  $\ell^* = -\frac{[12]}{[24]}\lambda_1\tilde{\lambda}_4$  and the residue of  $d\mathcal{I}_4$  in (1.5.10) on  $(\ell - \ell^*)^2 = 0$  is

$$\begin{aligned} \text{Res } d\mathcal{I}_4 &= d\log(\ell^2) \wedge d\log(\ell - k_1)^2 \wedge d\log(\ell - k_1 - k_2)^2 \\ &\quad - d\log(\ell^2) \wedge d\log(\ell - k_1)^2 \wedge d\log(\ell + k_4)^2 \\ &\quad + d\log(\ell^2) \wedge d\log(\ell - k_1 - k_2)^2 \wedge d\log(\ell + k_4)^2 \\ &\quad - d\log(\ell - k_1)^2 \wedge d\log(\ell - k_1 - k_2)^2 \wedge d\log(\ell + k_4)^2. \end{aligned} \quad (1.5.12)$$

The simplest way to see the cancellation is that on the solution of  $(\ell - \ell^*)^2 = 0$ , the following identity is satisfied

$$\ell^2(\ell - k_1 - k_2)^2 = (\ell - k_1)^2(\ell + k_4)^2. \quad (1.5.13)$$

Using this we can express, say,  $\ell^2$  in terms of other inverse propagators and substitute into Eq. (1.5.12). All terms in Eq. (1.5.12) then cancel pairwise because of the anti-symmetry property of the wedge product. A similar derivation can be carried out for the generic four-mass case, but we refrain from doing so here.

The *generalized box*, in terms of which Eq. (1.5.8) can be expanded, is

$$d\mathcal{I}_4 \left[ \begin{array}{c} F_1 \ F_2 \\ F_3 \ F_4 \end{array} \right] = \frac{d^4\ell \ N}{F_1 F_2 F_3 F_4} = d\log \frac{F_1}{F^*} \wedge d\log \frac{F_2}{F^*} \wedge d\log \frac{F_3}{F^*} \wedge d\log \frac{F_4}{F^*}, \quad (1.5.14)$$

where the numerator  $N$  is again a Jacobian (1.2.20) of the solution to the system of equations  $P_i = 0$  for  $P = \{F_1, F_2, F_3, F_4\}$  and  $F^* = (\ell - \ell^*)^2$ . Here  $\ell^*$  is the solution for  $\ell$  at  $F_i = 0$  for  $i = 1, 2, 3, 4$ . It is not automatic that  $d\mathcal{I}_4$  can be put into a  $d\log$  form for any set of  $F_i$ 's. This depends on whether  $d\mathcal{I}_4$  has only logarithmic singularities. If it has other types of singularities, then no change of variables will give a  $d\log$  representation for  $d\mathcal{I}_4$ . As a simple example of a form that cannot be rewritten in  $d\log$  form consider the generalized box

$$d^4\ell \frac{N_4}{\ell^2(\ell + k_1)^2(\ell + k_2)^2(\ell + k_4)^2}, \quad (1.5.15)$$

where the numerator is independent of loop momentum  $\ell$ . Using a parametrization of the type of Eq. (1.2.10), we find that on the collinear cut  $\ell^2 = (\ell + k_1)^2 = 0$  where  $\ell = \alpha_1 k_1$ , there is a double pole  $d\alpha_1/\alpha_1^2$ . Therefore no  $d\log$  form exists. In any case, at higher loops we will find the notion of a generalized box very useful for finding  $d\log$  forms.

Next we consider a generic one-loop pentagon form,

$$d\mathcal{I}_5 = \frac{d^4\ell \ N_5}{\ell^2(\ell - K_1)^2(\ell - K_1 - K_2)^2(\ell - K_1 - K_2 - K_3)^2(\ell + K_5)^2}, \quad (1.5.16)$$



with off-shell momenta  $K_j$ . The numerator  $N_5$  is not fixed by the normalization whereas it was in the case of the box. Also unlike in the case of the box, there are multiple numerators  $N_5$  that give unit leading singularities. The constraint of no poles at infinity constrains  $N_5$  to be quadratic:  $N_5 = g_1 \ell^2 + g_2 (\ell \cdot Q) + g_3$ , where the  $g_k$  are some constants and  $Q$  is a constant vector. The simplest way to decompose the pentagon form (1.5.16) is to start with a reference pentagon form,

$$d\tilde{\mathcal{I}}_5 \equiv d\log \frac{(\ell - K_1)^2}{\ell^2} \wedge d\log \frac{(\ell - K_1 - K_2)^2}{\ell^2} \wedge d\log \frac{(\ell + K_4 + K_5)^2}{\ell^2} \wedge d\log \frac{(\ell + K_5)^2}{\ell^2}, \quad (1.5.17)$$

in terms of which we express all other pentagons. This reference  $d\log$  form corresponds to a parity-odd integrand form and gives zero when integrating over Minkowski space. In Eq. (1.5.17) we single out  $\ell^2$ , but one can show that all five choices of singling out one of the inverse propagators are equivalent. We then can decompose the generic pentagon form (1.5.16) into the reference pentagon form (1.5.17)  $d\tilde{\mathcal{I}}_5$  plus box forms,

$$d\mathcal{I}_5 = c_0 d\tilde{\mathcal{I}}_5 + \sum_{j=1}^5 c_j d\mathcal{I}_4^{(j)}, \quad (1.5.18)$$

where  $c_j$  are coefficients most easily determined by imposing cut conditions on both sides of Eq. (1.5.18) and matching. While we can express Eq. (1.5.17) as a loop-integrand, its numerator  $\tilde{N}_5$  is complicated, and it is better to use directly the  $d\log$  form (1.5.17) for obtaining cuts.

The expansion (1.5.18) is always valid for up to two powers of loop momentum in the numerator  $N_5$ , but in higher-loop calculations it is often more convenient to use alternative decompositions. It is also possible to define generalized pentagons with propagators other than the standard ones. These will be useful in subsequent discussion.

### 1.5.2 Two loops

At two loops there are only two distinct integrand forms to consider: the planar and nonplanar double boxes displayed in Figs. 1.3 and 1.10. As shown in Ref. [119], we can choose the numerators such that all integrals individually have only logarithmic singularities and no poles at infinity. As already noted, in previous sections we suppressed a factor of  $\mathcal{K}$  (defined in Eq. (1.3.22)) that we now restore to make the connection to  $d\log$  forms and the leading singularity coefficients more straightforward.

We start with the planar double box of Fig. 1.3. It appears in the amplitude as

$$d\mathcal{I}^{(P)} = \frac{d^4 \ell_5 d^4 \ell_6 s^2 t C_1}{\ell_5^2 (\ell_5 + k_1)^2 (\ell_5 - k_2)^2 (\ell_5 + \ell_6 - k_2 - k_3)^2 \ell_6^2 (\ell_6 - k_3)^2 (\ell_6 + k_4)^2}, \quad (1.5.19)$$

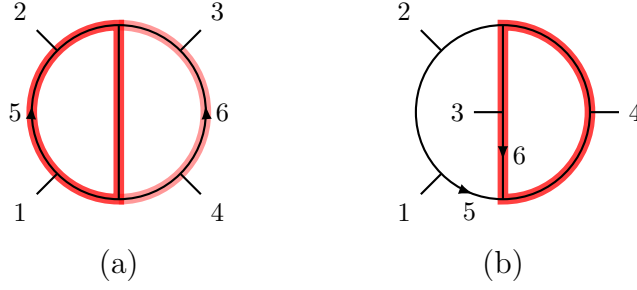


**Figure 1.10.** The (a) planar and (b) nonplanar two-loop four-point parent diagrams. In each case one-loop box subdiagrams are shaded (red). In the planar diagram, the Jacobian from the one-loop box subdiagram combines with the remaining three lightly shaded (light red) propagators to form a second box.

where  $C_1$  is defined in Eq. (1.3.32). It is straightforward to put this integrand form into a  $d\log$  form by iterating the one-loop single-box case in Eq. (1.3.32). We immediately obtain a product of two one-loop box integrand forms,

$$\begin{aligned}
 d\mathcal{I}^{(P)} &= C_1 \left[ \frac{d^4\ell_5 s(\ell_6 - k_2 - k_3)^2}{\ell_5^2(\ell_5 + k_1)^2(\ell_5 - k_2)^2(\ell_5 + \ell_6 - k_2 - k_3)^2} \right] \\
 &\quad \times \left[ \frac{d^4\ell_6 st}{\ell_6^2(\ell_6 - k_3)^2(\ell_6 + k_4)^2(\ell_6 - k_2 - k_3)^2} \right] \\
 &= C_1 d\mathcal{I}_4 \left[ \begin{array}{cc} \ell_5^2 & (\ell_5 + k_1)^2 \\ (\ell_5 - k_2)^2 & (\ell_5 + \ell_6 - k_2 - k_3)^2 \end{array} \right] \wedge d\mathcal{I}_4 \left[ \begin{array}{cc} \ell_6^2 & (\ell_6 - k_3)^2 \\ (\ell_6 + k_4)^2 & (\ell_6 - k_2 - k_3)^2 \end{array} \right].
 \end{aligned} \tag{1.5.20}$$

Thus,  $d\mathcal{I}^{(P)}$  is a  $d\log$  eight-form given by the wedge product of two  $d\mathcal{I}_4$  box four-forms, multiplied by the coefficient  $C_1$ . By symmetry, we can also reverse the order of iterating the one-loop box forms to instead obtain

$$d\mathcal{I}^{(P)} = C_1 d\mathcal{I}_4 \left[ \begin{array}{cc} \ell_5^2 & (\ell_5 + k_1)^2 \\ (\ell_5 - k_2)^2 & (\ell_5 - k_2 - k_3)^2 \end{array} \right] \wedge d\mathcal{I}_4 \left[ \begin{array}{cc} \ell_6^2 & (\ell_6 - k_3)^2 \\ (\ell_6 + k_4)^2 & (\ell_5 + \ell_6 - k_2 - k_3)^2 \end{array} \right]. \tag{1.5.21}$$

Despite the fact that the two  $d\log$  forms in Eqs. (1.5.20) and (1.5.21) look different, they are equal. This is another illustration that  $d\log$  forms are not unique, and there are many different ways to write them.

The nonplanar double box in Fig. 1.3 is more complicated, since it contains both box and pentagon subdiagrams. It is given by

$$d\mathcal{I}^{(NP)} = \frac{d^4\ell_5 d^4\ell_6 C_1 st [(\ell_5 - k_4)^2 + (\ell_5 - k_3)^2]}{\ell_5^2(\ell_5 + k_1)^2(\ell_5 + k_1 + k_2)^2 \ell_6^2(\ell_6 + k_3)^2(\ell_6 + \ell_5)^2(\ell_6 + \ell_5 - k_4)^2}. \tag{1.5.22}$$

We start by writing the  $\ell_6$  box subdiagram highlighted in Fig. 1.10 as a  $d\log$  form, so that

$$d\mathcal{I}^{(\text{NP})} = d\mathcal{I}_{\ell_6} \wedge d\mathcal{I}_{\ell_5}, \quad (1.5.23)$$

where

$$d\mathcal{I}_{\ell_6} = \frac{d^4 \ell_6 (\ell_5 \cdot q)(\ell_5 \cdot \bar{q})}{\ell_6^2 (\ell_6 + k_3)^2 (\ell_6 + \ell_5)^2 (\ell_6 + \ell_5 - k_4)^2} = d\mathcal{I}_4 \left[ \frac{\ell_6^2 (\ell_6 + \ell_5)^2}{(\ell_6 + k_3)^2 (\ell_6 + \ell_5 - k_4)^2} \right]. \quad (1.5.24)$$

The  $d\mathcal{I}_{\ell_6}$  form is normalized with the Jacobian numerator  $(\ell_5 \cdot q)(\ell_5 \cdot \bar{q})$ , where  $q = \lambda_3 \tilde{\lambda}_4$  and  $\bar{q} = \lambda_4 \tilde{\lambda}_3$ . This is just a relabeling of the two-mass-easy normalization given in Eq. (1.2.22). The remaining integral can then be divided into two parts:

$$d\mathcal{I}_{\ell_5} = C_1 d\mathcal{I}_5^{X1} + C_2 d\mathcal{I}_5^{X2}, \quad (1.5.25)$$

where we have used  $tC_1 = uC_2$  and

$$\begin{aligned} d\mathcal{I}_5^{X1} &\equiv \frac{d^4 \ell_5 \, st(\ell_5 - k_4)^2}{\ell_5^2 (\ell_5 + k_1)^2 (\ell_5 + k_1 + k_2)^2 (\ell_5 \cdot q)(\ell_5 \cdot \bar{q})}, \\ d\mathcal{I}_5^{X2} &\equiv d\mathcal{I}_5^{X1} \Big|_{k_3 \leftrightarrow k_4}. \end{aligned} \quad (1.5.26)$$

These are exactly generalized pentagons, of the type we discussed in the previous subsection. It is straightforward to check that there are only logarithmic singularities and no poles at infinity. Because of the two propagators linear in  $\ell_5$ , these two forms are not canonical one-loop integrand forms. Nevertheless, we can find a change of variables for  $d\mathcal{I}_5^{X1}$  and  $d\mathcal{I}_5^{X2}$  so that each is a single  $d\log$  form,

$$d\mathcal{I}_5^{X1} = d\log \frac{\ell_5^2}{(\ell_5 \cdot \bar{q})} \wedge d\log \frac{(\ell_5 + k_1)^2}{(\ell_5 \cdot \bar{q})} \wedge d\log \frac{(\ell_5 + k_1 + k_2)^2}{(\ell_5 \cdot q)} \wedge d\log \frac{(\ell_5 - \ell_5^*)^2}{(\ell_5 \cdot q)}, \quad (1.5.27)$$

where  $\ell_5^* = \frac{\langle 34 \rangle}{\langle 31 \rangle} \lambda_1 \tilde{\lambda}_4$  is the solution of cut conditions  $\ell_5^2 = (\ell_5 + k_1)^2 = (\ell_5 + k_1 + k_2)^2 = (\ell_5 \cdot q) = 0$ . A similar result is obtained for  $d\mathcal{I}_{\ell_5}^{X2}$  by swapping  $k_3$  and  $k_4$ . The final result for the  $d\log$  form of the nonplanar double box is

$$d\mathcal{I}^{(\text{NP})} = C_1 d\mathcal{I}_{\ell_6} \wedge d\mathcal{I}_{\ell_5}^{X1} + C_2 d\mathcal{I}_{\ell_6} \wedge d\mathcal{I}_{\ell_5}^{X2}. \quad (1.5.28)$$

Since each term carries a different normalization, this expression cannot be uniformly normalized to have unit leading singularities on all cuts. We choose a normalization such that  $C_1$  or  $C_2$  are the leading singularities of the integrand form, depending on which residue we take. This construction is useful at three loops, as we see below.

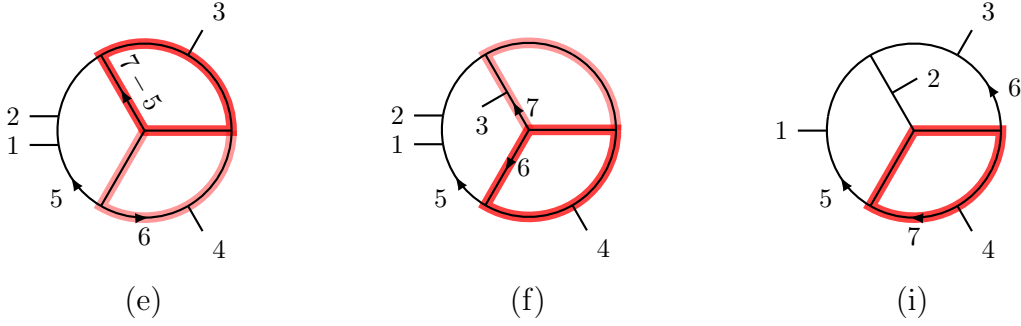


**Figure 1.11.** The three-loop diagrams with highlighted one-loop box subdiagrams used in the construction of  $d\log$  forms. In diagram (e) we start with the top (red) box whose Jacobian generates the missing fourth propagator for the bottom (light red) box. In diagram (f) we start with the bottom (red) box whose Jacobian generates the missing fourth propagator for the top (light red) box. In diagram (i), there is only one box on the bottom (red).

### 1.5.3 Three loops

We now turn to the main subject: constructing the three-loop four-point nonplanar  $d\log$  forms. Unfortunately, at present there is no general procedure to rewrite high-loop order integrand forms into  $d\log$  forms. Nevertheless, we can proceed with our general strategy: whenever there is a box subdiagram, we rewrite it in a  $d\log$  form and then deal with the remaining forms by again looking at subdiagrams. This tactic works well at three loops: we have worked out  $d\log$  forms for all diagrams that have box subdiagrams. This consists of all diagrams except for diagram (h), which is the most complicated case because it has only pentagon subdiagrams. Diagrams (a) and (b) are simple because they are directly related to the one- and two-loop cases. In this subsection we show explicit examples of diagrams (e), (f), and (i), which are less trivial. Each example shows how to overcome some new obstacle to constructing a  $d\log$  form. We start with diagram (e) in Figs. 1.4 and 1.11. The numerator is  $\mathcal{KN}^{(e)} = C_1 s^2 t (\ell_5 + k_4)^2$ . This gives us the integrand form,

$$d\mathcal{I}^{(e)} = \frac{d^4 \ell_5 d^4 \ell_6 d^4 \ell_7 C_1 s^2 t (\ell_5 + k_4)^2}{\ell_5^2 (\ell_5 - k_1)^2 (\ell_5 - k_1 - k_2)^2 (\ell_5 + \ell_6)^2 \ell_6^2 (\ell_6 - k_4)^2} \times \frac{1}{(\ell_7 - \ell_5)^2 (\ell_7 + \ell_6)^2 (\ell_7 + k_4)^2 (\ell_7 - k_1 - k_2)^2}, \quad (1.5.29)$$

where  $C_1$  is defined in Eq. (1.3.32). There are two box subdiagrams in this case, both of which are highlighted in Fig. 1.11(e). We start with the top (red) box in Fig. 1.11,

which carries loop momentum  $\ell_7$ . The  $d\log$  form for this box subdiagram is

$$d\mathcal{I}_{\ell_7} = d\mathcal{I}_4 \left[ \begin{array}{cc} (\ell_7 - \ell_5)^2 & (\ell_7 + k_4)^2 \\ (\ell_7 + \ell_6)^2 & (\ell_7 - k_1 - k_2)^2 \end{array} \right]. \quad (1.5.30)$$

Using Eq. (1.2.21) and relabeling, we find that this box carries a normalization factor

$$J_7 = (\ell_5 + k_4)^2 (\ell_6 - k_3 - k_4)^2 - (\ell_5 - k_1 - k_2)^2 (\ell_6 - k_4)^2, \quad (1.5.31)$$

which then goes into the denominator of the remaining  $\ell_5, \ell_6$  forms. The  $\ell_6$  integrand form is a generalized box formed from the three bottom (light red) propagators in Fig. 1.11 and a generalized propagator  $J_7$ . We can then rewrite the  $\ell_6$  integrand form as a  $d\log$  form,

$$d\mathcal{I}_{\ell_6} = d\mathcal{I}_4 \left[ \begin{array}{cc} \ell_6^2 & (\ell_6 + \ell_5)^2 \\ (\ell_6 - k_4)^2 & [(\ell_5 + k_4)^2 (\ell_6 - k_3 - k_4)^2 - (\ell_5 - k_1 - k_2)^2 (\ell_6 - k_4)^2] \end{array} \right]. \quad (1.5.32)$$

The normalization required by this generalized box can be computed from the generic Jacobian formula (1.2.20) and gives

$$J_6 = s[(\ell_5 + k_4)^2]^2, \quad (1.5.33)$$

exactly matching Eq. (1.4.7) which was obtained by searching for double poles. This confirms that a factor  $(\ell_5 + k_4)^2$  is needed in the numerator of Eq. (1.5.29): it cancels the double pole in the remaining  $\ell_5$  form. After canceling the double propagator against the numerator factor, we then have the last box form:

$$d\mathcal{I}_{\ell_5} = d\mathcal{I}_4 \left[ \begin{array}{cc} \ell_5^2 & (\ell_5 + k_4)^2 \\ (\ell_5 - k_1)^2 & (\ell_5 - k_1 - k_2)^2 \end{array} \right]. \quad (1.5.34)$$

The final result for the integrand form of Eq. (1.5.29) is thus

$$d\mathcal{I}^{(e)} = C_1 d\mathcal{I}_{\ell_5} \wedge d\mathcal{I}_{\ell_6} \wedge d\mathcal{I}_{\ell_7}. \quad (1.5.35)$$

The derivation of a  $d\log$  form for this case is relatively straightforward, because at each step we encounter only generalized box forms.

As a less straightforward example, consider the nonplanar diagram (f) in Figs. 1.4 and 1.11, using the numerator  $\mathcal{KN}_1^{(f)}$  in Table 1.1. This integrand form is

$$d\mathcal{I}^{(f)} = \frac{d^4 \ell_5 d^4 \ell_6 d^4 \ell_7}{\ell_5^2 (\ell_5 - k_1)^2 (\ell_5 - k_1 - k_2)^2 \ell_7^2 (\ell_7 - k_3)^2 (\ell_5 + \ell_7 + k_4)^2} \frac{C_1 st(\ell_5 + k_4)^2 [(\ell_5 + k_3)^2 + (\ell_5 + k_4)^2]}{1} \times \frac{1}{\ell_6^2 (\ell_6 - \ell_5)^2 (\ell_6 - \ell_5 - k_4)^2 (\ell_6 + \ell_7)^2}, \quad (1.5.36)$$

where we include numerator  $N_1^{(f)}$  from Table 1.1. As indicated in Fig. 1.11 for diagram (f), there are two box subdiagrams that can be put into  $d\log$  form. We write the  $\ell_6$  and  $\ell_7$  forms as box-forms straight away:

$$\begin{aligned} d\mathcal{I}_{\ell_6} &= d\mathcal{I}_4 \left[ \begin{array}{cc} \ell_6^2 & (\ell_6 - \ell_5 - k_4)^2 \\ (\ell_6 + \ell_7)^2 & (\ell_6 - \ell_5)^2 \end{array} \right], \\ d\mathcal{I}_{\ell_7} &= d\mathcal{I}_4 \left[ \begin{array}{cc} \ell_7^2 & (\ell_7 + \ell_5 + k_4)^2 \\ (\ell_7 - k_3)^2 & [(\ell_5 + k_4)^2(\ell_5 + \ell_7)^2 - \ell_5^2(\ell_5 + \ell_7 + k_4)^2] \end{array} \right]. \end{aligned} \quad (1.5.37)$$

The  $\ell_6$  box introduced a Jacobian which is then used in the  $\ell_7$  box as a new generalized propagator. The remaining  $\ell_5$  form, including also the Jacobian from the  $\ell_7$  generalized box, is then a generalized pentagon form,

$$d\mathcal{I}_{\ell_5} = \frac{d^4 \ell_5 C_1 st [(\ell_5 + k_3)^2 + (\ell_5 + k_4)^2]}{\ell_5^2 (\ell_5 - k_1)^2 (\ell_5 - k_1 - k_2)^2 (\ell_5 \cdot q) (\ell_5 \cdot \bar{q})}, \quad (1.5.38)$$

where  $q = \lambda_3 \tilde{\lambda}_4$ ,  $\bar{q} = \lambda_4 \tilde{\lambda}_3$ . This generalized pentagon form is a relabeling of the one we encountered for the two loop nonplanar double box so we can write,

$$d\mathcal{I}_{\ell_5} = C_1 d\mathcal{I}_5^{X1} + C_2 d\mathcal{I}_5^{X2}, \quad (1.5.39)$$

where the forms  $d\mathcal{I}_5^{X1}$  and  $d\mathcal{I}_5^{X2}$  are defined in Eq. (1.5.26). The final result for  $d\mathcal{I}^{(f)}$  in Eq. (1.5.36) is then

$$d\mathcal{I}^{(f)} = C_1 d\mathcal{I}_{\ell_6} \wedge d\mathcal{I}_{\ell_7} \wedge d\mathcal{I}_5^{X1} + C_2 d\mathcal{I}_{\ell_6} \wedge d\mathcal{I}_{\ell_7} \wedge d\mathcal{I}_5^{X2}. \quad (1.5.40)$$

An even more complicated example is diagram (i) in Figs. 1.4 and 1.11. Consider the first term in numerator  $N_1^{(i)}$  in Table 1.1 given by  $(\ell_6 + k_4)^2 (\ell_5 - k_1 - k_2)^2$ . We will explicitly write the  $d\log$  form for this part of the integrand but not the remaining pieces for the sake of brevity. Putting back the overall normalization  $C_1 st$ , we have the integrand form

$$\begin{aligned} d\mathcal{I}_1^{(i)} &= \frac{d^4 \ell_5 d^4 \ell_6 d^4 \ell_7 C_1 st (\ell_6 + k_4)^2 (\ell_5 - k_1 - k_2)^2}{\ell_5^2 (\ell_5 - k_1)^2 \ell_6^2 (\ell_6 - k_3)^2 (\ell_6 + \ell_5 - k_1 - k_3)^2 (\ell_6 + \ell_5 + k_4)^2} \\ &\quad \times \frac{1}{\ell_7^2 (\ell_7 + k_4)^2 (\ell_7 - \ell_5)^2 (\ell_7 + \ell_6 + k_4)^2}. \end{aligned} \quad (1.5.41)$$

As in all other cases we start with a box subintegral. Here there is only a single choice, as highlighted in Fig. 1.11(i):

$$d\mathcal{I}_{\ell_7} = \frac{d^4 \ell_7 [(\ell_5 + k_4)^2 (\ell_6 + k_4)^2 - \ell_5^2 \ell_6^2]}{\ell_7^2 (\ell_7 + k_4)^2 (\ell_7 - \ell_5)^2 (\ell_7 + \ell_6 + k_4)^2} = d\mathcal{I}_4 \left[ \begin{array}{cc} \ell_7^2 & (\ell_7 - \ell_5)^2 \\ (\ell_7 + k_4)^2 & (\ell_7 + \ell_6 + k_4)^2 \end{array} \right]. \quad (1.5.42)$$

The  $\ell_6$  integrand form is then a generalized pentagon,

$$d\mathcal{I}_{\ell_6} = \frac{d^4 \ell_6 \, st(\ell_6 + k_4)^2}{\ell_6^2 (\ell_6 - k_3)^2 (\ell_6 + \ell_5 - k_1 - k_3)^2 (\ell_6 + \ell_5 + k_4)^2 [(\ell_5 + k_4)^2 (\ell_6 + k_4)^2 - \ell_5^2 \ell_6^2]} . \quad (1.5.43)$$

In principle we could follow a general pentagon decomposition procedure, but there is a simpler way to obtain the result. We can rewrite the numerator as

$$(\ell_6 + k_4)^2 = \frac{1}{(\ell_5 + k_4)^2} [(\ell_5 + k_4)^2 (\ell_6 + k_4)^2 - \ell_5^2 \ell_6^2] + \frac{\ell_5^2}{(\ell_5 + k_4)^2} \ell_6^2 . \quad (1.5.44)$$

After canceling factors in each term against denominator factors, we get two generalized box integrand forms. The decomposition is

$$d\mathcal{I}_1^{(i)} = C_1 d\mathcal{I}_{\ell_7} \wedge d\mathcal{I}_{\ell_6}^{(1)} \wedge d\mathcal{I}_{\ell_5}^{(1)} + C_3 d\mathcal{I}_{\ell_7} \wedge d\mathcal{I}_{\ell_6}^{(2)} \wedge d\mathcal{I}_{\ell_5}^{(2)} , \quad (1.5.45)$$

where the  $\ell_6$  integrand forms can be put directly into  $d\log$  forms:

$$\begin{aligned} d\mathcal{I}_{\ell_6}^{(1)} &= \frac{d^4 \ell_6 [(\ell_5 - k_1 - k_2)^2 (\ell_5 - k_1 - k_3)^2 - (\ell_5 + k_4)^2 (\ell_5 - k_1)^2]}{\ell_6^2 (\ell_6 - k_3)^2 (\ell_6 + \ell_5 - k_1 - k_3)^2 (\ell_6 + \ell_5 + k_4)^2} \\ &= d\mathcal{I}_4 \left[ \frac{\ell_6^2}{(\ell_6 - k_3)^2} \frac{(\ell_6 + \ell_5 + k_4)^2}{(\ell_6 + \ell_5 - k_1 - k_3)^2} \right] , \\ d\mathcal{I}_{\ell_6}^{(2)} &= \frac{d^4 \ell_6 (\ell_5 \cdot q)(\ell_5 \cdot \bar{q})(\ell_5 - k_1 - k_2)^2}{(\ell_6 - k_3)^2 (\ell_6 + \ell_5 - k_1 - k_3)^2 (\ell_6 + \ell_5 + k_4)^2 [(\ell_5 + k_4)^2 (\ell_6 + k_4)^2 - \ell_5^2 \ell_6^2]} \\ &= d\mathcal{I}_4 \left[ \frac{(\ell_6 - k_3)^2}{(\ell_6 + \ell_5 + k_4)^2} \frac{(\ell_6 + \ell_5 - k_1 - k_3)^2}{(\ell_5 + k_4)^2 (\ell_6 + k_4)^2 - \ell_5^2 \ell_6^2} \right] , \end{aligned} \quad (1.5.46)$$

with  $q = \lambda_2 \tilde{\lambda}_4$  and  $\bar{q} = \lambda_4 \tilde{\lambda}_2$ . Here we have normalized both integrand forms properly to have unit leading singularities so that they are  $d\log$  forms. As indicated in Eq. (1.5.45), the remaining  $\ell_5$  integrand forms are different for  $d\mathcal{I}_{\ell_6}^{(1)}$  and  $d\mathcal{I}_{\ell_6}^{(2)}$ .

Writing the integrand form for  $\ell_5$  following from  $d\mathcal{I}_{\ell_6}^{(1)}$ ,

$$\begin{aligned} d\mathcal{I}_{\ell_5}^{(1)} &= \frac{d^4 \ell_5 \, st(\ell_5 - k_1 - k_2)^2}{\ell_5^2 (\ell_5 - k_1)^2 (\ell_5 + k_4)^2 [(\ell_5 - k_1 - k_2)^2 (\ell_5 - k_1 - k_3)^2 - (\ell_5 + k_4)^2 (\ell_5 - k_1)^2]} \\ &= \frac{d^4 \ell_5 \, st(\ell_5 - k_1 - k_2)^2}{\ell_5^2 (\ell_5 - k_1)^2 (\ell_5 + k_4)^2 ((\ell_5 - k_1) \cdot q)((\ell_5 - k_1) \cdot \bar{q})} , \end{aligned} \quad (1.5.47)$$

where  $q = \lambda_2 \tilde{\lambda}_3$  and  $\bar{q} = \lambda_3 \tilde{\lambda}_2$ . In the last expression we used the fact that the quartic expression was a two-mass-easy Jacobian of the  $\ell_6$  integrand, which factorizes into a product. Up to relabeling, this is the same integrand as the first nonplanar pentagon

form in Eq. (1.5.26), and we can write it as the  $d\log$  form

$$d\mathcal{I}_{\ell_5}^{(1)} = d\log \frac{(\ell_5 - k_1)^2}{((\ell_5 - k_1) \cdot \bar{q})} d\log \frac{\ell_5^2}{((\ell_5 - k_1) \cdot \bar{q})} d\log \frac{(\ell_5 + k_4)^2}{((\ell_5 - k_1) \cdot q)} d\log \frac{(\ell_5 - \ell_5^*)^2}{((\ell_5 - k_1) \cdot q)}, \quad (1.5.48)$$

where  $q = \lambda_3 \tilde{\lambda}_2$ ,  $\bar{q} = \lambda_2 \tilde{\lambda}_3$  and  $\ell_5^* = \frac{\langle 32 \rangle}{\langle 31 \rangle} \lambda_1 \tilde{\lambda}_2$ . For the second integrand form in Eq. (1.5.46), the remaining  $\ell_5$  integral is (for  $q = \lambda_2 \tilde{\lambda}_4$  and  $\bar{q} = \lambda_4 \tilde{\lambda}_2$ ) just a generalized box and can be directly written as the  $d\log$  form,

$$d\mathcal{I}_{\ell_5}^{(2)} = \frac{d^4 \ell_5 \, ut}{(\ell_5 - k_1)^2 (\ell_5 + k_4)^2 (\ell_5 \cdot q) (\ell_5 \cdot \bar{q})} = d\mathcal{I}_4 \left[ \begin{array}{c} (\ell_5 - k_1)^2 \ (\ell_5 \cdot q) \\ (\ell_5 + k_4)^2 \ (\ell_5 \cdot \bar{q}) \end{array} \right]. \quad (1.5.49)$$

To obtain this, we used the relation  $sC_1 = uC_3$  to write  $C_3$  as the overall factor of the second term in the assembled result given in Eq. (1.5.45).

We have carried out similar procedures on all contributions to the three-loop four-point amplitude, except for the relatively complicated case of diagram (h). In all these cases we find explicit  $d\log$  forms. These checks directly confirm that there are only logarithmic singularities in the integrand, as we found in Sect. 1.4. At relatively low loop orders, detailed analysis of the cut structure, as carried out in Sect. 1.4, provides a straightforward proof of this property. At higher loop orders, the space of all possible singularities grows rapidly and finding  $d\log$  forms, as we did in the present section, becomes a more practical way of showing that there are only logarithmic singularities. Even so, one cannot completely avoid detailed checks of the singularity structure because, in general,  $d\log$  forms do not necessarily make manifest that there are no poles at infinity.

## 1.6 Logarithmic singularities at higher loops

Complete, unintegrated four-point  $\mathcal{N} = 4$  sYM amplitudes, including their nonplanar parts, have been obtained at four and five loops in Refs. [129, 133, 141]. In principle, we could repeat the same procedure we did for three loops at higher loops to construct  $d\log$  numerators. However, the number of parent diagrams grows: at four loops there are 85 diagrams and by five loops there are 410 diagrams. Many of the diagrams are simple generalizations of the already analyzed three-loop diagrams, so their analysis is straightforward. Some, however, are new topologies, for which an exhaustive search for double or higher poles and poles at infinity would be nontrivial. Such an analysis would require either a more powerful means of identifying numerators with the desired properties, or computer automation to sweep through all dangerous kinematic regions of the integrands while looking for unwanted singularities. This of course is an interesting problem for the future.



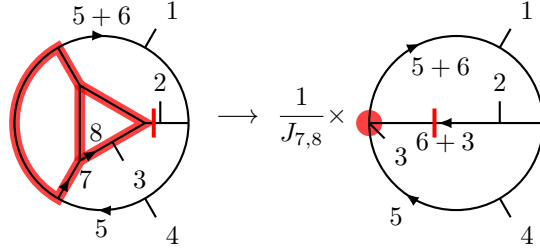


**Figure 1.12.** The left diagram contributes to the four-loop four-point  $\mathcal{N} = 4$  sYM amplitude [133]. The shaded (red) lines indicate propagators that are replaced by on-shell conditions as given in Eq. (1.6.1). These propagators are removed from the diagram and leave behind an inverse Jacobian, given in Eq. (1.6.2). The resulting simplified diagram is given on the right. The vertical shaded (red) line crossing the propagator carrying momentum  $\ell_6 + k_3$  indicates that it too is replaced with an on-shell condition at the start of this process.

Here we take initial steps at higher loops, investigating sample four- and five-loop cases to provide supporting evidence that only logarithmic singularities are present in the nonplanar sector. We do so by showing compatibility between  $d\log$  numerators and known expressions for the amplitudes [133, 141] on maximal cuts.

As a first example, consider the nonplanar four-loop diagram on the left in Fig. 1.12. We wish to show that the maximal cuts are compatible with a numerator that ensures only logarithmic singularities and no poles at infinity. Since this diagram has a hexagon subdiagram carrying loop momentum  $\ell_6$  and a pentagon subdiagram carrying loop momentum  $\ell_5$ , the overall dimensionality and asymptotic scaling constraints of Sect. 1.3 require  $N^{4\text{-loop}} \sim \mathcal{O}((\ell_6)^4, (\ell_5)^2)$ .

In order to derive the desired numerator for this diagram, we use the cut sequence

$$\text{cuts} = \{(\ell_6 + k_3)^2, B(\ell_8), B(\ell_7, \ell_7 - k_3)\}, \quad (1.6.1)$$

where the notation is defined in Sect. 1.2.3. The first cut setting  $(\ell_6 + k_3)^2 = 0$  is indicated in Fig. 1.12 by the vertical shaded (red) line crossing the corresponding propagator. The remaining cuts leave behind Jacobians; the propagators placed on-shell by these cuts are indicated by the shaded (red) thick lines. The resulting Jacobian is

$$J_{7,8} = (\ell_5 - k_3)^2 [\ell_6^2]^2. \quad (1.6.2)$$

Since the Jacobian appears in the denominator, this gives us an unwanted double pole in the integrand when  $\ell_6^2 = 0$ . Thus, to remove it on the cuts (1.6.1) we require the numerator be proportional to  $\ell_6^2$ :

$$N^{4\text{-loop}}(\ell_5, \ell_6)|_{\text{cut}} = \ell_6^2 \tilde{N}^{4\text{-loop}}(\ell_5, \ell_6)|_{\text{cut}}. \quad (1.6.3)$$

After canceling one factor of  $\ell_6^2$  from the Jacobian in Eq. (1.6.2) against a factor in the numerator, we can use the remaining  $\ell_6^2$  or  $(\ell_5 - k_3)^2$  from the Jacobian together with the remaining uncut propagators on the right of Fig. 1.12 to give two distinct relabelings of the two-loop nonplanar diagram in Fig. 1.3(b), if we also cancel the other propagator factor coming from the Jacobian. We then relabel the  $d\log$  numerators for the two-loop nonplanar diagram in Eq. (1.3.30) to match the labels of the simplified four-loop diagram on the right in Fig. 1.12. Including factors to cancel the double pole and unwanted Jacobian factor, we have two different  $d\log$  numerators for the four-loop diagram of Fig. 1.12:

$$\begin{aligned} N_1^{4\text{-loop}}(\ell_5, \ell_6)|_{\text{cut}} &= \ell_6^2(\ell_5 - k_3)^2 [(\ell_6 - k_4)^2 + (\ell_6 - k_1)^2]|_{\text{cut}}, \\ N_2^{4\text{-loop}}(\ell_5, \ell_6)|_{\text{cut}} &= [\ell_6^2]^2 [(\ell_5 - k_2 - k_3)^2 + (\ell_5 - k_1 - k_3)^2]|_{\text{cut}}. \end{aligned} \quad (1.6.4)$$

The integrands with these numerators then have only logarithmic singularities and no poles at infinity in the kinematic region of the cut, as inherited from the two-loop nonplanar double box.

Are these  $d\log$  numerators compatible with the known four-loop amplitude? Relabeling the numerator of the corresponding diagram 32 in Fig. 23 of Ref. [133] to match our labels, we see that a valid numerator that matches the maximal cuts is

$$N_{\text{old}}^{4\text{-loop}} = \ell_6^2(s\ell_6^2 - t(\ell_5 - k_3)^2 - s(\ell_6 + \ell_5)^2). \quad (1.6.5)$$

To check compatibility with our  $d\log$  numerators we take the maximal cut, replacing all propagators with on-shell conditions. This selects out a piece unique to this diagram.<sup>5</sup> On the maximal cut, Eq. (1.6.5) simplifies to

$$N_{\text{old}}^{4\text{-loop}}\Big|_{\text{max cut}} = \ell_6^2(s\ell_6^2 + t(2\ell_5 \cdot k_3)) = \left(N_1^{4\text{-loop}} - N_2^{4\text{-loop}}\right)\Big|_{\text{max cut}}. \quad (1.6.6)$$

This shows that the maximal cut of diagram 32 with the old numerator is a linear combination of the maximal cut of diagram 32 with the two  $d\log$  numerators in Eq. (1.6.4). We note that by following through the modified rung rule of Sect. 1.4.3, we obtain the same coefficients as those determined from the maximal cuts.

Next consider a five-loop example: the nonplanar five-loop diagram on the left of Fig. 1.13. As in the four-loop case, we identify potential double poles by choosing a sequence of cuts that uncovers a lower-loop embedding for which a  $d\log$  numerator is already known. Our order of taking cuts is

$$\text{cuts} = \{B(\ell_7), B(\ell_9, \ell_9 + k_1)\}, \quad (1.6.7)$$

---

<sup>5</sup>Other diagrams do not mix with the one under consideration if we use all solutions to the maximal cut.

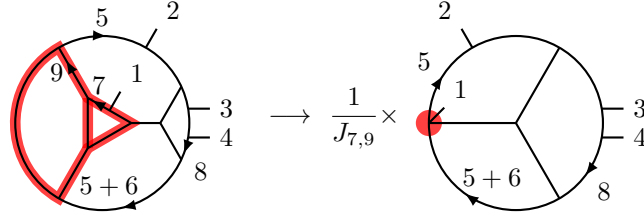


**Figure 1.13.** The left diagram contributes to the five-loop four-point  $\mathcal{N} = 4$  sYM amplitude [141]. The shaded (red) lines indicate propagators that are replaced by on-shell conditions as given in Eq. (1.6.1). These propagators are removed from the diagram and leave behind an inverse Jacobian, given in Eq. (1.6.8). The resulting simplified diagram is given on the right. The factor  $\ell_6^2$  in the Jacobian can be used to expand the shaded (red) region, resulting in a graph isomorphic to the three-loop diagram Fig. 1.4(g).

resulting in the Jacobian

$$J_{7,9} = \ell_6^2 [\ell_6^2(\ell_5 + k_1)^2 - \ell_5^2(\ell_6 - k_1)^2]. \quad (1.6.8)$$

Collecting the  $\ell_6^2$ -factor of this Jacobian with the remaining uncut propagators reproduces a relabeling of three-loop diagram (g), with numerator given in Eq. (1.4.32). To ensure this five-loop nonplanar integrand has a  $d\log$  numerator, we require the numerator to cancel the Jacobian, as well as to contain a factor of the three-loop numerator,

$$N^{(g)} = -s(\ell_8 - \ell_5)^2 + (\ell_5 + k_1)^2 [(\ell_8 - k_1)^2 + (\ell_8 - k_2)^2], \quad (1.6.9)$$

obtained from Eq. (1.4.32) and relabeled to match Fig. 1.13. We have not included the last three terms in the numerator given in Eq. (1.4.32), because they vanish on maximal cuts, which we impose below in our compatibility test. Here we are not trying to find all  $d\log$  numerators, but just those that we can use for testing compatibility with the known results. Combining the Jacobian (1.6.8) with the relabeled numerator  $N^{(g)}$  gives a valid  $d\log$  numerator,

$$N^{5\text{-loop}}|_{\text{cut}} = [\ell_6^2(\ell_5 + k_1)^2 - \ell_5^2(\ell_6 - k_1)^2] N^{(g)}|_{\text{cut}}. \quad (1.6.10)$$

A straightforward exercise then shows that on the maximal cut of the five-loop diagram in Fig. 1.13,  $N^{5\text{-loop}}$  matches the numerator from Ref. [141]:

$$N^{5\text{-loop}}|_{\text{cut}}^{\text{max}} = N_{\text{old}}^{5\text{-loop}}|_{\text{cut}}^{\text{max}} = -\frac{1}{2}s(\ell_8 \cdot k_1)(\ell_6 \cdot k_1)(\ell_5 \cdot k_1). \quad (1.6.11)$$

Here we have compared to diagram 70 of the ancillary file of Ref. [141] and shifted momentum labels to match ours. Again the modified rung rule matches the  $\ell_6^2(\ell_5 + k_1)^2$  term, which is the only non-vanishing contribution to  $N^{5\text{-loop}}$  on the maximal cut.

We have also checked a variety of other four- and five-loop examples. These provide higher-loop evidence that we should find only logarithmic singularities and no poles at infinity. We build on this theme in the next section by considering the consequences of  $d\log$  numerators at high loop-order in the planar sector.

## 1.7 Back to the planar integrand

How powerful is the requirement that an expression has only logarithmic singularities and no poles at infinity? To answer this we re-examine the planar sector of  $\mathcal{N} = 4$  sYM theory and argue that these requirements on the singularity structure are even more restrictive than dual conformal invariance. Specifically we make the following conjecture:

- Logarithmic singularities and absence of poles at infinity imply dual conformal invariance of local integrand forms to all loop orders in the planar sector.

To give supporting evidence for this conjecture, as well as to show that the constraints on the singularities are even stronger than implied by dual conformal symmetry, we work out a variety of nontrivial examples. In particular, we show in detail that at three- and four-loops the singularity conditions exactly select the dual conformal invariant integrand forms that appear in the amplitudes. We also look at a variety of other examples through seven loops. This conjecture means that by focusing on the singularity structure we can effectively carry over the key implications of dual conformal symmetry to the nonplanar sector even if we do not know how to carry over the symmetry itself. This suggests that there may be some kind of generalized version of dual conformal symmetry for the complete four-point amplitudes in  $\mathcal{N} = 4$  sYM theory, including the nonplanar sector. At the integrated level dual conformal symmetry leads to powerful anomalous Ward identities that constrain planar amplitudes [50]. An interesting question is whether anything analogous can be found for nonplanar amplitudes. We put off further speculation on these points until future work.

We also show that the conditions of no double poles are even more constraining than dual conformal symmetry. In fact, we demonstrate that the singularity constraints explain why certain dual conformal numerators cannot appear in the  $\mathcal{N} = 4$  sYM integrand. We describe simple rules for finding non-logarithmic poles in momentum twistor space. These rules follow the spirit of Ref. [48] and allow us to restrict the set of dual conformal numerators to a smaller subset of potential  $d\log$  numerators. While these rules do not fully eliminate all dual conformal numerators that lead to unwanted double poles, they offer a good starting point for finding a basis of  $d\log$  numerators.

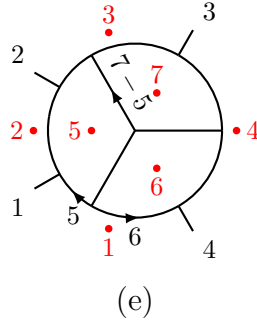


**Figure 1.14.** The planar three-loop diagram (e), including shaded (red) dots and labels to indicate the face or dual variables.

Furthermore, we give explicit examples at five and six loops where the pole constraints not only identify contributions with zero coefficient but also explain nonvanishing relative coefficients between various dual conformally invariant contributions. From this perspective, requiring only logarithmic singularities is a stronger constraint than requiring dual conformal symmetry.

In our study we use the four-loop results from Ref. [142] and results through seven-loops from Ref. [121]. Equivalent results at five and six loops can be found in Refs. [138, 144, 145].

### 1.7.1 Brief review of dual conformal invariance

Dual conformal symmetry [41–43] has been extensively studied for planar  $\mathcal{N} = 4$  sYM amplitudes. For a detailed review, see Ref. [13, 14]. Here we only require the part useful for multiloop four point amplitudes, which we briefly review. Dual or region variables are the natural variables to make dual conformal symmetry manifest. To indicate the dual variables, we draw graphs in momentum space with the corresponding dual faces marked with a shaded (red) dot and labeled with a shaded (red) number. This is illustrated in Fig. 1.14.

We define the relation between external momenta  $k_i$  and external dual variables (region momenta)  $x_i$  as

$$k_i = x_{i+1} - x_i, \quad i = 1, 2, 3, 4, \quad x_5 \equiv x_1. \quad (1.7.1)$$

In term of dual variables, the Mandelstam invariants are

$$s = (k_1 + k_2)^2 \equiv x_{13}^2, \quad t = (k_2 + k_3)^2 \equiv x_{24}^2. \quad (1.7.2)$$

The internal faces are parametrized by additional  $x_j$ , with  $j = 5, 6, \dots, 4 + L$  corresponding to loop momenta. In terms of the dual coordinates, loop momenta are defined

from the diagrams as:

$$\ell = x_{\text{right}} - x_{\text{left}}, \quad (1.7.3)$$

where  $x_{\text{right}}$  is the dual coordinate to the right of  $\ell$  when traveling in the direction of  $\ell$ , and  $x_{\text{left}}$  is the dual coordinate to the left of  $\ell$  when traveling in the direction of  $\ell$ .

The key symmetry property of the integrand forms is invariance under inversion,  $x_i^\mu \rightarrow x_i^\mu/x_i^2$  so that

$$x_{ij}^2 \rightarrow \frac{x_{ij}^2}{x_i^2 x_j^2}, \quad d^4 x_i \rightarrow \frac{d^4 x_i}{x_i^2}. \quad (1.7.4)$$

We say that a four-point planar integrand form is dual conformally invariant if  $d\mathcal{I} \rightarrow d\mathcal{I}$  under this transformation.

### 1.7.2 Dual conformal invariance at three and four loops

First consider three loops. There are two planar diagrams, diagrams (a) and (e) in Fig. 1.4. Diagram (a) is a bit trivial because the numerator does not contain any loop momenta, so we do not discuss it in any detail. Diagram (e), together with its face variables, is shown in Fig. 1.14. The only allowed  $d\log$  numerator for this diagram is given in Eq. (1.4.32) and Table 1.1. Written in dual coordinates, it is

$$N^{(e)} = s(\ell_5 + k_4)^2 = x_{13}^2 x_{45}^2. \quad (1.7.5)$$

This numerator exactly matches the known result [35, 120] for the three-loop planar amplitude consistent with dual conformal symmetry [41], giving (somewhat trivial) evidence for our conjecture. When counting the dual conformal weights via Eq. (1.7.4), we need to account for the factor of  $st = x_{13}^2 x_{24}^2$  in the prefactor  $\mathcal{K}$  defined in Eq. (1.3.22). We note that the conditions of logarithmic singularities do not fix the overall prefactor of  $s$ , but such loop momentum independent factors are easily determined from maximal cut or leading singularity constraints when expanding the amplitude.

A more interesting test of our conjecture starts at four loops. We construct a basis of  $d\log$ -integrand for the planar amplitude following the same techniques we used at three loops. We then compare these to known results for the amplitude that manifest dual conformal invariance [142]. Following the algorithm of Sect. 1.3, we define trivalent parent diagrams. These are given in Fig. 1.15.

We have constructed all  $d\log$  numerators for the four-loop four-point planar amplitude. To illustrate this construction, consider first diagram (4c) of Fig. 1.15. This is a particularly simple case, because it follows from taking diagram (e) at three loops in Fig. 1.14 and forming an additional box by inserting an extra propagator between two external lines. The extra box introduces only a factor of  $s$  to the three-loop numerator  $N^{(e)}$ .

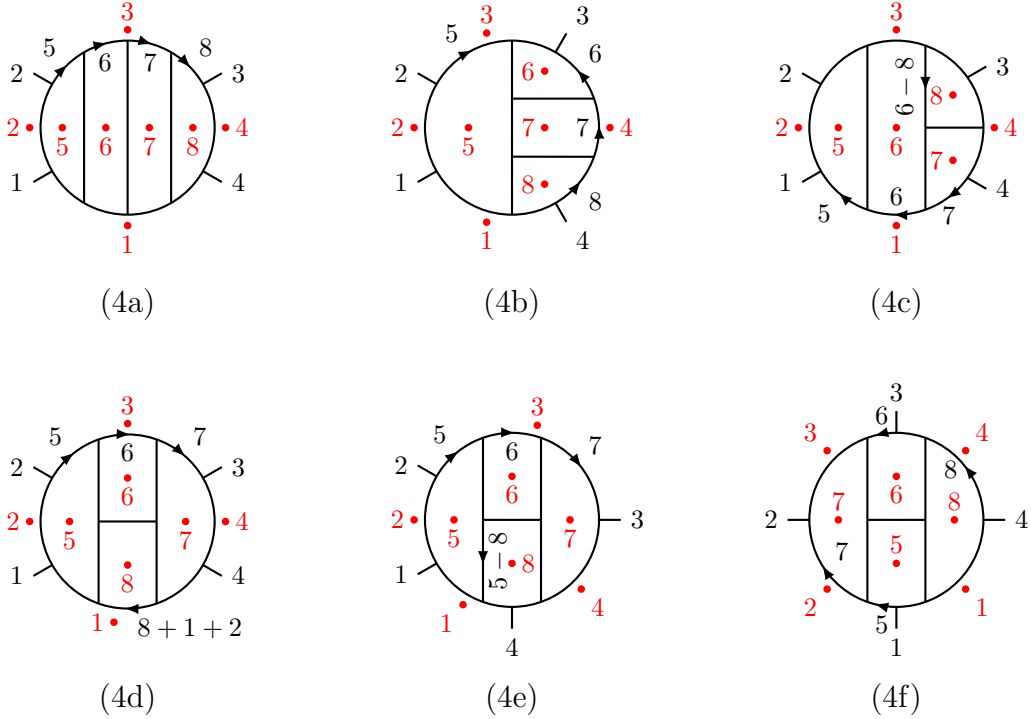


**Figure 1.15.** Parent diagrams contributing to the four-loop planar amplitude. The shaded (red) dots indicate the face or dual labels of the planar graph.

This then gives us the four loop numerator

$$N^{(4c)} = s N^{(e)}|_{\ell_5 \rightarrow \ell_6} = (x_{13}^2)^2 x_{46}^2, \quad (1.7.6)$$

where the relabeling  $\ell_5 \rightarrow \ell_6$  changes from the three-loop diagram (e) labels of Fig. 1.4 to the four-loop labels of diagram (4c).

As a more complicated example, consider diagram (4d) of Fig. 1.15. This contains two pentagon subdiagrams parametrized by  $\ell_5$  and  $\ell_7$  and so has a numerator scaling as  $N^{(4d)} \sim \mathcal{O}(\ell_5^2, \ell_7^2)$ . We skip the details here, and just list the two<sup>6</sup> independent numerators that result from applying all  $d\log$ -conditions:

$$N_1^{(4d)} = s^2 (\ell_5 - \ell_7)^2 = (x_{13}^2)^2 x_{57}^2, \quad (1.7.7)$$

$$N_2^{(4d)} = s \ell_7^2 (\ell_5 + k_1 + k_2)^2 = x_{13}^2 x_{37}^2 x_{15}^2 \longrightarrow N^{(4d_2)} = x_{13}^2. \quad (1.7.8)$$

In Eq. (1.7.8), we have indicated that the numerator  $N_2^{(4d)}$  cancels two propagators to produce exactly Fig. 1.16 (4d<sub>2</sub>), with numerator  $N^{(4d_2)}$ . The numerator  $N_1^{(4d)}$  is one of

<sup>6</sup>There is a third numerator  $s \ell_7^2 (\ell_5 + k_1 + k_2)^2$  that is a relabeling of  $N_2^{(4d)}$  under automorphisms of diagram (4d). Here and below we omit such relabelings.

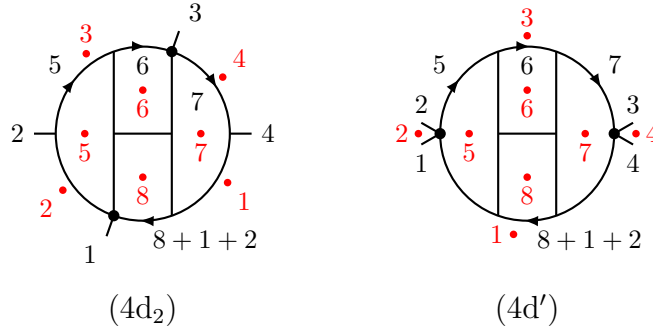


**Figure 1.16.** Diagram (4d<sub>2</sub>) contributes to the planar amplitude at four-loops. Diagram (4d') does not. Shaded (red) dots represent dual coordinates. Black dots represent contact terms.

the known dual conformal numerators, and the lower-propagator diagram Fig. 1.16(4d<sub>2</sub>) is also a well-known dual conformal diagram.

Interestingly, dual conformal invariance allows two additional numerators:

$$N_3^{(4d)} = x_{13}^2 x_{27}^2 x_{45}^2, \quad (1.7.9)$$

$$N_4^{(4d)} = x_{13}^2 x_{25}^2 x_{47}^2 \longrightarrow N^{(4d')} = x_{13}^2, \quad (1.7.10)$$

where again  $N_4^{(4d)}$  reduces to diagram (4d') in Fig. 1.16 upon canceling propagators. These two numerators do not meet the no double poles and no poles at infinity constraints. This is not a coincidence and fits nicely with the fact that these two numerators have zero coefficient in the amplitude [48, 142].

The other diagrams are similar, and we find that for all cases the  $d$ log-requirement selects out the dual conformal planar integrands that actually contribute to the amplitude and rejects those that do not. Our analysis also proves that, at least for this amplitude, each dual conformally invariant term in the amplitudes, as given in Ref. [142], is free of non-logarithmic singularities and poles at infinity.

### 1.7.3 Simple rules for eliminating double poles

In the previous subsection, we highlighted the relationship between dual conformal invariance and the singularity structure of integrands. Here we go further and demonstrate that the requirement of having no other singularities than logarithmic ones puts tighter constraints on the integrand than dual conformal symmetry.

We start from the observation of Drummond, Korchemsky, and Sokatchev (DKS) [48] that certain integrands upon integration are not well defined in the infrared, even with external off-shell legs. They found that if any set of four loop variables  $\{x_{i_1}, x_{i_2}, x_{i_3}, x_{i_4}\}$



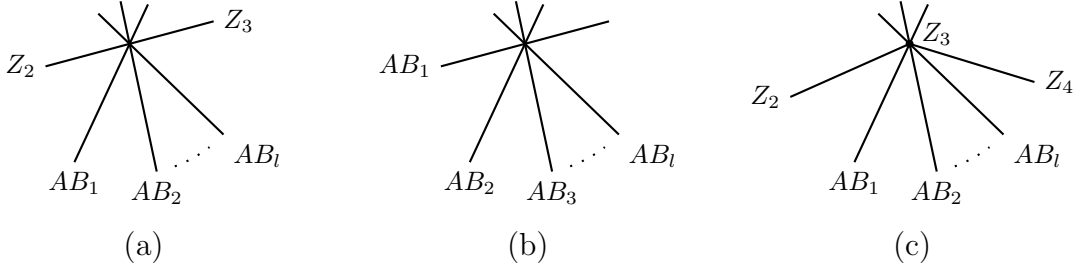


**Figure 1.17.** Cut configurations in momentum twistor geometry. Our type I conditions correspond to (b), type II to (a) and type III to (c).

approach the same external point  $x_j$  such that  $\rho^2 = x_{i_1j}^2 + x_{i_2j}^2 + x_{i_3j}^2 + x_{i_4j}^2 \rightarrow 0$  and the integrand scales as

$$d\mathcal{I} = \frac{d^4x_{i_1} \cdots d^4x_{i_4} N(x_i)}{D(x_i)} \sim \frac{d\rho}{\rho}. \quad (1.7.11)$$

The singularity  $\rho \rightarrow 0$  corresponds to an integrand double pole in our language, as we shall see below. The singularity (1.7.11) occurs in the region of integration and results in an infrared divergent integral even for off-shell external momenta. It is therefore not a sensible dual conformal integral. Such ill-defined integrals should not contribute, as DKS confirmed in various examples, leading to their all loop order conjecture [48]. A trivial generalization is to group  $l$  loop variables at a time,  $\rho^2 = x_{i_1j}^2 + x_{i_2j}^2 + \cdots + x_{i_lj}^2 \rightarrow 0$ . Again the requirement is that the integral not be divergent with off-shell external momenta. Of course, this rule was not meant to explain all vanishings of coefficients nor to explain why terms appear in certain linear combinations.

Here we wish to extend this line of reasoning using our new insight into the singularity structure of amplitudes. For this exercise it is convenient to switch to momentum twistor coordinates, for which the problem of approaching certain dangerous on-shell kinematic regions becomes purely geometric; see Ref. [47, 146] for a discussion of momentum twistor geometry. To facilitate comparisons to existing statements in the literature, we translate the results back to dual coordinates (region momenta) at the end.

First we rewrite the DKS observation in momentum twistor variables. To be concrete, we can take  $x_j = x_3$  to be the designated external point, but in fact there is nothing special about that choice. Consider the case of  $l$  loop variables. The  $l$  loop variables  $\{x_{i_1}, \dots, x_{i_l}\}$  correspond to  $l$  lines  $(AB)_1, \dots, (AB)_l$  in momentum twistor space. In our notation, the point  $x_3$  in dual coordinates corresponds to the line  $Z_2Z_3$  in momentum twistor space. Geometrically, the condition  $\rho^2 \rightarrow 0$  corresponds to a configuration in

momentum twistor space for which all  $l$  lines intersect the line  $Z_2Z_3$  at the same point, as in Fig. 1.17(a).

If we parametrize

$$A_i = Z_2 + \rho_i Z_3 + \sigma_i Z_4, \quad (1.7.12)$$

where  $\rho_i, \sigma_i$  are free parameters, then setting  $\rho_i = \rho^*$  and  $\sigma_i = 0$  results in the desired configuration, where  $\rho^*$  is arbitrary but the same for all  $i$ . We use a collective coordinate:

$$\rho_1 = \rho^*, \quad \rho_j = \rho^* + t\tilde{\rho}_j, \quad \sigma_i = \tilde{\sigma}_i t, \quad (1.7.13)$$

for  $j = 2, \dots, l$  and  $i = 1, \dots, l$ , which sets all parameters to the desired configuration in the limit  $t \rightarrow 0$ . In this limit, the measure scales as

$$\prod_{i=1, j=2}^l d\rho_j d\sigma_i \sim t^{2l-2} dt, \quad (1.7.14)$$

and all propagators of the form  $\langle (AB)_i (AB)_j \rangle$  and  $\langle (AB)_i Z_2 Z_3 \rangle$  scale like  $t$ . The result is that the integrand behaves as

$$d\mathcal{I} = \prod_{i=1, j=2}^l d\rho_j d\sigma_i \frac{N(\rho_j, \sigma_i)}{D(\rho_j, \sigma_i)} \sim dt t^{2l-2} \cdot \frac{t^N}{t^P} = \frac{dt}{t^{P-N-2l+2}}, \quad (1.7.15)$$

where  $N(t) \sim t^N$  is the behavior of the numerator in this limit and  $D(t) \sim t^P$  is the behavior of the denominator, meaning that  $P$  is the number of propagators that go to zero as  $t \rightarrow 0$ . To avoid unwanted double or higher poles, we demand that  $P < N + 2l$ . Note the shift by one in the counting rules with respect to Eq. (1.7.11). That equation counts overall scaling in the integration, while we study singularities in the integrand in an inherently on-shell manner. Either way we arrive at the same conclusion.

As an example consider diagram (4d). One of the numerators is  $N_1^{(4d)} = (x_{13})^2 x_{57}^2$  and so has  $N = 1$ , while there are  $l = 4$  loops, and there are a total of  $P = 8$  propagators of the form  $\langle (AB)_i (AB)_j \rangle$  and  $\langle (AB)_i Z_2 Z_3 \rangle$ . In this case

$$P = 8 < 9 = 1 + 2 \cdot 4 = N + 2l, \quad (1.7.16)$$

and so the numerator is allowed by this double pole constraint. In fact, both numerators  $N_1^{(4d)}$  and  $N_2^{(4d)}$  from Eqs. (1.7.7) and (1.7.8) have the same values of  $P, l$ , and  $N$ , and so each passes this double pole test and has only single poles. In contrast, the numerators  $N_3^{(4d)}$  and  $N_4^{(4d)}$  from Eqs. (1.7.9) and (1.7.10) have  $N = 0$  and fail the inequality, so they have double poles and do not contribute to the amplitude.

Now we can generalize this and consider two similar cases: all lines  $(AB)_i$  intersect at a generic point as in Fig. 1.17(b), or all lines intersect at a given external point as

in Fig. 1.17(c). The crux of the argument is the same as the first: if the integrand has a double pole we reject it. The resulting inequalities to avoid these singularities follow analogously; the only difference with the first case is the geometric issue of how many of the  $l$  lines are made to intersect. We summarize the results in terms of  $N$ , the number of numerator factors that vanish,  $P$ , the number of vanishing propagators, and the subset of  $l$  loop dual coordinates  $\{x\}_L \equiv \{x_{i_1}, \dots, x_{i_l}\}$ . Corresponding to each of the diagrams in Fig. 1.17, we obtain three types of conditions:

- Type I (Fig. 1.17(b)):

$$P < N + 2l - 2, \quad (1.7.17)$$

in the limit that loop dual coordinates are light-like separated from each other:  $x_{ij}^2 = 0$  for all  $x_i, x_j \in \{x\}_L$ .

- Type II (Fig. 1.17(a)):

$$P < N + 2l, \quad (1.7.18)$$

in the limit that loop dual coordinates are light-like separated from each other and from one external point:  $x_{ij}^2 = x_{ki}^2 = 0$  for all  $x_i, x_j \in \{x\}_L$ ,  $k = 1, 2, 3, 4$

- Type III (Fig. 1.17(c)):

$$P < N + 2l + 1, \quad (1.7.19)$$

in the limit that loop dual coordinates are light-like separated from each other and from two external points:  $x_{ij}^2 = x_{ki}^2 = x_{k'i}^2 = 0$ , for all  $x_i, x_j \in \{x\}_L$ ,  $k, k' = 1, 2, 3, 4$ .<sup>7</sup>

These rules prevent certain classes of non-logarithmic singularities from appearing. In the four-loop case, these rules are sufficient to reconstruct all dual conformal numerators, automatically precluding those that do not contribute to the amplitude. Up to seven loops, we used a computer code to systematically check that all contributions to the amplitude pass the above rules. Furthermore, we were able to explain all coefficient zero diagrams up to five loops and many coefficient zero diagrams up to seven loops using these rules and the available data provided in Ref. [121]. In the next subsection we give examples illustrating the above three conditions in action, as well as examples of non-logarithmic singularities not detected by these tests. Not surprisingly, as the number of loops increases there are additional types of nonlogarithmic singularities. Indeed, at sufficiently high loop order we expect that cancellations of unwanted singularities can involve multiple diagrams.

---

<sup>7</sup>The equations  $x_{ki}^2 = x_{k'i}^2 = 0$  have two solutions so we have to choose the same solution for all  $x_i$ .

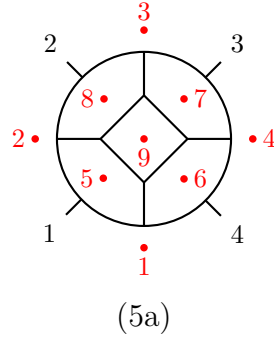


**Figure 1.18.** A sample five-loop planar diagram. Shaded (red) dots and labels represent dual coordinates.

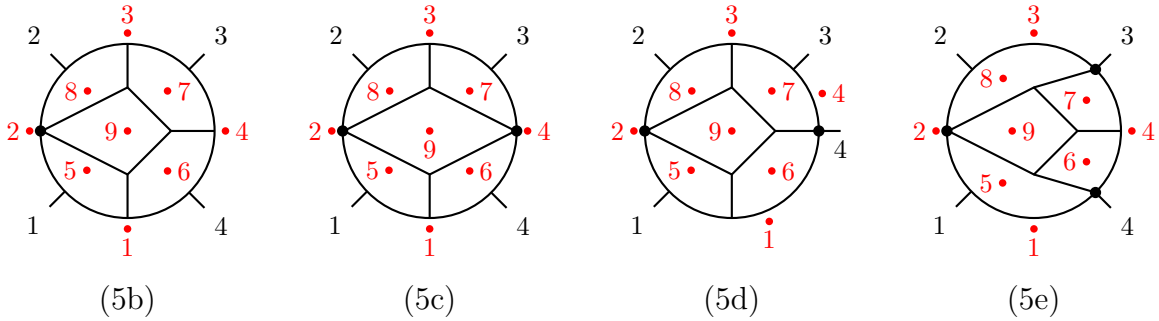


**Figure 1.19.** Descendants of the five-loop planar diagram of Fig. 1.18 with numerator coefficients determined to be *non-zero* by testing for non-logarithmic singularities.

#### 1.7.4 Applications of three types of rules

We now consider three examples to illustrate the rules. First we examine a five-loop example where the rules forbid certain dual conformal numerators from contributing to the amplitude. We will see in that example that double poles beyond the scope of the above three rules determine relative coefficients between integrands consistent with the reference data [121, 138]. We then consider two different six-loop diagrams that have zero coefficient in the expansion of the amplitude. In the first example, the three rules are sufficient to determine that the numerator has zero coefficient in the amplitude, while the integrand in the second example has hidden double poles not accounted for by the rules.

We first consider the diagram of Fig. 1.18. We take a slightly different approach here than in previous subsections. First we list the set of all dual conformal numerators allowed by power counting, and then eliminate numerators that do not pass the three

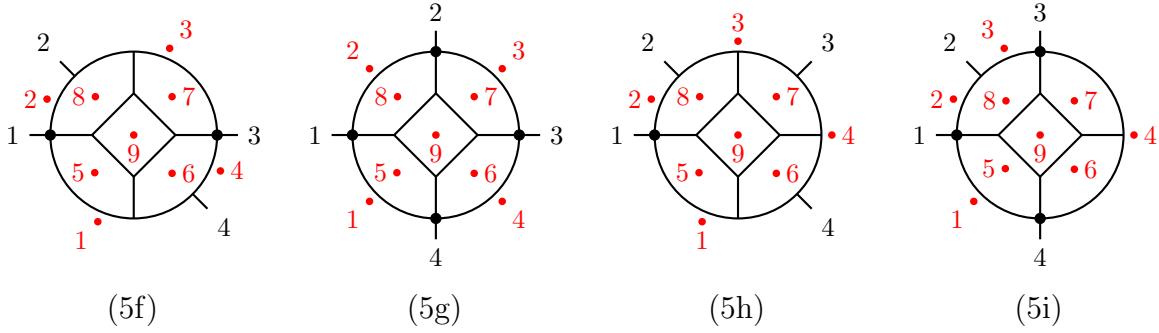


**Figure 1.20.** Descendants of the five-loop planar diagram of Fig. 1.18 with numerator coefficients determined to be *zero* by testing positive for non-logarithmic singularities.

rules of the previous subsection.

The dual conformal numerators that do not collapse any propagators in Fig. 1.18 are

$$\begin{aligned} N_1^{(5a)} &= x_{24}^2 x_{35}^2 x_{17}^2 x_{68}^2, & N_2^{(5a)} &= -x_{13}^2 x_{24}^2 x_{57}^2 x_{68}^2, \\ N_3^{(5a)} &= x_{18}^2 x_{27}^2 x_{36}^2 x_{45}^2, \end{aligned} \quad (1.7.20)$$

where we omit any dual conformal numerators that are relabelings of these numerators under automorphisms of the diagram. These three numerators correspond to diagrams 21, 22 and 35, respectively, of Ref. [138]. However, notice that in the notation used here an overall factor of  $st = x_{13}^2 x_{24}^2$  has been stripped off. For the three kinematic conditions of the rules, this diagram has three different values of  $P$ :

$$P_I = 8, \quad P_{II} = 10, \quad \text{and} \quad P_{III} = 12, \quad (1.7.21)$$

where the subscript denotes the kinematic case we consider. The type I kinematics is most constraining in this example, and for  $l = 5$  requires  $N > 0$ . Converting this back to a statement about the numerator, we conclude that all  $d\log$  numerators for this diagram must have at least one factor of the form  $x_{l_1 l_2}$ , for  $x_{l_1}$ , and  $x_{l_2}$  in the set of loop face variables. Only  $N_1^{(5a)}$  and  $N_2^{(5a)}$  have this correct loop dependence. So we conclude that both  $N_1^{(5a)}$  and  $N_2^{(5a)}$  can appear in the amplitude, while  $N_3^{(5a)}$  yields an integrand with non-logarithmic poles, and so has coefficient zero in the amplitude.

In addition to the numerators in Eq. (1.7.20), there are other dual conformal numerators that cancel propagators of the parent diagram, resulting in contact-term diagrams depicted in Figs. 1.19 and 1.20. If we consider only the contact terms that can be obtained from the diagram in Fig. 1.18, the numerators that pass the three types of checks are

$$N^{(5b)} = -x_{24}^2 x_{17}^2 x_{36}^2, \quad N^{(5c)} = x_{13}^2 x_{24}^2,$$

$$N^{(5d)} = -x_{13}^2 x_{27}^2, \quad N^{(5e)} = x_{24}^2, \quad (1.7.22)$$

where the four numerators respectively correspond to diagrams 31, 32, 33, and 34 in Ref. [138]. Besides  $N_3^{(5a)}$ , there are four more numerators that display dual conformal invariance at the integrand level, but are invalid by applying the type II rules, which is equivalent to the DKS observation that they are ill defined:

$$\begin{aligned} N^{(5f)} &= x_{18}^2 x_{36}^2, & N^{(5g)} &= 1, \\ N^{(5h)} &= x_{17}^2 x_{36}^2 x_{48}^2, & N^{(5i)} &= x_{35}^2. \end{aligned} \quad (1.7.23)$$

These correspond to diagrams 36, 37, 38, and 39, respectively, of Ref. [138]. The numerators listed in Eq. (1.7.22) are numerators for the lower-propagator topologies in Fig. 1.19, and the numerators listed in Eq. (1.7.23) are numerators for the lower-propagator topologies in Fig. 1.20. We again omit the other dual conformal numerators that are relabelings of these numerators under automorphism of the diagram.

With this analysis, we have not proved that  $N_{1,2}^{(5a)}$  through  $N^{(5e)}$  ensure a  $d\log$  form; we have only argued that the corresponding integrands do not contain the types of non-logarithmic singularities detected by our three rules. It is still possible for those integrands to have non-logarithmic poles buried in certain kinematic regimes deeper in the cut structure. Indeed, under more careful scrutiny we find additional constraints from the requirements of no double poles. In particular, we find that only the following combinations of integrands corresponding to Figs. 1.18 and 1.19 are free of double poles:

$$\mathcal{I}^{(A)} = \mathcal{I}_1^{(5a)} + \mathcal{I}^{(5b)} + \mathcal{I}^{(5e)}, \quad \mathcal{I}^{(B)} = \mathcal{I}_2^{(5a)} + \mathcal{I}^{(5c)}, \quad \mathcal{I}^{(D)} = \mathcal{I}^{(5d)}. \quad (1.7.24)$$

The notation is, for example, that the integrand  $\mathcal{I}_1^{(5a)}$  has the propagators of diagram (5a) and the numerator  $N_1^{(5a)}$  in Eq. (1.7.20). Similarly, the corresponding numerators for the integrands of diagrams (5b)–(5e) are given in Eq. (1.7.22). The integrand for diagram (5a) with numerator  $N_3^{(5a)}$  is not present, because no contact terms can remove all double poles of  $\mathcal{I}_3^{(5a)}$ . In this case, all cancellations of double poles are between the parent and descendant diagrams. However, at higher loops the situation can very well be more complicated: unwanted singularities can cancel between different parent diagrams as well.

We now illustrate how pole constraints can explain why some six-loop diagrams enter the planar amplitude with zero coefficient. We choose two examples that both fall outside the type II classification of the effective rules of the previous subsection. This means both numerators escape detection by the original DKS rule, and so far could not be easily identified as coefficient-zero terms. The two examples are the six-loop “bowtie” in Fig. 1.21(6a) and another six-loop diagram with two contact terms in

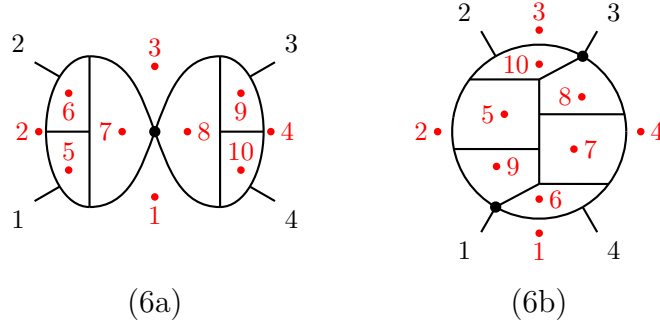


**Figure 1.21.** Two six-loop diagrams that have coefficient zero in the amplitude because they have non-logarithmic singularities. Diagram (6a) has non-logarithmic poles detected by our rules. Diagram (6b) requires explicit checks to locate double poles.

Fig. 1.21(6b). The dual conformal numerators of these diagrams are [121]<sup>8</sup>

$$N^{(6a)} = x_{13}^3 x_{24}, \quad N^{(6b)} = x_{24}^2 x_{27}^2 x_{45}^2. \quad (1.7.25)$$

There are other dual conformal numerators for (6b), but they belong to lower-propagator diagrams, so we ignore them in this discussion.

We first consider diagram (6a). This integrand suffers from poles of type III. We see this by cutting

$$x_{25}^2 = x_{26}^2 = x_{36}^2 = x_{37}^2 = x_{56}^2 = x_{57}^2 = x_{67}^2 = 0. \quad (1.7.26)$$

We are then looking at the  $l = 3$ ,  $N = 0$ ,  $P = 7$  case and the corresponding inequality  $P < N + 2l + 1$  is violated, indicating a non-logarithmic pole. This means the non-logarithmic rules immediately offer a reason why this diagram contributes to the amplitude with coefficient zero. This agrees with Ref. [121].

The six-loop example (6b) in Fig. 1.21 is more subtle, since it is not ruled out by the three rules. However, it does have a double pole. We know from Ref. [121] that this diagram with numerator  $N^{(6b)}$  does not enter the expansion of the amplitude but has coefficient zero. Presumably, the double pole cannot cancel against other diagrams.

We also conducted a variety of checks at seven loops using the integrand given in Ref. [121]. We applied the three rules to all 2329 potential contributions and found that all 456 contributions that failed the tests did not appear in the amplitude, as expected. We also checked dozens of examples that have vanishing coefficients and we were able to identify problematic singularities. More generally, as we saw at five loops,

<sup>8</sup>These diagrams and numerators can be found in the associated files of Ref. [121] in the list of six loop integrands that do not contribute to the amplitude. In our notation, we have again stripped off a factor of  $st = x_{13}^2 x_{24}^2$ .

the double poles can cancel nontrivially between different contributions. We leave a detailed study of the restrictions that logarithmic singularities and poles at infinity place on higher-loop planar amplitudes to future work. In any case, the key implication is that we should be able to carry over the key consequences of dual conformal symmetry to the nonplanar sector, even though we do not know how to define the symmetry in this sector.

## 1.8 From gauge theory to gravity

Ref. [119] noted that the two-loop four-point amplitude of  $\mathcal{N} = 8$  supergravity has only logarithmic singularities and no poles at infinity. Does this remain true at higher loops? In this section we use BCFJ duality to analyze this question. Indeed, we make the following conjecture:

- At finite locations, the four-point momentum-space integrand forms of  $\mathcal{N} = 8$  supergravity have only logarithmic singularities.

However, we will prove that in  $\mathcal{N} = 8$  supergravity there are poles at infinity whose degree grows with the loop order, as one might have guessed from power counting. This conjecture relies on two other conjectures: the duality between color and kinematics [114], and the conjecture that nonplanar  $\mathcal{N} = 4$  sYM amplitudes have only logarithmic singularities and are free of poles at infinity [119]. Explicit local expressions for numerators that satisfy the duality between color and kinematics are known at four points through four loops [129]. At higher loops the duality is a conjecture and it may require nonlocal numerators for it to hold, resulting in poles at finite points in momentum space for supergravity amplitudes. Our conjecture proposes that if this were to happen it would introduce no worse than logarithmic singularities. With modifications it should be possible to extend our conjecture beyond four points, but for  $N^k$ MHV amplitudes with  $k \geq 3$ , the second sYM conjecture that we rely on holds only in the Grassmannian space and not momentum space, as noted earlier. Given that all our explicit studies are at four points, we leave our conjecture at this level for now.

We note that our conjecture effectively states that one of the key properties linked to dual conformal symmetry not only transfers to the nonplanar sector of  $\mathcal{N} = 4$  sYM theory, but transfers to  $\mathcal{N} = 8$  supergravity as well. Because there are poles at infinity, dual conformal symmetry is not quite present in supergravity. However, a strong echo remains in  $\mathcal{N} = 8$  supergravity.

To gather evidence for our conjecture, we construct the complete three-loop four-point amplitude of  $\mathcal{N} = 8$  supergravity, and do so in a form that makes it obvious that the conjecture is true for this case. To demonstrate that there are poles at infinity, we



analyze a certain easy-to-construct cut of the four-point amplitude to all loop orders. Using the duality between color and kinematics [113, 114], it is easy to obtain the complete three-loop four-point amplitude of  $\mathcal{N} = 8$  supergravity in a format that makes the singularity structure manifest. Here, we simply quote a main result of the duality, and refer to Ref. [147] for a recent review. According to the duality conjecture,  $\mathcal{N} = 8$  supergravity numerators may be constructed by replacing the color factors of each diagram of an  $\mathcal{N} = 4$  sYM amplitude by kinematic numerators of a second copy, constrained to the same algebraic relations as the color factors. Although the general existence of numerators with the required property is unproven, here we only need the three-loop case, for which such numerators are explicitly known. Whenever duality satisfying numerators are available we immediately have the  $\mathcal{N} = 8$  diagram numerators in terms of gauge-theory ones:

$$N_{\mathcal{N}=8}^{(x)} = N^{(x)} N_{\text{BCJ}}^{(x)}, \quad (1.8.1)$$

where  $(x)$  labels the diagram. The gauge-theory numerator  $N^{(x)}$  is exactly one of the numerators in Eq. (1.4.32), while  $N_{\text{BCJ}}^{(x)}$  is one of the  $\mathcal{N} = 4$  sYM BCJ numerators from Ref. [114].

To be concrete, we construct the  $\mathcal{N} = 8$  supergravity numerator for diagram (f) in Fig. 1.4. Multiplying the sYM  $d$ log numerator  $N^{(f)}$  in Eq. (1.4.32) by the corresponding BCJ numerator gives the  $\mathcal{N} = 8$  supergravity numerator:

$$N_{\mathcal{N}=8}^{(f)} = - \left[ (\ell_5 + k_4)^2 ((\ell_5 + k_3)^2 + (\ell_5 + k_4)^2) \right] \\ \times \left[ (s(-\tau_{35} + \tau_{45} + t) - t(\tau_{25} + \tau_{45}) + u(\tau_{25} - \tau_{35}) - s^2)/3 \right], \quad (1.8.2)$$

where  $\tau_{ij} = 2k_i \cdot \ell_j$ . As for the gauge-theory case, we remove overall factors of  $\mathcal{K}$  (defined in Eq. (1.3.22)). The construction of the complete three-loop supergravity amplitude is then trivial using Eq. (1.8.1), Eq. (1.4.32) and Table 1 of Ref. [114]. This construction is designed to give correct  $\mathcal{N} = 8$  supergravity unitarity cuts.

Based on the BCJ construction, we immediately learn some nontrivial properties about  $\mathcal{N} = 8$  supergravity. Since the supergravity and sYM diagrams have identical propagators, and each numerator has a factor of  $N^{(x)}$ , all unwanted double poles located at finite values are canceled. However, in general the factor  $N_{\text{BCJ}}^{(x)}$  in Eq. (1.8.1) carries additional powers of loop momenta. These extra powers of loop momentum in the numerator compared to the  $\mathcal{N} = 4$  sYM case generically lead to poles at infinity, as we prove below. However, because the three-loop BCJ numerators are at most linear in loop momentum, only single poles, or equivalently logarithmic singularities, can develop at infinity. At higher loops, the BCJ numerators contribute ever larger powers of

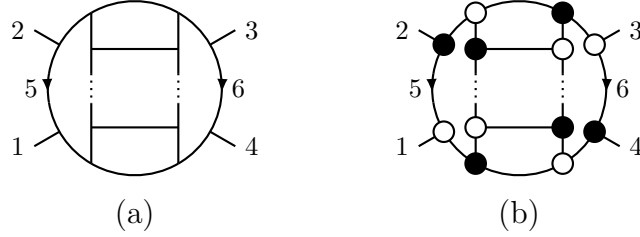


**Figure 1.22.** At  $L > 3$  loops, diagram (a) contains a pole at infinity that cannot cancel against other diagrams. By cutting all propagators in diagram (a) we obtain the corresponding on-shell diagram (b), which gives a residue of the amplitude on one of the solutions of the  $L$ -loop maximal cut. This is the only contribution.

loop momenta. These additional loop momenta generate non-logarithmic singularities as the orders of the poles at infinity grow.

To analyze the poles at infinity, we turn to a particular set of cuts chosen so that we can study poles at infinity at any loop order. While we do not yet know the four-point  $\mathcal{N} = 8$  supergravity amplitude at five or higher loops, we do have partial information about the structure of the amplitude to all loop orders. In particular, we know the value of the maximal cut of the diagram in Fig. 1.22(a) that is displayed in Fig. 1.22(b). One could evaluate the cut directly in terms of amplitudes, using superspace machinery [148, 149]. However, it is much simpler to use the rung rule [120], which is equivalent to evaluating iterated two-particle cuts. This gives the value for the numerator

$$N = [(\ell_5 + \ell_6 + k_2 + k_3)^2]^{\delta(L-3)}, \quad (1.8.3)$$

up to terms that vanish on the maximal cut. Here  $\delta = 1$  for  $\mathcal{N} = 4$  sYM theory and  $\delta = 2$  for  $\mathcal{N} = 8$  supergravity. As usual factors of  $\mathcal{K}$  have been removed.

We carefully<sup>9</sup> choose a set of maximal cuts as encoded in Fig. 1.22(b) so that only a single diagram is selected. On this solution, the two loop momenta labeled in Fig. 1.22 have solutions

$$\ell_5 = \alpha \lambda_1 \tilde{\lambda}_2, \quad \ell_6 = \beta \lambda_3 \tilde{\lambda}_4. \quad (1.8.4)$$

The Jacobian for this cut is

$$J = s^2 \alpha \beta [(\ell_5 + \ell_6 + k_2 + k_3)^2]^{L-2} F(\sigma_1, \dots, \sigma_{L-3}), \quad (1.8.5)$$

where the function  $F$  depends on the remaining  $L-3$  parameters,  $\sigma_i$ , of the cut solution, and not on  $\alpha$  or  $\beta$ . On the cut, the parametrization Eq. (1.8.4) implies that

$$(\ell_5 + \ell_6 + k_2 + k_3)^2 \Big|_{\text{cut}} = (\alpha \langle 13 \rangle + \langle 23 \rangle) (\beta [24] + [23]). \quad (1.8.6)$$

<sup>9</sup>To avoid mixing in any additional solutions, we must first take a next-to-maximal cut, and then make a final cut to hone in on the single solution in Eq. (1.8.4).

Then the residue in the sYM case is

$$\text{Res}_{\text{cut}} d\mathcal{I}_{\text{YM}} \sim \frac{d\alpha}{\alpha(\alpha - \alpha_0)} \wedge \frac{d\beta}{\beta(\beta - \beta_0)} \wedge \frac{d\sigma_1 \dots d\sigma_{L-3}}{F(\sigma_1, \dots, \sigma_{L-3})}, \quad (1.8.7)$$

with  $\alpha_0 = -\langle 23 \rangle / \langle 13 \rangle$ ,  $\beta_0 = -[23] / [24]$ . So the sYM integrand has only logarithmic singularities and no pole at infinity in  $\alpha$  or  $\beta$ . On the other hand, in the supergravity case the residue is

$$\text{Res}_{\text{cut}} d\mathcal{I}_{\text{GR}} \sim \frac{d\alpha}{\alpha(\alpha - \alpha_0)^{4-L}} \wedge \frac{d\beta}{\beta(\beta - \beta_0)^{4-L}} \wedge \frac{d\sigma_1 \dots d\sigma_{L-3}}{F(\sigma_1, \dots, \sigma_{L-3})}. \quad (1.8.8)$$

We see that these forms have the same structure as sYM for  $L = 3$ , but for  $L > 3$  they differ. In the latter case, the sYM expression in Eq. (1.8.7) stays logarithmic with no poles at  $\alpha, \beta \rightarrow \infty$ , while the supergravity residue Eq. (1.8.8) loses the poles at  $\alpha_0$  and  $\beta_0$  for  $L = 4$  and develops a logarithmic pole at infinity. However, for  $L \geq 5$  the poles at infinity become non-logarithmic, and the degree grows linearly with  $L$ . Since the cut was carefully chosen so that no other diagrams can mix with Fig. 1.22(a), the poles at infinity identified in Eq. (1.8.8) for  $L \geq 4$  cannot cancel against other diagrams, and so the  $\mathcal{N} = 8$  supergravity amplitudes indeed have poles at infinity. This can also be verified by the direct evaluation of the on-shell diagram in Fig. 1.22(b). In fact, at three loops there is another contribution (different from Fig. 1.22) that leads to a pole at infinity as well. As it does not offer qualitatively new insights, we will not show this example here.

We conclude that in contrast to  $\mathcal{N} = 4$  sYM theory,  $\mathcal{N} = 8$  supergravity has poles at infinity with a degree that grows linearly with the loop order. An interesting question is what this might imply about the ultraviolet properties of  $\mathcal{N} = 8$  supergravity. While it is true that a lack of poles at infinity implies an amplitude is ultraviolet finite, the converse argument that poles at infinity imply divergences is not necessarily true. There are a number of reasons to believe that this converse fails in supergravity. First, at three and four loops the four-point  $\mathcal{N} = 8$  supergravity amplitudes have exactly the same degree of divergence as the corresponding  $\mathcal{N} = 4$  sYM amplitudes [122, 128, 129], even though the supergravity amplitudes have poles at infinity. Indeed, when calculating supergravity divergences in critical dimensions where the divergences first appear, they are proportional to divergences in subleading-color parts of gauge-theory amplitudes [129]. In addition, recent work in  $\mathcal{N} = 4$  and  $\mathcal{N} = 5$  supergravity shows that non-trivial cancellations, beyond those that have been understood by standard-symmetry considerations, occur between the diagrams of any covariant formulation [111, 150]. Furthermore, suppose that under the rescaling  $\ell_i \rightarrow t\ell_i$  with  $t \rightarrow \infty$  the supergravity integrand scales as  $1/t^m$ . If  $m \leq 4L$ , where  $L$  is the number of loops, we can interpret

this behavior as a pole at infinity. However, as we have demonstrated in this paper, after applying cuts this pole can still be present or disappear, and other poles at infinity can appear. Thus, the relation between ultraviolet properties of integrated results and the presence of poles at infinity is nontrivial. It will be fascinating to study this relation.

## 1.9 Conclusion

In this paper, we have studied in some detail the singularity structure of integrands of  $\mathcal{N} = 4$  sYM theory, including nonplanar contributions. These contributions were recently conjectured to have only logarithmic singularities and no poles at infinity [119], just as for the planar case [67]. In this paper, besides providing nontrivial evidence in favor of this conjecture, we made two additional conjectures. First, we conjectured that in the planar sector of  $\mathcal{N} = 4$  sYM theory, constraints on the amplitudes that follow from dual conformal symmetry can instead be obtained from requirements on singularities. The significance of this conjecture is that it implies that consequences of dual conformal symmetry on the analytic structure of amplitudes carry over to the nonplanar sector. We described evidence in favor of this conjecture through seven loops. Our second conjecture involves  $\mathcal{N} = 8$  supergravity. While we proved that the amplitudes of this theory have poles at infinity, we conjectured that at finite locations, at least the four-point amplitude should have only logarithmic singularities, matching the  $\mathcal{N} = 4$  sYM behavior.

To carry out our checks we developed a procedure for analyzing the singularity structure, which we then applied to the three-loop four-point amplitude of  $\mathcal{N} = 4$  sYM theory. Using this approach we found an explicit representation of this amplitude, where the desired properties hold term by term. We also partially analyzed the singularity structure of four-point amplitudes through seven loops. We illustrated at three loops how to make the logarithmic singularity property manifest by finding  $d\log$  forms. Our strategy for studying the nonplanar singularity structure required subdividing the integrand into diagrams and assuming that we could impose the desired properties on individual diagram integrands. Unitarity constraints then allowed us to find the appropriate linear combinations of integrands to build an integrand valid for the full amplitude. Interestingly, many coefficients of the basis integrands follow a simple pattern dictated by the rung rule [120].

More generally, the study of planar  $\mathcal{N} = 4$  sYM amplitudes has benefited greatly by identifying hidden symmetries. Dual conformal symmetry, in particular, imposes an extremely powerful constraint on planar  $\mathcal{N} = 4$  sYM amplitudes. When combined with superconformal symmetry, it forms a Yangian symmetry which is tied to the presumed

integrability of the planar theory. However, at present we do not know how to extend this symmetry to the nonplanar sector. Nevertheless, as we argued in this paper, the key analytic restrictions on the amplitude do, in fact, carry over straightforwardly to the nonplanar sector. This bodes well for future studies of full amplitudes in  $\mathcal{N} = 4$  sYM theory.

Our basis integrands are closely related to the integrals used by Henn et al. [123–126] to find a simplified basis of master integrals determined from integration-by-parts identities [151, 152]. In this simplified basis, all master integrals have uniform transcendental weight, which then leads to simple differential equations for the integrals. This basis overlaps with our construction, except that we include only cases where the integrands do not have poles at infinity, since those are the ones relevant for  $\mathcal{N} = 4$  sYM theory. The  $d\log$  forms we described are in some sense partway between the integrand and the integrated expressions.

An interesting avenue of further exploration is to apply these ideas to  $\mathcal{N} = 8$  supergravity. Using BCJ duality [113, 114], we converted the four-point three-loop  $\mathcal{N} = 4$  sYM integrand forms with into ones for  $\mathcal{N} = 8$  supergravity. We proved that the three-loop four-point integrand form of  $\mathcal{N} = 8$  supergravity has only logarithmic singularities. However, there are singularities at infinity. Indeed, we proved that, to all loop orders, there are poles at infinity whose degree grows with the loop order. A deeper understanding of these poles might shed new light on the surprisingly tame ultraviolet properties of supergravity amplitudes, and in particular on recently uncovered [111] “enhanced ultraviolet cancellations”, which are nontrivial cancellations that occur between diagrams.

In summary, by directly placing constraints on the singularity structure of integrands in  $\mathcal{N} = 4$  sYM theory, we have a means for carrying over the key consequences of dual conformal symmetry and more to the nonplanar sector. A key conclusion of our study is that the nonplanar sector of  $\mathcal{N} = 4$  sYM theory is more similar to the planar sector than arguments based on symmetry considerations suggest. Of course, one would like to do better by finding a formulation that makes manifest the singularity structure. The explicit results presented in this paper should aid that goal.

# Evidence for a nonplanar amplituhedron

The scattering amplitudes of planar  $\mathcal{N} = 4$  super-Yang-Mills exhibit a number of remarkable analytic structures, including dual conformal symmetry and logarithmic singularities of integrands. The amplituhedron is a geometric construction of the integrand that incorporates these structures. This geometric construction further implies the amplitude is fully specified by constraining it to vanish on spurious residues. By writing the amplitude in a  $d\log$  basis, we provide nontrivial evidence that these analytic properties and “zero conditions” carry over into the nonplanar sector. This suggests that the concept of the amplituhedron can be extended to the nonplanar sector of  $\mathcal{N} = 4$  super-Yang-Mills theory.

## 2.1 Introduction

In this paper, we investigate how some of the remarkable properties of planar  $\mathcal{N} = 4$  super-Yang-Mills carry over to the nonplanar sector. A basic difficulty in the nonplanar sector is that it is currently unclear how to define a unique integrand, largely due to the lack of global variables with which to describe a nonplanar integrand. Such ambiguities greatly obscure the desired structures that might be hiding in the amplitude. In addition, we lose Yangian symmetry and presumably any associated integrability constraints, as well as the connection between amplitudes and Wilson loops. Naively we also lose the ability to construct amplitudes using on-shell diagrams, the positive Grassmannian, and the amplituhedron.

Nevertheless, one might suspect that many features of the planar theory can be extended to the full theory including nonplanar contributions. In particular, the conjectured duality between color and kinematics [113, 114] suggests that nonplanar integrands are obtainable directly from planar ones, and hence properties of the nonplanar theory should be related to properties of the planar sector. However, it is not a priori obvious which features can be carried over.

The dual formulation of planar  $\mathcal{N} = 4$  super-Yang-Mills scattering amplitudes using on-shell diagrams and the positive Grassmannian makes manifest that the integrand has only logarithmic singularities, and can be written in a *dlog form*. Furthermore, the integrand has no poles at infinity as a consequence of dual conformal symmetry. Recently, Arkani-Hamed, Bourjaily, Cachazo, and Trnka conjectured the same singularity properties hold to all loop orders for all maximally helicity violating (MHV) amplitudes in the nonplanar sector as well [119]. In a previous paper [1], we confirmed this explicitly for the full three-loop four-point integrand of  $\mathcal{N} = 4$  SYM by finding a basis of diagram integrands where each term manifests these properties. We also conjectured that to all loop orders the constraints give us the key analytic information contained in dual conformal symmetry. Additional evidence for this was provided from studies of the four- and five-loop amplitudes. These results then offer concrete evidence that analytic structures present in the planar amplitudes do indeed carry over to the nonplanar sector of the theory.

Now we take this further and show that in the planar case dual conformal invariance is equivalent to integrands with (i) no poles at infinity, and (ii) special values of leading singularities (maximal codimension residues). In the MHV sector, property (ii) and superconformal invariance imply that leading singularities are necessarily  $\pm 1$  times the usual Parke-Taylor factor [17, 153]. Moreover, the existence of a dual formulation using on-shell diagrams and the positive Grassmannian implies that (iii) integrands have only logarithmic singularities. While (i) and (iii) can be directly conjectured also

for nonplanar amplitudes, property (ii) must be modified. As proven in Ref. [112] for both planar and nonplanar cases, the leading singularities are linear combinations of Parke-Taylor factors with different orderings and with coefficients  $\pm 1$ . This set of conditions was first conjectured in [119], and here we give a more detailed argument as to why the content of dual conformal symmetry in the MHV sector is exhausted by this set of conditions. We also provide direct nontrivial evidence showing they hold for the two-loop five-point amplitude and the three-loop four-point amplitude. While we might expect this structure to hold in the MHV sector, beyond this we expect  $R$  invariants [43] to play an important role.

The main purpose of this paper is to present evidence for the amplituhedron concept [18] beyond the planar limit. The amplituhedron is defined in momentum twistor variables which intrinsically require cyclic ordering of amplitudes, making direct nonplanar tests in these variables impossible. However, we can test specific implications even for nonplanar amplitudes. In Ref. [154], Arkani-Hamed, Hodges, and Trnka argued that the existence of the “dual” amplituhedron implies certain positivity conditions of amplitude integrands. Indeed, these conditions were proven analytically for some simple cases and numerically in a large number of examples. (Interestingly, these conditions appear to hold even post-integration [99, 154]). The dual amplituhedron can be interpreted as a geometric region of which the amplitude is literally a volume, in contrast to the original definition where the amplitude is a form with logarithmic singularities on the boundaries of the amplituhedron space. This implies a very interesting property when the integrand is combined into a single rational function: its numerator represents a codimension one surface which lies outside the dual amplituhedron space. The surface is simply described as a polynomial in momentum twistor variables and therefore can be fully determined by the zeros of the polynomial, which correspond to points violating positivity conditions defining the amplituhedron. A nontrivial statement implied by the amplituhedron geometry is that *all* these zeros can be interpreted as cuts where the amplitude vanishes.

This leads to a concrete feature that can be tested even in a diagrammatic representation of a nonplanar amplitude:

The integrand should be determined entirely from homogeneous conditions,  
up to an overall normalization.

Concretely, by “homogeneous conditions” we mean the conditions of no poles at infinity, only logarithmic singularities, and also unitarity cuts that vanish. That is, in the unitarity method, the only required cut equations are the ones where one side of the equation is zero, as opposed to a nontrivial kinematical function. These zeros occur either because the amplitude vanishes on a particular branch of the cut solutions or



because the cut is spurious<sup>10</sup>. This conjecture has exciting implications because this feature is closely related to the underlying geometry in the planar sector, suggesting that the nonplanar contributions to amplitudes admit a similar structure.

To test this conjecture we use the three-loop four-point and two-loop five-point nonplanar amplitudes as nontrivial examples. A key assumption is that the desired properties can all be made manifest diagram-by-diagram [1]. While it is unknown if this assumption holds for all amplitudes at all loop orders, at the relatively low loop orders that we work our results confirm that this is a good hypothesis. The three-loop four-point integrand was first obtained in Ref. [122], while the two-loop five-point integrand was first calculated in Ref. [155] in a format that makes the duality between color and kinematics manifest. Here we construct different representations that make manifest that the amplitudes have only logarithmic singularities and no poles at infinity. These representations are then compatible with the notion that there exists a nonplanar analog of dual conformal symmetry and a geometric formulation of nonplanar amplitudes. We organize the amplitudes in terms of basis integrands that have only  $\pm 1$  leading singularities. The coefficients of these integrals in the amplitudes are then simply sums of Parke-Taylor factors, as proved in Ref. [112]. We also show that homogeneous conditions are sufficient to determine both amplitudes up to an overall factor, as expected if a nonplanar analog of the amplituhedron were to exist.

This paper is organized as follows. In Sect. 2.2 we summarize properties connected to the amplituhedron picture of amplitudes in planar  $\mathcal{N} = 4$  SYM. Then in Sect. 2.3 we turn to a discussion of properties of nonplanar amplitudes, showing in various examples that the consequences of dual conformal invariance and the logarithmic singularity condition do carry over to the nonplanar sector. Finally, in Sect. 2.4 we give evidence for a geometric interpretation of the amplitude by showing that the coefficients in the diagrammatic expansion are determined by zero conditions. In Sect. 2.5 we give our conclusions.

## 2.2 Dual picture for planar integrands

In this section we summarize known properties of planar amplitudes in  $\mathcal{N} = 4$  SYM theory that we wish to carry beyond the planar limit to amplitudes of the full theory. We emphasize those features associated with the amplituhedron construction. In the planar case, we strip the amplitude of color factors. Later when we deal with the nonplanar case, we restore them.

---

<sup>10</sup>A spurious cut is one that exposes a non-physical singularity, i.e. a singularity that is not present in the full amplitude.

The classic representation of scattering amplitudes uses Feynman diagrams. At loop level the diagrams can be expressed in terms of scalar and tensor integrals. We can then write the amplitude as<sup>11</sup>

$$\mathcal{M} = \sum_j d_j \int d\mathcal{I}^j, \quad (2.2.1)$$

where the sum is over a set of basis integrands  $d\mathcal{I}^j$  and  $d_j$  are functions of the momenta of external particles, hereafter called kinematical functions. In general the integrations should be performed in  $D = 4 - 2\epsilon$  dimensions as a means for regulating both infrared and ultraviolet divergences. While the integrand can contain pieces that differ between four dimensions and  $D$  dimensions, in the present paper we ignore any potential contributions proportional to  $(-2\epsilon)$  components of loop momenta. At four-points we do not expect any such contribution through at least six loops [132], but they can enter at lower loop orders as the number of legs increases [156]. We will not deal with such contributions in this paper, but we expect that they can be treated systematically as corrections to any uncovered four-dimensional structure.

In  $\mathcal{N} = 4$  SYM we can split off an MHV prefactor, including the supermomentum conserving delta function  $\delta^8(Q)$ , from all  $d_j$ ,

$$\text{PT}(1234 \cdots n) = \frac{\delta^8(Q)}{\langle 12 \rangle \langle 23 \rangle \langle 34 \rangle \cdots \langle n1 \rangle}, \quad (2.2.2)$$

which defines a Parke-Taylor factor [17, 153]. Usually, we describe the  $d\mathcal{I}^j$  in terms of local integrals that share the same Feynman propagators as corresponding Feynman diagrams. However, in the planar sector of the amplitude we do not need to rely on those diagrams. Instead we can choose *dual coordinates*  $k_i = x_i - x_{i-1}$  to encode external kinematics, as well as analogously defined  $y_j$  for different loop momenta. The variables are associated with the faces of each diagram, are globally defined for all diagrams, and allow us to define a unique integrand by appropriately symmetrizing over the faces [40]. With these variables, we can sum all diagrams under one integration symbol and write an  $L$ -loop amplitude as

$$\mathcal{M} \sim \int d\mathcal{I}(x_i, y_j) = \int d^4 y_1 d^4 y_2 \cdots d^4 y_L \mathcal{I}(x_i, y_j), \quad (2.2.3)$$

where  $d\mathcal{I}$  is the integrand form and  $\mathcal{I}$  is the unique *integrand* of the scattering amplitude. The integrand form  $d\mathcal{I}$  for the  $n$ -point amplitude is a unique rational function

---

<sup>11</sup>In general we drop overall factors of  $1/(2\pi)^D$  and couplings from the amplitude, since these play no role in our discussion.

with many extraordinary properties that we will review in this section. Particularly effective ways of constructing the integrand are unitarity cut methods [23, 138, 157] or BCFW recursion relations [39, 40].

### 2.2.1 Dual conformal symmetry

A key property of  $\mathcal{N} = 4$  SYM planar amplitudes is that they possess *dual conformal symmetry* [41–43]. This symmetry acts like ordinary conformal symmetry on the dual variables  $x_i$  and  $y_j$  mentioned above. This can be supersymmetrically extended to a dual *superconformal* symmetry, and in combination with the ordinary superconformal symmetry it closes into the infinite dimensional Yangian symmetry [44]. This is a symmetry of tree-level amplitudes, and at loop level is a symmetry of quantities such as the integrand  $d\mathcal{I}$ , and IR safe quantities like ratio functions [43].

We are interested in understanding the implications of dual conformal symmetry on the analytic structure of the amplitude. Good variables for doing so are the momentum twistor variables  $Z_i$ , introduced in Ref. [47]. These are points in complex projective space  $\mathbb{CP}^3$  and are related to the spinor helicity variables  $\lambda_i \equiv |i\rangle$ ,  $\tilde{\lambda}_i \equiv |i]$  via

$$Z_i = \begin{pmatrix} \lambda_i \\ \mu_i \end{pmatrix} \quad \text{where} \quad \mu_i^{\dot{a}} = x_i^{a\dot{a}} \lambda_{i,a}, \quad (2.2.4)$$

where  $x_i^{a\dot{a}}$  are the dual variables defined above in spinor indices. The set of  $n$  on-shell external momenta are then described by  $n$  momentum twistors  $Z_i$ ,  $i = 1, 2, \dots, n$ . Momentum twistors are unconstrained variables and trivialize momentum conservation, which is a quadratic condition on the  $\lambda_i, \tilde{\lambda}_i$  spinors. Each off-shell loop momentum  $\ell_i$  is equivalent to a point  $y_i$  in dual momentum space, which in turn is represented by a line  $Z_{A_i} Z_{B_i}$  in momentum twistor space.

Dual conformal symmetry acts as  $SL(4)$  on  $Z_i$ , and we can construct invariants from a contraction of four different  $Z$ 's,

$$\langle ijkl \rangle \equiv \langle Z_i Z_j Z_k Z_l \rangle = \epsilon_{\alpha\beta\rho\sigma} Z_i^\alpha Z_j^\beta Z_k^\rho Z_l^\sigma. \quad (2.2.5)$$

Any dual conformal invariant can be written using these four-brackets. The contractions of spinor helicity variables  $\lambda$  can be written as

$$\langle ij \rangle \equiv \epsilon_{ab} \lambda_i^a \lambda_j^b = \epsilon_{\alpha\beta\rho\sigma} Z_i^\alpha Z_j^\beta I^{\rho\sigma}, \quad (2.2.6)$$

where  $I^{\rho\sigma}$  is the *infinity twistor* defined in Ref. [47]. An expression containing  $I^{\rho\sigma}$  breaks dual conformal symmetry because  $I^{\rho\sigma}$  does not transform as a tensor. There is a simple dictionary between momentum space and momentum twistor invariants; we refer the reader to Ref. [47] for details.

A simple example of a dual conformal invariant integrand is the zero-mass box,

$$d\mathcal{I} = \frac{d^4\ell (k_1 + k_2)^2 (k_2 + k_3)^2}{\ell^2 (\ell - k_1)^2 (\ell - k_1 - k_2)^2 (\ell + k_4)^2} = \frac{\langle AB d^2 A \rangle \langle AB d^2 B \rangle \langle 1234 \rangle^2}{\langle AB12 \rangle \langle AB23 \rangle \langle AB34 \rangle \langle AB41 \rangle}. \quad (2.2.7)$$

This represents the full one-loop four-point integrand form in  $\mathcal{N} = 4$  SYM. Note that the integrand in Eq. (2.2.7) is completely projective in all variables  $Z$ , and the infinity twistor is absent in this expression. This is true for any dual conformal invariant integrand.

This brings us to a key question we would like to answer here:

*What is the content of dual conformal symmetry for momentum-space integrands?*

In momentum twistor space the answer is obvious: the infinity twistor  $I^{\rho\sigma}$  is absent. Suppose instead the infinity twistor is present. What is the implication in momentum space? The first trivial case is when the prefactor of the integrand is not chosen properly. For example, if the factor  $(k_2 + k_3)^2$  in the numerator of the zero-mass box in Eq. (2.2.7) is replaced with say  $(k_1 + k_2)^2$ , this will introduce a dependence on  $I$ , signaling broken dual conformal invariance. In this case, the only dependence on the infinity twistor is through four-brackets  $\langle ijI \rangle$  involving only external variables. The presence of these is easily avoided by correctly normalizing  $d\mathcal{I}$ .

The nontrivial interesting cases occur when the infinity twistor appears in combination with the line  $Z_A Z_B$  that represents a loop momentum, e.g.  $\langle ABI \rangle$ . In this case no prefactor depending only on external kinematics can fix it, and the integrand form necessarily violates dual conformal symmetry. The factor  $\langle ABI \rangle$  (or its powers) can appear either in the numerator or the denominator. If it is in the denominator, the integrand has a spurious singularity at  $\langle ABI \rangle = 0$ . In momentum space this corresponds to sending  $\ell \rightarrow \infty$ . To see this, consider a simple example: the one-loop triangle given by

$$d\mathcal{I} = \frac{d^4\ell (k_1 + k_2)^2}{\ell^2 (\ell - k_1)^2 (\ell - k_1 - k_2)^2} = \frac{\langle AB d^2 A \rangle \langle AB d^2 B \rangle \langle 1234 \rangle \langle 23I \rangle}{\langle AB12 \rangle \langle AB23 \rangle \langle AB34 \rangle \langle ABI \rangle}. \quad (2.2.8)$$

If we parametrize the loop momentum as  $\ell = \alpha \lambda_1 \tilde{\lambda}_1 + \beta \lambda_2 \tilde{\lambda}_2 + \gamma \lambda_1 \tilde{\lambda}_2 + \delta \lambda_2 \tilde{\lambda}_1$  and send  $\gamma \rightarrow \infty$  while keeping  $\gamma\delta = \text{finite}$ , there is a pole which corresponds to  $\ell \rightarrow \infty$ . Bubble integrals even have a double pole at infinity, which corresponds to a double pole  $\langle ABI \rangle^2$  when written in momentum twistor space.

If the  $\langle ABI \rangle$  factor is in the numerator there is a problem with the values of leading singularities. For an  $L$ -loop integrand these are  $4L$ -dimensional residues that are just rational functions of external kinematics [134]. If the integrand form is dual conformal invariant, all its leading singularities are dual conformal cross ratios (defined

in Ref. [158]). A special case is when they are all  $\pm 1$ , as for the box integrand in Eq. (2.2.7).

If the integrand has  $\langle ABI \rangle$  in the numerator, the values of leading singularities, denoted  $LS(\cdot)$ , depend on  $\langle (AB)^* I \rangle$ ,

$$LS(d\mathcal{I}) = \langle (AB)^* I \rangle \cdot \mathcal{F}(Z_i, \langle ab \rangle), \quad (2.2.9)$$

where  $(AB)^*$  is the position of the line  $AB$  with the leading singularity solution substituted in. The function  $\mathcal{F}$  is dual conformal invariant up to some two-brackets of external twistors  $\langle ab \rangle$  from normalization. For one particular leading singularity we can choose the normalization of  $d\mathcal{I}$  and therefore force  $\mathcal{F}$  to cancel  $\langle (AB)^* I \rangle$ , restoring dual conformal symmetry. However, different leading singularities – of which each integrand has at least two by the residue theorem – are located at different  $(AB)^*$  so that it is not possible to simultaneously normalize all leading singularities correctly using only external data. As a result, some of the leading singularities are not necessarily dual conformal invariant. A simple example is the scalar one-loop pentagon,

$$\begin{aligned} d\mathcal{I} &= \frac{d^4\ell (k_1 + k_2)^2 (k_2 + k_3)^2 (k_3 + k_4)^2}{\ell^2 (\ell - k_1)^2 (\ell - k_1 - k_2)^2 (\ell - k_1 - k_2 - k_3)^2 (\ell + k_5)^2} \\ &= \frac{\langle AB d^2 A \rangle \langle AB d^2 B \rangle \langle ABI \rangle \langle 1234 \rangle \langle 2345 \rangle \langle 5123 \rangle}{\langle AB12 \rangle \langle AB23 \rangle \langle AB34 \rangle \langle AB45 \rangle \langle AB51 \rangle \langle 23I \rangle}, \end{aligned} \quad (2.2.10)$$

which is not dual conformal invariant, as implied by the appearance of the infinity twistor. The numerator of this pentagon can be modified to a chiral version studied in Ref. [146], which restores dual conformal symmetry.

Based on these considerations, we can summarize the content of dual conformal symmetry of individual integrands in momentum space in two conditions:

1. There are no poles as  $\ell \rightarrow \infty$ .
2. All leading singularities are dual conformal cross ratios.

Any integrand that satisfies these properties necessarily is dual conformal invariant.

In the context of integrands for MHV amplitudes in planar  $\mathcal{N} = 4$  SYM, if we strip off the MHV tree-level amplitude, i.e. the Parke-Taylor factor  $\text{PT}(123 \dots n)$  Eq. (2.2.2),

$$\mathcal{M} = \text{PT}(123 \dots n) \int d\mathcal{I}, \quad (2.2.11)$$

then the integrand  $d\mathcal{I}$  is dual conformal invariant satisfying both properties above. There are even stronger constraints: superconformal symmetry requires that all leading singularities are holomorphic functions [36] of  $\lambda_i$ 's alone. The only functions that are

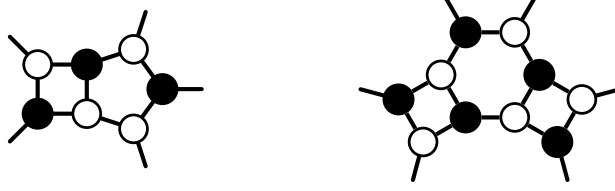


**Figure 2.23.** Sample on-shell diagrams. The black and white dots respectively represent MHV and  $\overline{\text{MHV}}$  three-point amplitudes. Black lines are on-shell particles.

holomorphic, satisfy property 2 above, and have the correct mass dimension and little-group weight, are pure numbers. In the normalization conventions adopted here, they are  $\pm 1$  or 0. While we do not have a direct formulation of dual conformal symmetry in the nonplanar sector, we shall find analogous analytic structures in the amplitudes for all the examples we study. The role of the Parke-Taylor factor will have to be modified slightly however.

### 2.2.2 On-shell diagrams

*On-shell diagrams* provide another novel representation of the integrand [67]. These are diagrams with black and white vertices connected by lines, as illustrated in Fig. 2.23. Black vertices represent MHV three-point amplitudes, white vertices  $\overline{\text{MHV}}$  three-point amplitudes, and all lines, both internal and external, represent on-shell particles. There are two indices associated with any on-shell diagram: the number of external legs  $n$  and the helicity index  $k$ . The  $k$ -index is defined as

$$k = \sum_V k_V - P, \quad (2.2.12)$$

where the sum is over all vertices  $V$ ,  $k_V$  is the  $k$ -count of the tree-level amplitude in a given vertex, and  $P$  is the number of on-shell internal propagators. Black and white vertices have  $k_B = 2$  and  $k_W = 1$ , respectively. As an example, the first diagram in Fig. 2.23 has  $k = (2 + 2 + 2) + (1 + 1 + 1 + 1) - 8 = 2$ . This  $k$  corresponds to the total number of external negative helicities.

The values of the diagrams are computed by integrating over the phase space  $d\Omega_i$  of on-shell internal particles the product of tree-level amplitudes  $A_j$  for each vertex

$$d\Omega = \prod_i \int d\Omega_i \prod_j A_j. \quad (2.2.13)$$

An on-shell diagram may be interpreted as a specific generalized unitarity cut of an amplitude. In this interpretation, the internal lines of an on-shell diagram represent cut

propagators. The on-shell diagram represents a nonvanishing valid cut of the amplitude only if the labels  $n, k$  of the on-shell diagram coincide with the same labels of the amplitude.

A very different way to describe and calculate planar on-shell diagrams is as cells of a positive Grassmannian  $G_+(k, n)$  [67]. For each diagram we define variables  $\alpha_j$  associated with edges or faces of the diagram. Using certain rules [67], we build a  $(k \times n)$  matrix  $C$  with positive main minors – a cell in the positive Grassmannian. Then the value of the diagram is given by a logarithmic form in the variables of the diagram, multiplied by a delta function which connects the  $C$  matrix with external variables (ordinary momenta or momentum twistors),<sup>12</sup>

$$d\Omega = \frac{d\alpha_1}{\alpha_1} \frac{d\alpha_2}{\alpha_2} \frac{d\alpha_3}{\alpha_3} \dots \frac{d\alpha_m}{\alpha_m} \delta(C \cdot Z). \quad (2.2.14)$$

This is known as a “ $d\log$  form” since all singularities have the structure  $d\log \alpha_i \equiv d\alpha_i/\alpha_i$ . For further details we refer the reader to Ref. [67].

Since the planar integrand can be expressed as a sum of these on-shell diagrams via recursion relations [67], all its singularities are also logarithmic. That is, if we approach a singularity of the amplitude for  $\alpha_j \rightarrow 0$  the integrand develops a pole

$$d\mathcal{I} \xrightarrow{\alpha_j=0} \frac{d\alpha_j}{\alpha_j} d\tilde{\mathcal{I}} \quad \text{where } d\tilde{\mathcal{I}} \text{ does not depend on } \alpha_j. \quad (2.2.15)$$

This property is not at all obvious in more traditional diagrammatic representations of scattering amplitudes.

The on-shell diagrams are individually both dual conformal and Yangian invariant and therefore are good building blocks that make both symmetries manifest. On the other hand, rewriting the variables  $\alpha_j$  in terms of momenta results in spurious poles which only cancel in the sum over all contributions.

While Eq. (2.2.15) holds for all planar  $\mathcal{N} = 4$  integrands for all helicities, in general the variables  $\alpha_j$  are variables of on-shell diagrams that are nontrivially related to the loop and external variables through the delta function  $\delta(C \cdot Z)$ . For MHV, NMHV (next-to-MHV), and N<sup>2</sup>MHV (next-to-next-to-MHV), this change of variables implies that the integrand also has logarithmic singularities directly in momentum space. For higher N<sup>*m*</sup>MHV amplitudes with  $m > 2$ , the fermionic Grassmann variables enter in the change of variables so that the integrand is not a  $d\log$  form in momentum variables directly. In this paper, we only deal with the case of MHV amplitudes, so that the  $d\log$  structure is straightforwardly visible in momentum space. As conjectured in Ref. [119], the same properties hold at the nonplanar level.

---

<sup>12</sup>We suppress wedge notation for forms throughout:  $dx dy \equiv dx \wedge dy$ .

## Pure integrand diagrams

In the MHV sector, we can check the  $d\log$  property for individual momentum-space planar diagrams with only Feynman propagators. In this check, we consider different cuts<sup>13</sup> of a diagram and probe whether Eq. (2.2.15) is always valid in momentum space. If so, its integrand form indeed has logarithmic singularities and can in principle be written as a sum of  $d\log$  forms

$$d\mathcal{I}^j = \sum_k b_k d\log f_1^{(k)} d\log f_2^{(k)} \dots d\log f_{4L}^{(k)}, \quad (2.2.16)$$

where  $f_m^{(k)}$  are some functions of external and loop momenta. Constraining these integrands to be dual conformal invariant further enforces that the functions  $d\log f_m^{(k)}$  never generate a pole if any of the loop momenta approach infinity,  $\ell_i \rightarrow \infty$ . In addition, for appropriately normalized diagrams the coefficients  $b_k$  are all equal to  $\pm 1$ . A form  $d\mathcal{I}^j$  with all these properties is called a *pure integrand form*. A simple example of such a form is the box integrand in Eq. (2.2.7) which can be expressed explicitly as a single  $d\log$  form [67]. More complicated  $d\log$  integrands have been used to write explicit expressions for one-loop and two-loop planar integrands for all multiplicities [159, 160]. Whenever the amplitude is built from  $d\mathcal{I}^j$ 's that are individually pure integrands, we will refer to such an expansion as a *pure integrand representation* of the amplitude, and to the set of  $d\mathcal{I}^j$ 's as a *pure integrand basis*.

We can now expand the  $n$ -point planar MHV integrand with Parke-Taylor tree amplitudes factored out as a sum of pure integrands,

$$d\mathcal{I} = \sum_j a_j d\mathcal{I}^j. \quad (2.2.17)$$

The existence of a diagram basis of pure integrands  $d\mathcal{I}^j$  with only local poles is a conjecture. There is no guarantee that we can fix the  $a_j$  coefficients of this ansatz to match the integrand of the amplitude; it might have been necessary to use non-pure integrands where unwanted singularities cancel between diagrams. Presently, it seems that pure integrands are sufficient up to relatively high loop order. The coefficients must all be  $a_j = \pm 1, 0$  based on the requirements of superconformal and dual conformal symmetry. Their precise values are determined by calculating leading singularities or other unitarity cuts.

We note that the representation in Eq. (2.2.17) does not make the full Yangian symmetry manifest, as there is a tension between this symmetry and locality. However, the representation does make manifest both dual conformal symmetry and logarithmic singularities.

---

<sup>13</sup>We use the words “cuts” and “residues” interchangeably throughout this paper.



### 2.2.3 Zero conditions from the amplituhedron

With on-shell diagrams, scattering amplitudes are built from abstract mathematical objects with no reference to spacetime dynamics. This is an important step towards finding a new description of physics where locality and unitarity are not fundamental, but rather are derived from geometric properties of amplitudes. The on-shell diagrams individually have this flavor, but the particular sum that gives the amplitude is dictated by recursion relations that are based on unitarity properties. A procedure that dictates which particular sum of on-shell diagrams gives the amplitude without reference to unitarity would therefore be an improvement on recursion relations. The amplituhedron exactly has this property [18] as it is a self-consistent geometric definition of the planar integrand. Here we will not need the details of this object, just some of its basic properties.

We focus mainly on the fact that the integrand of scattering amplitudes is defined as a differential form  $d\Omega$  with logarithmic singularities on the boundaries of the amplituhedron space. This space is defined as a certain map of the positive Grassmannian through the matrix of positive (bosonized) external data  $Z$  for the tree-level case, and its generalization to loops. A particular representation of the amplitude in terms of on-shell diagrams provides a triangulation of this space, but the definition of the amplituhedron is independent of any particular triangulation.

The underlying assumptions in this construction are *logarithmic singularities*, in terms of which the form  $d\Omega$  is defined, and *dual conformal symmetry*, which is manifest in momentum twistor space and generalizations thereof. All other properties of the integrand, including locality and unitarity, are derived from the amplituhedron geometry. This gives a complete definition of the integrand in a geometric language; yet, as mentioned in Ref. [154], it is desirable to find another formulation which calculates the integrand as a volume of an object rather than as a differential form with special properties. In search of this *dual amplituhedron* it was conjectured in Ref. [154] and checked in a variety of cases that the integrand  $\mathcal{I}$  (without the measure) is positive when evaluated inside the amplituhedron. This is exactly the property we expect to be true for a volume function. If we write  $\mathcal{I}$  as a numerator divided by all local poles,

$$\mathcal{I} = \frac{N}{\prod (\text{local poles})}, \quad (2.2.18)$$

then, since  $N$  is a polynomial in the loop variables  $(AB)_j$  (and for non-MHV cases also in other objects), it must be completely fixed by its zeros (roots). An interesting conjecture is that the zeros of  $N$  have two simple interpretations:

- The zeros correspond to forbidden cuts generated by the denominator; geometrically these are points outside the amplituhedron.

- The zeros cancel higher poles in the denominator to ensure that all singularities are logarithmic.

This should be true for all singularities of the integrand, both in external and loop variables. In the context of MHV amplitudes however, only the loop part is nontrivial. As an example, we can write the MHV one-loop integrand in the following way,

$$\mathcal{I} = \frac{N(AB, Z_i)}{\langle AB12 \rangle \langle AB23 \rangle \langle AB34 \rangle \dots \langle ABn1 \rangle}, \quad (2.2.19)$$

where  $N(AB, Z_i)$  is a degree  $n-4$  polynomial in  $AB$  with proper little group weights in  $Z_i$ . In this case the denominator generates only logarithmic poles on the cuts, and the numerator  $N$  is completely fixed (up to an overall constant) only by requiring that it vanishes on all forbidden cuts. There are two types of forbidden cut solutions for MHV amplitudes:

- *Unphysical cut solutions*: all helicity amplitudes vanish. In the on-shell diagram representation: no on-shell diagram exists.
- *Non-MHV cut solutions*: only MHV amplitudes vanish while other helicity amplitudes can be non-zero. In the on-shell diagram representation: the corresponding on-shell diagram has  $k \neq 2$ .

A simple example of the first case is the collinear cut  $\ell = \alpha k_1$  followed by cutting another propagator  $(\ell - k_1 - k_2 - k_3)^2$  of the pentagon integral in Eq. (2.2.10). In momentum twistor geometry this corresponds to  $\langle AB12 \rangle = \langle AB23 \rangle = \langle AB45 \rangle = 0$  (as well as setting a Jacobian to zero), which localizes  $Z_A = Z_2$ ,  $Z_B = (123) \cap (45)$ . This is an example of an unphysical cut which vanishes for all amplitudes including MHV, and the numerator  $N$  in Eq. (2.2.19) vanishes for this choice of  $Z_A, Z_B$ .

All forbidden cuts correspond to points outside the amplituhedron and therefore we can think about  $N$  as a codimension one surface outside the amplituhedron. The amplituhedron and the surface  $N$  can only touch on lower dimensional boundaries. This is completely consistent with the picture of the amplitude being the actual volume of the dual amplituhedron, making a clear distinction between inside and outside of the space.

Consider the simple example discussed in Ref. [154] and shown in Fig. 2.24. In this case the amplituhedron is the area of the pentagon. The numerator  $N$  is given by the conic that passes through five given points cyclically labeled by the  $X_{i,i+2}$ . These points correspond to “unphysical” singularities of the form  $d\Omega$ . Knowing the positions of the  $X_{i,i+2}$  fully fixes the numerator  $N$ , as there is a unique conic passing through five

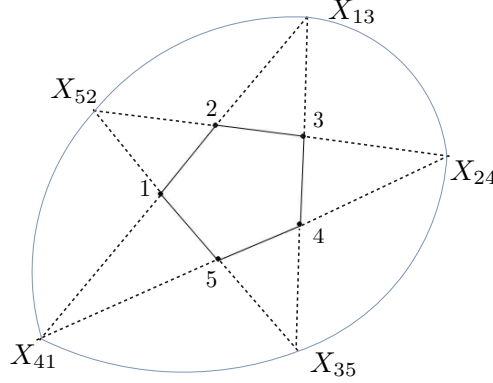


**Figure 2.24.** A simple amplituhedron example [154]. The area of the pentagon formed by the black solid line is the amplituhedron. The points  $X_{i,i+2}$  define zeros of a numerator, so the conic given by the outer (blue) solid lines connecting the points represents the numerator.

points. Knowing  $N$  fixes the integrand  $\mathcal{I}$ , per Eq. (2.2.18). Note that all five  $X_{i,i+2}$  are outside the amplituhedron (in this case the pentagon). The existence of a zero surface outside the amplituhedron in this example directly leads to a geometric construction of the integrand. The same happens for more complicated amplituhedra, which may lack such an intuitive visualization.

Now let us go several steps back and consider the standard expansion for the integrand, Eq. (2.2.17), in momentum space as the starting point, and think about the zero conditions as coming from physics (unphysical cuts) rather than geometry (forbidden boundaries). We can reformulate the conjecture about fixing  $N$  in Eq. (2.2.18) in terms of unknown coefficients  $a_j$  in the expansion in Eq. (2.2.17):

All coefficients  $a_j$  are fixed by *zero conditions*, up to an overall normalization.

By zero conditions we mean both unphysical and non-MHV cuts (as defined above) for which the integrand vanishes,  $0 = d\mathcal{I}|_{\text{cuts}}$ . The overall normalization just means the overall scale of the amplitude is one undetermined coefficient of the  $a_j$ , which may be fixed by one non-zero condition.

Assuming the integrand may be expanded as in Eq. (2.2.17) automatically assumes the presence of only logarithmic singularities as well as the cancellation of some unphysical cuts, viz. those which do not correspond to planar diagrams. On one hand, we can think about this conjecture as a reduced version of the one stated in Ref. [154] where both logarithmic singularities and diagram-like cuts were nontrivial conditions on the numerator  $N$  of the planar integrand Eq. (2.2.18). On the other hand, a (dual) ampli-

$$\mathcal{M}_4^{2\text{-loop}} = a_1 n_1 \quad \begin{array}{c} 2 \quad 3 \\ \diagdown \quad \diagup \\ \square \quad \square \\ \diagup \quad \diagdown \\ 1 \quad 4 \end{array} \quad + \quad a_2 n_2 \quad \begin{array}{c} 3 \quad 4 \\ \diagdown \quad \diagup \\ \square \quad \square \\ \diagup \quad \diagdown \\ 2 \quad 1 \end{array}$$

**Figure 2.25.** The planar two-loop four-point amplitude can be represented in terms of double-box diagrams.

tuhedron exactly implies our conjecture about zero conditions given the diagrammatic expansion of the integrand in Eq. (2.2.17). And most importantly, our new conjecture is now formulated in a language which allows us to carry it over to the nonplanar sector later in the paper.

A first simple example that illustrates our zero conditions conjecture is the planar two-loop four-point amplitude [120], which can be represented using the diagrammatic expansion in Fig. 2.25. The diagrams represent the denominators of individual integrands and their unit leading singularity normalizations are  $n_1 = s^2 t$ ,  $n_2 = s t^2$ . The overall planar Parke-Taylor factor  $\text{PT}(1234)$  is suppressed. We can consider a simple non-MHV cut on which the amplitude should vanish and relate the coefficients as  $a_1 = a_2$ , which is indeed correct. We will elaborate on this example in section 2.4 in the context of nonplanar amplitudes where more diagrams contribute.

### 2.3 Nonplanar amplitudes

As already noted, there is an essential difference between the planar and nonplanar sectors. In the nonplanar case, it is not known how to construct a unique integrand prior to integration. This is a direct consequence of the lack of global variables. Without those, the choice of variables in one nonplanar diagram relative to the choice in another diagram is arbitrary. This is a nontrivial obstruction to carrying over the planar amplituhedron construction directly to the full amplitude.

Here we circumvent this problem and follow the same strategy as in Refs. [1, 119], which is to consider diagrams as individual objects and to impose all desired properties diagram-by-diagram. These elements then form a basis for the complete amplitude and give us a representation in terms of a linear combination of said objects. Each integral is furthermore dressed by color factors  $c_j$  and with some kinematical coefficients  $d_j$  that need to be determined,

$$\mathcal{M} = \sum_j d_j c_j \int d\mathcal{I}^j. \quad (2.3.1)$$

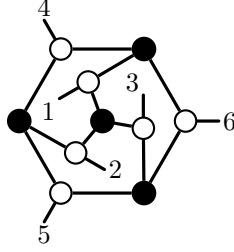


**Figure 2.26.** Example of a nonplanar on-shell diagram.

The individual pieces  $d\mathcal{I}^j$  interpreted as integrand forms are not really well defined because of the arbitrariness in their choice of variables, and they become well-defined only when integrated over loop momenta. However, we can still impose nontrivial requirements on the singularity structure of individual diagrams as was done in Refs. [1, 119]. This is because unitarity cuts of the amplitude impose constraints in terms of a well defined set of cut momenta, just as they do in the planar sector. This implies that the integrand forms  $d\mathcal{I}^j$  are interesting in their own right and that we can systematically study their properties with the tools at hand. In particular, we will see concrete examples where MHV integrands may be expanded in a pure integrand basis.

### 2.3.1 Nonplanar conjectures

In the context of  $\mathcal{N} = 4$  SYM it is natural to propose the following properties of the “integrand” even in nonplanar cases:

- (i) The integrand has only logarithmic singularities.
- (ii) The integrand has no poles at infinity.
- (iii) The leading singularities of the integrand all take on special values.

The presence of only logarithmic singularities (i) would be an indication of the “volume” interpretation of nonplanar amplitudes. We will give more detailed evidence for such an interpretation in the next section. Demonstrating properties (ii) and (iii) would provide nontrivial evidence for the existence of an analog of dual conformal symmetry for full  $\mathcal{N} = 4$  SYM amplitudes, including the nonplanar sector. Since we lack nonplanar momentum twistor variables we cannot formulate an analogous symmetry directly, yet the basic constraints of properties (ii) and (iii) on nonplanar amplitudes would be identical to the constraints of dual conformal symmetry on planar amplitudes.

The first property (i) can be directly linked to the properties of on-shell diagrams, which are well-defined beyond the planar sector [79, 112]. Nonplanar on-shell diagrams,

one of which is illustrated in Fig. 2.26, are calculated following the same rules as in the planar case [67]. In particular, they are given by the same logarithmic form Eq. (2.2.14), where the  $C$ -matrix is now some cell in the (not necessarily positive) Grassmannian  $G(k, n)$ . However, the singularities are again logarithmic and for MHV, NMHV, and  $N^2$ MHV amplitudes; this property holds directly in momentum space like in the planar case. At present it is not known whether this is a property of the full amplitude, including nonplanar contributions. Unlike the planar case, we do not currently have an on-shell diagram representation of the amplitude since it is not known how to unambiguously implement recursion relations. If such a construction exists then the amplitude would share the properties of the on-shell diagrams, including their singularity structure. Therefore it is very natural to conjecture that the full amplitude indeed has only logarithmic singularities [119].

Because there is no global definition for the integrand, it is reasonable to assume that there exist  $d\mathcal{I}^j$  as in Eq. (2.3.1) such that each  $d\mathcal{I}^j$  has only logarithmic singularities [1]. That is, we assume that there exists a  $d\log$  representation Eq. (2.2.16) for each diagram,

$$d\mathcal{I}^j = \sum_k b_k d\log f_1^{(k)} d\log f_2^{(k)} \dots d\log f_{4L}^{(k)}, \quad (2.3.2)$$

where  $f_i^{(k)}$  are some functions of external and loop momenta and the coefficients  $b_k$  are numerical coefficients independent of external kinematics.

In the planar sector, the other two properties (ii) and (iii) are closely related to dual conformal symmetry. As discussed in Sect. 2.2.1, the exact constraints of dual conformal symmetry on MHV amplitudes are that the amplitudes have unit leading singularities (when combined with ordinary superconformal symmetry and stripped off Parke-Taylor factor) and no poles at infinity. Property (ii) can be directly carried over to any nonplanar integrand, in particular it would imply that the  $d\log$  forms in Eq. (2.3.2) never generate a pole as  $\ell \rightarrow \infty$ . As for property (iii), the value of leading singularities cannot be directly translated to the nonplanar case, since there is no single overall Parke-Taylor factor to strip off. Superconformal invariance only allows us to write leading singularities as any holomorphic function  $\mathcal{F}_n(\lambda)$ , but as proven in Ref. [112], the only allowed functions are

$$\mathcal{F}_n = \sum_{\sigma} a_{\sigma} \text{PT}_{\sigma}, \quad (2.3.3)$$

where  $a_{\sigma} = (\pm 1, 0)$  and PT stands for a Parke-Taylor factor with a given ordering,

$$\text{PT}_{\sigma} \equiv \text{PT}(\sigma_1 \sigma_2 \sigma_3 \dots \sigma_n) = \frac{\delta^8(Q)}{\langle \sigma_1 \sigma_2 \rangle \langle \sigma_2 \sigma_3 \rangle \dots \langle \sigma_n \sigma_1 \rangle}. \quad (2.3.4)$$

The sum over  $\sigma$  runs over the Parke-Taylor amplitudes independent under the Kleiss-Kuijf relations [161]. There are additional relations between the amplitudes, but those introduce ratios of kinematic invariants [113] — which introduce spurious poles in external kinematics since they involve  $\tilde{\lambda}$  — and so we will not make use of them here. As an example, consider the on-shell diagram from Fig. 2.26 above, which is equal to the sum of seven Parke-Taylor factors (see Eq. (3.11) of Ref. [112]),

$$\begin{aligned} \mathcal{F}_6 = & \text{PT}(123456) + \text{PT}(124563) + \text{PT}(142563) + \text{PT}(145623) \\ & + \text{PT}(146235) + \text{PT}(146253) + \text{PT}(162345). \end{aligned} \quad (2.3.5)$$

This is a nontrivial property since there exist many holomorphic functions  $\mathcal{F}_n(\lambda)$  for  $n \geq 6$  which are not of the form of Eq. (2.3.3).

Analogously to how it works in the planar sector, we can define a pure integrand to take the form Eq. (2.2.16), so that the integrand has unit logarithmic singularities with no poles at infinity. Putting together the results from Refs. [1, 112, 119], our conjecture is that all MHV amplitudes in  $\mathcal{N} = 4$  SYM theory can be written as

$$\mathcal{M} = \sum_{k,\sigma,j} a_{\sigma,k,j} c_k \text{PT}_\sigma \int d\mathcal{I}^j, \quad (2.3.6)$$

where  $a_{\sigma,k,j}$  are numerical rational coefficients and  $d\mathcal{I}^j$  are pure integrands with leading singularities  $(\pm 1, 0)$ . The  $\text{PT}_\sigma$  are as in Eq. (2.3.4), and  $c_k$  are color factors. For contributions with the maximum number of propagators, the unique color factors can be read off directly from the corresponding diagrams, but contact term contributions may have multiple contributing color factors. The  $a_{\sigma,k,j}$  coefficients are such that, up to sums of Parke-Taylor factors, the leading singularities of the amplitude are normalized to be  $(\pm 1, 0)$ , reflecting a known property of the amplitude.

#### *Uniqueness and total derivatives*

There is an important question about the uniqueness of our result. The standard wisdom is that the final amplitude  $\mathcal{M}$  is a unique object while the planar integrand  $d\mathcal{I}$  is ambiguous, as we can add any total derivative  $d\mathcal{I}^{\text{tot}}$ ,

$$\int d\mathcal{I}^{\text{tot}} = 0, \quad (2.3.7)$$

that leaves  $\mathcal{M}$  invariant. Note that this is not true in our way of constructing the integrand, which relies on matching the cuts of the amplitude. This was sharply stated in Ref. [40]: there is only one function which satisfies all constraints (logarithmic singularities, dual conformal symmetry) and cut conditions. Any total derivative  $d\mathcal{I}^{\text{tot}}$

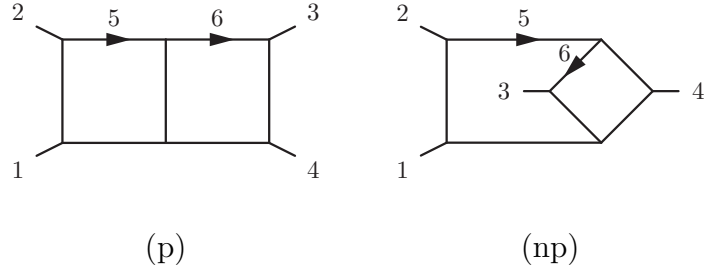


**Figure 2.27.** The integrals appearing in the two-loop four-point amplitude of  $\mathcal{N} = 4$  SYM theory.

would violate one or the other. In other words, if we demand dual conformal invariance and logarithmic singularities then any integrand would necessarily contribute to some of the cuts; the integrand therefore cannot be left undetected by all cuts. It does not matter if it integrates to zero or not, its coefficient is completely fixed by cut conditions. The same is true in the case of nonplanar amplitudes in general. In practice, our bases of pure integrands for all examples in the following subsections are complete. The pure integrand representation does not distinguish between forms that do integrate to zero and those that do not. Therefore, once the cuts are matched, the pure integrand basis does not miss any total derivatives that satisfy our constraints, and thus we cannot add any terms like  $\int d\mathcal{I}^{\text{tot}}$  to our amplitude. In fact, some linear combination of the basis elements  $d\mathcal{I}^j$  in Eq. (2.3.6) might be total derivatives, but the linear combination must contribute to the amplitude prior to integration with fixed coefficients to match all cuts. There is no freedom to change this coefficient to some other value. As a result, like in the planar sector, the nonplanar result is unique once we impose all constraints.

In the remainder of this section, we explicitly demonstrate that the two-loop four-point, three-loop four-point, and two-loop five-point amplitudes may be written in this pure integrand expansion. In Sect. 2.4, we furthermore demonstrate that the coefficients  $a_{\sigma,k,j}$  are all determined from homogeneous information.

### 2.3.2 Two-loop four-point amplitude

The simplest multi-loop example is the two-loop four-point amplitude, which was first obtained in Refs. [120, 127]. In Ref. [119] these results were reorganized in terms of individual integrals with only logarithmic singularities and no poles at infinity. There are two topologies: planar and nonplanar double boxes, as illustrated in Fig. 2.27. The numerators for the planar and nonplanar double box integrals with these properties are

$$\tilde{N}^{(\text{p})} = s, \quad \tilde{N}^{(\text{np})} = (\ell_5 - k_3)^2 + (\ell_5 - k_4)^2, \quad (2.3.8)$$



up to overall factors independent of loop momentum,  $\ell_i$ . The labels on the momenta in Eq. (2.3.8) correspond to the leg labels in Fig. 2.27. The integrand  $d\mathcal{I}^{(\text{np})}$  with this numerator has logarithmic singularities and no poles at infinity, but it is not a pure integrand. That is, the leading singularities are not all  $\pm 1$  but also contain ratios of the form,  $\pm u/t$ . The kinematic invariants  $s = (k_1 + k_2)^2$ ,  $t = (k_2 + k_3)^2$  and  $u = (k_1 + k_3)^2$  are the usual Mandelstam invariants.

Here we want to decompose the  $\tilde{N}$  numerators so that the resulting integrands  $d\mathcal{I}^j$  are pure, and express the amplitude in terms of the resulting pure integrand basis. In practice, we do this by retaining (with respect to Ref. [119]) the permutation invariant function  $\mathcal{K} = st\text{PT}(1234) = su\text{PT}(1243)$ , and by requiring each basis integrand to have correct mass dimension — six in this case — and unit leading singularities  $\pm 1$ . This gives us three basis elements:

$$N^{(\text{p})} = s^2 t, \quad N_1^{(\text{np})} = su(\ell_5 - k_3)^2, \quad N_2^{(\text{np})} = st(\ell_5 - k_4)^2. \quad (2.3.9)$$

The two nonplanar basis integrals are related by the symmetry of the diagram, but to maintain unit leading singularities we keep the terms distinct. The corresponding pure integrand forms  $d\mathcal{I}^{(\text{p})}$ ,  $d\mathcal{I}_1^{(\text{np})}$ ,  $d\mathcal{I}_2^{(\text{np})}$  are obtained by including the integration measure and the appropriate propagators that can be read off from Fig. 2.27

We note that for the planar double box, an explicit  $d\log$  form is known [119],

$$d\mathcal{I}^{(\text{p})} = d\log \frac{\ell_5^2}{(\ell_5 - \ell_5^*)^2} d\log \frac{(\ell_5 + k_2)^2}{(\ell_5 - \ell_5^*)^2} d\log \frac{(\ell_5 + k_1 + k_2)^2}{(\ell_5 - \ell_5^*)^2} d\log \frac{(\ell_5 - k_3)^2}{(\ell_5 - \ell_5^*)^2} \\ \times d\log \frac{(\ell_5 - \ell_6)^2}{(\ell_6 - \ell_6^*)^2} d\log \frac{\ell_6^2}{(\ell_6 - \ell_6^*)^2} d\log \frac{(\ell_6 - k_3)^2}{(\ell_6 - \ell_6^*)^2} d\log \frac{(\ell_6 - k_3 - k_4)^2}{(\ell_6 - \ell_6^*)^2}, \quad (2.3.10)$$

where

$$\ell_5^* = -\frac{\langle 12 \rangle}{\langle 13 \rangle} \lambda_3 \tilde{\lambda}_2, \quad \ell_6^* = k_3 + \frac{(\ell_5 - k_3)^2}{\langle 4 | \ell_5 | 3 \rangle} \lambda_4 \tilde{\lambda}_3, \quad (2.3.11)$$

denote one of the solutions to the on-shell conditions. Ref. [119] gave the  $d\log$  form for the nonplanar double box with numerators as in Eq. (2.3.9) as a sum of four  $d\log$  forms with prefactors (leading to different Parke-Taylor factors). This representation has the advantage that it naturally separates parity even and odd pieces. In Ref. [1] this was rewritten in a way that manifestly splits into unit leading singularity pieces, so that there are single  $d\log$  forms corresponding to each of the nonplanar numerators  $N_1^{(\text{np})}$  and  $N_2^{(\text{np})}$ . As usual, we suppress the wedge notation and write,

$$d\mathcal{I}_1^{(\text{np})} = d\Omega_1 d\Omega_{2,(1)}, \quad d\mathcal{I}_2^{(\text{np})} = d\Omega_1 d\Omega_{2,(2)}. \quad (2.3.12)$$

More explicitly, these forms are

$$d\Omega_1 = d\log \frac{\ell_6^2}{(\ell_6 - \ell_6^*)^2} d\log \frac{(\ell_6 - k_3)^2}{(\ell_6 - \ell_6^*)^2} d\log \frac{(\ell_6 - \ell_5)^2}{(\ell_6 - \ell_6^*)^2} d\log \frac{(\ell_6 - \ell_5 + k_4)^2}{(\ell_6 - \ell_6^*)^2},$$

$$\begin{aligned}
d\Omega_{2,(1)} &= d\log \frac{\ell_5^2}{\langle 4|\ell_5|3\rangle} d\log \frac{(\ell_5 + k_2)^2}{\langle 4|\ell_5|3\rangle} d\log \frac{(\ell_5 + k_1 + k_2)^2}{\langle 3|\ell_5|4\rangle} d\log \frac{(\ell_5 - \ell_{5,1}^*)^2}{\langle 3|\ell_5|4\rangle}, \\
d\Omega_{2,(2)} &= d\log \frac{\ell_5^2}{\langle 3|\ell_5|4\rangle} d\log \frac{(\ell_5 + k_2)^2}{\langle 3|\ell_5|4\rangle} d\log \frac{(\ell_5 + k_1 + k_2)^2}{\langle 4|\ell_5|3\rangle} d\log \frac{(\ell_5 - \ell_{5,2}^*)^2}{\langle 4|\ell_5|3\rangle}. \quad (2.3.13)
\end{aligned}$$

where the cut solutions read

$$\ell_6^* = -\frac{\lambda_3 \ell_5 \cdot \lambda_4}{\langle 34\rangle}, \quad \ell_{5,1}^* = -\frac{\langle 34\rangle}{\langle 31\rangle} \lambda_1 \tilde{\lambda}_4 - k_1 - k_2, \quad \ell_{5,2}^* = -\frac{\langle 43\rangle}{\langle 41\rangle} \lambda_1 \tilde{\lambda}_3 - k_1 - k_2. \quad (2.3.14)$$

Using these basis integrals, the full two-loop four-point amplitude can be written as a linear combination dressed with the appropriate color and Parke-Taylor factors,

$$\begin{aligned}
\mathcal{M}_4^{2\text{-loop}} &= \frac{1}{4} \sum_{S_4} \left[ c_{1234}^{(p)} a^{(p)} \text{PT}(1234) \int d\mathcal{I}^{(p)} \right. \\
&\quad \left. + c_{1234}^{(\text{np})} \left( a_1^{(\text{np})} \text{PT}(1243) \int d\mathcal{I}_1^{(\text{np})} + a_2^{(\text{np})} \text{PT}(1234) \int d\mathcal{I}_2^{(\text{np})} \right) \right], \quad (2.3.15)
\end{aligned}$$

where we sum over all 24 permutations of the external legs  $S_4$ . The overall 1/4 divides out the symmetry factor for each diagram to remove the overcount from the permutation sum. The planar and nonplanar double-box color factors are

$$\begin{aligned}
c_{1234}^{(p)} &= \tilde{f}^{a_1 a_7 a_9} \tilde{f}^{a_2 a_5 a_7} \tilde{f}^{a_5 a_6 a_8} \tilde{f}^{a_9 a_8 a_{10}} \tilde{f}^{a_3 a_{11} a_6} \tilde{f}^{a_4 a_{10} a_{11}}, \\
c_{1234}^{(\text{np})} &= \tilde{f}^{a_1 a_7 a_8} \tilde{f}^{a_2 a_5 a_7} \tilde{f}^{a_5 a_{11} a_6} \tilde{f}^{a_8 a_9 a_{10}} \tilde{f}^{a_3 a_6 a_9} \tilde{f}^{a_4 a_{10} a_{11}}, \quad (2.3.16)
\end{aligned}$$

where the  $\tilde{f}^{abc} = i\sqrt{2}f^{abc}$  are appropriately normalized color structure constants.

Matching the amplitude on unitarity cuts determines the coefficients to be

$$a^{(p)} = 1, \quad a_1^{(\text{np})} = -1, \quad a_2^{(\text{np})} = -1, \quad (2.3.17)$$

so that the amplitude in Eq. (2.3.15) is equivalent to the one presented in Ref. [119]. The trivial difference is that there the two pieces  $d\mathcal{I}_1^{(\text{np})}$  and  $d\mathcal{I}_2^{(\text{np})}$  are combined into one numerator.

### 2.3.3 Three-loop four-point amplitude

Now consider the three-loop four-point amplitude. This amplitude has been discussed already in various papers [1, 114, 122, 129]. Here we will express the amplitude in a pure integrand basis. In order to find such a basis we follow the strategy of Ref. [1], wherein integrands with only logarithmic singularities were identified. We proceed in the same way, but at the end impose the additional requirement that the leading singularities be  $\pm 1$  or 0. The construction of diagram numerators which lead to pure integrands is

very similar to the previous representation of Ref. [1], so we will only summarize the construction here.

The construction starts from a general  $\mathcal{N} = 4$  SYM power counting of loop momenta. For a given loop variable we require the overall scaling of a given integrand to behave like a box in that variable. For example, if there is a pentagon subdiagram for loop variable  $\ell$ , we allow a nontrivial numerator in  $\ell$ ,  $N \sim \rho_1 \ell^2 + \rho_2 (\ell \cdot Q) + \rho_3$ , where  $Q$  is some complex momentum (not necessarily massless). Similarly, if there is a hexagon subdiagram in loop variable  $\ell$ , we allow  $N \sim \rho_1 (\ell^2)^2 + \rho_2 (\ell^2) (\ell \cdot Q) + \rho_3 (\ell \cdot Q_1) (\ell \cdot Q_2) + \dots$ , and so on. Our conventions require that the overall mass dimension of  $d\mathcal{I}_j$  is zero<sup>14</sup> which fixes the mass dimension of the  $\rho_j$ .

In Ref. [1], we then directly constructed the amplitude by constraining the ansatz numerators to obey the symmetry of the diagrams and to vanish on poles at infinity and double (or multiple) poles. We now take a slightly different approach and instead of constructing the amplitude directly, focus on constructing the pure integrand basis.

#### *Basis of unit leading singularity numerators*

The next step in constructing the pure integrand basis is to require that the elements have unit leading singularities. We write each basis element as an ansatz that has the same power counting as the diagram numerators. We then constrain the elements so that *any* leading singularity — codimension  $4L$  residue — is either  $\pm 1$  or 0.

The resulting basis elements differ slightly from those of Ref. [1]. Terms that were originally grouped so that the numerator obeyed diagram symmetry are now split to make the unit leading singularity property manifest. This is exactly the same reason we rewrote Eq. (2.3.8) as Eq. (2.3.9) in the two-loop four-point example. Additionally, the basis elements are scaled by products  $st$ ,  $su$ , or  $tu$  to account for differing normalizations. The results of our construction of basis numerators yielding pure integrands are summarized in Table 2.4.

In Table 2.4 we use the relabeling convention  $N|_{i \leftrightarrow j}$ : “redraw the graph associated with numerator  $N$  with the indicated exchanges of external momenta  $i, j$  and also relabel loop momenta accordingly.” As a simple example look at  $N_1^{(i)}|_{1 \leftrightarrow 3}$ ,

$$N_1^{(i)} = tu(\ell_6 + k_4)^2(\ell_5 - k_1 - k_2)^2, \quad N_2^{(i)} = N_1^{(i)}|_{1 \leftrightarrow 3}. \quad (2.3.18)$$

Under this relabeling, the Mandelstam variables  $s$  and  $t$  transform into one another  $s = (k_1 + k_2)^2 \leftrightarrow (k_3 + k_2)^2 = t$  and  $u$  stays invariant. As usual we take the labels of the

---

<sup>14</sup>This mass dimension is different than in Ref. [1], where we factored out the totally crossing symmetric  $\mathcal{K} = st\text{PT}(1234) = su\text{PT}(1243) = tu\text{PT}(1324)$ .

Diagram	Numerators
(a)	$N_1^{(a)} = s^3 t,$
(b)	$N_1^{(b)} = s^2 u (\ell_6 - k_3)^2, \quad N_2^{(b)} = N_1^{(b)} _{3 \leftrightarrow 4},$
(c)	$N_1^{(c)} = s^2 u (\ell_5 - \ell_7)^2, \quad N_2^{(c)} = N_1^{(c)} _{1 \leftrightarrow 2},$
(d)	$N_1^{(d)} = su \left[ (\ell_6 - k_1)^2 (\ell_6 + k_3)^2 - \ell_6^2 (\ell_6 - k_1 - k_2)^2 \right],$ $N_2^{(d)} = N_1^{(d)} _{3 \leftrightarrow 4}, \quad N_3^{(d)} = N_1^{(d)} _{1 \leftrightarrow 2}, \quad N_4^{(d)} = N_1^{(d)} _{\substack{1 \leftrightarrow 2 \\ 3 \leftrightarrow 4}},$
(e)	$N_1^{(e)} = s^2 t (\ell_5 + k_4)^2,$
(f)	$N_1^{(f)} = st (\ell_5 + k_4)^2 (\ell_5 + k_3)^2, \quad N_2^{(f)} = su (\ell_5 + k_4)^2 (\ell_5 + k_4)^2,$
(g)	$N_1^{(g)} = s^2 t (\ell_5 + \ell_6 + k_3)^2,$ $N_2^{(g)} = st (\ell_5 + k_3)^2 (\ell_6 + k_1 + k_2)^2, \quad N_3^{(g)} = N_2^{(g)} _{3 \leftrightarrow 4},$
(h)	$N_1^{(h)} = st \left[ (\ell_6 + \ell_7)^2 (\ell_5 + k_2 + k_3)^2 - \ell_5^2 (\ell_6 + \ell_7 - k_1 - k_2)^2 \right. \\ \left. - (\ell_5 + \ell_6)^2 (\ell_7 + k_2 + k_3)^2 - (\ell_5 + \ell_6 + k_2 + k_3)^2 \ell_7^2 \right. \\ \left. - (\ell_6 + k_1 + k_4)^2 (\ell_5 - \ell_7)^2 - (\ell_5 - \ell_7 + k_2 + k_3)^2 \ell_6^2 \right],$ $N_2^{(h)} = tu \left[ [(\ell_5 - k_1)^2 + (\ell_5 - k_4)^2] [(\ell_6 + \ell_7 - k_1)^2 + (\ell_6 + \ell_7 - k_2)^2] \right. \\ \left. - 4 \ell_5^2 (\ell_6 + \ell_7 - k_1 - k_2)^2 \right. \\ \left. - (\ell_7 + k_4)^2 (\ell_5 + \ell_6 - k_1)^2 - (\ell_7 + k_3)^2 (\ell_5 + \ell_6 - k_2)^2 \right. \\ \left. - (\ell_6 + k_4)^2 (\ell_5 - \ell_7 + k_1)^2 - (\ell_6 + k_3)^2 (\ell_5 - \ell_7 + k_2)^2 \right],$ $N_3^{(h)} = N_1^{(h)} _{2 \leftrightarrow 4}, \quad N_4^{(h)} = N_2^{(h)} _{2 \leftrightarrow 4},$
(i)	$N_1^{(i)} = tu (\ell_6 + k_4)^2 (\ell_5 - k_1 - k_2)^2, \quad N_2^{(i)} = N_1^{(i)} _{1 \leftrightarrow 3}$ $N_3^{(i)} = st [(\ell_6 + k_4)^2 (\ell_5 - k_1 - k_3)^2 - \ell_5^2 (\ell_6 - k_2)^2], \quad N_4^{(i)} = N_3^{(i)} _{1 \leftrightarrow 3}$
(j)	$N^{(j)} = stu.$
(k)	$N^{(k)} = su,$

**Table 2.4.** The basis of numerators for pure integrands for the three-loop four-point amplitude. The notation  $N|_{i \leftrightarrow j}$  is defined in the text.

momenta to follow the labels of the corresponding diagrams. Here it is the labels of diagram (i) in Table 2.4. Besides changing the external labels, we are instructed to relabel the loop momenta as well. In the chosen example, this corresponds to interchanging  $\ell_5 \leftrightarrow \ell_6$ , so that

$$N_2^{(i)} = N_1^{(i)} \Big|_{1 \leftrightarrow 3} = su(\ell_5 + k_4)^2 (\ell_6 - k_3 - k_2)^2. \quad (2.3.19)$$

### *Matching the amplitude*

The three-loop four-point amplitude is assembled from the basis numerators as

$$\mathcal{M}_4^{3\text{-loop}} = \sum_{S_4} \sum_x \frac{1}{\mathcal{S}_x} \int d^4\ell_5 d^4\ell_6 d^4\ell_7 \frac{\mathcal{N}^{(x)}}{\prod_{\alpha_x} p_{\alpha_x}^2}, \quad (2.3.20)$$

analogously to Eq. (2.3.15). Now the sum over  $x$  runs over all diagrams in the basis listed in Table 2.4, the sum over  $S_4$  is a sum over all 24 permutations of the external legs, and  $\mathcal{S}_x$  is the symmetry factor of diagram  $x$  determined by counting the number of automorphisms of diagram  $x$ . The product over  $\alpha_x$  indicates the product of Feynman propagators  $p_{\alpha_x}^2$  of diagram  $x$ , as read from the graphs in Table 2.4. The Parke-Taylor factors, color factors, and coefficients are absorbed in  $\mathcal{N}^{(x)}$ , which we list in Table 2.5. For four external particles, there are only two independent Parke-Taylor factors. We abbreviate these as

$$\text{PT}_1 = \text{PT}(1234), \quad \text{PT}_2 = \text{PT}(1243). \quad (2.3.21)$$

The third possible factor,  $\text{PT}(1423)$ , is related to the other two by a  $U(1)$  decoupling identity or dual Ward identity [162]

$$\text{PT}(1423) = -\text{PT}(1234) - \text{PT}(1243), \quad (2.3.22)$$

and is therefore linearly dependent on  $\text{PT}_1$  and  $\text{PT}_2$ .

When checking cuts of the amplitude, certain cuts may combine contributions from different terms in the permutation sum of Eq. (2.3.20), resulting in a cut expression that involves diagrams that are relabellings of those in Table 2.4. In that case, the procedure is to relabel the numerators, propagators, Parke-Taylor factors, and color factors given in the tables into the cut labels. The resulting Parke-Taylor factors may not be in the original basis of Parke-Taylor factors; however every Parke-Taylor in the relabeled expression can be expanded in the original Parke-Taylor basis.

The diagrams with 10 propagators contain only three-point vertices and therefore have unique color factors included in  $\mathcal{N}^{(x)}$ . For the two diagrams with less than 10 propagators, we include in our ansatz for  $\mathcal{N}$  all independent color factors from all 10-propagator

diagrams that are related to the lower-propagator diagrams by collapsing internal legs. For example, three 10-propagator diagrams are related to diagram (j) in this way, with color factors  $c_{1234}^{(i)}$ ,  $c_{1243}^{(i)}$  and  $c_{3241}^{(i)}$ , where

$$c_{1234}^{(i)} = \tilde{f}^{a_1 a_8 a_5} \tilde{f}^{a_6 a_2 a_9} \tilde{f}^{a_3 a_{11} a_{10}} \tilde{f}^{a_{12} a_4 a_{13}} \tilde{f}^{a_9 a_{10} a_8} \tilde{f}^{a_{11} a_{12} a_{14}} \tilde{f}^{a_{13} a_5 a_7} \tilde{f}^{a_{14} a_7 a_6} , \quad (2.3.23)$$

is the standard color factor in terms of appropriately normalized structure constants, and the others  $c$ 's are relabellings of 1234 of this color factor. The Jacobi relation between the three color factors allows us to eliminate, say  $c_{1243}^{(i)}$ . This is exactly what we do for diagram (j). In diagram (k), there are nine contributing parent diagrams. Typically there are four independent color factors in the solution to the set of six Jacobi relations, but in this case two of the color factors that contribute happen to be identical up to a sign, and thus there are only three independent color factors.

In Ref. [1], the final representation of the amplitude contained arbitrary free parameters associated with the color Jacobi identity that allowed contact terms to be moved between parent diagrams without altering the amplitude. Here we removed this freedom by assigning the contact terms to their own diagrams and keeping only a basis of independent color factors for each.

One advantage of the Parke-Taylor expansion of the amplitude is that we can compactly express the solution to the cut equations in the set of matrices listed on the right hand side of Table 2.5. For example,  $\mathcal{N}^{(i)}$  can be read off from the table as

$$\mathcal{N}^{(i)} = c_{1234}^{(i)}(-1)(N_1^{(i)}(\text{PT}_1 + \text{PT}_2) + N_2^{(i)}\text{PT}_2 - N_3^{(i)}\text{PT}_1 + N_4^{(i)}\text{PT}_1) . \quad (2.3.24)$$

This expression supplies the Parke-Taylor and color dependence required for Eq. (2.3.20), in agreement with the general form of Eq. (2.3.6).

### 2.3.4 Two-loop five-point amplitude

The integrand for the two-loop five-point amplitude was first obtained in Ref. [155] in a format that makes the duality between color and kinematics manifest. Here we find a pure integrand representation. An additional feature of our representation is that it is manifestly free of spurious poles in external kinematics.

#### *Basis of unit leading-singularity numerators*

Following the three-loop four-point case, our first step is to construct a pure integrand basis. Constructing this basis is similar to constructing the three-loop four-point amplitude in Ref. [1] and summarized in Sec. 2.3.3. Although deriving the numerators for the two-loop five-point case is in principle straightforward, it does require a nontrivial amount of algebra, which we suppress. We again split the basis elements according

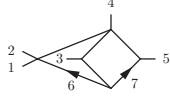
Color Dressed Numerators	PT Matrices
$\mathcal{N}^{(a)} = c_{1234}^{(a)} \sum_{1 \leq \sigma \leq 2} N_1^{(a)} \mathbf{a}_{1\sigma}^{(a)} \text{PT}_\sigma,$	$\mathbf{a}_{1\sigma}^{(a)} = (1 \ 0),$
$\mathcal{N}^{(b)} = c_{1234}^{(b)} \sum_{\substack{1 \leq \nu \leq 2 \\ 1 \leq \sigma \leq 2}} N_\nu^{(b)} \mathbf{a}_{\nu\sigma}^{(b)} \text{PT}_\sigma,$	$\mathbf{a}_{\nu\sigma}^{(b)} = (-1) \begin{pmatrix} 0 & 1 \\ 1 & 0 \end{pmatrix},$
$\mathcal{N}^{(c)} = c_{1234}^{(c)} \sum_{\substack{1 \leq \nu \leq 2 \\ 1 \leq \sigma \leq 2}} N_\nu^{(c)} \mathbf{a}_{\nu\sigma}^{(c)} \text{PT}_\sigma,$	$\mathbf{a}_{\nu\sigma}^{(c)} = (-1) \begin{pmatrix} 0 & 1 \\ 1 & 0 \end{pmatrix},$
$\mathcal{N}^{(d)} = c_{1234}^{(d)} \sum_{\substack{1 \leq \nu \leq 4 \\ 1 \leq \sigma \leq 2}} N_\nu^{(d)} \mathbf{a}_{\nu\sigma}^{(d)} \text{PT}_\sigma,$	$\mathbf{a}_{\nu\sigma}^{(d)} = \begin{pmatrix} 0 & 1 & 1 & 0 \\ 1 & 0 & 0 & 1 \end{pmatrix}^T,$
$\mathcal{N}^{(e)} = c_{1234}^{(e)} \sum_{1 \leq \sigma \leq 2} N_1^{(e)} \mathbf{a}_{1\sigma}^{(e)} \text{PT}_\sigma,$	$\mathbf{a}_{1\sigma}^{(e)} = (1 \ 0),$
$\mathcal{N}^{(f)} = c_{1234}^{(f)} \sum_{\substack{1 \leq \nu \leq 2 \\ 1 \leq \sigma \leq 2}} N_\nu^{(f)} \mathbf{a}_{\nu\sigma}^{(f)} \text{PT}_\sigma,$	$\mathbf{a}_{\nu\sigma}^{(f)} = (-1) \begin{pmatrix} 1 & 0 \\ 0 & 1 \end{pmatrix},$
$\mathcal{N}^{(g)} = c_{1234}^{(g)} \sum_{\substack{1 \leq \nu \leq 3 \\ 1 \leq \sigma \leq 2}} N_\nu^{(g)} \mathbf{a}_{\nu\sigma}^{(g)} \text{PT}_\sigma,$	$\mathbf{a}_{\nu\sigma}^{(g)} = \begin{pmatrix} -1 & 1 & 0 \\ 0 & 0 & 1 \end{pmatrix}^T,$
$\mathcal{N}^{(h)} = c_{1234}^{(h)} \sum_{\substack{1 \leq \nu \leq 4 \\ 1 \leq \sigma \leq 2}} N_\nu^{(h)} \mathbf{a}_{\nu\sigma}^{(h)} \text{PT}_\sigma,$	$\mathbf{a}_{\nu\sigma}^{(h)} = \frac{1}{2} \begin{pmatrix} 1 & 1 & 1 & 0 \\ 0 & 1 & 0 & -1 \end{pmatrix}^T,$
$\mathcal{N}^{(i)} = c_{1234}^{(i)} \sum_{\substack{1 \leq \nu \leq 4 \\ 1 \leq \sigma \leq 2}} N_\nu^{(i)} \mathbf{a}_{\nu\sigma}^{(i)} \text{PT}_\sigma,$	$\mathbf{a}_{\nu\sigma}^{(i)} = (-1) \begin{pmatrix} 1 & 0 & -1 & 1 \\ 1 & 1 & 0 & 0 \end{pmatrix}^T,$
$\mathcal{N}^{(j)} = c_{1234}^{(i)} \sum_{1 \leq \sigma \leq 2} N_1^{(j)} \mathbf{a}_{1\sigma, (1234)}^{(j)} \text{PT}_\sigma$ $+ c_{3241}^{(i)} \sum_{1 \leq \sigma \leq 2} N_1^{(j)} \mathbf{a}_{1\sigma, (3241)}^{(j)} \text{PT}_\sigma,$	$\mathbf{a}_{1\sigma, (1234)}^{(j)} = (1 \ 1),$ $\mathbf{a}_{1\sigma, (3241)}^{(j)} = (-1 \ 0),$
$\mathcal{N}^{(k)} = c_{1234}^{(g)} \sum_{1 \leq \sigma \leq 2} N_1^{(k)} \mathbf{a}_{1\sigma, (1234)}^{(k)} \text{PT}_\sigma$ $+ c_{4312}^{(g)} \sum_{1 \leq \sigma \leq 2} N_1^{(k)} \mathbf{a}_{1\sigma, (4312)}^{(k)} \text{PT}_\sigma$ $+ c_{2431}^{(f)} \sum_{1 \leq \sigma \leq 2} N_1^{(k)} \mathbf{a}_{1\sigma, (2431)}^{(k)} \text{PT}_\sigma.$	$\mathbf{a}_{1\sigma, (1234)}^{(k)} = (-2 \ 0),$ $\mathbf{a}_{1\sigma, (4312)}^{(k)} = 0,$ $\mathbf{a}_{1\sigma, (2431)}^{(k)} = 0.$

**Table 2.5.** The three-loop four-point numerators that contribute to the amplitude. The  $N_\nu^{(x)}$  are listed in Table 2.4. The four-point Parke-Taylor factors  $\text{PT}_\sigma$  are listed in Eq. (2.3.21). The numerators including color factors are denoted as  $\mathcal{N}^{(x)}$ . The symbol ‘ $T$ ’ denotes a transpose.

Diagram	Numerators
	$N_1^{(a)} = \langle 13 \rangle \langle 24 \rangle \left[ [24][13] \left( \ell_7 + \frac{[45]}{[24]} \lambda_5 \tilde{\lambda}_2 \right)^2 \left( \ell_6 - \frac{Q_{12} \cdot \tilde{\lambda}_3 \tilde{\lambda}_1}{[13]} \right)^2 - [14][23] \left( \ell_7 + \frac{[45]}{[14]} \lambda_5 \tilde{\lambda}_1 \right)^2 \left( \ell_6 - \frac{Q_{12} \cdot \tilde{\lambda}_3 \tilde{\lambda}_2}{[23]} \right)^2 \right],$ $N_2^{(a)} = N_1^{(a)} \Big _{\substack{1 \leftrightarrow 2 \\ 4 \leftrightarrow 5}}, \quad N_3^{(a)} = N_1^{(a)} \Big _{\substack{2 \leftrightarrow 4 \\ 1 \leftrightarrow 5}}, \quad N_4^{(a)} = N_1^{(a)} \Big _{\substack{1 \leftrightarrow 4 \\ 2 \leftrightarrow 5}},$ $N_5^{(a)} = \overline{N}_1^{(a)}, \quad N_6^{(a)} = \overline{N}_2^{(a)}, \quad N_7^{(a)} = \overline{N}_3^{(a)}, \quad N_8^{(a)} = \overline{N}_4^{(a)},$
	$N_1^{(b)} = \langle 15 \rangle [45] \langle 43 \rangle s_{45} [13] \left( \ell_6 + \frac{Q_{45} \cdot \tilde{\lambda}_3 \tilde{\lambda}_1}{[13]} \right)^2,$ $N_2^{(b)} = \overline{N}_1^{(b)},$
	$N_1^{(c)} = [13] \left( \ell_6 + \frac{Q_{45} \cdot \tilde{\lambda}_3 \tilde{\lambda}_1}{[13]} \right)^2 \langle 15 \rangle [54] \langle 43 \rangle (\ell_6 + k_4)^2,$ $N_2^{(c)} = N_1^{(c)} \Big _{4 \leftrightarrow 5}, \quad N_3^{(c)} = \overline{N}_1^{(c)}, \quad N_4^{(c)} = \overline{N}_2^{(c)},$
	$N_1^{(d)} = s_{34} (s_{34} + s_{35}) \left( \ell_7 - k_5 + \frac{(35)}{(34)} \lambda_4 \tilde{\lambda}_5 \right)^2,$ $N_2^{(d)} = N_1^{(d)} \Big _{4 \leftrightarrow 5}, \quad N_3^{(d)} = \overline{N}_1^{(d)}, \quad N_4^{(d)} = \overline{N}_2^{(d)},$
	$N_1^{(e)} = s_{15} s_{45}^2,$
	$N_1^{(f)} = s_{14} s_{45} (\ell_6 + k_5)^2, \quad N_2^{(f)} = N_1^{(f)} \Big _{4 \leftrightarrow 5},$
	$N_1^{(g)} = s_{12} s_{45} s_{24},$
	$N_1^{(h)} = \langle 15 \rangle [35] \langle 23 \rangle [12] \left( \ell_6 - \frac{\langle 12 \rangle}{\langle 32 \rangle} \lambda_3 \tilde{\lambda}_1 \right)^2, \quad N_2^{(h)} = N_1^{(h)} \Big _{3 \leftrightarrow 5},$ $N_3^{(h)} = s_{12} \langle 13 \rangle [15] \langle 5   \ell_6   3 \rangle, \quad N_4^{(h)} = s_{12} [13] \langle 15 \rangle \langle 3   \ell_6   5 \rangle,$ $N_5^{(h)} = \overline{N}_1^{(h)}, \quad N_6^{(h)} = \overline{N}_2^{(h)},$
	$N_1^{(i)} = \langle 2   4   3 \rangle \langle 3   5   2 \rangle - \langle 3   4   2 \rangle \langle 2   5   3 \rangle.$

**Table 2.6.** The parent diagram numerators that give pure integrands for the two-loop five-point amplitude. Each basis diagram is consistent with requiring logarithmic singularities and no poles at infinity. The overline notation means  $[\cdot] \leftrightarrow \langle \cdot \rangle$  and  $Q_{ij} \cdot \tilde{\lambda}_k = [ik] \lambda_i + [jk] \lambda_j$ . As usual, the momentum labels match the diagram labels.



Diagram	Numerators
(j) 	$N_1^{(j)} = s_{12}s_{35} = (N_2^{(h)} - N_1^{(h)})/(\ell_6 - k_1)^2,$

**Table 2.7.** A diagram and numerator that gives a pure integrand. However, as indicated in the table and explained in the text, it is not an independent basis element. As usual, the momentum labels match the diagram labels.

to diagram topologies and distinguish between parent diagrams and contact diagrams. The numerators of each pure integrand are given in Table 2.6.

Table 2.7 contains an additional pure integrand. However we do not include it in our basis because it is linearly dependent on two other basis elements:  $N_1^{(h)} - N_2^{(h)} + N_1^{(j)}(\ell_6 - k_1)^2 = 0$ . In our result, we choose  $N_1^{(h)}$  and  $N_2^{(h)}$  as our linearly independent pure integrands, and only mention  $N_1^{(j)}$  because it might be an interesting object in future studies.

In contrast to the three-loop four-point basis, in the two-loop five-point case it is useful to allow spinor helicity variables associated with external momenta. Specifically, several of the expressions in Table 2.6 have the structure  $(\ell + \alpha\lambda_i\tilde{\lambda}_j)^2$ , where  $\alpha$  is such that both mass dimension and little group weights are consistent. For example, the penta-box numerator

$$N_1^{(b)} \sim \left( \ell_6 + \frac{Q_{45} \cdot \tilde{\lambda}_3 \tilde{\lambda}_1}{[13]} \right)^2 = (\ell_6 - \ell_6^*)^2, \quad (2.3.25)$$

is a “chiral” numerator that manifestly vanishes on the  $\overline{\text{MHV}}$  solution  $\ell_6 = \ell_6^*$  [146]. As a shorthand notation, we use  $Q_{ij} = k_i + k_j$  and  $Q_{ij} \cdot \tilde{\lambda}_k = [ik]\lambda_i + [jk]\lambda_j$ .

### *Matching the amplitude*

Following the construction of the pure integrand basis in Sect. 2.3.4 we are ready to build up the amplitude. In complete analogy to Eq. (2.3.20), the two-loop five-point amplitude is assembled from the basis numerators as,

$$\mathcal{M}_5^{2\text{-loop}} = \sum_{S_5} \sum_x \frac{1}{\mathcal{S}_x} \int d^4\ell_6 d^4\ell_7 \frac{\mathcal{N}^{(x)}}{\prod_{\alpha_x} p_{\alpha_x}^2}, \quad (2.3.26)$$

where the sum over  $x$  runs over all diagrams in the basis listed in Table 2.6, the sum over  $S_5$  is a sum over all 120 permutations of the external legs, and  $\mathcal{S}_x$  is the symmetry

factor of diagram  $x$ . The product over  $\alpha_x$  indicates the product of Feynman propagators  $p_{\alpha_x}^2$  of diagram  $x$ , as read from the graphs in Table 2.6.

We refer the reader to the discussion in Sect. 2.3.3 for explicit examples on how to read Table 2.8. We choose the following set of independent five-point Parke-Taylor basis elements:

$$\begin{aligned} \text{PT}_1 &= \text{PT}(12345), & \text{PT}_2 &= \text{PT}(12354), & \text{PT}_3 &= \text{PT}(12453), \\ \text{PT}_4 &= \text{PT}(12534), & \text{PT}_5 &= \text{PT}(13425), & \text{PT}_6 &= \text{PT}(15423). \end{aligned} \quad (2.3.27)$$

The basis elements  $\overline{N}^{(x)}$  in Table 2.8 do not contribute to the MHV amplitude so those data are omitted from the  $\mathbf{a}_{\nu\sigma}^{(x)}$ .

## 2.4 Zeros of the integrand

In the previous section we gave explicit examples of the expansion of the amplitude, Eq. (2.3.1), in terms of a basis of pure integrands, giving new nontrivial evidence that the analytic consequences of dual conformal symmetry hold beyond the planar sector. In this section we take a further step and present evidence that the amplituhedron concept, which is a complete and self-contained geometric definition of the integrand, may exist beyond the planar sector as well.

As already mentioned in previous sections, beyond the planar limit we currently have no alternative other than to use diagrams representing local integrals, Eq. (2.3.1), as a starting point for defining nonplanar integrands. The lack of global variables makes it unclear how to directly test for a geometric construction analogous to the amplituhedron in the nonplanar sector. However, as discussed in Sect. 2.2, in the planar sector the (dual) amplituhedron construction implies that all coefficients in the expansion in Eq. (2.2.17) are determined by zero conditions, up to an overall normalization. We expect that if an analogous geometric construction exists in the nonplanar sector, then zero conditions should also determine the amplitude. This can be tested directly. Indeed, we conjecture that for the representation in Eq. (2.3.1):

All coefficients  $d_j$  are fixed by *zero conditions*, up to overall normalization.

This is the direct analog of the corresponding planar statement in Sect. 2.2. In the MHV case, which we consider here, the coefficients  $d_j$  are linear combinations of Parke-Taylor factors, so that only numerical coefficients  $a_{\sigma,k,j}$  in Eq. (2.3.6) need to be determined. The above conjecture is a statement that we can obtain these coefficients using only zero conditions, up to an overall constant. Here we confirm this proposal for all amplitudes constructed in the previous section.

Color Dressed Numerators	PT Matrices
$\mathcal{N}^{(a)} = c_{12345}^{(a)} \sum_{\substack{1 \leq \nu \leq 4 \\ 1 \leq \sigma \leq 6}} N_\nu^{(a)} \mathbf{a}_{\nu\sigma}^{(a)} \text{PT}_\sigma,$	$\mathbf{a}_{\nu\sigma}^{(a)} = \frac{1}{4} \begin{pmatrix} -1 & 0 & 1 & 0 & 0 & 2 \\ 1 & 0 & -1 & 0 & 0 & 2 \\ -3 & 0 & -1 & 0 & 0 & 2 \\ -1 & 0 & -3 & 0 & 0 & 2 \end{pmatrix},$
$\mathcal{N}^{(b)} = c_{12345}^{(b)} \sum_{1 \leq \sigma \leq 6} N_1^{(b)} \mathbf{a}_{1\sigma}^{(b)} \text{PT}_\sigma,$	$\mathbf{a}_{1\nu}^{(b)} = (-1 \ 0 \ 0 \ 0 \ 0 \ 0),$
$\mathcal{N}^{(c)} = c_{12345}^{(c)} \sum_{\substack{1 \leq \nu \leq 2 \\ 1 \leq \sigma \leq 6}} N_\nu^{(c)} \mathbf{a}_{\nu\sigma}^{(c)} \text{PT}_\sigma,$	$\mathbf{a}_{\nu\sigma}^{(c)} = \begin{pmatrix} -1 & 0 & 0 & 0 & 0 & 0 \\ 0 & -1 & 0 & 0 & 0 & 0 \end{pmatrix},$
$\mathcal{N}^{(d)} = \mathcal{N}^{(e)} = \mathcal{N}^{(f)} = 0,$	
$\mathcal{N}^{(g)} = c_{12345}^{(a)} \sum_{1 \leq \sigma \leq 6} N_1^{(g)} \mathbf{a}_{1\sigma,(12345)}^{(g)} \text{PT}_\sigma$ $+ c_{31245}^{(b)} \sum_{1 \leq \sigma \leq 6} N_1^{(g)} \mathbf{a}_{1\sigma,(31245)}^{(g)} \text{PT}_\sigma,$	$\mathbf{a}_{1\sigma,(12345)}^{(g)} = \frac{1}{4} (1 \ 0 \ 3 \ 0 \ 0 \ -2),$ $\mathbf{a}_{1\sigma,(31245)}^{(g)} = (0 \ 0 \ -1 \ 0 \ 0 \ 0),$
$\mathcal{N}^{(h)} = c_{12345}^{(a)} \sum_{\substack{1 \leq \nu \leq 4 \\ 1 \leq \sigma \leq 6}} N_\nu^{(h)} \mathbf{a}_{\nu\sigma,(12345)}^{(h)} \text{PT}_\sigma$ $+ c_{12543}^{(a)} \sum_{\substack{1 \leq \nu \leq 4 \\ 1 \leq \sigma \leq 6}} N_\nu^{(h)} \mathbf{a}_{\nu\sigma,(12543)}^{(h)} \text{PT}_\sigma,$	$\mathbf{a}_{\nu\sigma,(12345)}^{(h)} = \frac{1}{4} \begin{pmatrix} 4 & 0 & 4 & 0 & 0 & -4 \\ 2 & 0 & 3 & 0 & 1 & -2 \\ -2 & 0 & -3 & 0 & -1 & 2 \\ 4 & 0 & 4 & 0 & 0 & -4 \end{pmatrix},$ $\mathbf{a}_{\nu\sigma,(12543)}^{(h)} = \mathbf{a}_{\nu\sigma,(12345)}^{(h)},$
$\mathcal{N}^{(i)} = c_{12345}^{(a)} \sum_{1 \leq \sigma \leq 6} N_1^{(i)} \mathbf{a}_{1\sigma,(12345)}^{(i)} \text{PT}_\sigma$ $+ c_{13245}^{(a)} \sum_{1 \leq \sigma \leq 6} N_1^{(i)} \mathbf{a}_{1\sigma,(13245)}^{(i)} \text{PT}_\sigma$ $+ c_{12543}^{(a)} \sum_{1 \leq \sigma \leq 6} N_1^{(i)} \mathbf{a}_{1\sigma,(12543)}^{(i)} \text{PT}_\sigma$ $+ c_{15243}^{(a)} \sum_{1 \leq \sigma \leq 6} N_1^{(i)} \mathbf{a}_{1\sigma,(15243)}^{(i)} \text{PT}_\sigma,$	$\mathbf{a}_{1\sigma,(12345)}^{(i)} = 2 (0 \ 0 \ -1 \ 0 \ 0 \ 1),$ $\mathbf{a}_{1\sigma,(13245)}^{(i)} = 2 (0 \ 0 \ 0 \ 0 \ 0 \ 1),$ $\mathbf{a}_{1\sigma,(12543)}^{(i)} = 2 (1 \ 0 \ 1 \ 0 \ 1 \ -1),$ $\mathbf{a}_{1\sigma,(15243)}^{(i)} = 2 (0 \ 0 \ 0 \ 0 \ -1 \ 0).$

**Table 2.8.** The two-loop five-point numerators that contribute to the amplitude. The  $N_\nu^{(x)}$  are listed in Table 2.6. The five-point  $\text{PT}_\sigma$  are listed in Eq. (2.3.27). We denote the numerators including color information as  $\mathcal{N}^{(x)}$ .

As a simple first example, consider the two-loop four-point amplitude. The integrand is given as a linear combination of planar and nonplanar double boxes, c.f. Sect. 2.3.2. The only required condition to determine the unknown conditions is the cut in Fig. 2.28.

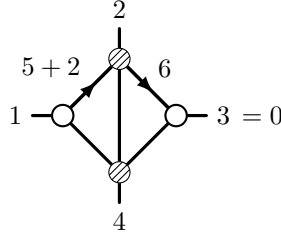


**Figure 2.28.** The two-loop four-point MHV amplitude vanishes on this cut. The four-point trees in the diagram have  $k = 2$ , so the overall helicity counting is  $k = 1$ .

$$\begin{aligned}
 \mathcal{M}_4^{2\text{-loop}} \Big|_{\text{cut}} = & N_{1234}^{(\text{p})} c_{1234}^{(\text{p})} \begin{array}{c} 2 \\ \text{---} \\ 1 \end{array} \begin{array}{c} \text{---} \\ \text{---} \\ \text{---} \\ \text{---} \\ 3 \\ 4 \end{array} + N_{4123}^{(\text{p})} c_{4123}^{(\text{p})} \begin{array}{c} 1 \\ \text{---} \\ 4 \end{array} \begin{array}{c} \text{---} \\ \text{---} \\ \text{---} \\ \text{---} \\ 2 \\ 3 \end{array} \\
 + & N_{1234}^{(\text{np})} c_{1234}^{(\text{np})} \begin{array}{c} 2 \\ \text{---} \\ 1 \end{array} \begin{array}{c} \text{---} \\ \text{---} \\ \text{---} \\ \text{---} \\ 3 \\ 4 \end{array} + N_{4123}^{(\text{np})} c_{4123}^{(\text{np})} \begin{array}{c} 1 \\ \text{---} \\ 4 \end{array} \begin{array}{c} \text{---} \\ \text{---} \\ \text{---} \\ \text{---} \\ 2 \\ 3 \end{array} \\
 + & N_{3214}^{(\text{np})} c_{3214}^{(\text{np})} \begin{array}{c} 2 \\ \text{---} \\ 3 \end{array} \begin{array}{c} \text{---} \\ \text{---} \\ \text{---} \\ \text{---} \\ 1 \\ 4 \end{array} + N_{3412}^{(\text{np})} c_{3412}^{(\text{np})} \begin{array}{c} 4 \\ \text{---} \\ 3 \end{array} \begin{array}{c} \text{---} \\ \text{---} \\ \text{---} \\ \text{---} \\ 1 \\ 2 \end{array} \\
 + & N_{4213}^{(\text{np})} c_{4213}^{(\text{np})} \begin{array}{c} 2 \\ \text{---} \\ 4 \end{array} \begin{array}{c} \text{---} \\ \text{---} \\ \text{---} \\ \text{---} \\ 1 \\ 3 \end{array}
 \end{aligned}$$

**Figure 2.29.** The two-loop four-point amplitude evaluated on the cut of Fig. 2.28. In each diagram the two shaded propagators are uncut, and every other propagator is cut. Eq. (2.4.7) gives the value of the cut.

In the full amplitude, we have contributions from the planar and nonplanar double boxes in Fig. 2.27 and their permutations of external legs. All permutations of diagrams that contribute to the cut in Fig. 2.28 are shown in Fig. 2.29, along with their numerators and color factors. For convenience, we indicate the permutation labels of external legs of the seven contributing diagrams. There are only seven diagrams rather than nine because two of the nine diagrams have triangle subdiagrams, and so have vanishing numerators in  $\mathcal{N} = 4$  SYM.

For the cut in Fig. 2.28, five propagators are put on-shell so that the cut solution depends on  $\alpha$ ,  $\gamma$ , and  $\delta$ , three unfixed parameters of the loop momenta. Explicitly, the

cut solution is

$$\begin{aligned}\ell_5^* + k_2 &= \lambda_1 \left[ \alpha \tilde{\lambda}_1 + \frac{1}{\delta \langle 13 \rangle [23]} (\delta t - \alpha (s + \delta u + \gamma \langle 13 \rangle [12])) \tilde{\lambda}_2 \right], \\ \ell_6^* &= \lambda_3 \left[ \delta \tilde{\lambda}_3 + \gamma \tilde{\lambda}_2 \right].\end{aligned}\tag{2.4.1}$$

On this  $k = 1$  cut, the MHV amplitude vanishes for any values of  $\alpha$ ,  $\gamma$ ,  $\delta$ . By cutting the Jacobian

$$J = \gamma (\delta t - \alpha (s + \delta u + \gamma \langle 13 \rangle [12])),\tag{2.4.2}$$

the amplitude remains zero, and this condition simplifies. Specifically, this allows us to localize  $\ell_5 + k_2$  to be collinear with  $k_1$  and to localize  $\ell_6$  to be collinear with  $k_3$ . This is equivalent to taking further residues of the already-cut integrand at  $\gamma = 0$ ,  $\alpha = \delta t / (s + \delta u)$ . On this cut, the solution for the loop momenta simplifies,

$$\ell_5^* + k_2 = \frac{\delta t}{s + \delta u} \lambda_1 \tilde{\lambda}_1, \quad \ell_6^* = \delta \lambda_3 \tilde{\lambda}_3,\tag{2.4.3}$$

with the overall Jacobian  $J' = s + u\delta$ . Even in this simplified setting with one parameter  $\delta$  left, the single zero cut condition Fig. 2.28 is sufficient to fix the integrand up to an overall constant.

The numerators for the pure integrands, using the labels in Fig. 2.27, are given in Eq. (2.3.9). Including labels for the external legs to help us track relabellings, these are

$$N_{1234}^{(p,1)} = s^2 t, \quad N_{1234}^{(np,1)} = su (\ell_5 - k_3)^2, \quad N_{1234}^{(np,2)} = st (\ell_5 - k_4)^2.\tag{2.4.4}$$

As noted near Eq. (2.3.21) there are only two Parke-Taylor factors independent under  $U(1)$  relations for four-particle scattering, namely  $\text{PT}_1 = \text{PT}(1234)$  and  $\text{PT}_2 = \text{PT}(1243)$ . Therefore the numerator ansatz for the planar diagram is

$$N_{1234}^{(p)} = \left( a_{1,1}^{(p)} \text{PT}_1 + a_{1,2}^{(p)} \text{PT}_2 \right) N_{1234}^{(p,1)}.\tag{2.4.5}$$

For the nonplanar diagram, there are two pure integrands, each of which gets decorated with the two independent Parke-Taylor factors, so that the ansatz takes the form

$$\begin{aligned}N_{1234}^{(np)} &= \left[ \left( a_{1,1}^{(np)} \text{PT}_1 + a_{1,2}^{(np)} \text{PT}_2 \right) N_{1234}^{(np,1)} \right. \\ &\quad \left. + \left( a_{2,1}^{(np)} \text{PT}_1 + a_{2,2}^{(np)} \text{PT}_2 \right) N_{1234}^{(np,2)} \right],\end{aligned}\tag{2.4.6}$$

and both numerators are then decorated with corresponding color factors  $c_{1234}^{(p)}$ ,  $c_{1234}^{(np)}$ , and propagators. The  $a_{i,j}^{(x)}$  coefficients are determined by demanding the integrand vanishes on the cut solution in Eq. (2.4.3).

Explicitly, the zero condition from the cut corresponding to Fig. 2.29 is:

$$\begin{aligned}
0 = & \left( \frac{c_{1234}^{(p)} N_{1234}^{(p)}}{\ell_5^2 (\ell_6 - k_3 - k_4)^2} + \frac{c_{4123}^{(p)} N_{4123}^{(p)}}{(\ell_5 - k_3)^2 (\ell_6 + k_2)^2} + \frac{c_{1234}^{(\text{np})} N_{1234}^{(\text{np})}}{\ell_5^2 (\ell_5 - \ell_6 - k_4)^2} \right. \\
& + \frac{c_{4123}^{(\text{np})} N_{4123}^{(\text{np})}}{(\ell_5 - k_3)^2 (\ell_5 - \ell_6 + k_2)^2} + \frac{c_{3214}^{(\text{np})} N_{3214}^{(\text{np})}}{(\ell_6 + k_2)^2 (\ell_5 - \ell_6 - k_4)^2} \\
& \left. + \frac{c_{3412}^{(\text{np})} N_{3412}^{(\text{np})}}{(\ell_6 - k_3 - k_4)^2 (\ell_5 - \ell_6 + k_2)^2} + \frac{c_{4213}^{(\text{np})} N_{4213}^{(\text{np})}}{(\ell_5 - \ell_6 + k_2)^2 (\ell_5 - \ell_6 - k_4)^2} \right) \Bigg|_{\ell_5^*, \ell_6^*} \quad (2.4.7)
\end{aligned}$$

The sum runs over the seven contributing diagrams, following the order displayed in Fig. 2.29. The denominators are the two propagators that are left uncut in each diagram when performing this cut. One of the terms in the cut equation, for example, is

$$\begin{aligned}
\frac{N_{3214}^{(\text{np})}}{(\ell_6 + k_2)^2 (\ell_5 - \ell_6 - k_4)^2} &= \frac{1}{(\ell_6 + k_2)^2 (\ell_5 - \ell_6 - k_4)^2} \quad (2.4.8) \\
&\times \left[ \left( a_{1,1}^{(\text{np})} \text{PT}(3214) + a_{1,2}^{(\text{np})} \text{PT}(4213) \right) tu (\ell_6 + k_1 + k_2)^2 \right. \\
&\quad \left. + \left( a_{2,1}^{(\text{np})} \text{PT}(3214) + a_{2,2}^{(\text{np})} \text{PT}(4213) \right) st (\ell_6 + k_2 + k_4)^2 \right].
\end{aligned}$$

This has been relabeled from the master labels of Eq. (2.4.4) to the labels of the third nonplanar diagram in Fig. 2.29, including the two uncut propagators. Specifically  $\ell_5 \mapsto -\ell_6 - k_2$  and  $\ell_6 \mapsto -\ell_5 - k_1$  is the relabeling for this diagram. A key simplifying feature is that the  $a_{i,j}^{(x)}$  coefficients do not change under this relabeling so as to maintain crossing symmetry; the same four coefficients contribute to all five of the nonplanar double boxes that appear, for example. As discussed in Sect. 2.3.3, the Parke-Taylor factors that appear in Eq. (2.4.8) do not necessarily need to be in the chosen basis, although here  $\text{PT}(3214) = \text{PT}_1$  and  $\text{PT}(4213) = \text{PT}_2$ .

The single zero condition Eq. (2.4.7) determines five of the six  $a_{ij}^{(x)}$  parameters. This is, consistent with our conjecture above, the maximum amount of information that we can extract from all zero conditions. To do so in this example, we reduce to the two-member Parke-Taylor basis mentioned before, and also use Jacobi identities to reduce the seven contributing color factors to a basis of four. Since the remaining Parke-Taylor and color factors are independent, setting the coefficients of  $\text{PT} \cdot c$  to zero yields eight potentially independent equations for the six coefficients. It turns out only five are independent:

$$\begin{aligned}
a_{1,2}^{(p)} &= a_{1,1}^{(p)} + 3a_{1,1}^{(\text{np})} + a_{2,1}^{(\text{np})} = a_{1,1}^{(p)} + a_{1,1}^{(\text{np})} + a_{2,1}^{(\text{np})} = 0, \quad (2.4.9) \\
2a_{1,2}^{(p)} - a_{1,1}^{(\text{np})} + a_{1,2}^{(\text{np})} - a_{2,1}^{(\text{np})} + a_{2,2}^{(\text{np})} &= a_{1,2}^{(p)} + a_{1,1}^{(\text{np})} + a_{1,2}^{(\text{np})} - a_{2,1}^{(\text{np})} + 3a_{2,2}^{(\text{np})} = 0.
\end{aligned}$$

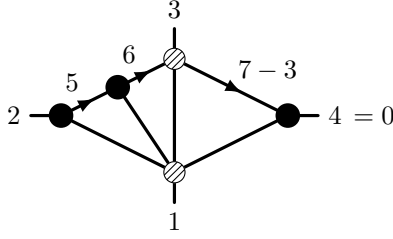


**Figure 2.30.** The three-loop four-point MHV amplitude vanishes on this cut. The five-point tree at the bottom of the diagram has  $k = 2$  or  $k = 3$ , so the overall helicity counting is  $k = 3$  or  $k = 4$ .

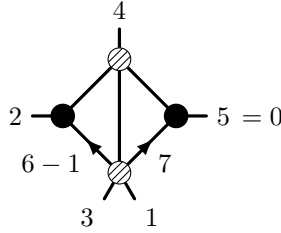


**Figure 2.31.** The two-loop five-point MHV amplitude vanishes on this cut. The five-point tree at the bottom of the diagram has  $k = 2$  or  $k = 3$ , so the overall helicity counting is  $k = 3$  or  $k = 4$ .

The solution for this system is

$$a_{1,2}^{(p)} = a_{1,1}^{(\text{np})} = a_{2,2}^{(\text{np})} = 0, \quad a_{1,2}^{(\text{np})} = a_{2,1}^{(\text{np})} = -a_{1,1}^{(p)}, \quad (2.4.10)$$

and any of  $a_{1,2}^{(\text{np})}$ ,  $a_{2,1}^{(\text{np})}$ , or  $a_{1,1}^{(p)}$  is the overall undetermined parameter. This matches the result in Eq. (2.3.17), if we take  $a_{1,1}^{(p)} = 1$ . This last condition is exactly the overall scale that the zero conditions cannot determine.

Finally, we confirmed that the three-loop four-point and two-loop five-point amplitudes can also be uniquely determined via a zero cut condition up to a single overall constant. We used the cut in Fig. 2.30 to determine the arbitrary parameters in the three-loop four-point amplitude, and we used the cut in Fig. 2.31 to determine the parameters of the two-loop five-point amplitude. We also confirmed in both cases that using one cut where the amplitude does not vanish is sufficient to determine the overall unfixed parameter to the correct value. To confirm that the so-constructed amplitudes are correct, we verified a complete set of unitarity cuts needed to fully determine the amplitudes, matching to the corresponding cuts of previously known results in Refs. [114, 122, 155].

We thus conclude that in all three examples that we analyzed, the coefficients in the expansion Eq. (2.3.6) are determined up to one constant by zero conditions. The set of relations is more complicated in the three-loop four-point and two-loop five-point examples than in the two-loop four-point example, but in all cases all coefficients are determined as simple rational numbers without any kinematic dependence, leaving one overall coefficient free.

While far from a proof, these results point to the existence of an amplituhedron-like construction in the nonplanar sector of the theory. As discussed in Sect. 2.2, in the planar sector the existence of such a construction implies that homogeneous conditions determine the amplitudes up to an overall normalization. This is indeed what we have found in the various nonplanar examples studied above: the homogeneous requirements of only logarithmic singularities, no poles at infinity, and vanishing of unphysical cuts do determine the amplitudes. In any case, the notion that homogeneous conditions fully determine amplitudes opens a door to applying these ideas to other theories where no geometric properties are expected. Of course, we ultimately would like a direct amplituhedron-like geometric formulation of  $\mathcal{N} = 4$  SYM amplitudes, including the nonplanar contributions. As a next step we would need sensible global variables that allow us to define a unique integrand.

## 2.5 Conclusion

In this paper we found evidence that an amplituhedron-like construction of nonplanar  $\mathcal{N} = 4$  SYM theory scattering amplitudes may exist. We did so by checking the expected consequences of such a construction: that the integrand should be determined by homogeneous conditions, such as vanishing on certain cut solutions. We also gave additional nontrivial evidence for the conjecture that only logarithmic singularities appear in nonplanar amplitudes [1, 119], which is another characteristic feature of planar amplitudes resulting from the amplituhedron construction.

An important complication is that unlike in the planar sector, there is no unique integrand of scattering amplitudes which can be directly interpreted as a volume of some space. This forced us to chop up the amplitude into local diagrams containing only Feynman propagators. As pointed out in Ref. [119] and further developed in Ref. [1], analytic properties that follow from dual conformal invariance can be imposed on such local diagrams. We developed the notion of a pure integrand basis: a basis of integrands with only logarithmic singularities, no poles at infinity and only unit leading singularities. The first property is motivated by the analogous statement for on-shell diagrams in  $\mathcal{N} = 4$  SYM. If, like in the planar case, we understood how to formulate



nonplanar recursion relations, we expect that it would then be possible to express nonplanar amplitudes directly as sums of on-shell diagrams [67, 112, 163] and manifestly expose their  $d\log$  structure. The latter two properties lift the exact content of dual conformal symmetry in the planar sector to the nonplanar one.

We constructed a pure integrand basis for each of the two-loop four-point, three-loop four-point and two-loop five-point amplitudes, and showed that the amplitudes could be expanded in their respective bases. This confirmed that the three example amplitudes share the three properties of the pure integrands. Our pure integrand representations here are closely related to Refs. [1, 119] for four-point amplitudes at two- and three-loops, while our representation of the two-loop five-point amplitude has completely novel properties compared to the result in Ref. [155]. The fact that we exposed analytic properties in the nonplanar sector similar to those connected to dual conformal symmetry in the planar sector suggests that an analog of dual conformal symmetry may exist in the nonplanar sector. (For Yangian symmetry a similar statement is less clear.)

One particularly bold future goal is to lift the amplituhedron [18] paradigm from the planar sector to the nonplanar sector of  $\mathcal{N} = 4$  SYM. The amplituhedron provides a geometric picture of the planar integrand where all standard physical principles like locality and unitarity are derived. In such a picture, traditional ways of organizing amplitudes, be it via Feynman diagrams, unitarity cuts, or even on-shell diagrams, are consequences of amplituhedron geometry, rather than a priori organizational principles. The amplituhedron reverses traditional logic, as logarithmic singularities and dual conformal symmetry, rather than locality and unitarity, are fundamental inputs into the definition of the amplituhedron. The definition then invokes intuitive geometric ideas about the inside of a projective triangle, generalized to the more complicated setting of Grassmannian geometry.

We would like to carry this geometric picture over to the nonplanar sector. However, a lack of global variables limits us to demanding that the amplitude be a sum of local integrals. This already imposes locality and some unitarity constraints. Nevertheless, after imposing special analytic structures on the basis integrals — unit logarithmic singularities with no poles at infinity — one can extract the “remaining” geometric information. Motivated by the discussion in Ref. [154], in this paper we conjectured that this remaining information is a set of *zero conditions*, i.e. cuts on which the amplitude vanishes. This is exactly the statement which we successfully carried over to the nonplanar sector and tested in examples in Sect. 2.4. Here we propose that after constructing a pure integrand basis, zero conditions are sufficient for finding the complete amplitude.

This provides nontrivial evidence that an amplituhedron-like construction might very

well exist beyond the planar limit for amplitudes in  $\mathcal{N} = 4$  SYM theory. However there are still many obstacles including, among other things, a choice of good variables and a geometric space in which nonplanar scattering amplitudes are defined as volumes. If such a nonplanar amplituhedron really exists, it would be phrased in terms of very interesting mathematical structures going beyond those of the planar amplituhedron. If our zero condition conjecture indeed holds, how might it extend to other theories? The most naive possibility is that  $\mathcal{N} = 4$  SYM amplitudes are the most constrained amplitudes and so need no inhomogeneous conditions except for overall normalization, while amplitudes in other theories, with less supersymmetry for example, do need additional inhomogeneous information. Even in such theories the zero conditions would still constrain the amplitudes, and it would be interesting to see which and how many additional inhomogeneous conditions are required to completely determine the amplitudes.

It may be possible to link the  $\mathcal{N} = 4$  SYM results we presented here directly to identical helicity amplitudes in quantum chromodynamics (QCD) via dimension shifting relations [164, 165]. These relations were recently employed to aid in the construction of a representation of the two-loop five-point identical helicity QCD amplitude where the duality between color and kinematics holds [166]. It should also be possible to find a new representation of the identical helicity QCD amplitude in terms of the  $\mathcal{N} = 4$  SYM representation we gave here.

Another line of research is to concentrate on individual integrals rather than on the full amplitude. After integration, integrands with only logarithmic singularities are expected to have uniform maximum transcendental weight at the loop order of the integrand [115]. This provides a nice connection between properties of the integrand and conjectured properties of final integrated amplitudes. On the practical level, having a good basis of master integrals under integral reduction is important for many problems, including applications to phenomenology. As explained in Refs. [123, 124], uniformly transcendental integrals obey relatively simple differential equations, making them easy to work with [126, 167]. This also makes our basis of pure integrands useful for five-point scattering in NNLO QCD. For a recent discussion of the planar case see Ref. [168].

As already noted in Ref. [1], the types of gauge-theory results described here can have a direct bearing on issues in quantum gravity, through the double-copy relation of Yang-Mills theories to gravity [114]. We expect that developing a better understanding of the nonplanar sector of  $\mathcal{N} = 4$  SYM will aid our ability to construct corresponding gravity amplitudes, where no natural separation of planar and nonplanar contributions exists.

In summary, we have presented evidence that nonplanar integrands of  $\mathcal{N} = 4$  SYM share important analytic structure with planar ones. We have also presented evidence

for a geometric structure similar to the amplituhedron [18] based on the idea that such a structure implies that zero conditions are sufficient to fix the amplitude, up to an overall normalization. While there is much more to do, these results suggest that the full theory has structure at least as rich as the planar theory.

# Gravity on-shell diagrams

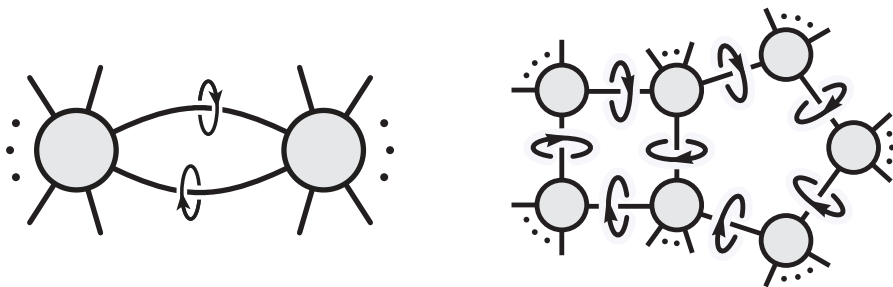
We study on-shell diagrams for gravity theories with any number of supersymmetries and find a compact Grassmannian formula in terms of edge variables of the graphs. Unlike in gauge theory where the analogous form involves only  $d\log$ -factors, in gravity there is a non-trivial numerator as well as higher degree poles in the edge variables. Based on the structure of the Grassmannian formula for  $\mathcal{N} = 8$  supergravity we conjecture that gravity loop amplitudes also possess similar properties. In particular, we find that there are only logarithmic singularities on cuts with finite loop momentum, poles at infinity are present, and loop amplitudes show special behavior on certain collinear cuts. We demonstrate on 1-loop and 2-loop examples that the behavior on collinear cuts is a highly non-trivial property which requires cancellations between all terms contributing to the amplitude.

### 3.1 Introduction

Within the field of scattering amplitudes, a great number of developments in the last decade or so are based on powerful on-shell methods [23, 38, 39, 134, 138, 157, 169]. Amongst others, BCFW-recursion [38, 39] and generalized unitarity [23, 138, 157] allowed us to push the boundary of computable amplitudes in terms of number of loops and legs. The core idea behind these methods is that on-shell amplitudes break up into products of simpler amplitudes on all factorization channels. In the traditional picture of Quantum Field Theory, locality and unitarity dictate the form and locations of all these residues. In particular, they arise in kinematic regions where either internal particles or sums of external particles become on-shell. Associated with these residues are vanishing propagators and in this context we talk about *cuts* of the amplitude. Symbolically, one can write the two types of elementary cuts (singularities) as [40],

$$\partial \left| \begin{array}{c} \cdot \\ \cdot \\ \cdot \\ \cdot \\ \cdot \\ \cdot \\ \cdot \\ \cdot \\ \cdot \\ \cdot \end{array} \right| \begin{array}{c} \cdot \\ \cdot \\ \cdot \\ \cdot \\ \cdot \\ \cdot \\ \cdot \\ \cdot \\ \cdot \\ \cdot \end{array} \left| \right. = \sum_{L,R} \begin{array}{c} \cdot \\ \cdot \\ \cdot \\ \cdot \\ \cdot \\ \cdot \\ \cdot \\ \cdot \\ \cdot \\ \cdot \end{array} \left| \begin{array}{c} \cdot \\ \cdot \\ \cdot \\ \cdot \\ \cdot \\ \cdot \\ \cdot \\ \cdot \\ \cdot \\ \cdot \end{array} \right| \begin{array}{c} \cdot \\ \cdot \\ \cdot \\ \cdot \\ \cdot \\ \cdot \\ \cdot \\ \cdot \\ \cdot \\ \cdot \end{array} \left| \right. + \sum_a \begin{array}{c} \cdot \\ \cdot \\ \cdot \\ \cdot \\ \cdot \\ \cdot \\ \cdot \\ \cdot \\ \cdot \\ \cdot \end{array} \left| \begin{array}{c} \cdot \\ \cdot \\ \cdot \\ \cdot \\ \cdot \\ \cdot \\ \cdot \\ \cdot \\ \cdot \\ \cdot \end{array} \right| \begin{array}{c} \cdot \\ \cdot \\ \cdot \\ \cdot \\ \cdot \\ \cdot \\ \cdot \\ \cdot \\ \cdot \\ \cdot \end{array} \left| \right. \quad (3.1.1)$$

where the first term corresponds to the factorization into a product of lower point amplitudes (keeping the total loop degree fixed) while the second term is the forward limit of an  $(L - 1)$ -loop,  $(n + 2)$ -point amplitude. In general field theories this term suffers from IR-divergencies [170] and therefore, in many cases the fundamental cut is the well-known *unitarity cut* [171, 172]. Iterating these cuts one can calculate multi-dimensional residues by setting an increasing number of propagators to zero. This is known in the literature as *generalized unitarity* [23, 138, 157].



Generically, it is not possible to set to zero more than two propagators in a given loop while simultaneously also requiring real kinematics. Therefore, the loop momenta are complex when constrained by the set of on-shell conditions which implies that these singularities are outside the physical integration region. The main success of generalized unitarity then relies on the fact that the integrands are rational functions

that can be analytically continued so that complex residues (given by a sufficient set of cuts) completely specify them.

A natural next step in this line of thought is to cut the maximum number of propagators which factorizes the amplitude into the simplest building blocks [138]. The most elementary case occurs when all factors are three-point amplitudes. As we will describe in a moment, these are rather special due to the particular features of three-point kinematics. In this scenario we talk about *on-shell diagrams* [67].

### 3.1.1 On-shell diagrams

For massless particles, the three-point amplitudes are completely fixed by Poincare symmetry to all loop orders in perturbation theory up to an overall constant [173]. This statement holds in any Quantum Field Theory with massless states and just follows from the fact that there are no kinematic invariants one can build out of three on-shell momenta. For real external kinematics, the on-shell conditions,  $p_1^2 = p_2^2 = p_3^2 = 0$  and momentum conservation  $p_1 + p_2 + p_3 = 0$  would force all three point amplitudes to vanish. However, for complex kinematics in  $D = 4$  we have two distinct solutions [36] which can be conveniently written using spinor-helicity [174] variables  $p^\mu = \sigma_{\alpha\dot{\alpha}}^\mu \lambda_\alpha \tilde{\lambda}_{\dot{\alpha}}$ .

$$\text{I.) } \tilde{\lambda}_1 \sim \tilde{\lambda}_2 \sim \tilde{\lambda}_3 \text{ (MHV)}, \quad \text{II.) } \lambda_1 \sim \lambda_2 \sim \lambda_3 \text{ (}\overline{\text{MHV}}\text{)}.$$

Any three-point amplitude is then either of type I.) or II.). In particular, for the gluon-amplitudes in Yang-Mills theory we have two elementary amplitudes with MHV (+ - -) or  $\overline{\text{MHV}}$  (- + +) helicity configuration (ignoring higher dimensional operators that could lead to ( $\pm\pm\pm$ ) amplitudes, see e.g. [175]). In the maximally supersymmetric case of  $\mathcal{N} = 4$  sYM theory these gluonic amplitudes are embedded in the MHV, resp.  $\overline{\text{MHV}}$  superamplitudes (see e.g. [43]) which we denote by blobs with different colors,

$$\begin{array}{c} 2 \\ \diagup \\ \text{---} \bullet \text{---} \\ \diagdown \\ 3 \end{array} = \frac{\delta^4(P)\delta^8(Q)}{\langle 12\rangle\langle 23\rangle\langle 31\rangle}, \quad \begin{array}{c} 2 \\ \diagup \\ \text{---} \circ \text{---} \\ \diagdown \\ 3 \end{array} = \frac{\delta^4(P)\delta^4(\tilde{Q})}{[12][23][31]}, \quad (3.1.2)$$

where  $\langle ij \rangle = \epsilon_{\alpha\beta} \lambda_i^\alpha \lambda_j^\beta$  and  $[ij] = \epsilon_{\dot{\alpha}\dot{\beta}} \tilde{\lambda}_i^{\dot{\alpha}} \tilde{\lambda}_j^{\dot{\beta}}$ . Using the anti-commuting  $\tilde{\eta}^I$ ,  $I = 1, \dots, 4$  variables to write the on-shell multiplet as [176],

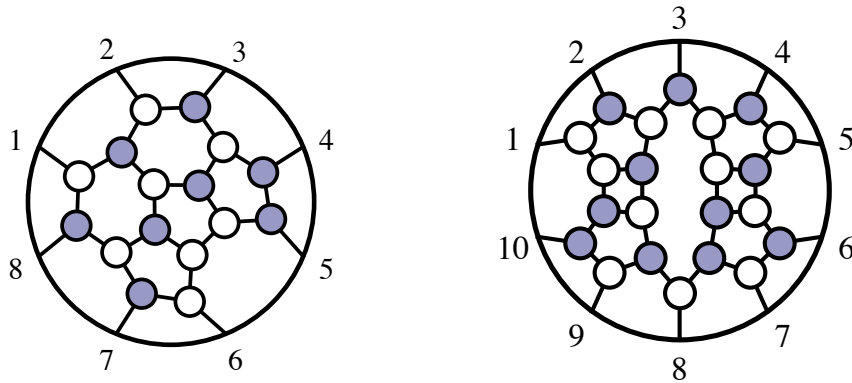
$$\Phi(\tilde{\eta}) = g^+ + \tilde{\eta}^I \tilde{g}_I + \frac{1}{2!} \tilde{\eta}^I \tilde{\eta}^J \phi_{IJ} + \frac{1}{3!} \epsilon_{IJKL} \tilde{\eta}^I \tilde{\eta}^J \tilde{\eta}^K \tilde{g}^L + \frac{1}{4!} \epsilon_{IJKL} \tilde{\eta}^I \tilde{\eta}^J \tilde{\eta}^K \tilde{\eta}^L g^-,$$

the arguments of the respective delta-functions in (3.1.2) are given by (neglecting all spinor- and  $SU(4)$   $R$ -symmetry indices),

$$P \equiv \lambda \cdot \tilde{\lambda} = \lambda_1 \tilde{\lambda}_1 + \lambda_2 \tilde{\lambda}_2 + \lambda_3 \tilde{\lambda}_3, \quad Q \equiv \lambda \cdot \tilde{\eta} = \lambda_1 \tilde{\eta}_1 + \lambda_2 \tilde{\eta}_2 + \lambda_3 \tilde{\eta}_3, \quad \tilde{Q} = [12] \tilde{\eta}_3 + [23] \tilde{\eta}_1 + [31] \tilde{\eta}_2.$$

Here and in the following we denote  $\lambda \cdot \tilde{\lambda} \equiv \sum_{a=1}^n \lambda_a \tilde{\lambda}_a$ ,  $\lambda \cdot \tilde{\eta} \equiv \sum_{a=1}^n \lambda_a \tilde{\eta}_a$  as the sum over all external particles.

Having completed the discussion of three-particle amplitudes, we are now in the position to introduce on-shell diagrams. For us, an on-shell diagram is any graph formed from the two types of three-point amplitudes (3.1.2) connected by edges,



that all represent on-shell particles (both internal and external). In this section we review properties of on-shell diagrams in planar  $\mathcal{N} = 4$  sYM and introduce all concepts relevant for our gravity discussion later. Further details can be found directly in [67] and the review article [13]. With this definition, the value of the diagram is given by the product of three-point amplitudes satisfying the on-shell conditions for all edges. In practice, the delta functions of the elementary three-point amplitudes can be used for solving for  $\lambda_I$ ,  $\tilde{\lambda}_I$ , and  $\tilde{\eta}_I$  of the internal particle and writing the overall result (including delta functions), using external data only. In this case we talk about *leading singularities* [134]. If the number of on-shell conditions exceeds the number of internal degrees of freedom, we get additional constraints on the external kinematics, while in the opposite case the on-shell diagram depends on some unfixed parameters. These cases are easily classified by a parameter  $n_\delta$  counting the number of constraints on external kinematics  $n_\delta = 0$ ,  $n_\delta > 0$ , and  $n_\delta < 0$ .

The simplest example of a reduced on-shell diagram ( $n_\delta = 0$ ) actually represents the color-ordered four-point tree-level amplitude which consists of four vertices. The simpler looking on-shell diagram with only two vertices is the residue of the amplitude on the  $t$ -channel factorization pole and imposes a constraint ( $n_\delta = 1$ ) on the external

momenta.

$$\begin{aligned}
 & \text{Diagram 1} = \frac{\delta^4(\lambda \cdot \tilde{\lambda}) \delta^8(\lambda \cdot \tilde{\eta})}{\langle 12 \rangle \langle 23 \rangle \langle 34 \rangle \langle 41 \rangle} \\
 & \text{Diagram 2} = \frac{\delta^4(\lambda \cdot \tilde{\lambda}) \delta^8(\lambda \cdot \tilde{\eta}) \delta(\langle 14 \rangle)}{\langle 12 \rangle \langle 23 \rangle \langle 34 \rangle}
 \end{aligned}
 \tag{3.1.3}$$

As an example for the third possibility ( $n_\delta < 0$ ), we can draw a diagram which depends on one unfixed parameter  $z$ .

$$\text{Diagram} = \frac{\delta^4(\lambda \cdot \tilde{\lambda}) \delta^8(\lambda \cdot \tilde{\eta})}{z \langle 12 \rangle \langle 23 \rangle (\langle 34 \rangle + z \langle 31 \rangle) \langle 41 \rangle}
 \tag{3.1.4}$$

The counting is easy to understand if we think about the diagram as a hepta-cut of the two loop amplitude: there are seven on-shell conditions imposed on two off-shell loop momenta, leaving one degree of freedom unfixed. In the diagram  $z$  parametrizes the momentum flow along the edge between external legs 1 and 4,  $\ell(z) = z \lambda_1 \tilde{\lambda}_4$  but also other internal legs will depend on  $z$ . In the standard approach of generalized unitarity, this diagram represents a *maximal cut* as there are no further propagators available to cut and localize the remaining degree of freedom. However, the amplitude does have further residues at  $z = 0$  and  $z = \frac{\langle 34 \rangle}{\langle 13 \rangle}$ . Each residue corresponds to erasing an edge of (3.1.4) giving the one-loop on-shell diagram on the left of (3.1.3). This is a leading singularity of the amplitude – all degrees of freedom in loop momenta are fixed by on-shell conditions.

It turns out that not all on-shell diagrams are independent, but rather there are equivalence classes of diagrams related by certain identity moves. The first is the *merge and expand* move represented in (3.1.5). The black vertices enforce all  $\tilde{\lambda}$ 's to be proportional, which is independent of the way the individual three-point amplitudes are



connected,

(3.1.5)

One further nontrivial move is the *square move* [177], which can be motivated by the cyclic invariance of the four-particle tree level amplitude,

(3.1.6)

Together with *bubble deletion* which does not play a role in our discussion here, these are all the equivalence moves for planar  $\mathcal{N} = 4$  sYM. Modulo the aforementioned moves, it is possible to give a complete classification of on-shell diagrams [67] in this theory.

Besides representing cuts of loop amplitudes, on-shell diagrams serve directly as building blocks for constructing amplitudes. In particular, the BCFW recursion relation for tree-level amplitudes and loop integrands in planar  $\mathcal{N} = 4$  sYM theory is represented by [40, 67]

This equation is a solution to the question what on-shell function has singularities given by (3.1.1). Here planarity was crucial because it permitted a unique definition of the *integrand* as a rational function with certain properties. It is this integrand which can be constructed recursively. The key point was the existence of global variables

(dual variables and momentum twistors [47]) common to all terms in the expansion. Currently, it is the lack of global labels that hampers the extension of the recursion relations beyond the planar limit.

While the recursion relations are only formulated in planar  $\mathcal{N} = 4$  sYM so far, the on-shell diagrams are well defined gauge invariant objects in any Quantum Field Theory, planar or non-planar, with or without supersymmetry. They are defined as products of on-shell three-point amplitudes (for theories with fundamental three point amplitudes) and at the least represent cuts of loop amplitudes. From that point of view they encode an important amount of information about amplitudes in any theory and their properties are well worth studying in its own right.

### 3.1.2 Grassmannian formulation

Besides viewing on-shell diagrams as gluing of three-point amplitudes integrated over the on-shell phase space (including the sum over all physical states that can cross the cut) there is a completely different way how to calculate on-shell diagrams. This *dual formulation* expresses on-shell diagrams as differential forms on the (positive) Grassmannian [67]. There are a number of ways how to motivate this picture starting from classifying configurations of points with linear dependencies to representing the permutation group in terms of planar bi-colored graphs [86]. Physically, the most direct way to discover the Grassmannian picture for on-shell diagrams is to think about momentum conservation more seriously. Starting from the innocuous equation,

$$\delta^4(P) \equiv \delta^4(\lambda \cdot \tilde{\lambda}) = \delta^4(\lambda_1 \tilde{\lambda}_1 + \lambda_2 \tilde{\lambda}_2 + \cdots + \lambda_n \tilde{\lambda}_n), \quad (3.1.7)$$

one notes that this is a quadratic condition on the spinor-helicity variables. Naturally, one can ask if there is a way to trivialize the quadratic constraints and rewrite them as sets of linear relations between  $\lambda$ s and  $\tilde{\lambda}$ s separately. The solution to this problem is to introduce an auxiliary  $k$ -plane in  $n$ -dimensions represented by a  $(k \times n)$ -matrix  $C$  modulo a  $GL(k)$  redundancy arising from row operations that leave the  $k$ -plane invariant. This space is known as the Grassmannian  $G(k, n)$ . Using these auxiliary variables, momentum conservation is then enforced geometrically [68–70] via the following set of delta functions (similar relations hold in twistor and momentum twistor spaces),

$$\delta^{(k \times 2)}(C_{\alpha a} \tilde{\lambda}_a) \delta^{((n-k) \times 2)}(C_{\beta a}^\perp \lambda_a), \quad (3.1.8)$$

where  $C^\perp$  denotes the  $((n-k) \times n)$ -matrix orthogonal to  $C$ ,  $C \cdot C^\perp = 0$ . There are  $2n$  delta functions in total; four of them give the overall momentum conservation while the remaining  $2n - 4$  constrain the parameters of the  $C$ -matrix.

The study of Grassmannians is a vast and active topic in the mathematics community ranging, amongst others, from combinatorics to algebraic geometry [85–90]. There is

a close connection to on-shell diagrams which was simultaneously discovered both by physicists in the context of scattering amplitudes and by mathematicians (in the math literature these diagrams are called *plabic graphs*) in searching for positive parameterizations of Grassmannians. In particular, each on-shell diagram gives a parameterization for the  $C$ -matrix using a set of variables  $\alpha_j$ . When these variables are real with definite signs, the matrix  $C$  has all main minors positive and then we talk about positive Grassmannian  $G_+(k, n)$ . These variables are associated with either faces or edges of the diagram. The face variables are more invariant but they can be used only in planar diagrams. Since in this paper we will include non-planar examples we use *edge variables* instead to parametrize the Grassmannian matrix.

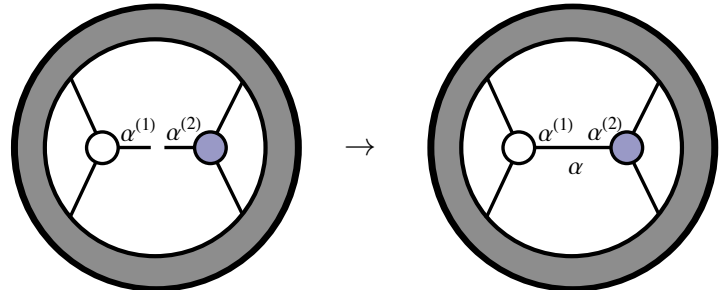
Like in the physical picture where on-shell diagrams are products of three-point amplitudes we also start our discussion with elementary three point vertices. We first choose a *perfect orientation* in which we attach arrows to all legs. For all black vertices two of the arrows are incoming and one outgoing while for white vertices one is incoming and two outgoing. Then we associate a  $(2 \times 3)$ -matrix with the black (MHV,  $k = 2$ ) vertex and a  $(1 \times 3)$ -matrix with the white ( $\overline{\text{MHV}}$ ,  $k = 1$ ) vertex in the following way:

$$\begin{array}{ccc}
 \begin{array}{c} 2 \\ \swarrow \alpha_2 \\ \bullet \\ \nearrow \alpha_1 \\ 1 \end{array} & & \begin{array}{c} 2 \\ \swarrow \alpha_2 \\ \circ \\ \nearrow \alpha_1 \\ 1 \end{array} \\
 \updownarrow & & \updownarrow \\
 C = \begin{pmatrix} 1 & 0 & \alpha_1\alpha_3 \\ 0 & 1 & \alpha_2\alpha_3 \end{pmatrix} & & C = (\alpha_1\alpha_3 \ \alpha_2\alpha_3 \ 1) .
 \end{array} \tag{3.1.9}$$

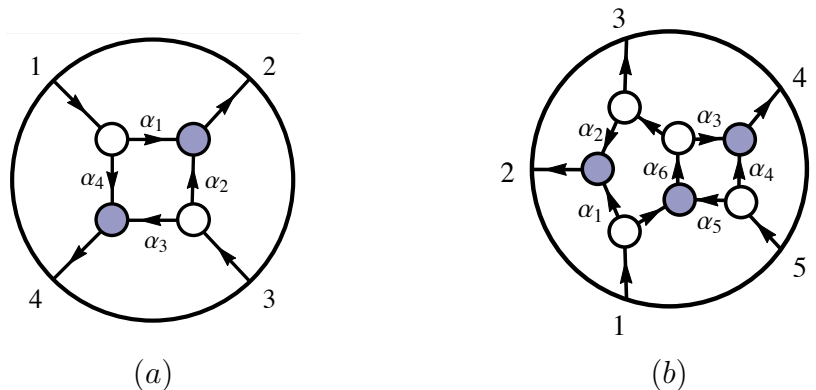
Choosing a perfect orientation fixes a part of the general  $GL(k)$ -redundancy of the  $C$ -matrix that represents a point in the Grassmannian. With the remaining  $GL(1)_v$ -freedom we are allowed to fix any one of the variables associated to the half-edges of that vertex to some arbitrary value. The canonical choice would be  $\alpha_3 = 1$ , but any other finite, nonzero value is allowed as well. For the moment though, let us keep this freedom unfixed.

In the next step we glue the atomic three-point vertices together into an arbitrary planar on-shell diagram to which we associate some bigger  $(k \times n)$ -matrix  $C$ . In the gluing process, we identify two half-edges of the vertices involved in the fusion to form an internal edge of the bigger on-shell diagram. Each internal edge of this big diagram is then parametrized by two variables,  $\alpha^{(1)}$  and  $\alpha^{(2)}$ , coming from the two vertices

involved in the gluing process so that the  $C$ -matrix will only depend on their product  $\alpha = \alpha^{(1)}\alpha^{(2)}$ . Pictorially, this process is simple to state (the grey blob denotes the rest of the diagram),


(3.1.10)

and illustrates that it is natural to directly use edge-variables  $\alpha_k$  rather than the individual vertex variables introduced by the little Grassmannians. The identification is as follows; in the gluing process we encounter another  $GL(1)_e$  redundancy stemming from the fact that the internal momentum of that edge is invariant under little group rescaling  $\lambda_I \rightarrow t_I \lambda_I$ ,  $\tilde{\lambda}_I \rightarrow t_I^{-1} \tilde{\lambda}_I$  which allows us to combine two of the vertex-variables into a single edge-variable. Doing this for all internal edges, we are only left with the  $GL(1)_v$  redundancies for each vertex in the big on-shell diagram which we can use to set certain edge weights to one for instance.


(3.1.11)

In terms of edge-variables, the rule how to obtain the  $C$ -matrix from the graph is quite simple. First, we have to choose a perfect orientation for the diagram by consistently decorating all edges with arrows. The external legs with incoming arrows are called *sources*, while the external legs with outgoing arrows are called *sinks*. For the diagram with  $k$  sources and  $n - k$  sinks we construct a  $(k \times n)$  matrix  $C$ . Note that these numbers do not depend on the way we choose a perfect orientation but are an invariant property of the on-shell diagram itself. Each row of the matrix is associated with one source while the columns are linked to both sources and sinks. Now each entry  $C_{\alpha a}$  is

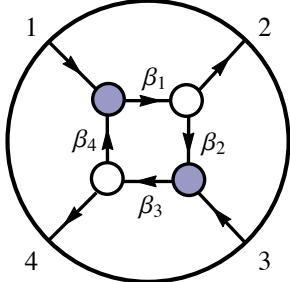
calculated as

$$C_{\alpha a} = \sum_{\Gamma_{\alpha \rightarrow a}} \prod_j \alpha_j, \quad (3.1.12)$$

where we sum over all directed paths  $\Gamma_{\alpha \rightarrow a}$  from the source  $\alpha$  to the sink  $a$  by following the arrows. Along the way we take the product of all edge variables. If the label  $a = \alpha$  is the same source we fix the matrix entry to 1 if  $a = \alpha'$  is a different source the matrix entry is 0. For the examples above the  $C$ -matrices are,

$$C^{(a)} = \begin{pmatrix} 1 & \alpha_1 & 0 & \alpha_4 \\ 0 & \alpha_2 & 1 & \alpha_3 \end{pmatrix}, \quad C^{(b)} = \begin{pmatrix} 1 & \alpha_1 + \alpha_2\alpha_6 & \alpha_6 & \alpha_3\alpha_6 & 0 \\ 0 & \alpha_5\alpha_6\alpha_2 & \alpha_5\alpha_6 & \alpha_4 + \alpha_3\alpha_5\alpha_6 & 1 \end{pmatrix}. \quad (3.1.13)$$

Different choices for the sources and sinks corresponds to different gauge fixings of the  $C$ -matrix that are related by  $GL(k)$ -transformations. For some gauge choices, the perfect orientation can involve closed loops. In these cases there are infinitely many paths from  $\alpha$  to  $a$  and we have to sum over all of them,



$$\Leftrightarrow C = \begin{pmatrix} 1 & \beta_1\delta & 0 & \beta_1\beta_2\beta_3\delta \\ 0 & \beta_3\beta_4\beta_1\delta & 1 & \beta_3\delta \end{pmatrix}, \quad (3.1.14)$$

where  $\delta$  is given by a geometric series,

$$\delta = \sum_{\sigma=0}^{\infty} (\beta_1\beta_2\beta_3\beta_4)^\sigma = \frac{1}{1 - \beta_1\beta_2\beta_3\beta_4}. \quad (3.1.15)$$

The important connection between the Grassmannian formulation and physics is that the same on-shell diagram that labels the  $C$ -matrix also represents a cut of a scattering amplitude in planar  $\mathcal{N} = 4$  sYM. The nontrivial relation is that the value of the on-shell diagram as calculated by multiplying three-point amplitudes is equal to the following differential form

$$d\Omega = \frac{d\alpha_1}{\alpha_1} \frac{d\alpha_2}{\alpha_2} \dots \frac{d\alpha_m}{\alpha_m} \delta(C \cdot Z). \quad (3.1.16)$$

All the dependence on external kinematics is pushed into the delta functions,

$$\delta(C \cdot Z) \equiv \delta^{(k \times 2)}(C_{ab} \tilde{\lambda}_b) \delta^{((n-k) \times 2)}(C_{cb}^\perp \lambda_b) \delta^{(k \times \mathcal{N})}(C_{ab} \tilde{\eta}_b), \quad (3.1.17)$$

which linearize both momentum and super-momentum conservation  $\delta^4(P) \delta^8(\mathcal{Q})$  using the auxiliary Grassmannian  $C$ -matrix associated with the diagram. Depending on the details of the given diagram, the delta functions (3.1.17) allow us to fix a certain number of edge variables  $\alpha_j$ . In the case of on-shell diagrams relevant for tree-level amplitudes (leading singularities), all variables are fixed, while the on-shell diagrams appearing in the loop recursion relations have  $4L$  unfixed parameters  $\alpha_j$  which are related to the  $4L$  degrees of freedom of  $L$  off-shell loop momenta  $\ell_i$ .

So far, the  $((n-k) \times n)$ -matrix  $C^\perp$  orthogonal to  $C$ , defined via  $C \cdot C^\perp = 0$ , has played no significant role in our discussion but is crucial for momentum conservation in (3.1.8) and (3.1.17). Given a gauge fixed  $C$ -matrix, there is a simple rule how to obtain  $C^\perp$ . One takes the  $(n-k)$  columns of the  $C$ -matrix that correspond to the  $(n-k)$  sinks of the on-shell diagram. For each such column of  $C$ , one forms a row of  $C^\perp$  by writing the negative entries of the column into the slots that correspond to the sources. The remaining  $((n-k) \times (n-k))$  matrix entries of  $C^\perp$  are then filled by a  $((n-k) \times (n-k))$  identity-matrix. Let us apply the construction procedure to some concrete examples. For the  $C$ -matrices in (3.1.13) corresponding to the on-shell diagrams (3.1.11), we get the following  $C^\perp$ -matrices:

$$C_{(a)}^\perp = \begin{pmatrix} -\alpha_1 & 1 & -\alpha_2 & 0 \\ -\alpha_4 & 0 & -\alpha_3 & 1 \end{pmatrix}, \quad C_{(b)}^\perp = \begin{pmatrix} -(\alpha_1 + \alpha_2\alpha_6) & 1 & 0 & 0 & -\alpha_5\alpha_6\alpha_2 \\ -\alpha_6 & 0 & 1 & 0 & -\alpha_5\alpha_6 \\ -\alpha_6\alpha_3 & 0 & 0 & 1 & -(\alpha_4 + \alpha_5\alpha_6\alpha_3) \end{pmatrix}. \quad (3.1.18)$$

Now that we have all ingredients together, we can go ahead and consider a simple on-shell diagram in detail. Specifically, we calculate the box on-shell diagram (3.1.11)(a), in which case the delta functions (3.1.17) are equal to

$$\delta(C \cdot Z) = \frac{1}{\langle 13 \rangle^4} \delta \left[ \alpha_1 - \frac{\langle 23 \rangle}{\langle 13 \rangle} \right] \delta \left[ \alpha_2 - \frac{\langle 12 \rangle}{\langle 13 \rangle} \right] \delta \left[ \alpha_3 - \frac{\langle 14 \rangle}{\langle 13 \rangle} \right] \delta \left[ \alpha_4 - \frac{\langle 43 \rangle}{\langle 13 \rangle} \right] \delta^4(P) \delta^8(\mathcal{Q}) \quad (3.1.19)$$

and the differential form becomes a function of external kinematics only,

$$d\Omega = \frac{d\alpha_1}{\alpha_1} \frac{d\alpha_2}{\alpha_2} \frac{d\alpha_3}{\alpha_3} \frac{d\alpha_4}{\alpha_4} \delta(C \cdot Z) = \frac{\delta^4(P) \delta^8(\mathcal{Q})}{\langle 12 \rangle \langle 23 \rangle \langle 34 \rangle \langle 41 \rangle}. \quad (3.1.20)$$

This is equal to formula (3.1.3) found by multiplying three-point amplitudes.

The same procedure can be applied to planar on-shell diagrams in  $\mathcal{N} < 4$  sYM. The important difference is that the diagrams are necessarily oriented unlike in the maximally supersymmetric case where the perfect orientations only played an auxiliary role for constructing the  $C$ -matrix. This corresponds to the fact that in less supersymmetric theories we need two on-shell multiplets to capture the positive and negative helicity

gluons (and their respective superpartners) and the arrows specify which multiplet we are talking about. For the external states, we can choose the orientation of the arrows of a given on-shell diagram depending on the helicity structure we want to consider, but for internal legs we have to sum over all possible orientations. In addition, for perfect orientations with closed internal loops we have to add an extra factor,  $\mathcal{J}$ , in the measure,

$$d\Omega = \frac{d\alpha_1}{\alpha_1} \frac{d\alpha_2}{\alpha_2} \dots \frac{d\alpha_m}{\alpha_m} \mathcal{J}^{\mathcal{N}-4} \cdot \delta(C \cdot Z). \quad (3.1.21)$$

This modification arises when passing from vertex-variables to edge-variables and  $\mathcal{J}$  is defined as the determinant of the adjacency matrix  $A_{ij}$  of the graph

$$\mathcal{J} = \det(1 - A). \quad (3.1.22)$$

The entries of  $A$  are given by,

$$A_{ij} = \text{weight of the directed edge } i \rightarrow j \text{ (if any)}. \quad (3.1.23)$$

If there is a collection of closed orbits bounding “faces”  $f_i$ , with *disjoint* pairs  $(f_i, f_j)$ , disjoint triples  $(f_i, f_j, f_k)$  etc., then the Jacobian  $\mathcal{J}$  can be expressed as,

$$\mathcal{J} = 1 + \sum_i f_i + \sum_{\substack{\text{disjoint} \\ \text{pairs } i,j}} f_i f_j + \sum_{\substack{\text{disjoint} \\ \text{triples } i,j,k}} f_i f_j f_k + \dots, \quad (3.1.24)$$

where each “face”  $f_i$  denotes the product of edge-variables along that orbit,

$$f_i = \prod_{r \subset \text{orbit}_i^{\text{closed}}} \alpha_r. \quad (3.1.25)$$

This factor cancels in  $\mathcal{N} = 4$  sYM but in the case of lower supersymmetries it is present. For further details, we refer the reader directly to [67], Sec. 14. Here we included a brief discussion of  $\mathcal{J}$  as it will play a role in our gravity formulas later.

### 3.1.3 Hidden properties of $\mathcal{N} = 4$ sYM amplitudes

The Grassmannian formulation of on-shell diagrams make several important properties of scattering amplitudes in planar  $\mathcal{N} = 4$  sYM completely manifest. The Yangian symmetry [44] is realized as positivity preserving diffeomorphisms [67], and the recursion relations (3.1.1) make manifest that it is also present in tree-level amplitudes and the loop integrands. The loop integration breaks the Yangian symmetry due to the presence of IR-divergencies [48] and all known regulators would break it as well.

There is an ongoing search for a new regulator which would preserve the Yangian using integrability techniques [104–107].

The other important property which is inherited in the formula (3.1.16) is the presence of logarithmic singularities only. This property is much stronger than just the presence of single poles since we require  $\frac{dx}{x}$  behavior near any pole in the cut structure. Each on-shell diagram is given by a  $d\log$  form ( $d\log x \equiv \frac{dx}{x}$ ) in terms of edge variables multiplied by a set of delta functions (3.1.16). One can solve for  $\alpha_k$  in terms of external momenta and off-shell loop momenta, and the full integrand can be written as

$$d\mathcal{I} = \sum_j d\log f_j^{(1)} d\log f_j^{(2)} d\log f_j^{(3)} \dots d\log f_j^{(4L)} \delta(C_j^* \cdot \tilde{\eta}), \quad (3.1.26)$$

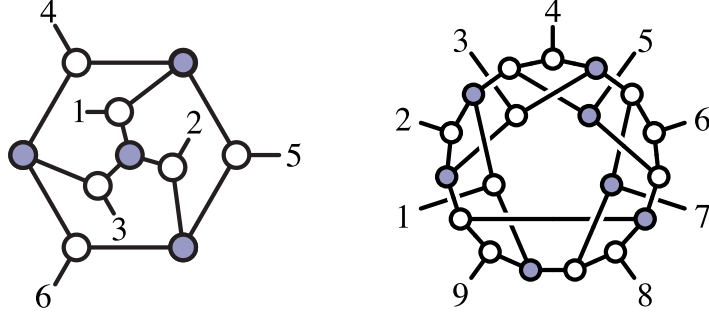
where the  $f_j^{(k)}$  depend both on external and internal momenta and  $C_j$  is the Grassmannian matrix with  $\alpha_k$  substituted for. This representation of the loop integrand is very closely connected to the maximal transcendentality of  $\mathcal{N} = 4$  planar amplitudes [46, 67, 91, 92]. For  $k \leq 4$  the fermionic delta function does not depend on the loop momenta and the representation (3.1.26) can in principle be integrated directly so that one can obtain the final result in terms of polylogarithms [60–66]. For  $k > 4$  the loop momenta are present in the fermionic delta function and the result is not a  $d\log$  form in momentum space, but it still is in terms of edge variables. This gives rise to elliptic functions after integration, which suggests that our notion of  $d\log$  forms and transcendentality should be generalized to include these cases.

Finally, the on-shell diagrams make another important property completely manifest and that is the absence of poles at infinity [67]. In other words, the loop integrand in planar  $\mathcal{N} = 4$  sYM as well as individual on-shell diagrams never generate a singularity which would correspond to sending the loop momentum to infinity,  $\ell \rightarrow \infty$ . This is a consequence of dual conformal symmetry and the representation of on-shell diagrams (and loop integrand) makes that manifest when using momentum twistor variables.

## 3.2 Non-planar on-shell diagrams

On-shell diagrams are well defined for any Quantum Field Theory with fundamental three point amplitudes and do not rely on the planarity of graphs. We can consider an arbitrary bi-colored graph with three-point vertices,





and define the on-shell function as the corresponding product of three-point amplitudes evaluated at specific on-shell kinematics dictated by the graph.

To each diagram we can associate a point in the Grassmannian, represented by the matrix  $C$ . This identification uses the rules explained in the previous section: associate variables with edges  $\alpha_k$ , choose a perfect orientation and calculate the entries of the  $C$ -matrix using Eq. (3.1.12). If the diagram is planar and the edge variables are chosen real and with definite sign, we obtain a cell in the positive Grassmannian  $G_+(k, n)$ , and in other cases we end up in some cell in a generic Grassmannian  $G(k, n)$ .

In general, we want to associate a form  $d\Omega$  which reproduces the on-shell function given by the product of three point amplitudes,

$$d\Omega = df(\alpha_k) \delta(C \cdot Z), \quad (3.2.1)$$

where the measure  $df(\alpha_k)$  depends on the theory while the delta function  $\delta(C \cdot Z)$  only depends on the diagram and external kinematics. Therefore the problem naturally splits into two parts: finding the measure  $df(\alpha_k)$  and the  $C$ -matrix. While the  $C$ -matrix associated to a given on-shell diagram can be found using Eq. (3.1.12), the classification of all possible non-planar diagrams and their associated particular subspace in  $G(k, n)$  represent an important problem. For the case of MHV leading singularities the answer was given in [112] but understanding more general cases is a part of ongoing research [163, 178].

For a generic Quantum Field Theory the measure  $df(\alpha_k)$  associated with a given diagram is not known. However, for the case of Yang-Mills theory the answer has been worked out in [67] and turns out to be surprisingly simple,

$$d\Omega = \frac{d\alpha_1}{\alpha_1} \frac{d\alpha_2}{\alpha_2} \dots \frac{d\alpha_m}{\alpha_m} \mathcal{J}^{\mathcal{N}-4} \cdot \delta(C \cdot Z). \quad (3.2.2)$$

The  $\mathcal{J}$ -factor is given by the determinant of the adjacency matrix (3.1.23) and the singularities coming from this part of the measure are closely related to the UV-sector of the theory. In  $\mathcal{N} = 4$  sYM this term is absent and we get a pure  $d\log$ -form. From

the discussion so far it is clear that writing the form (3.2.2) did not depend on the planarity of the diagram so that the formula is identical to (3.1.16) described in the planar sector. The goal of this section is to extend the knowledge of the Grassmannian formulation beyond the Yang–Mills case and find the analogue of (3.2.2) for gravity on-shell diagrams.

### 3.2.1 First look: MHV leading singularities

The leading singularities are reduced on-shell diagrams ( $n_\delta = 0$ ) associated with on-shell functions  $\Omega$  (rather than forms) and they represent codimension  $4L$  cuts of loop amplitudes. The simplest leading singularities are of MHV-type. In planar  $\mathcal{N} = 4$  sYM they are all equal to the MHV tree-level amplitude given by the Parke-Taylor factor,

$$\text{PT}(123 \dots n) = \frac{1}{\langle 12 \rangle \langle 23 \rangle \langle 34 \rangle \dots \langle n1 \rangle}. \quad (3.2.3)$$

Beyond the planar limit all MHV leading singularities must be holomorphic functions  $F(\lambda)$  [36]. Furthermore, it was shown in [112] that all MHV leading singularities can be decomposed into linear combinations of Parke-Taylor factors with different orderings  $\sigma$ ,

$$\Omega = \sum_{\sigma} c_{\sigma} \text{PT}(\sigma_1 \sigma_2 \dots \sigma_n), \quad \text{where } c_{\sigma} = \pm 1, 0. \quad (3.2.4)$$

This representation makes manifest the fact that all singularities are logarithmic as each Parke-Taylor factor behaves like  $\frac{1}{x}$  near any singularity and one can infer the existence of the logarithmic form directly from the expression (3.2.4). Following the same logic, it is very natural to look at the MHV leading singularities in  $\mathcal{N} = 8$  supergravity and study their expressions in more detail.

Gluing together three-point amplitudes we find some suggestive expressions for a few simple on-shell diagrams (dropping the overall (super-) momentum conserving  $\delta$ -functions in  $\mathcal{N} = 8$  supergravity  $\delta^4(\lambda \cdot \tilde{\lambda}) \delta^{16}(\lambda \cdot \tilde{\eta})$ ),

$$\begin{array}{ccc} \begin{array}{c} 1 \quad 2 \\ \diagdown \quad / \\ \circ \quad \bullet \\ | \quad | \\ \bullet \quad \circ \\ / \quad \diagdown \\ 4 \quad 3 \end{array} & \begin{array}{c} 3 \\ | \\ \circ \\ / \quad \diagdown \\ \bullet \quad \circ \\ | \quad | \\ \bullet \quad \circ \\ / \quad \diagdown \\ 2 \quad 4 \\ | \quad | \\ \bullet \quad \circ \\ / \quad \diagdown \\ 1 \quad 5 \end{array} & \begin{array}{c} 3 \\ | \\ \circ \\ / \quad \diagdown \\ \bullet \quad \circ \\ | \quad | \\ \bullet \quad \circ \\ / \quad \diagdown \\ 2 \quad 4 \\ | \quad | \\ \bullet \quad \circ \\ / \quad \diagdown \\ 1 \quad 5 \end{array} \\ \downarrow & \downarrow & \downarrow \\ \frac{[13][24]}{\langle 12 \rangle \langle 13 \rangle \langle 14 \rangle \langle 23 \rangle \langle 24 \rangle \langle 34 \rangle} & \frac{[12][23][45]^2}{\langle 12 \rangle \langle 13 \rangle \langle 15 \rangle \langle 23 \rangle \langle 34 \rangle \langle 45 \rangle} & \frac{[12][23][45]^2}{\langle 12 \rangle \langle 14 \rangle \langle 15 \rangle \langle 23 \rangle \langle 34 \rangle \langle 35 \rangle} \end{array}$$

From these examples one could conjecture that all poles  $\langle ij \rangle$  are linear and the numerator involves only anti-holomorphic brackets  $[ij]$ . However, looking at more complicated diagrams we learn that this is not the case and one gets both more complicated numerators and higher degree poles in the denominator.

$$\frac{\langle 5|Q_{16}|2\rangle\langle 2|Q_{34}|5\rangle[16]^2[34]^2}{\langle 12\rangle\langle 23\rangle\langle 34\rangle\langle 45\rangle\langle 56\rangle\langle 61\rangle\langle 25\rangle^2} \quad \frac{[23]^2\langle 1|Q_{23}|4\rangle\langle 4|Q_{23}|1\rangle\langle 1|Q_{67}|5\rangle\langle 1|Q_{57}|6\rangle\langle 4|Q_{56}|7\rangle^2}{\langle 14\rangle^3\langle 12\rangle\langle 15\rangle\langle 17\rangle\langle 23\rangle\langle 34\rangle\langle 45\rangle\langle 46\rangle\langle 56\rangle\langle 67\rangle}$$

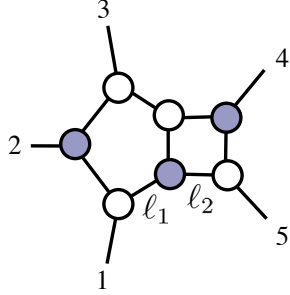
Analyzing the data more closely, especially looking at the on-shell solutions for the momenta of the internal edges, one can make the following statement:

*On-shell diagram vanishes if three momenta in a white vertex are collinear.*

Concretely, the white vertex already enforces the  $\lambda$ 's to be proportional. If, on top of that, the  $\tilde{\lambda}$ 's become collinear as well (which implies the collinearity of momenta) the on-shell diagram vanishes. Interestingly, each factor in the numerator of the on-shell function exactly corresponds to such a condition which is why the number of factors in the numerators equals the number of white vertices in a given MHV on-shell diagram. Taking a closer look at the denominator of the expressions one realizes that all factors which correspond to erasing edges from the on-shell diagram (by sending the momentum of that edge to zero) are single poles. In contrast, all higher poles (and some single poles) correspond to sending the momenta of an internal loop to infinity. Such poles are completely absent in the  $\mathcal{N} = 4$  sYM case – this is related to the statement of no poles at infinity [1, 2, 119] – but in gravity they are present.

To clarify some of these statements, we discuss a concrete example and analyze the

following on-shell diagram:



$$\begin{aligned}
 \ell_1 &= \frac{\lambda_1 Q_{12} \cdot \lambda_3}{\langle 13 \rangle}, & \ell_2 &= \frac{\lambda_5 Q_{12} \cdot \lambda_3}{\langle 35 \rangle}, \\
 \ell_1 - 1 &= \frac{\langle 23 \rangle}{\langle 13 \rangle} \lambda_1 \tilde{\lambda}_2, & \ell_2 - 5 &= \frac{\langle 34 \rangle}{\langle 35 \rangle} \lambda_5 \tilde{\lambda}_4, \\
 \ell_1 - Q_{12} &= \frac{\langle 12 \rangle}{\langle 13 \rangle} \lambda_3 \tilde{\lambda}_2, & \ell_2 - Q_{45} &= \frac{\langle 45 \rangle}{\langle 35 \rangle} \lambda_3 \tilde{\lambda}_4, \\
 \ell_1 - Q_{123} &= \frac{\lambda_3 Q_{23} \cdot \lambda_1}{\langle 13 \rangle}, & \ell_1 + \ell_2 &= \frac{\langle 15 \rangle}{\langle 13 \rangle \langle 35 \rangle} \lambda_3 Q_{12} \cdot \lambda_3.
 \end{aligned}$$

$$\Omega = \frac{[12][23][45]^2}{\langle 12 \rangle \langle 13 \rangle \langle 15 \rangle \langle 23 \rangle \langle 34 \rangle \langle 45 \rangle}. \quad (3.2.5)$$

As explained above, most of the poles  $\langle ij \rangle$  correspond to erasing edges in the on-shell diagram which is equivalent to setting the internal momentum of that edge to zero. In our example  $\langle 13 \rangle$  corresponds to a pole at infinity and on this pole, all momenta associated with this loop blow up. Finally, let's look at the structure of the numerator. Focusing on the white vertex adjacent to external leg 1, the respective on-shell solutions for  $\ell_1$  and  $\ell_1 - p_1$  as well as the external leg become collinear when  $[12] = 0 \Rightarrow \tilde{\lambda}_2 \sim \tilde{\lambda}_1$ ,  $\ell_1 \xrightarrow{[12] \rightarrow 0} \sim \lambda_1 \tilde{\lambda}_1$ ,  $\ell_1 - p_1 \xrightarrow{[12] \rightarrow 0} \sim \lambda_1 \tilde{\lambda}_1$ . As noted earlier, the gravity on-shell form vanishes in this limit due to the factor  $[12]$  in the numerator. For the remaining white vertices, a similar analysis recovers all other square brackets  $[ij]$  in the numerator of the gravity form (3.2.5).

We can take these observations as a starting point in the search for the Grassmannian formulation of gravity on-shell diagrams. We learned that on-shell diagrams can have multiple poles associated with poles at infinity, and importantly the numerator factor must capture the curious collinear behavior observed above.

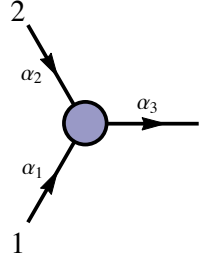
### 3.2.2 Three point amplitudes with spin $s$

The most natural starting point for a Grassmannian representation of gravity on-shell diagrams focuses on the atomic building blocks, the three-point amplitudes, first. We start with a maximally supersymmetric theory of particles with spin  $s$ . In that case, the amount of supersymmetry is given by  $\mathcal{N} = 4s$ . As noted before, in massless theories, the elementary three-point amplitudes are completely fixed by their little group weight to all orders in perturbation theory (up to an overall constant). In particular, the three-point MHV-amplitude for spin  $s$  particles is given by,

$$A_3^{(2)} = \frac{\delta^4(P) \delta^{2\mathcal{N}}(Q)}{\langle 12 \rangle^s \langle 23 \rangle^s \langle 31 \rangle^s}. \quad (3.2.6)$$

The on-shell diagram for this amplitude is just a single black vertex to which we can give a perfect orientation in exactly the same manner as for  $\mathcal{N} = 4$  sYM discussed in

section 3.1.2. We can use exactly the same rules from before to write the  $C$ -matrix,



$$C = \begin{pmatrix} 1 & 0 & \alpha_1 \alpha_3 \\ 0 & 1 & \alpha_2 \alpha_3 \end{pmatrix}. \quad (3.2.7)$$

Here we purposely do not choose any  $GL(1)_v$  gauge fixing in the vertex because gauge-independence will be one of our criteria for finding the correct formula. The first step towards the Grassmannian representation of (3.2.6) is to write the linearized delta functions, which have a very similar form to (3.1.17),

$$\delta^{(2 \times 2)}(C \cdot \tilde{\lambda}) \delta^{(1 \times 2)}(C^\perp \cdot \lambda) \delta^{(2 \times \mathcal{N})}(C \cdot \tilde{\eta}) = \frac{1}{\alpha_3^2 \langle 12 \rangle^{\mathcal{N}-1}} \delta^{(4)}(P) \delta^{(2\mathcal{N})}(\mathcal{Q}). \quad (3.2.8)$$

Using the two bosonic delta-functions from  $\delta^{(1 \times 2)}(C^\perp \cdot \lambda)$ , we can solve for two of the auxiliary  $\alpha_k$  variables,

$$\alpha_1 = \frac{\langle 23 \rangle}{\alpha_3 \langle 12 \rangle}, \quad \alpha_2 = \frac{\langle 13 \rangle}{\alpha_3 \langle 12 \rangle}. \quad (3.2.9)$$

The general form of the Grassmannian representation of (3.2.6), for which the measure depends only on the  $\alpha_k$ -variables and is permutation invariant in all three legs, is

$$d\Omega_\sigma = \frac{d\alpha_1}{\alpha_1^\sigma} \frac{d\alpha_2}{\alpha_2^\sigma} \frac{d\alpha_3}{\alpha_3^\sigma} \delta^{(2 \times 2)}(C \cdot \tilde{\lambda}) \delta^{(1 \times 2)}(C^\perp \cdot \lambda) \delta^{(2 \times \mathcal{N})}(C \cdot \tilde{\eta}), \quad (3.2.10)$$

for some integer  $\sigma$ . We can plug (3.2.8) and (3.2.9) into (3.2.10) to get

$$d\Omega_\sigma = \frac{d\alpha_3}{\alpha_3^{2-\sigma}} \cdot \frac{\delta^{(4)}(P) \delta^{(2\mathcal{N})}(\mathcal{Q})}{\langle 12 \rangle^{\mathcal{N}-1-2\sigma} \langle 23 \rangle^\sigma \langle 31 \rangle^\sigma}. \quad (3.2.11)$$

This expression must be permutation invariant in  $\langle 12 \rangle$ ,  $\langle 23 \rangle$ ,  $\langle 31 \rangle$  and independent of the gauge-choice for  $\alpha_3$ . In order to ensure  $GL(1)$ -invariance,  $\frac{d\alpha_3}{\alpha_3}$  has to factor out as the volume of  $GL(1)$ -transformations. These two requirements leave us with a unique choice:  $\sigma = s = 1$  which corresponds to  $\mathcal{N} = 4$  sYM with the logarithmic measure. Of course, one can also make a special choice,  $\alpha_3 = \frac{1}{\langle 12 \rangle}$  so that  $\alpha_1 = \langle 23 \rangle$ ,  $\alpha_2 = \langle 13 \rangle$ , which allows us to write any three point amplitude (3.2.6) using edge variables only. But our goal is to find a form which is independent of any such choices. Consequently, the form (3.2.10) is not able to reproduce the gravity or any higher spin three-point amplitude.

The natural modification of the form (3.2.10) involves some dimensionful, permutation invariant object  $\Delta$ . The  $\delta(C^\perp \cdot \lambda)$  allows us to relate  $\alpha_1 \lambda_1 + \alpha_2 \lambda_2 + \frac{1}{\alpha_3} \lambda_3 = 0$  which we use in the definition of  $\Delta$  as follows:

$$\Delta \equiv \langle AB \rangle = \langle BE \rangle = \langle EA \rangle \quad \text{where} \quad A = \alpha_1 \lambda_1, \quad B = \alpha_2 \lambda_2, \quad E = \frac{1}{\alpha_3} \lambda_3. \quad (3.2.12)$$

Note that this object has exactly the property suggested by our study of MHV leading singularities: it vanishes when all three momenta are collinear. Now we consider a form

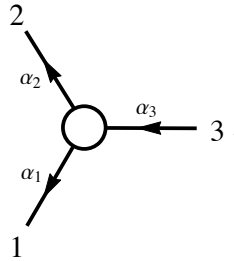
$$d\Omega = \frac{\Delta^\rho \cdot d\alpha_1 d\alpha_2 d\alpha_3}{\alpha_1^{\sigma_1} \alpha_2^{\sigma_2} \alpha_3^{\sigma_3}} \delta^{(2 \times 2)}(C \cdot \tilde{\lambda}) \delta^{(1 \times 2)}(C^\perp \cdot \lambda) \delta^{(2 \times \mathcal{N})}(C \cdot \tilde{\eta}). \quad (3.2.13)$$

Repeating the same exercise that led to (3.2.11) by solving for edge variables, converting the delta functions, imposing permutation invariance and the independence on  $\alpha_3$  uniquely fixes  $\rho = s - 1$  and  $\sigma_1 = \sigma_2 = \sigma_3 = 2s - 1$ . The modified form becomes

$$d\Omega_s = \frac{\Delta^{s-1} \cdot d\alpha_1 d\alpha_2 d\alpha_3}{\alpha_1^{2s-1} \alpha_2^{2s-1} \alpha_3^{2s-1}} \delta^{(2 \times 2)}(C \cdot \tilde{\lambda}) \delta^{(1 \times 2)}(C^\perp \cdot \lambda) \delta^{(2 \times \mathcal{N})}(C \cdot \tilde{\eta}), \quad (3.2.14)$$

which is a Grassmannian representation of (3.2.6). We would find the same unique solution even if we consider  $\Delta = \langle 12 \rangle$  or any other function of  $\alpha_1, \alpha_2, \alpha_3$  and  $\langle 12 \rangle$  ( $\langle 23 \rangle$  and  $\langle 13 \rangle$  are proportional to  $\langle 12 \rangle$  and  $\alpha$ 's). Note that this formula is well defined for all integer spins  $s$  and maximal supersymmetry  $\mathcal{N} = 4s$ . In particular, for  $s = 1$  it reproduces the logarithmic form of  $\mathcal{N} = 4$  sYM.

There is an analogous Grassmannian representation for the  $\overline{\text{MHV}}$  ( $k = 1$ ) three-point amplitudes,



$$C = (\alpha_1 \alpha_3 \quad \alpha_2 \alpha_3 \quad 1). \quad (3.2.15)$$

which can be encoded by the form,

$$d\tilde{\Omega}_s = \frac{\tilde{\Delta}^{s-1} \cdot d\alpha_1 d\alpha_2 d\alpha_3}{\alpha_1^{2s-1} \alpha_2^{2s-1} \alpha_3^{2s-1}} \delta^{(1 \times 2)}(C \cdot \tilde{\lambda}) \delta^{(2 \times 2)}(C^\perp \cdot \lambda) \delta^{(1 \times \mathcal{N})}(C \cdot \tilde{\eta}), \quad (3.2.16)$$

where  $\tilde{\Delta} = [AB] = [BE] = [EA]$  with  $A = \alpha_1 \tilde{\lambda}_1, B = \alpha_2 \tilde{\lambda}_2$  and  $E = \frac{1}{\alpha_3} \tilde{\lambda}_3$ .

### 3.2.3 Grassmannian formula

Equipped with the Grassmannian representation of the three-point amplitudes (3.2.14) and (3.2.16), we can write the Grassmannian representation for any spin  $s$  on-shell diagram. Much like in  $\mathcal{N} = 4$  sYM, using the amalgamation procedure [67] to glue the three-point vertices into larger diagrams, we write the form in terms of edge variables,

$$d\Omega_s = \Gamma \cdot \frac{d\alpha_1 d\alpha_2 \dots d\alpha_d}{\alpha_1^{2s-1} \alpha_2^{2s-1} \dots \alpha_d^{2s-1}} \cdot \prod_{b \in B_v} \Delta_b^{s-1} \cdot \prod_{w \in W_v} \tilde{\Delta}_w^{s-1} \quad (3.2.17)$$

$$\times \mathcal{J}^{\mathcal{N}-4} \cdot \delta^{(k \times 2)}(C \cdot \tilde{\lambda}) \delta^{((n-k) \times 2)}(C^\perp \cdot \lambda) \delta^{(k \times \mathcal{N})}(C \cdot \tilde{\eta}),$$

where  $\Gamma$  denotes any color factor/coupling constant associated with the diagram. The products of  $\Delta_b$  and  $\tilde{\Delta}_w$  are associated with the set of black ( $B_v$ ) and white ( $W_v$ ) vertices respectively. They can be easily calculated using edge variables and external spinor-helicity variables. We are going to show some explicit examples in section 3.3. Note that the Jacobian factor  $\mathcal{J}$  is the same as for  $\mathcal{N} < 4$  sYM on-shell diagrams (3.1.22). The reason is that it originates from rewriting the (super-)momentum conserving delta functions in the linearized form using the  $C$ -matrix. In particular, it does not depend on the measure  $df(\alpha_k)$  in (3.2.1) and therefore is the same for theories of arbitrary spin and number of supersymmetries. However, depending on the number of fermionic delta functions related to the amount of supersymmetry  $\mathcal{N}$ , the respective power  $\mathcal{J}^{\mathcal{N}-4}$  changes and for  $\mathcal{N} = 4$  always cancels. While the formula has been originally derived for  $\mathcal{N} = 4s$  it is actually valid for any  $s$  and any  $\mathcal{N}$ , so it also captures theories with lower supersymmetries. The reason is that  $\mathcal{J}$  comes from solving the delta functions in the gluing three point vertices and also depends on the number supersymmetries, not the measure for a given theory.

Before proceeding further, note that the on-shell diagrams for spin  $s > 2$  make perfect sense as they are obtained from gluing elementary three point amplitudes together – which in turn are well defined. However, in Minkowski space, we know that there are no consistent long range forces mediated by spin  $s > 2$  particles [179, 180]. From the point of on-shell diagrams, we can see that  $s = 1, 2$  are special if we look at the identity moves on on-shell diagrams. There are two moves satisfied by planar on-shell diagrams: the square move (3.1.6) and merge-expand (3.1.5). These moves leave invariant the cell in the positive Grassmannian  $G_+(k, n)$  as well as the logarithmic form  $d\Omega$  which calculates the value of the on-shell diagram in  $\mathcal{N} = 4$  sYM theory.

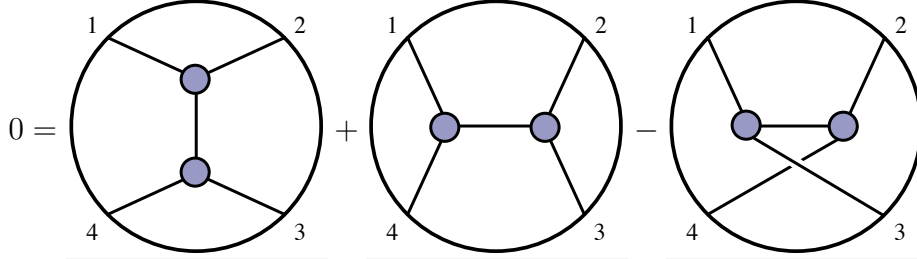
The content of the first move is the parity symmetry of a four point amplitude, and it does not really depend on planarity. Indeed, calculating the four point on-shell diagram

(3.1.11)(a) we find that for general  $s$  it is equal to

$$\Omega_s = \left( \frac{[12][24]}{\langle 13 \rangle \langle 34 \rangle} \right)^{s-1} \cdot \frac{\delta^{(4)}(P) \delta^{(2\mathcal{N})}(\mathcal{Q})}{\langle 12 \rangle \langle 23 \rangle \langle 34 \rangle \langle 41 \rangle}, \quad (3.2.18)$$

which is indeed invariant under the parity flip due to the totally crossing symmetric prefactor.

The merge-expand move gets modified beyond the planar limit. In fact, it is not a two-term relation (3.1.5) but now involves a third (non-planar) contribution,



Calculating all three diagrams either by gluing three point amplitudes or using the Grassmannian formula (3.2.17) we find that the invariance under this move requires

$$\Gamma_s(\langle 12 \rangle \langle 34 \rangle)^{s-1} + \Gamma_t(\langle 14 \rangle \langle 23 \rangle)^{s-1} = \Gamma_u(\langle 13 \rangle \langle 24 \rangle)^{s-1} \quad (3.2.19)$$

where  $\Gamma_k$  are the group factors for  $s$ -,  $t$ - and  $u$ -channels. There are only two solutions to this equation: either  $s = 1$  and  $\Gamma_s + \Gamma_t = \Gamma_u$ , which is nothing but the Jacobi identity for the color factors  $\Gamma_s = f^{12a} f^{34a}$ ,  $\Gamma_t = f^{14a} f^{23a}$ ,  $\Gamma_u = f^{13a} f^{24a}$ . Here we easily recognize  $\mathcal{N} = 4$  sYM. The other option for which the merge-expand move holds is  $s = 2$  and  $\Gamma_s = \Gamma_t = \Gamma_u$  (and equal to some constant) due to the Shouten identity. This case corresponds to  $\mathcal{N} = 8$  supergravity. All higher spin cases (as well as for  $s = 0$ ) are not consistent with the merge-expand move.

The merge-expand move is not an essential property of on-shell diagrams, indeed the  $\mathcal{N} < 4$  SYM diagrams do not satisfy it. But for maximally supersymmetric theories it seems like a good guide when the theory is healthy. From now on, we will focus on the  $s = 2$  case of  $\mathcal{N} = 8$  supergravity. For this theory, the Grassmannian representation becomes

$$d\Omega = \frac{d\alpha_1 d\alpha_2 \dots d\alpha_d}{\alpha_1^3 \alpha_2^3 \dots \alpha_d^3} \prod_{b \in B_v} \Delta_b \prod_{w \in W_v} \tilde{\Delta}_w \quad (3.2.20)$$

$$\times \mathcal{J}^4 \cdot \delta^{(k \times 2)}(C \cdot \tilde{\lambda}) \delta^{((n-k) \times 2)}(C^\perp \cdot \lambda) \delta^{(k \times 8)}(C \cdot \tilde{\eta}).$$

Note that a similar formula is valid for  $\mathcal{N} < 8$  SUGRA subject to the simple replacement  $\mathcal{J}^4 \rightarrow \mathcal{J}^{\mathcal{N}-4}$ . In these cases we also have to sum over all possible orientations of internal edges, in complete analogy to the Yang-Mills case.



### 3.3 Properties of gravity on-shell diagrams

In this section we are going to elaborate on the Grassmannian formula for gravity (3.2.20) obtained in the last section. We will show in examples how to use the formula to calculate particular on-shell diagrams and comment on their properties.

#### 3.3.1 Calculating on-shell diagrams

After deriving the Grassmannian formulation for on-shell diagrams in  $\mathcal{N} = 8$  supergravity in an abstract setting, let's consider a few concrete examples to show that we can reproduce the correct values of the on-shell functions derived before. As a first non-trivial example, we consider a reduced on-shell diagram for five external particles. For the construction of the  $C$ -matrix, we chose a convenient perfect orientation. Of course, the final result will be independent of the particular choice. Since we were able to choose a perfect orientation without any closed loops, the Jacobian factor  $\mathcal{J}$  in Eq. (3.1.22) from converting between vertex- and edge-variables is trivial,  $\mathcal{J} = 1$ .

In complete analogy to the Yang Mills case, we have used the  $GL(1)_v$ -freedom from all vertices to gauge fix several of the edge-weights to 1. Starting from the gauge-fixed on-shell diagram, we can follow the same rules described in Sec. 3.1.2 to construct the boundary-measurement matrix  $C$  by summing over paths from sources to sinks and multiplying the edge weights along the path.

$$C = \begin{pmatrix} 1 & \alpha_1 + \alpha_2\alpha_6 & \alpha_6 & \alpha_3\alpha_6 & 0 \\ 0 & \alpha_5\alpha_6\alpha_2 & \alpha_5\alpha_6 & \alpha_4 + \alpha_3\alpha_5\alpha_6 & 1 \end{pmatrix} \quad (3.3.1)$$

The orthogonal matrix  $C^\perp$  is then given by

$$C^\perp = \begin{pmatrix} -(\alpha_1 + \alpha_2\alpha_6) & 1 & 0 & 0 & -\alpha_5\alpha_6\alpha_2 \\ -\alpha_6 & 0 & 1 & 0 & -\alpha_5\alpha_6 \\ -\alpha_3\alpha_6 & 0 & 0 & 1 & -(\alpha_4 + \alpha_3\alpha_5\alpha_6) \end{pmatrix}. \quad (3.3.2)$$

We can use the  $\delta^{(3 \times 2)}(C^\perp \cdot \lambda)$  delta-functions to solve for all edge variables  $\alpha_i$ ,

$$\alpha_1 = \frac{\langle 23 \rangle}{\langle 13 \rangle}, \quad \alpha_2 = \frac{\langle 12 \rangle}{\langle 13 \rangle}, \quad \alpha_3 = \frac{\langle 45 \rangle}{\langle 35 \rangle}, \quad \alpha_4 = \frac{\langle 34 \rangle}{\langle 35 \rangle}, \quad \alpha_5 = \frac{\langle 13 \rangle}{\langle 35 \rangle}, \quad \alpha_6 = \frac{\langle 35 \rangle}{\langle 15 \rangle}. \quad (3.3.3)$$

Solving for all the  $\alpha_i$  induces a Jacobian  $J_{C^\perp, \lambda} = (\langle 35 \rangle^2 \langle 13 \rangle)^{-1}$ . Plugging these solutions  $\alpha_i = \alpha_i^*$  back into the remaining  $\delta$ -functions, we find,

$$\delta^{(2 \times 2)}(C \cdot \tilde{\lambda}) = \langle 15 \rangle^2 \delta^4(\lambda \cdot \tilde{\lambda}), \quad \delta^{(2 \times \mathcal{N})}(C \cdot \tilde{\eta}) = \frac{1}{\langle 15 \rangle^{\mathcal{N}}} \delta^{2\mathcal{N}}(\lambda \cdot \tilde{\eta}). \quad (3.3.4)$$

As a quick sanity check, we can recover the  $\mathcal{N} = 4$  sYM result,

$$\begin{aligned} d\Omega_{\mathcal{N}=4} &= \prod_{i=1}^6 \frac{d\alpha_i}{\alpha_i} \delta^{(2 \times 2)}(C \cdot \tilde{\lambda}) \delta^{(3 \times 2)}(C^\perp \cdot \lambda) \delta^{(2 \times 4)}(C \cdot \tilde{\eta}) \\ &= \text{PT}(12345) \delta^{(4)}(\lambda \cdot \tilde{\lambda}) \delta^{(2 \times 4)}(\lambda \cdot \tilde{\eta}). \end{aligned} \quad (3.3.5)$$

The only missing ingredient for the gravity result are the various  $\Delta_b$  and  $\tilde{\Delta}_w$  factors required in the definition of the measure (3.2.20). In order to calculate  $\Delta_b$  and  $\tilde{\Delta}_w$  the knowledge of the adjacent  $\lambda$  and  $\tilde{\lambda}$  are required. Naively one could think that one has to solve for all internal momenta explicitly in order to construct the  $\Delta$ 's and  $\tilde{\Delta}$ 's. However, the on-shell diagram knows about all relations between the internal  $\lambda$ 's and  $\tilde{\lambda}$ 's and the external kinematic data automatically. That is the point of constructing the  $C$  matrix using the paths and there are simple rules how to read off  $\Delta_b$  and  $\tilde{\Delta}_w$  directly from the diagram.

Let us first formulate the rule for the white vertices  $\tilde{\Delta}_w$ , which is defined as a contraction of two incoming  $\tilde{\lambda}$  spinors in the vertex,

$$\tilde{\Delta}_w = [\tilde{\lambda}_A \tilde{\lambda}_B]. \quad (3.3.6)$$

This naively depends on the split of the internal momenta  $p_I = \lambda_I \tilde{\lambda}_I$  into spinors as well as the choice which two of the  $\tilde{\lambda}$ 's to pick. However the on-shell diagram gives us the correct split automatically, similar to how it is provided in the delta functions (3.2.20). Furthermore, since the  $\tilde{\lambda}$ -spinor is conserved in each vertex—which is exactly the purpose of the linearized delta functions—it does not matter which two we pick. Following the rules used in the construction of the  $C$ -matrix, we choose two of the outgoing  $\tilde{\lambda}$ . Then we track each of them back to the external momenta following the rules:

*If we hit a black vertex we follow the path, and if we hit a white vertex we sum over both paths. At each step we multiply by the edge variables on the way.*

Note that this is exactly how the  $C$ -matrix is constructed, except that there we start with the incoming external legs rather than with the legs attached to an internal vertex.

In case of closed internal loops, it might be necessary to sum a geometric series as in the construction of the  $C$ -matrix.

The rule for  $\Delta_b$  is similar, it is a contraction of two  $\lambda$  spinors,

$$\Delta_b = \langle \lambda_A \lambda_B \rangle. \quad (3.3.7)$$

Now we choose the two incoming arrows in the black vertex and trace them back to external legs going against the arrows rather than following the arrows. This can be trivially understood from the linearized delta functions, where the  $\tilde{\lambda}$  spinors are coupled to the  $C$ -matrix but the  $\lambda$  spinors are coupled to the  $C^\perp$ , which can be thought of as the  $C$ -matrix for on-shell diagrams where all black and white vertices as well as all arrows are flipped.

In our example (3.3.1), let us start with the white vertices. Following the arrows from the vertex  $W_1$  we leave the diagram via the *sinks*, and the spinors are

$$\tilde{\lambda}_A = \alpha_4 \tilde{\lambda}_4, \quad \tilde{\lambda}_B = \alpha_5 \alpha_6 (\alpha_3 \tilde{\lambda}_4 + \tilde{\lambda}_3 + \alpha_2 \tilde{\lambda}_2), \quad (3.3.8)$$

corresponding to  $\tilde{\Delta}_1$ ,

$$\tilde{\Delta}_1 = [\tilde{\lambda}_A \tilde{\lambda}_B] = -\alpha_4 \alpha_5 \alpha_6 ([34] + \alpha_2 [24]). \quad (3.3.9)$$

Similarly, for the other vertices we get,

$$\tilde{\Delta}_2 = \alpha_1 (\alpha_3 [24] + [23]), \quad \tilde{\Delta}_3 = \alpha_2 [23], \quad \tilde{\Delta}_4 = \alpha_3 ([34] + \alpha_2 [24]). \quad (3.3.10)$$

For the black vertices we just go against the arrows and leave the diagram via the *sources*.

$$\Delta_1 = \alpha_3 \alpha_4 \alpha_6 \langle 15 \rangle, \quad \Delta_2 = \alpha_5 \langle 15 \rangle, \quad \Delta_3 = \alpha_1 \alpha_2 \alpha_5 \alpha_6 \langle 15 \rangle. \quad (3.3.11)$$

Collecting all terms in (3.2.20) our formula for the on-shell diagram is (omitting  $d\alpha_k$ )

$$d\Omega = \frac{([23] + \alpha_3 [24])^2 ([34] + \alpha_2 [34]) [23] \langle 15 \rangle^3}{\alpha_1 \alpha_2 \alpha_3 \alpha_4} \delta^{(2 \times 2)}(C \cdot \tilde{\lambda}) \delta^{(3 \times 2)}(C^\perp \cdot \lambda) \delta^{(2 \times 8)}(C \cdot \tilde{\eta}). \quad (3.3.12)$$

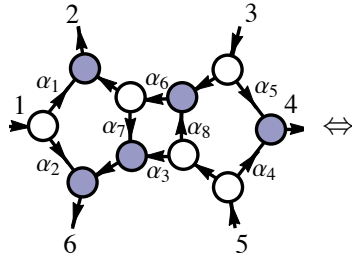
Substituting the solutions for the edge variables (3.3.3), converting the  $\delta$ -functions and including the Jacobians reproduces the same gravity result (3.2.5) we obtained from gluing three-point amplitudes directly,

$$d\Omega = \frac{[12][23][45]^2}{\langle 12 \rangle \langle 23 \rangle \langle 34 \rangle \langle 45 \rangle \langle 51 \rangle \langle 13 \rangle} \delta^4(\lambda \cdot \tilde{\lambda}) \delta^{16}(\lambda \cdot \tilde{\eta}). \quad (3.3.13)$$

Note that the formula (3.3.12) has only single poles in  $\alpha_k$  in contrast to the cubic poles in the general form (3.2.20). We will expand on this point later in this section.

### 3.3.2 More examples

So far we have mostly considered simple MHV examples. Here we would like to stress that our Grassmannian formulation for gravity on-shell diagrams is not restricted to the MHV sector but works for arbitrary  $k$  as well. To illustrate this point, let us consider a simple NMHV on-shell diagram,



$$C = \begin{pmatrix} 1 & \alpha_1 & 0 & 0 & 0 & \alpha_2 \\ 0 & \alpha_6 & 1 & \alpha_5 & 0 & \alpha_6 \alpha_7 \\ 0 & \alpha_6 \alpha_8 & 0 & \alpha_4 & 1 & \alpha_3 + \alpha_6 \alpha_7 \alpha_8 \end{pmatrix}$$

$$C^\perp = \begin{pmatrix} -\alpha_1 & 1 & -\alpha_6 & 0 & -\alpha_6 \alpha_8 & 0 \\ 0 & 0 & -\alpha_5 & 1 & -\alpha_4 & 0 \\ -\alpha_2 & 0 & -\alpha_6 \alpha_7 & 0 & -(\alpha_3 + \alpha_6 \alpha_7 \alpha_8) & 1 \end{pmatrix}.$$

Here we are going to have additional fermionic  $\delta$ -functions which exactly give us eight extra powers of  $\tilde{\eta}$  required for NMHV on-shell functions. Solving the bosonic  $\delta$ -functions for the edge variables we find,

$$\alpha_1 = -\frac{[16]}{[26]}, \quad \alpha_2 = \frac{[12]}{[26]}, \quad \alpha_3 = \frac{s_{345}}{\langle 5|Q_{345}|6\rangle}, \quad \alpha_4 = \frac{\langle 34\rangle}{\langle 35\rangle}, \quad \alpha_5 = \frac{\langle 45\rangle}{\langle 35\rangle},$$

$$\alpha_6 = \frac{\langle 5|Q_{345}|6\rangle}{\langle 35\rangle[26]}, \quad \alpha_7 = -\frac{\langle 5|Q_{345}|2\rangle}{\langle 5|Q_{345}|6\rangle}, \quad \alpha_8 = -\frac{\langle 3|Q_{345}|6\rangle}{\langle 5|Q_{345}|6\rangle}.$$

Converting the  $\delta$ -functions,

$$\delta(C \cdot Z) = \frac{[26]\langle 35\rangle \prod_{i=1}^8 \delta(\alpha_i - \alpha_i^*)}{\langle 5|Q_{345}|6\rangle \langle 35\rangle^8 [26]^8} \delta^4(P) \delta^{16}(\mathcal{Q}) \delta^8([26]\tilde{\eta}_1 + [61]\tilde{\eta}_2 + [12]\tilde{\eta}_6), \quad (3.3.14)$$

and writing all numerator factors  $\Delta_{b_i}, \tilde{\Delta}_{w_j}$  exactly as before, the on-shell function is,

$$d\Omega = \frac{\langle 12\rangle \langle 16\rangle [34][45] \delta^8([26]\tilde{\eta}_1 + [61]\tilde{\eta}_2 + [12]\tilde{\eta}_6)}{[12][26][61] s_{345} \langle 34\rangle \langle 45\rangle \langle 53\rangle \langle 5|Q_{345}|2\rangle \langle 3|Q_{345}|6\rangle} \delta^4(P) \delta^{16}(\mathcal{Q}). \quad (3.3.15)$$

As a further example, we can check that our Grassmannian formula for gravity on-shell diagrams also reproduces the correct result in cases where the graphs are non-reduced, i.e. contain additional degrees of freedom not localized by the bosonic  $\delta$ -functions. The

simplest case to consider is the following:

$$C = \begin{pmatrix} 1 & 0 & \alpha_3 \alpha_4 \alpha_5 & \alpha_1 + \alpha_2 \alpha_3 \\ 0 & 1 & \alpha_4 + \alpha_3 \alpha_5 & \alpha_3 \\ -\alpha_2 \alpha_3 \alpha_5 & -(\alpha_4 + \alpha_3 \alpha_5) & 1 & 0 \\ -(\alpha_1 + \alpha_2 \alpha_3) & -\alpha_3 & 0 & 1 \end{pmatrix}$$

$$C^\perp = \begin{pmatrix} -\alpha_2 \alpha_3 \alpha_5 & -(\alpha_4 + \alpha_3 \alpha_5) & 1 & 0 \\ -(\alpha_1 + \alpha_2 \alpha_3) & -\alpha_3 & 0 & 1 \end{pmatrix}.$$

Choosing  $\alpha_1$  to be the free parameter, we solve for the remaining edge-variables:

$$\alpha_2 = \frac{\langle 42 \rangle - \alpha_1 \langle 12 \rangle}{\langle 14 \rangle}, \quad \alpha_3 = \frac{\langle 14 \rangle}{\langle 12 \rangle}, \quad \alpha_4 = \frac{\langle 43 \rangle - \alpha_1 \langle 13 \rangle}{\langle 42 \rangle - \alpha_1 \langle 12 \rangle}, \quad \alpha_5 = \frac{\langle 32 \rangle}{\langle 42 \rangle - \alpha_1 \langle 12 \rangle}.$$

As a cross check, we can again look at the Yang–Mills result  $d\Omega_{\text{YM}} = \frac{1}{\alpha_1 \langle 12 \rangle \langle 14 \rangle \langle 23 \rangle \langle 43 \rangle - \alpha_1 \langle 13 \rangle}$ , which agrees with the form found earlier in (3.1.4) once we identify  $\alpha_1 \leftrightarrow -z$ .

The gravity result can be obtained using our rules from the previous sections,

$$d\Omega = \frac{[24][23][41]}{\alpha_1 \langle 12 \rangle \langle 13 \rangle \langle 23 \rangle \langle 41 \rangle \langle 43 \rangle - \alpha_1 \langle 13 \rangle} \delta^4(P) \delta^{16}(\mathcal{Q}) \quad (3.3.16)$$

All previous examples were in the context of maximal supersymmetry. Here we will explicitly consider a non-supersymmetric case to demonstrate that our Grassmannian formula also holds there. Since the only difference to the maximally supersymmetric theory is the Jacobian  $\mathcal{J}$  for on-shell diagrams with a perfect orientation containing closed internal cycles (c.f. (3.2.20)), we look at the simplest diagrams:

$$C^{(a)} = \begin{pmatrix} \alpha_2 \alpha_3 \alpha_4 \delta_a & 1 & \alpha_2 \delta_a & 0 \\ \alpha_4 \delta_a & 0 & \alpha_4 \alpha_1 \alpha_2 \delta_a & 1 \end{pmatrix}$$

$$C^{(b)} = \begin{pmatrix} \beta_1 \delta_b & 1 & \beta_1 \beta_4 \beta_3 \delta_b & 0 \\ \beta_3 \beta_2 \beta_1 \delta_b & 0 & \beta_3 \delta_b & 1 \end{pmatrix}$$

As mentioned before, in order to obtain the correct result, we have to sum over all possible orientations of the internal loop which is why we include both diagrams. Introducing the usual short-hand notation for the geometric series  $\delta_a = (1 - \alpha_1 \cdots \alpha_4)^{-1}$ ,  $\delta_b = (1 - \beta_1 \cdots \beta_4)^{-1}$  and solving for the edge variables, we find

$$\delta(C^{(a)}.Z) = \frac{\langle 24 \rangle^4 \delta^4(P)}{\langle 12 \rangle^2 \langle 34 \rangle^2} \delta \left[ \alpha_1 + \frac{\langle 23 \rangle}{\langle 13 \rangle} \right] \delta \left[ \alpha_2 - \frac{\langle 13 \rangle}{\langle 12 \rangle} \right] \delta \left[ \alpha_3 + \frac{\langle 14 \rangle}{\langle 13 \rangle} \right] \delta \left[ \alpha_4 + \frac{\langle 13 \rangle}{\langle 34 \rangle} \right], \quad (3.3.17)$$

$$\delta(C^{(b)}.Z) = \frac{\langle 24 \rangle^4 \delta^4(P)}{\langle 14 \rangle^2 \langle 23 \rangle^2} \delta \left[ \beta_1 - \frac{\langle 13 \rangle}{\langle 23 \rangle} \right] \delta \left[ \beta_2 - \frac{\langle 21 \rangle}{\langle 13 \rangle} \right] \delta \left[ \beta_3 - \frac{\langle 13 \rangle}{\langle 14 \rangle} \right] \delta \left[ \beta_4 - \frac{\langle 34 \rangle}{\langle 13 \rangle} \right]. \quad (3.3.18)$$

We can easily find the respective numerators and Jacobians  $\mathcal{J}$  (3.1.22) required for our gravity formula (3.2.20),

$$N^{(a)} = \alpha_1^2 \alpha_3^2 s_{12}^2, \quad \mathcal{J}^{(a)} = 1 - \alpha_1 \alpha_2 \alpha_3 \alpha_4, \quad N^{(b)} = \beta_2^2 \beta_4^2 s_{14}^2, \quad \mathcal{J}^{(b)} = 1 - \beta_1 \beta_2 \beta_3 \beta_4,$$

to put everything together ( $\mathcal{N} = 0 \Leftrightarrow \mathcal{J}^{-4}$ ),

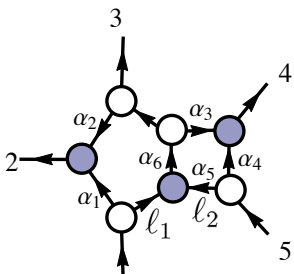
$$d\Omega^{\mathcal{N}=0} = \frac{\langle 24 \rangle^4}{\langle 13 \rangle^4} \left( s_{12}^2 \frac{\langle 12 \rangle \langle 34 \rangle}{\langle 14 \rangle \langle 23 \rangle} \left[ \frac{\langle 13 \rangle \langle 24 \rangle}{\langle 12 \rangle \langle 34 \rangle} \right]^{-4} + s_{14}^2 \frac{\langle 14 \rangle \langle 23 \rangle}{\langle 12 \rangle \langle 34 \rangle} \left[ \frac{\langle 13 \rangle \langle 24 \rangle}{\langle 14 \rangle \langle 23 \rangle} \right]^{-4} \right) \delta^4(P), \quad (3.3.19)$$

which agrees with the formula obtained by simply gluing three-point amplitudes together. This serves as a further verification of our Grassmannian formula for gravity on-shell diagrams (3.2.20).

### 3.3.3 Structure of singularities

There are two different types of singularities of on-shell diagrams. In terms of edge-variables, these are  $\alpha_k \rightarrow 0$  or  $\alpha_k \rightarrow \infty$  which correspond to either erasing edges or are associated with poles at infinity when all on-shell momenta in a given loop are located at  $\ell \rightarrow \infty$ .

Let us show the different cases for the on-shell diagram discussed in previous subsections, and also calculated in section 3.1. when we first looked at gravity on-shell diagrams.



$$\begin{aligned} l_1 &= \frac{\lambda_1 Q_{12} \cdot \lambda_3}{\langle 13 \rangle}, & l_2 &= \frac{\lambda_5 Q_{12} \cdot \lambda_3}{\langle 35 \rangle}, \\ l_1 - 1 &= \frac{\langle 23 \rangle}{\langle 13 \rangle} \lambda_1 \tilde{\lambda}_2, & l_2 - 5 &= \frac{\langle 34 \rangle}{\langle 35 \rangle} \lambda_5 \tilde{\lambda}_4, \\ l_1 - Q_{12} &= \frac{\langle 12 \rangle}{\langle 13 \rangle} \lambda_3 \tilde{\lambda}_2, & l_2 - Q_{45} &= \frac{\langle 45 \rangle}{\langle 35 \rangle} \lambda_3 \tilde{\lambda}_4, \\ l_1 - Q_{123} &= \frac{\lambda_3 Q_{23} \cdot \lambda_1}{\langle 13 \rangle}, & l_1 + l_2 &= \frac{\langle 15 \rangle}{\langle 13 \rangle \langle 35 \rangle} \lambda_3 Q_{12} \cdot \lambda_3. \end{aligned}$$

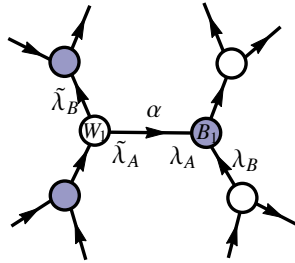
$$\alpha_1 = \frac{\langle 23 \rangle}{\langle 13 \rangle}, \quad \alpha_2 = \frac{\langle 12 \rangle}{\langle 13 \rangle}, \quad \alpha_3 = \frac{\langle 45 \rangle}{\langle 35 \rangle}, \quad \alpha_4 = \frac{\langle 34 \rangle}{\langle 35 \rangle}, \quad \alpha_5 = \frac{\langle 13 \rangle}{\langle 35 \rangle}, \quad \alpha_6 = \frac{\langle 35 \rangle}{\langle 15 \rangle}.$$

Here we can see that four of the edge variables,  $\alpha_1$ ,  $\alpha_2$ ,  $\alpha_3$ , and  $\alpha_4$ , directly parametrize the momentum flow in a given edge. If we send one of them to zero, the zero momentum

flow effectively erases that edge. Similarly, sending  $\alpha_6 \rightarrow \infty$  erases the corresponding  $(\ell_1 + \ell_2)$ -edge. Whether the location of the pole is at 0 or  $\infty$  is determined by the orientation of the arrow on the edge, flipping the orientation of the arrow inverts the edge variable  $\alpha_k \rightarrow \frac{1}{\alpha_k}$  and the location of the pole changes. Independent of the details of the orientation, the important statement is that all of the discussed edges are erasable by sending  $\alpha_k \rightarrow 0$  or  $\infty$ . Note that the edge corresponding to  $\alpha_5$  is not erasable. The reason is that if we tried to erase this edge, the remaining diagram would enforce both  $[45] = \langle 13 \rangle = 0$ , which imposes too many constraints. In fact, sending  $\alpha_5 \rightarrow 0$  or  $\infty$  blows up one of the loops with  $\ell_1 \rightarrow \infty$  or  $\ell_2 \rightarrow \infty$ . The same happens if we set  $\alpha_1, \alpha_2, \alpha_3, \alpha_4$  to infinity or  $\alpha_6$  to zero. In the example above, we have already chosen a particular  $GL(1)_v$  gauge-fixing, corresponding to the fact that some edge-variables are set to 1. For a different gauge-fixing we could analyze these edges as well, leading to the same set of erasable edges described above.

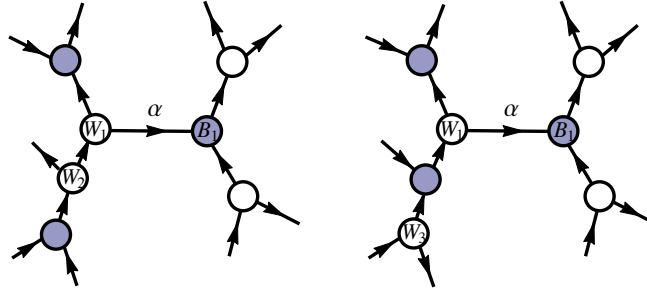
In the case of  $\mathcal{N} = 4$  sYM theory the form is logarithmic in all edge variables independent whether an edge is erasable or not. Furthermore, the final expression does not contain any poles that send loop-momenta to infinity so that all singularities correspond to erasing edges only. This is an important distinction to  $\mathcal{N} = 8$  supergravity, where poles at infinity do appear.

Let us investigate the properties of our Grassmannian form for gravity on-shell diagrams a little more closely. First, it is relatively easy to see that the form (3.2.20) has only linear poles for  $\alpha_k \rightarrow 0$ , when the corresponding edge is erasable. The denominator contains the third power of this edge variable,  $\alpha_k^3$  but the numerator always generates two powers leaving only a single pole. We remove the erasable edge in the on-shell diagram for  $\alpha_k \rightarrow 0$  if the arrow points from a white to a black vertex, while it is erased by  $\alpha_k \rightarrow \infty$  if the arrow points from a black to a white vertex. The edges between same colored vertices are never removable.



The numerator for such subgraph is given by the products of  $\Delta_b$  and  $\tilde{\Delta}_w$ . Based on our rules, we have  $\Delta_{b_1} = \langle \lambda_A \lambda_B \rangle \sim \alpha$  and  $\tilde{\Delta}_{w_1} = [\tilde{\lambda}_A \tilde{\lambda}_B] \sim \alpha$ , while all other  $\Delta_b$  and  $\tilde{\Delta}_w$  do not depend on  $\alpha$ . Therefore the numerator generates  $\sim \alpha^2$ . We can also consider

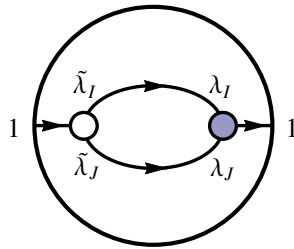
a modification of the subgraph by adding another white vertex (or in general a chain of white vertices), or consider some more distant vertex and look if they can possibly generate additional  $\alpha$  factors in the numerator,



In both cases the numerator will have further  $\alpha$ -dependence but in either situation, it will look like  $\tilde{\Delta}_{w2}, \tilde{\Delta}_{w3} \sim \alpha(\dots) + (\dots)$  and the linearity of the pole in  $\alpha$  is not changed. The argument for erasable edges would be similar when the arrow points from black to white vertex. The only difference is that we have to keep track of the pole  $\alpha \rightarrow \infty$  but we would again find a linear pole only. Alternatively, we can take the same diagram and consider a different perfect orientation in which the arrow again points from white to black so that the pole is localized at zero. As a result, all poles corresponding to erasable edges are linear. This immediately implies that all higher poles (including some simple poles) correspond to poles at infinity, when internal on-shell momenta in one or more loops are sent to infinity.

### Bubbles

Let us comment on one important property of gravity on-shell diagrams which is a trivial consequence of the formula (3.2.20): any internal bubble **vanishes**. Let us consider a diagram with an internal bubble.



Independent of the rest of the diagram, the perfect orientation chosen and the directions of arrows, the numerator factors  $\Delta_b$  and  $\tilde{\Delta}_w$  vanish for both vertices separately. All  $\tilde{\lambda}$ 's in the black vertex are proportional, and so are all  $\lambda$ 's in the white vertex, which implies that  $\lambda_1 \sim \lambda_I \sim \lambda_J$  and  $\tilde{\lambda}_1 \sim \tilde{\lambda}_I \sim \tilde{\lambda}_J$  and  $\Delta_b = \tilde{\Delta}_w = 0$ .



This fact will have dramatic consequences on properties of loop amplitudes. We will discuss them in greater detail in the next section. Furthermore, there is one interesting aspect related to vanishing bubbles: in planar  $\mathcal{N} = 4$  sYM, the loop integrand is expressed in terms of on-shell diagrams containing bubbles. In fact, via equivalence moves, one can show that four bubbles built the four degrees of freedom of the off-shell loop momentum for each loop [67]. We do not have any recursion relations in the gravity case (as well as in  $\mathcal{N} = 4$  sYM beyond the planar limit) but if such formulation exists, it must take this fact into account. In the planar case we could always use the identity moves to eliminate the bubble from the diagram in the form (see figure above). The non-planar identity moves for  $\mathcal{N} = 8$  SUGRA (and also non-planar  $\mathcal{N} = 4$  SYM) are different, which might lead to a different role of bubbles in the loop integrand.

### 3.4 From on-shell diagrams to scattering amplitudes

In the last sections we initiated a detailed study of gravity on-shell diagrams and gave their Grassmannian representation. This formula (3.2.20) exhibited some interesting properties: (a) higher poles associated with sending internal momenta to infinity and (b) vanishing whenever three momenta in any vertex become collinear. As it was stressed several times, the on-shell diagrams represent cuts of loop integrands and they contain a considerable amount of information about the structure of loop amplitudes themselves even though we do not yet know how to express the integrand directly in terms of on-shell diagrams. There are two obvious paths beyond the well-understood case of planar  $\mathcal{N} = 4$  sYM theory: (i) going to lower supersymmetry or (ii) going non-planar. The recursion relations for planar non-supersymmetric Yang-Mills theory suffers from divergencies in the forward limit term. Resolving that problem is an active area of research [181] and it appears to be a question of properly defining the forward limit term in these theories rather than some fundamental obstruction.

The extension to non-planar theories, even with maximal supersymmetry, seems more difficult because it is not even clear which object should recurse in the first place. Beyond the planar limit we do not have global variables and loop momenta are normally associated with individual diagrams in the Feynman expansion, or its refined version using a set of integrals in the unitarity method. Therefore it is not clear how to associate the "loop-momentum" degrees of freedom with those in on-shell diagrams or how to cancel spurious poles. Making progress on this problem would certainly open doors to many new directions of research. However, even without having the recursion relations at hand, there is an immediate question one can ask:

*Does the loop amplitude have the same properties as individual on-shell diagrams?*

This analysis was done in particular examples for amplitudes in full non-planar  $\mathcal{N} = 4$  sYM theory and the answer is positive [1, 2, 119]. Additionally, many of the structures present in the planar limit seem to survive in non-planar amplitudes despite the absence of good kinematic variables. We review this progress in the next subsection and then motivated by this success we will test the properties found for gravity on-shell diagrams on explicit expressions for gravity amplitudes.

### 3.4.1 Non-planar $\mathcal{N} = 4$ sYM amplitudes

In the  $\mathcal{N} = 4$  sYM case we are able to take the step to non-planar amplitudes. On one hand we have a detailed understanding of the planar sector of the theory and the properties of the amplitudes: logarithmic singularities, dual conformal [41–43] and Yangian [44] symmetries as well as the Amplituhedron [18] construction. On the other hand, we have the non-planar on-shell diagrams which have logarithmic singularities, and for MHV leading singularities we even know that they are expressed in terms of planar ones.

All these ingredients lead to the following conjectures [1, 2, 119]:

- The loop amplitudes have only **logarithmic singularities**, as in the planar limit. For  $k > 4$  (perhaps even for lower  $k$ ) we expect the presence of elliptic cuts but at least for  $k = 2$  the logarithmic singularities must be present directly in momentum space.
- There are **no poles at infinity**. This was one of the consequence of the dual conformal symmetry of planar amplitudes, but also motivated by the observation about MHV leading singularities.

These conjectures were tested in [1, 2, 119] on the four-point amplitudes at two- and three-loops, and on the five-point amplitude at two-loops. These tests rely on a two-step process. First one constructs the basis of integrals  $\mathcal{I}_k$  with the above two properties (also with unit leading singularities) and second one expands the loop amplitudes in this basis. The correctness of the result is guaranteed by satisfying all unitarity cuts.

$$\mathcal{A} = \sum_k c_k \mathcal{I}_k \tag{3.4.1}$$

As was argued in [1, 2] this is a strong evidence for a new hidden symmetry (analogue of dual conformal symmetry) in the full  $\mathcal{N} = 4$  sYM theory.

Finally, the step towards the geometric Amplituhedron-like construction was also made in [2]. The presence of logarithmic singularities only was one of the ingredients of the

Amplituhedron, where the  $d\log$  forms can be thought of as volumes in the Grassmannian. Moreover, motivated by the work [154] it was checked that all coefficients  $c_k$  in (3.4.1) can be fixed only from vanishing cuts. This means that the full amplitude is fixed entirely by homogeneous conditions providing nontrivial evidence for an Amplituhedron-type geometric formulation.

Motivated by this success we can now turn to gravity and see what structures we can carry over from on-shell diagrams directly to the amplitude. In particular, we want to test two statements:

- All singularities are logarithmic unless it is a pole at infinity.
- The amplitude **vanishes** on all collinear cuts.

The first statement is motivated by the singularity structure of gravity on-shell diagrams described in Sec. 3.3.3. There, we saw that certain single poles correspond to erasable edges, and all higher poles are associated with sending internal momenta to infinity. The second statement is the crucial ingredient in the Grassmannian formula (3.2.20) and checking it for gravity amplitudes will be a main result of this section.

### 3.4.2 Gravity from Yang-Mills

The relation between scattering amplitudes in Yang-Mills theory and gravity has been a long standing area of research starting by the work of Kawai, Lewellen, and Tye (KLT) [182], to the recent discovery of Bern, Carrasco and Johansson (BCJ) [113, 114]. The BCJ-relations state that there exists a representation of the Yang-Mills amplitude (with or without supersymmetry) in terms of cubic graphs,

$$\mathcal{A}_{YM} = \sum_{i \in \text{cubic}} \frac{n_i c_i}{s_i}, \quad (3.4.2)$$

where  $n_i$  are kinematic numerators,  $c_i$  are color factors and  $s_i$  is the denominator of the cubic graph given by Feynman propagators BCJ [113, 114] states that whenever the color factors  $c_i$  satisfy the Jacobi identity  $c_i + c_j = c_k$  then the numerators satisfy the same relation  $n_i + n_j = n_k$ . Once we have (3.4.2) the gravity amplitude can be then obtained by the simple formula<sup>15</sup>,

$$\mathcal{M}_{GR} = \sum_{i \in \text{cubic}} \frac{n_i \tilde{n}_i}{s_i}, \quad (3.4.3)$$

---

<sup>15</sup>There is a natural identification of coupling constants which does not play a role in our discussion and we suppress them altogether.

where the set of numerators  $\tilde{n}_i$  do not necessarily have to satisfy the Jacobi relation, i.e. they can belong to a non-BCJ representation of the Yang-Mills amplitude. If we start with two copies of  $\mathcal{N} = 4$  sYM then we obtain an  $\mathcal{N} = 8$  supergravity amplitude. There is a dictionary for the squaring relations between amplitudes in lower supersymmetric theories with different matter content (see e.g. [183]) and even for some effective field theories [184]. The BCJ-relations are a conjecture which was proven for tree-level amplitudes and tested up to high loop order for loop amplitudes (there it is a statement about integrands).

In order to prove that the amplitudes in  $\mathcal{N} = 8$  supergravity have only logarithmic singularities (except poles at infinity) we first assume the loop BCJ-relations (3.4.3) and also the statement that the  $\mathcal{N} = 4$  sYM amplitudes can always be expressed in (3.4.1) where all basis integrals  $\mathcal{I}_k$  have only logarithmic singularities. This is certainly true up to high loop order [1, 2, 119] and it is reasonable to assume it holds to all loops. Then we can use one copy of the Yang-Mills amplitude written in this manifest  $d\log$  form, and the other copy written in the BCJ-form (3.4.2). The gravity amplitude is then given by (3.4.3). While the numerator in the  $d\log$  form  $\tilde{n}_i$  already guarantees that term-by-term all singularities are logarithmic in the Yang-Mills amplitude, then the expression (3.4.3) will also have only logarithmic singularities term-by-term. This is not true for poles at infinity, as adding the extra numerator  $n_i$  introduces further loop momentum dependence in the numerator, but for finite  $\ell$  all singularities stay logarithmic. This argument was already used in [1] but we repeat it here because it is in perfect agreement with the results we get from the gravity on-shell diagrams.

Let us comment on the poles at infinity explicitly. The on-shell diagrams have higher poles at infinite momentum and this is what we also expect from the BCJ-form (3.4.3) as adding two copies of  $n_i$  increases the power counting in the numerator. Indeed, looking at the explicit results we can see that the loop amplitudes in  $\mathcal{N} = 8$  supergravity do have poles at infinity. The simplest example is the 3-loop four-point amplitude. The cut represented by the following (non-reduced) on-shell diagram,

$$\begin{array}{ccc} \begin{array}{c} \text{1} \quad \text{2} \\ \diagup \quad \diagdown \\ \bullet \\ \diagdown \quad \diagup \\ \text{---} \quad \text{---} \\ \diagup \quad \diagdown \\ \text{---} \quad \text{---} \\ \diagdown \quad \diagup \\ \text{---} \quad \text{---} \\ \text{4} \quad \text{3} \end{array} & \xrightarrow{a \rightarrow 0} & \begin{array}{c} \text{1} \quad \text{2} \\ \diagup \quad \diagdown \\ \circ \quad \bullet \\ \diagdown \quad \diagup \\ \text{---} \quad \text{---} \\ \diagup \quad \diagdown \\ \text{---} \quad \text{---} \\ \diagdown \quad \diagup \\ \text{---} \quad \text{---} \\ \text{4} \quad \text{3} \end{array} \sim \int \frac{dz}{z} \times F(\wp), \end{array} \quad (3.4.4)$$

has a pole at  $z \rightarrow \infty$ , corresponding to  $\ell \rightarrow \infty$ . The detailed expression for the  $z$ -independent function  $F(\wp)$  is not particularly illuminating but can be obtained by

either gluing together tree-amplitudes or by evaluating the known representation of the gravity amplitude [128] on the cut. Starting with the cut on the left hand side of (3.4.4), the relevant loop momentum  $\ell$  is parameterized by two degrees of freedom,  $a$  and  $z$ ,

$$\ell(a, z) = (1 - a)\lambda_1\tilde{\lambda}_1 + a\lambda_2\tilde{\lambda}_2 + \frac{a(1 - a)}{z}\lambda_2\tilde{\lambda}_1 + z\lambda_1\tilde{\lambda}_2.$$

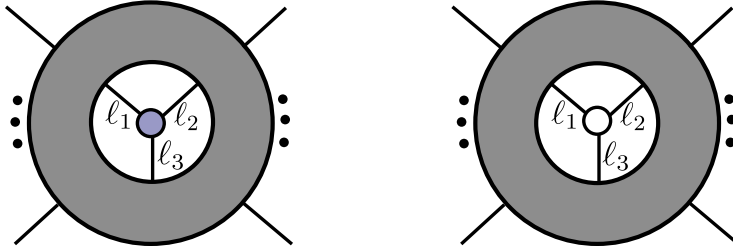
By localizing  $a \rightarrow 0$ , we go to the maximal cut and select a unique contribution where no further cancellations are possible. Since we are on the maximal cut, the gravity numerator in the diagrammatic expansion of the amplitude can be obtained by squaring the respective  $\mathcal{N} = 4$  sYM numerator of any representation and we take [1],

$$N^{\text{GR}} \Big|_{\text{cut}} \sim stu\mathcal{M}_4^{\text{tree}} \cdot \left[ s(\ell + p_4)^2 \right]_{\text{cut}}^2,$$

where  $stu\mathcal{M}_4^{\text{tree}} = \left( \frac{[34][41]}{\langle 12 \rangle \langle 23 \rangle} \right)^2$  is the totally crossing symmetric prefactor depending on external kinematics only. The important observation is that the integrand in (3.4.4) behaves like  $\frac{dz}{z}$  leading to the pole at infinity in  $\ell(z) \rightarrow \infty$ . At higher loops we even get multiple poles at infinity [1]. In general, poles at infinity can indicate potential UV-divergencies after integration as is the case for the bubble integral. However, a direct association of poles at infinity with a UV-divergence is not possible. The triangle integral for example also has a pole at infinity but it is UV-finite. Finding a precise rule between the interplay of poles at infinity and the UV-behavior of gravity amplitudes is an active area of research and would have a direct bearing on the UV-finiteness question of  $\mathcal{N} = 8$  supergravity [185].

### 3.4.3 Collinear behavior

Based on the numerator factors in the Grassmannian formula for gravity on-shell diagrams (3.2.20) it is natural to conjecture that the residue of loop amplitudes on cuts that involve a three-point vertex (where the grey blob is any tree or loop amplitude),



factorize in a particular way,

$$\mathcal{M} = \langle \ell_1 \ell_2 \rangle \cdot \mathcal{R} \quad \text{for MHV vertex, i.e. } \tilde{\lambda}_{\ell_1} \sim \tilde{\lambda}_{\ell_2} \sim \tilde{\lambda}_{\ell_3}, \quad (3.4.5)$$

$$\mathcal{M} = [\ell_1 \ell_2] \cdot \overline{\mathcal{R}} \quad \text{for } \overline{\text{MHV}} \text{ vertex, i.e. } \lambda_{\ell_1} \sim \lambda_{\ell_2} \sim \lambda_{\ell_3}, \quad (3.4.6)$$

where  $\mathcal{R}$  and  $\overline{\mathcal{R}}$  are functions regular in  $\langle \ell_1 \ell_2 \rangle$  and  $[\ell_1 \ell_2]$  respectively. If both  $\ell_1$  and  $\ell_2$  are external particles this reduces to the well known behavior of gravity amplitudes in the collinear limit [165, 186],

$$\mathcal{M} \sim \frac{[12]}{\langle 12 \rangle} \cdot \widetilde{\mathcal{M}} \quad \text{for } \langle 12 \rangle \rightarrow 0, \quad \mathcal{M} \sim \frac{\langle 12 \rangle}{[12]} \cdot \widetilde{\mathcal{M}} \quad \text{for } [12] \rightarrow 0. \quad (3.4.7)$$

Let us stress that our claim is more general as one or both of the  $\ell_k$  can be loop momenta and there is no such statement available in the literature. It is fair to say that this statement does not follow from formula (3.2.20) for on-shell diagrams but it is rather motivated by it. The reason is that the lower cuts can not be directly written as the sums of on-shell diagrams. There are some extra  $1/s_{ij}$  factors one has to add when going from on-shell diagram to generalized cuts, and therefore our statement does not immediately apply to the other cuts. If we calculate the residue of the amplitude on the cut when the three point amplitude (say MHV) factorizes then this piece factorizes  $\langle \ell_1 \ell_2 \rangle$  but it is not guaranteed that the rest of the diagram does not give additional  $\frac{1}{\langle \ell_1 \ell_2 \rangle}$  and cancel this factor. This does not happen in the case of on-shell diagrams but it could for generalized cuts. Our conjecture is that indeed it does not happen and any cut of the amplitude of this type would be proportional to  $\langle \ell_1 \ell_2 \rangle$ . We will test this conjecture explicitly in several examples.

#### Four point one-loop

The four-point one-loop  $\mathcal{N} = 8$  supergravity amplitude was first given by Green, Schwarz and Brink [22] as a sum of three box integrals<sup>16</sup>,

$$\mathcal{M}_4^1(1234) = i stu \mathcal{M}_4^{\text{tree}}(1234) \left[ I_4^1(s, t) + I_4^1(t, u) + I_4^1(u, s) \right], \quad (3.4.8)$$

where the corresponding tree amplitude  $\mathcal{M}_4^{\text{tree}}(1234)$  carries the helicity information. Multiplying by  $stu$  one finds the totally permutation invariant four-point gravity prefactor (see e.g. [187]),

$$stu \mathcal{M}_4^{\text{tree}}(1234) = \underbrace{\left( \frac{[34][41]}{\langle 12 \rangle \langle 23 \rangle} \right)^2}_{\equiv \mathcal{K}_8}. \quad (3.4.9)$$

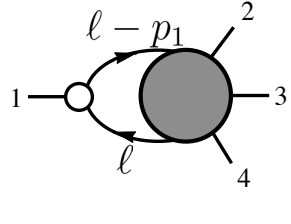
<sup>16</sup>The gravitational coupling constant  $(\kappa/2)^{n-2}$  for n-pt tree level amplitudes and  $(\kappa/2)^n$  for n-pt one-loop amplitudes will be suppressed ( $\kappa = \sqrt{32\pi G_N}$ ).

The one-loop box integrals  $I_4^1(-, -)$  are defined without the usual  $st$ -type normalization which was put into the permutation invariant prefactor  $\mathcal{K}_8$ . All integrals have numerator  $N = 1$  and therefore do not have unit leading singularity  $\pm 1, 0$  on all residues,

$$I_4^1(s; t) = \begin{array}{c} 2 \quad 3 \\ \square \\ 1 \quad \ell \quad 4 \end{array} \quad I_4^1(t; u) = \begin{array}{c} 2 \quad 3 \\ \diagdown \quad \diagup \\ 1 \quad \ell \quad 4 \end{array} \quad I_4^1(u; s) = \begin{array}{c} 2 \quad 3 \\ \diagup \quad \diagdown \\ 1 \quad \ell \quad 4 \end{array} \quad (3.4.10)$$

As there is no unique origin in loop momentum space, there is a general problem how to label the loop momentum  $\ell$  in individual diagrams; we will come back to this point shortly. In the definition (3.4.10), we chose an arbitrary origin for the loop momentum routing in each of the three boxes.

Let us consider a double cut of the amplitude where  $\ell^2 = (\ell - p_1)^2 = 0$  which chooses natural labels on the cut. For complex momenta, there are two solutions to the on-shell conditions. Here we choose the one with  $\ell = \lambda_1 \tilde{\lambda}_\ell$  for some  $\tilde{\lambda}_\ell$ , which corresponds to the cut diagram. The grey blob corresponds to five point  $(L - 1)$  loop amplitude, but in our case  $L = 1$  and it is just tree:



$$(3.4.11)$$

Note that for  $\ell^2 = 0$  the loop momentum  $\ell$  becomes null and can be written as  $\ell = \lambda_\ell \tilde{\lambda}_\ell$  so that the other propagator factorizes  $(\ell - p_1)^2 = \langle \ell 1 \rangle [\ell 1]$ . The solution we chose sets  $\langle \ell 1 \rangle = 0$  and the Jacobian of this double cut is

$$\mathcal{J} = \frac{1}{[\ell 1]}. \quad (3.4.12)$$

Using the box-expansion of the one-loop amplitude (3.4.8) we can calculate the residue on this cut for all three boxes (3.4.10) individually and get

$$\begin{aligned} & \left[ I_4^1(s, t) + I_4^1(t, u) + I_4^1(u, s) \right] \Big|_{\ell = \lambda_1 \tilde{\lambda}_\ell} = \\ & = \frac{1}{[\ell 1]} \left[ \frac{1}{(\ell - p_1 - p_2)^2 (\ell + p_4)^2} + \frac{1}{(\ell - p_1 - p_3)^2 (\ell + p_4)^2} + \frac{1}{(\ell - p_1 - p_2)^2 (\ell + p_3)^2} \right] \Big|_{\ell = \lambda_1 \tilde{\lambda}_\ell} \end{aligned}$$

$$\begin{aligned}
&= \frac{1}{[\ell 1]} \left[ \frac{1}{\langle 12 \rangle ([12] - [\ell 2]) \langle 14 \rangle [\ell 4]} + \frac{1}{\langle 13 \rangle ([13] - [\ell 3]) \langle 14 \rangle [\ell 4]} + \frac{1}{\langle 12 \rangle ([12] - [\ell 2]) \langle 13 \rangle [\ell 3]} \right] \\
&= \frac{[\ell 1] \cdot [34] \langle 14 \rangle}{[\ell 1] \cdot [\ell 3] [\ell 4] ([12] - [\ell 2]) ([13] - [\ell 3]) \langle 12 \rangle \langle 13 \rangle \langle 14 \rangle} .
\end{aligned} \tag{3.4.13}$$

From the Jacobian (3.4.12), each term contains a factor  $\frac{1}{[\ell 1]}$  but combining all three boxes we generate an expression with  $[\ell 1]$  in the numerator which cancels  $\mathcal{J}$ . However, this is not enough. Our conjecture was that on this cut the amplitude behaves like  $\sim [\ell 1]$ . The computation above seems to immediately contradict the conjecture but due to labeling issues mentioned earlier, the calculation is incomplete. In labeling the box diagrams in (3.4.10), we made a particular choice. We could have labeled the three boxes in a different way,

$$\tilde{I}_4^1(s; t) = \begin{array}{c} 2 \quad 3 \\ \square \\ 1 \quad 4 \end{array} \quad \tilde{I}_4^1(t; u) = \begin{array}{c} 2 \quad 3 \\ \diagup \quad \diagdown \\ 1 \quad 4 \end{array} \quad \tilde{I}_4^1(u; s) = \begin{array}{c} 2 \quad 3 \\ \diagdown \quad \diagup \\ 1 \quad 4 \end{array} \tag{3.4.14}$$

which gives a different residue on the cut (3.4.11),

$$\begin{aligned}
&\left. \left[ \tilde{I}_4^1(s, t) + \tilde{I}_4^1(t, u) + \tilde{I}_4^1(u, s) \right] \right|_{\ell = \lambda_1 \tilde{\lambda}_\ell} = \\
&\frac{1}{[\ell 1]} \left[ \frac{1}{(\ell - p_1 - p_4)^2 (\ell + p_2)^2} + \frac{1}{(\ell - p_1 - p_4)^2 (\ell + p_3)^2} + \frac{1}{(\ell - p_1 - p_3)^2 (\ell + p_2)^2} \right] \Big|_{\ell = \lambda_1 \tilde{\lambda}_\ell} \\
&= \frac{[\ell 1] \cdot [23] \langle 12 \rangle}{[\ell 1] \cdot [\ell 2] [\ell 3] ([13] - [\ell 3]) ([14] - [\ell 4]) \langle 12 \rangle \langle 13 \rangle \langle 14 \rangle}
\end{aligned} \tag{3.4.15}$$

Summing over both expression (3.4.13) and (3.4.15) (we should include a factor  $\frac{1}{2}$  but that is irrelevant here) and using  $[23] \langle 12 \rangle = [34] \langle 14 \rangle$ , we get

$$\mathcal{M}_4^1(1234) \Big|_{\ell = \lambda_1 \tilde{\lambda}_\ell} \sim \frac{[23] \langle 12 \rangle [24] \cdot [\ell 1]^2}{[\ell 1] \cdot [\ell 2] [\ell 3] [\ell 4] ([12] - [\ell 2]) ([13] - [\ell 3]) ([14] - [\ell 4]) \langle 12 \rangle \langle 13 \rangle \langle 14 \rangle}, \tag{3.4.16}$$

so that our conjecture indeed passes this check as the amplitude vanishes for  $[\ell 1] = 0$ , i.e.  $\ell \sim p_1$ . This example clearly demonstrates that the symmetrization over labels is important to getting the correct result. Note that the sum over six terms naturally arises when one starts directly from the cut-picture (3.4.11). To get all contributions, one is instructed to expand the five-point tree in all possible ways and find the contributions of all basis integrals. This procedure automatically takes into account all labellings of loop-momenta.



### Four point two-loop

We will now test the same property for the four-point two-loop amplitude which is given as a sum of planar- and non-planar double-box integrals including a numerator factor [127],

$$I_{(1234)}^{(P)} = s^2 \times \begin{array}{c} 2 \\ \square \square \\ 1 \quad 4 \\ 3 \end{array} \quad I_{(1234)}^{(NP)} = s^2 \times \begin{array}{c} 3 \\ \diamond \\ 2 \\ \square \\ 4 \end{array} \quad (3.4.17)$$

$$\mathcal{M}_4^2 = \frac{\mathcal{K}_8}{4} \sum_{\sigma \in \mathfrak{S}_4} \left[ I_{\sigma}^{(P)} + I_{\sigma}^{(NP)} \right], \quad (3.4.18)$$

where the sum over  $\sigma$  runs over all 24 permutations of  $\mathfrak{S}_4$ .

The full calculation can be performed numerically, but here we present a simplified version in which we calculate the residue on  $\ell^2 = \langle \ell 1 \rangle = [\ell 1] = 0$  which sets  $\ell = \alpha p_1$  directly. When combining all pieces, the numerator again generates  $[\ell 1]^2$  so that the residue on the  $\frac{1}{[\ell 1]}$  pole vanishes quadratically. Going directly to the kinematic region, where  $\ell = \alpha p_1$ , we are only able to see a pure vanishing  $\mathcal{M}_4^2(1234) \Big|_{\ell = \alpha p_1} = 0$ , but even this weaker statement requires an intricate cancellation between a large number of different terms.

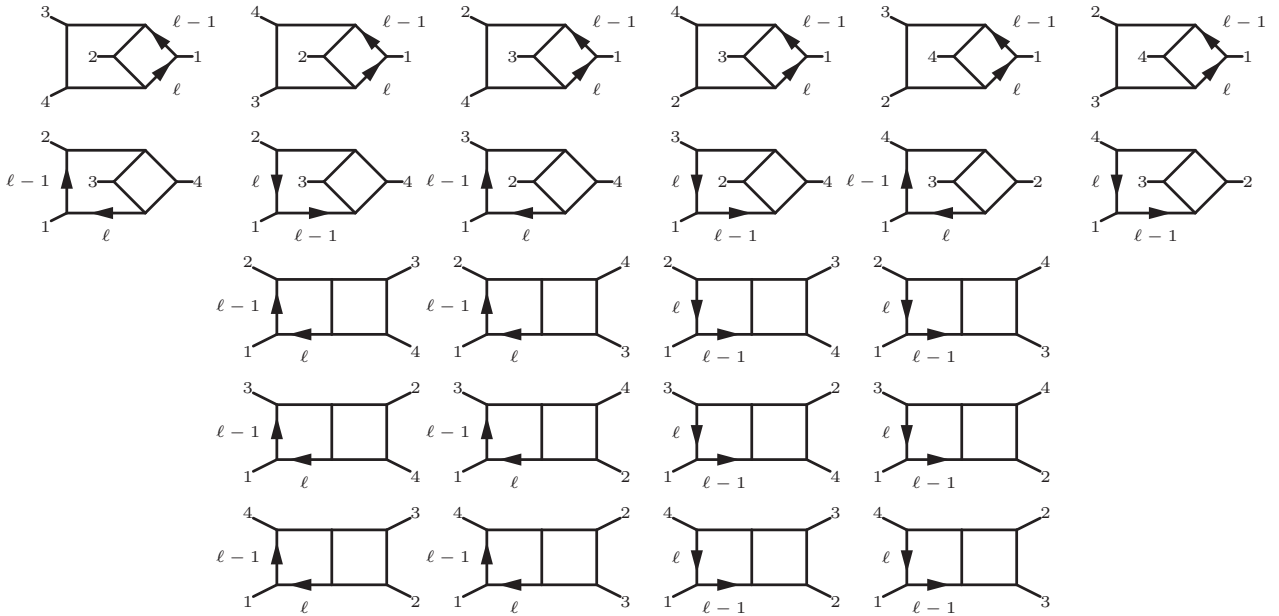


**Figure 3.32.** Contributing integrals on the collinear cut.

Starting with the collinear cut  $\ell^2 = \langle \ell 1 \rangle = [\ell 1] = 0$ , there are 24 terms contributing. If we look at the nonplanar integrals, for collinear kinematics  $\ell = \alpha p_1$ , we can use one

factor of  $s$  of the numerator (3.4.17) to decompose the pentagon as a sum of boxes. This is only possible for this special kinematics.

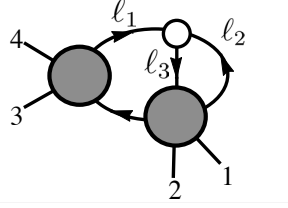
$$\begin{aligned}
 & \alpha 1 \quad 2 \quad (1-\alpha)1 \\
 & \quad \quad \quad s \quad \quad \quad 3 \\
 & \quad \quad \quad 4 \quad \quad \quad 3 \\
 & = \frac{1}{\alpha} \times \begin{array}{c} 2 \quad (1-\alpha)1 \\ \alpha 1+4 \quad 3 \end{array} \quad - \frac{1}{\alpha} \times \begin{array}{c} \alpha 1+2 \quad (1-\alpha)1 \\ 4 \quad 3 \end{array} \\
 & - \frac{1}{1-\alpha} \times \begin{array}{c} \alpha 1 \quad (1-\alpha)1+2 \\ 4 \quad 3 \end{array} \quad + \frac{1}{1-\alpha} \times \begin{array}{c} \alpha 1 \quad 2 \\ 4 \quad (1-\alpha)1+3 \end{array} \\
 & \hspace{20em} (3.4.19)
 \end{aligned}$$

If one uses the pentagon decomposition (3.4.19) on all nonplanar integrals in the first line of Fig. 3.32 and rewrites the  $\frac{1}{\alpha}$  and  $\frac{1}{1-\alpha}$  coefficients of the boxes in terms of propagators by multiplying and dividing by appropriate Mandelstam variables, one can see that all the planar double-boxes cancel. Each nonplanar integral in the first line cancels exactly two planar double boxes, so that the counting works perfectly. The remaining two terms of the decomposition that come with a plus sign are almost as straight-forward. One has to collect all these terms and re-express them as non-planar integrals. Combined with the non-planar integrals of the second line in Fig. 3.32, one can show that they always come in the combination  $(s + t + u) = 0$  so that they also cancel. This concludes our calculation and indeed we find our conjecture to hold. All signs work out such that the two-loop four-point amplitude in fact vanishes on the collinear cut  $\ell = \alpha p_1$ .

### Internal collinear region

Finally we can show one more example when the collinear region is between internal loops only corresponding to the cases described in the beginning of Sec. 3.4.3. The simplest example where we can study this kinematic region is for the two-loop four-point amplitude discussed above. Instead of going to the triple cut  $\ell_1^2 = \ell_2^2 = (\ell_1 + \ell_2)^2 = 0$  we can cut one more propagator to simplify the analysis by limiting the number of

contributing terms:



$$(3.4.20)$$

Parameterizing the cut solution on  $\ell_1^2 = \ell_2^2 = 0$  as

$$\ell_1 = \left[ \lambda_1 + \alpha_1 \lambda_2 \right] \left[ \alpha_2 \tilde{\lambda}_2 + \alpha_3 \tilde{\lambda}_1 \right], \quad \ell_2 = \left[ \lambda_1 + \beta_1 \lambda_2 \right] \left[ \beta_2 \tilde{\lambda}_2 + \beta_3 \tilde{\lambda}_1 \right],$$

the third propagator  $\ell_3^2 \equiv (\ell_1 + \ell_2)^2$  factorizes and we cut  $\langle \ell_1 \ell_2 \rangle = 0$  by setting  $\beta_1 = \alpha_1$ . The remaining part of the factorized propagator becomes,  $[\ell_1 \ell_2] = [21](\alpha_2 \beta_3 - \alpha_3 \beta_2)$ . As mentioned before, we simplify our life by further cutting  $(\ell_1 + p_3 + p_4)^2 = 0$ , which sets  $\alpha_3 = 1 - \alpha_1 \alpha_2$ .

Blowing up the blobs in (3.4.20) into planar and non-planar double-boxes (3.4.17) of different labels and combining all  $(8 + 4)$  terms, we checked numerically that the two-loop amplitude behaves as,

$$M_4^2 \Big|_{\langle \ell_1 \ell_2 \rangle = 0} \sim \frac{[\ell_1 \ell_2]^2}{[\ell_1 \ell_2]} \cdot \overline{\mathcal{R}}, \quad (3.4.21)$$

where the numerator generates the  $[\ell_1 \ell_2]^2$ -factor consistent with our conjecture.

### 3.5 Conclusion

In this paper we studied on-shell diagrams in gravity theories. We wrote a Grassmannian representation using edge variables and our formulation includes a non-trivial numerator factor in the measure as well as higher degree poles in the denominator. We showed that all higher poles correspond to cases where internal momenta in the loop are sent to infinity while all erasable edges are represented by single poles only. The numerator factor can be interpreted as a set of collinearity conditions on the on-shell momenta. We provide several examples in the paper for both leading singularities as well as diagrams with unfixed parameters. Because on-shell diagrams are also cuts of gravity loop amplitudes it is natural to conjecture that loop amplitudes share the same properties. We tested this conjecture on the cases of 1-loop and 2-loop amplitudes in  $\mathcal{N} = 8$  SUGRA and found a perfect agreement. Unlike in the Yang-Mills case these properties of on-shell diagrams can not be implemented term-by-term and require non-trivial cancellations between diagrams (even at four-point one-loop).

There was one aspect of gravity on-shell diagrams we did not discuss in more detail: *poles at infinity*. While absent in gauge theory they are present in gravity on-shell diagrams as poles of arbitrary degree. Poles at finite locations in momentum space correspond to erasing edges in on-shell diagrams but there is no such interpretation for poles at infinity. It is not clear how to embed them in the Grassmannian and what is the on-shell diagrammatic interpretation for them. This also prevents us from writing homological identities between different on-shell diagrams which was an important ingredient in the Yang-Mills case. Finally, the poles at infinity are closely related to the UV-behavior of gravity loop amplitudes and further study of their role in on-shell diagrams could lead to new insights there.

**Note:** While this work was completed, [188] appeared and has some overlap with our results.

# Bibliography

- [1] Z. Bern, E. Herrmann, S. Litsey, J. Stankowicz, and J. Trnka, *Logarithmic Singularities and Maximally Supersymmetric Amplitudes*, *JHEP* **06** (2015) 202, [[arXiv:1412.8584](#)].
- [2] Z. Bern, E. Herrmann, S. Litsey, J. Stankowicz, and J. Trnka, *Evidence for a Nonplanar Amplituhedron*, *JHEP* **06** (2016) 098, [[arXiv:1512.0859](#)].
- [3] E. Herrmann and J. Trnka, *Gravity On-shell Diagrams*, *JHEP* **11** (2016) 136, [[arXiv:1604.0347](#)].
- [4] S. Weinberg, *The Quantum theory of fields. Vol. 1: Foundations*. Cambridge University Press, 2005.
- [5] M. E. Peskin and D. V. Schroeder, *An Introduction to quantum field theory*. 1995.
- [6] W. Nahm, *Supersymmetries and their Representations*, *Nucl. Phys.* **B135** (1978) 149.
- [7] N. Seiberg, *Five-dimensional SUSY field theories, nontrivial fixed points and string dynamics*, *Phys. Lett.* **B388** (1996) 753–760, [[hep-th/9608111](#)].
- [8] E. Witten, *Conformal Field Theory In Four And Six Dimensions*, in *Topology, geometry and quantum field theory. Proceedings, Symposium in the honour of the 60th birthday of Graeme Segal, Oxford, UK, June 24-29, 2002*, 2007. [arXiv:0712.0157](#).
- [9] O. Aharony, M. Berkooz, S. Kachru, and E. Silverstein, *Matrix description of (1,0) theories in six-dimensions*, *Phys. Lett.* **B420** (1998) 55–63, [[hep-th/9709118](#)].
- [10] O. Aharony, M. Berkooz, and N. Seiberg, *Light cone description of (2,0) superconformal theories in six-dimensions*, *Adv. Theor. Math. Phys.* **2** (1998) 119–153, [[hep-th/9712117](#)].
- [11] O. Aharony, A. Hanany, and B. Kol, *Webs of (p,q) five-branes, five-dimensional field theories and grid diagrams*, *JHEP* **01** (1998) 002, [[hep-th/9710116](#)].
- [12] S. J. Parke and T. R. Taylor, *Gluonic Two Goes to Four*, *Nucl. Phys.* **B269** (1986) 410–420.
- [13] H. Elvang and Y.-t. Huang, *Scattering Amplitudes*, [arXiv:1308.1697](#).
- [14] J. M. Henn and J. C. Plefka, *Scattering Amplitudes in Gauge Theories*, *Lect. Notes Phys.* **883** (2014) 1–195.
- [15] L. J. Dixon, *Calculating scattering amplitudes efficiently*, [hep-ph/9601359](#).

- [16] S. Weinzierl, *Tales of 1001 Gluons*, 2016. [arXiv:1610.0531](#).
- [17] S. J. Parke and T. R. Taylor, *An Amplitude for  $n$  Gluon Scattering*, *Phys. Rev. Lett.* **56** (1986) 2459.
- [18] N. Arkani-Hamed and J. Trnka, *The Amplituhedron*, [arXiv:1312.2007](#).
- [19] J. M. Maldacena, *The Large  $N$  limit of superconformal field theories and supergravity*, *Int. J. Theor. Phys.* **38** (1999) 1113–1133, [[hep-th/9711200](#)]. [Adv. Theor. Math. Phys.2,231(1998)].
- [20] L. Brink, J. H. Schwarz, and J. Scherk, *Supersymmetric Yang-Mills Theories*, *Nucl.Phys.* **B121** (1977) 77.
- [21] F. Gliozzi, J. Scherk, and D. I. Olive, *Supersymmetry, Supergravity Theories and the Dual Spinor Model*, *Nucl.Phys.* **B122** (1977) 253–290.
- [22] M. B. Green, J. H. Schwarz, and L. Brink,  *$N=4$  Yang-Mills and  $N=8$  Supergravity as Limits of String Theories*, *Nucl.Phys.* **B198** (1982) 474–492.
- [23] Z. Bern, L. J. Dixon, D. C. Dunbar, and D. A. Kosower, *One loop  $n$  point gauge theory amplitudes, unitarity and collinear limits*, *Nucl.Phys.* **B425** (1994) 217–260, [[hep-ph/9403226](#)].
- [24] C. F. Berger, Z. Bern, L. J. Dixon, F. Febres Cordero, D. Forde, H. Ita, D. A. Kosower, and D. Maitre, *An Automated Implementation of On-Shell Methods for One-Loop Amplitudes*, *Phys. Rev.* **D78** (2008) 036003, [[arXiv:0803.4180](#)].
- [25] Z. Bern, L. J. Dixon, and D. A. Kosower, *Progress in one loop QCD computations*, *Ann.Rev.Nucl.Part.Sci.* **46** (1996) 109–148, [[hep-ph/9602280](#)].
- [26] F. Cachazo and P. Svrcek, *Lectures on twistor strings and perturbative Yang-Mills theory*, *PoS RTN2005* (2005) 004, [[hep-th/0504194](#)].
- [27] N. Beisert, C. Ahn, L. F. Alday, Z. Bajnok, J. M. Drummond, et al., *Review of AdS/CFT Integrability: An Overview*, *Lett.Math.Phys.* **99** (2012) 3–32, [[arXiv:1012.3982](#)].
- [28] J. Drummond, *Tree-level amplitudes and dual superconformal symmetry*, *J.Phys.* **A44** (2011) 454010, [[arXiv:1107.4544](#)].
- [29] S. Caron-Huot, L. J. Dixon, A. McLeod, and M. von Hippel, *Bootstrapping a Five-Loop Amplitude Using Steinmann Relations*, *Phys. Rev. Lett.* **117** (2016), no. 24 241601, [[arXiv:1609.0066](#)].
- [30] L. J. Dixon, J. Drummond, T. Harrington, A. J. McLeod, G. Papathanasiou, and M. Spradlin, *Heptagons from the Steinmann Cluster Bootstrap*, [arXiv:1612.0897](#).
- [31] L. J. Dixon, J. M. Drummond, and J. M. Henn, *Analytic result for the two-loop*

- six-point NMHV amplitude in  $N=4$  super Yang-Mills theory*, *JHEP* **1201** (2012) 024, [[arXiv:1111.1704](#)].
- [32] L. J. Dixon, J. M. Drummond, C. Duhr, M. von Hippel, and J. Pennington, *Bootstrapping six-gluon scattering in planar  $N=4$  super-Yang-Mills theory*, *PoS LL2014* (2014) 077, [[arXiv:1407.4724](#)].
- [33] L. J. Dixon, J. M. Drummond, C. Duhr, and J. Pennington, *The four-loop remainder function and multi-Regge behavior at NNLLA in planar  $N = 4$  super-Yang-Mills theory*, *JHEP* **1406** (2014) 116, [[arXiv:1402.3300](#)].
- [34] L. J. Dixon and M. von Hippel, *Bootstrapping an NMHV amplitude through three loops*, [[arXiv:1408.1505](#)].
- [35] Z. Bern, L. J. Dixon, and V. A. Smirnov, *Iteration of planar amplitudes in maximally supersymmetric Yang-Mills theory at three loops and beyond*, *Phys.Rev.* **D72** (2005) 085001, [[hep-th/0505205](#)].
- [36] E. Witten, *Perturbative gauge theory as a string theory in twistor space*, *Commun.Math.Phys.* **252** (2004) 189–258, [[hep-th/0312171](#)].
- [37] R. Roiban, M. Spradlin, and A. Volovich, *A Googly amplitude from the B model in twistor space*, *JHEP* **0404** (2004) 012, [[hep-th/0402016](#)].
- [38] R. Britto, F. Cachazo, and B. Feng, *New recursion relations for tree amplitudes of gluons*, *Nucl.Phys.* **B715** (2005) 499–522, [[hep-th/0412308](#)].
- [39] R. Britto, F. Cachazo, B. Feng, and E. Witten, *Direct proof of tree-level recursion relation in Yang-Mills theory*, *Phys.Rev.Lett.* **94** (2005) 181602, [[hep-th/0501052](#)].
- [40] N. Arkani-Hamed, J. L. Bourjaily, F. Cachazo, S. Caron-Huot, and J. Trnka, *The All-Loop Integrand For Scattering Amplitudes in Planar  $N=4$  SYM*, *JHEP* **1101** (2011) 041, [[arXiv:1008.2958](#)].
- [41] J. Drummond, J. Henn, V. Smirnov, and E. Sokatchev, *Magic identities for conformal four-point integrals*, *JHEP* **0701** (2007) 064, [[hep-th/0607160](#)].
- [42] L. F. Alday and J. M. Maldacena, *Gluon scattering amplitudes at strong coupling*, *JHEP* **0706** (2007) 064, [[arXiv:0705.0303](#)].
- [43] J. Drummond, J. Henn, G. Korchemsky, and E. Sokatchev, *Dual superconformal symmetry of scattering amplitudes in  $N=4$  super-Yang-Mills theory*, *Nucl.Phys.* **B828** (2010) 317–374, [[arXiv:0807.1095](#)].
- [44] J. M. Drummond, J. M. Henn, and J. Plefka, *Yangian symmetry of scattering amplitudes in  $N=4$  super Yang-Mills theory*, *JHEP* **0905** (2009) 046, [[arXiv:0902.2987](#)].

- [45] N. Beisert and M. Staudacher, *The  $N=4$  SYM integrable super spin chain*, *Nucl.Phys.* **B670** (2003) 439–463, [[hep-th/0307042](#)].
- [46] N. Beisert, B. Eden, and M. Staudacher, *Transcendentality and Crossing*, *J. Stat. Mech.* **0701** (2007) P01021, [[hep-th/0610251](#)].
- [47] A. Hodges, *Eliminating spurious poles from gauge-theoretic amplitudes*, *JHEP* **1305** (2013) 135, [[arXiv:0905.1473](#)].
- [48] J. Drummond, G. Korchemsky, and E. Sokatchev, *Conformal properties of four-gluon planar amplitudes and Wilson loops*, *Nucl.Phys.* **B795** (2008) 385–408, [[arXiv:0707.0243](#)].
- [49] A. Brandhuber, P. Heslop, and G. Travaglini, *MHV amplitudes in  $N=4$  super Yang-Mills and Wilson loops*, *Nucl. Phys.* **B794** (2008) 231–243, [[arXiv:0707.1153](#)].
- [50] J. Drummond, J. Henn, G. Korchemsky, and E. Sokatchev, *Conformal Ward identities for Wilson loops and a test of the duality with gluon amplitudes*, *Nucl.Phys.* **B826** (2010) 337–364, [[arXiv:0712.1223](#)].
- [51] L. Mason and D. Skinner, *The Complete Planar S-matrix of  $N=4$  SYM as a Wilson Loop in Twistor Space*, *JHEP* **1012** (2010) 018, [[arXiv:1009.2225](#)].
- [52] S. Caron-Huot, *Notes on the scattering amplitude / Wilson loop duality*, *JHEP* **1107** (2011) 058, [[arXiv:1010.1167](#)].
- [53] L. F. Alday, B. Eden, G. P. Korchemsky, J. Maldacena, and E. Sokatchev, *From correlation functions to Wilson loops*, *JHEP* **1109** (2011) 123, [[arXiv:1007.3243](#)].
- [54] B. Eden, G. P. Korchemsky, and E. Sokatchev, *From correlation functions to scattering amplitudes*, *JHEP* **1112** (2011) 002, [[arXiv:1007.3246](#)].
- [55] B. Eden, G. P. Korchemsky, and E. Sokatchev, *More on the duality correlators/amplitudes*, *Phys.Lett.* **B709** (2012) 247–253, [[arXiv:1009.2488](#)].
- [56] B. Basso, A. Sever, and P. Vieira, *Spacetime and Flux Tube S-Matrices at Finite Coupling for  $N=4$  Supersymmetric Yang-Mills Theory*, *Phys.Rev.Lett.* **111** (2013), no. 9 091602, [[arXiv:1303.1396](#)].
- [57] B. Basso, J. Caetano, L. Cordova, A. Sever, and P. Vieira, *OPE for all Helicity Amplitudes*, *JHEP* **08** (2015) 018, [[arXiv:1412.1132](#)].
- [58] B. Basso, A. Sever, and P. Vieira, *Hexagonal Wilson Loops in Planar  $\mathcal{N} = 4$  SYM Theory at Finite Coupling*, [[arXiv:1508.0304](#)].
- [59] L. J. Dixon, J. M. Drummond, and J. M. Henn, *Bootstrapping the three-loop hexagon*, *JHEP* **1111** (2011) 023, [[arXiv:1108.4461](#)].
- [60] L. J. Dixon, J. M. Drummond, M. von Hippel, and J. Pennington, *Hexagon functions and the three-loop remainder function*, *JHEP* **12** (2013) 049, [[arXiv:1308.2276](#)].



- [61] L. J. Dixon and M. von Hippel, *Bootstrapping an NMHV amplitude through three loops*, *JHEP* **10** (2014) 065, [[arXiv:1408.1505](#)].
- [62] L. J. Dixon, M. von Hippel, and A. J. McLeod, *The four-loop six-gluon NMHV ratio function*, [arXiv:1509.0812](#).
- [63] J. M. Drummond, G. Papathanasiou, and M. Spradlin, *A Symbol of Uniqueness: The Cluster Bootstrap for the 3-Loop MHV Heptagon*, *JHEP* **03** (2015) 072, [[arXiv:1412.3763](#)].
- [64] A. B. Goncharov, M. Spradlin, C. Vergu, and A. Volovich, *Classical Polylogarithms for Amplitudes and Wilson Loops*, *Phys.Rev.Lett.* **105** (2010) 151605, [[arXiv:1006.5703](#)].
- [65] J. Golden, A. B. Goncharov, M. Spradlin, C. Vergu, and A. Volovich, *Motivic Amplitudes and Cluster Coordinates*, *JHEP* **1401** (2014) 091, [[arXiv:1305.1617](#)].
- [66] D. Parker, A. Scherlis, M. Spradlin, and A. Volovich, *Hedgehog bases for  $A_n$  cluster polylogarithms and an application to six-point amplitudes*, *JHEP* **11** (2015) 136, [[arXiv:1507.0195](#)].
- [67] N. Arkani-Hamed, J. L. Bourjaily, F. Cachazo, A. B. Goncharov, A. Postnikov, and J. Trnka, *Scattering Amplitudes and the Positive Grassmannian*, [arXiv:1212.5605](#).
- [68] N. Arkani-Hamed, F. Cachazo, C. Cheung, and J. Kaplan, *A Duality For The S Matrix*, *JHEP* **1003** (2010) 020, [[arXiv:0907.5418](#)].
- [69] N. Arkani-Hamed, F. Cachazo, and C. Cheung, *The Grassmannian Origin Of Dual Superconformal Invariance*, *JHEP* **1003** (2010) 036, [[arXiv:0909.0483](#)].
- [70] L. Mason and D. Skinner, *Dual Superconformal Invariance, Momentum Twistors and Grassmannians*, *JHEP* **0911** (2009) 045, [[arXiv:0909.0250](#)].
- [71] N. Arkani-Hamed, J. Bourjaily, F. Cachazo, and J. Trnka, *Unification of Residues and Grassmannian Dualities*, *JHEP* **1101** (2011) 049, [[arXiv:0912.4912](#)].
- [72] N. Arkani-Hamed, J. Bourjaily, F. Cachazo, and J. Trnka, *Local Spacetime Physics from the Grassmannian*, *JHEP* **1101** (2011) 108, [[arXiv:0912.3249](#)].
- [73] Y.-T. Huang and C. Wen, *ABJM amplitudes and the positive orthogonal grassmannian*, *JHEP* **1402** (2014) 104, [[arXiv:1309.3252](#)].
- [74] Y.-t. Huang, C. Wen, and D. Xie, *The Positive orthogonal Grassmannian and loop amplitudes of ABJM*, [arXiv:1402.1479](#).
- [75] J. Kim and S. Lee, *Positroid Stratification of Orthogonal Grassmannian and ABJM Amplitudes*, *JHEP* **1409** (2014) 085, [[arXiv:1402.1119](#)].
- [76] H. Elvang, Y.-t. Huang, C. Keeler, T. Lam, T. M. Olson, et al., *Grassmannians for scattering amplitudes in 4d  $\mathcal{N} = 4$  SYM and 3d ABJM*, [arXiv:1410.0621](#).

- [77] B. Chen, G. Chen, Y.-K. E. Cheung, Y. Li, R. Xie, et al., *Nonplanar On-shell Diagrams and Leading Singularities of Scattering Amplitudes*, [arXiv:1411.3889](#).
- [78] N. Arkani-Hamed and J. Trnka, *Into the Amplituhedron*, [arXiv:1312.7878](#).
- [79] S. Franco, D. Galloni, A. Mariotti, and J. Trnka, *Anatomy of the Amplituhedron*, [arXiv:1408.3410](#).
- [80] T. Lam, *Amplituhedron cells and Stanley symmetric functions*, [arXiv:1408.5531](#).
- [81] Y. Bai and S. He, *The Amplituhedron from Momentum Twistor Diagrams*, [arXiv:1408.2459](#).
- [82] Y. Bai, S. He, and T. Lam, *The Amplituhedron and the One-loop Grassmannian Measure*, [arXiv:1510.0355](#).
- [83] L. Ferro, T. Lukowski, A. Orta, and M. Parisi, *Towards the Amplituhedron Volume*, [arXiv:1512.0495](#).
- [84] N. Arkani-Hamed, Y. Bai, and T. Lam, *Positive Geometries and Canonical Forms*, [arXiv:1703.0454](#).
- [85] G. Lusztig, *Total positivity in partial flag manifolds*, *Represent. Theory* **2** (1998) 70–78.
- [86] A. Postnikov, *Total positivity, Grassmannians, and networks*, *ArXiv Mathematics e-prints* (Sept., 2006) [[math/0609764](#)].
- [87] A. Postnikov, D. Speyer, and L. Williams, *Matching polytopes, toric geometry, and the non-negative part of the Grassmannian*, *ArXiv e-prints* (June, 2007) [[arXiv:0706.2501](#)].
- [88] L. K. Williams, *Enumeration of totally positive Grassmann cells*, *ArXiv Mathematics e-prints* (July, 2003) [[math/0307271](#)].
- [89] A. B. Goncharov and R. Kenyon, *Dimers and cluster integrable systems*, *ArXiv e-prints* (July, 2011) [[arXiv:1107.5588](#)].
- [90] A. Knutson, T. Lam, and D. Speyer, *Positroid Varieties: Juggling and Geometry*, *ArXiv e-prints* (Nov., 2011) [[arXiv:1111.3660](#)].
- [91] A. Kotikov and L. Lipatov, *On the highest transcendentality in  $N=4$  SUSY*, *Nucl.Phys.* **B769** (2007) 217–255, [[hep-th/0611204](#)].
- [92] B. Eden and M. Staudacher, *Integrability and transcendentality*, *J.Stat.Mech.* **0611** (2006) P11014, [[hep-th/0603157](#)].
- [93] A. E. Lipstein and L. Mason, *From  $d$  logs to dilogs the super Yang-Mills MHV amplitude revisited*, *JHEP* **1401** (2014) 169, [[arXiv:1307.1443](#)].
- [94] C. Duhr, *Mathematical aspects of scattering amplitudes*, in *Theoretical Advanced Study Institute in Elementary Particle Physics: Journeys Through the Precision*

- Frontier: Amplitudes for Colliders (TASI 2014) Boulder, Colorado, June 2-27, 2014*, 2014. [arXiv:1411.7538](#).
- [95] E. Panzer, *Feynman integrals and hyperlogarithms*. PhD thesis, Humboldt U., Berlin, Inst. Math., 2015. [arXiv:1506.0724](#).
- [96] F. Brown, *Periods and Feynman amplitudes*, in *18th International Congress on Mathematical Physics (ICMP2015) Santiago de Chile, Chile, July 27-August 1, 2015*, 2015. [arXiv:1512.0926](#).
- [97] J. Golden, M. F. Paulos, M. Spradlin, and A. Volovich, *Cluster Polylogarithms for Scattering Amplitudes*, [arXiv:1401.6446](#).
- [98] J. Golden and M. Spradlin, *A Cluster Bootstrap for Two-Loop MHV Amplitudes*, [arXiv:1411.3289](#).
- [99] L. J. Dixon, M. von Hippel, A. J. McLeod, and J. Trnka, *Multi-Loop Positivity of the Planar  $\mathcal{N} = 4$  SYM Six-Point Amplitude*, [arXiv:1611.0832](#).
- [100] B. Basso, A. Sever, and P. Vieira, *Space-time S-matrix and Flux tube S-matrix II. Extracting and Matching Data*, *JHEP* **1401** (2014) 008, [[arXiv:1306.2058](#)].
- [101] B. Basso, A. Sever, and P. Vieira, *Space-time S-matrix and Flux-tube S-matrix III. The two-particle contributions*, *JHEP* **1408** (2014) 085, [[arXiv:1402.3307](#)].
- [102] B. Basso, A. Sever, and P. Vieira, *On the collinear limit of scattering amplitudes at strong coupling*, [arXiv:1405.6350](#).
- [103] B. Basso, A. Sever, and P. Vieira, *Space-time S-matrix and Flux-tube S-matrix IV. Gluons and Fusion*, *JHEP* **1409** (2014) 149, [[arXiv:1407.1736](#)].
- [104] L. Ferro, T. Lukowski, C. Meneghelli, J. Plefka, and M. Staudacher, *Harmonic R-matrices for Scattering Amplitudes and Spectral Regularization*, *Phys.Rev.Lett.* **110** (2013), no. 12 121602, [[arXiv:1212.0850](#)].
- [105] L. Ferro, T. Lukowski, C. Meneghelli, J. Plefka, and M. Staudacher, *Spectral Parameters for Scattering Amplitudes in  $N=4$  Super Yang-Mills Theory*, *JHEP* **1401** (2014) 094, [[arXiv:1308.3494](#)].
- [106] N. Beisert, J. Broedel, and M. Rosso, *On Yangian-invariant regularization of deformed on-shell diagrams in  $\mathcal{N} = 4$  super-Yang-Mills theory*, *J.Phys.* **A47** (2014) 365402, [[arXiv:1401.7274](#)].
- [107] J. Broedel, M. de Leeuw, and M. Rosso, *Deformed one-loop amplitudes in  $N = 4$  super-Yang-Mills theory*, [arXiv:1406.4024](#).
- [108] L. Ferro, T. Lukowski, and M. Staudacher,  *$N=4$  Scattering Amplitudes and the Deformed Grassmannian*, [arXiv:1407.6736](#).

- [109] T. Bargheer, Y.-t. Huang, F. Loebbert, and M. Yamazaki, *Integrable Amplitude Deformations for  $N=4$  Super Yang–Mills and ABJM Theory*, [arXiv:1407.4449](#).
- [110] N. Beisert, A. Garus, and M. Rosso, *Yangian Symmetry and Integrability of Planar  $N=4$  Super-Yang-Mills Theory*, [arXiv:1701.0916](#).
- [111] Z. Bern, S. Davies, and T. Dennen, *Enhanced Ultraviolet Cancellations in  $N = 5$  Supergravity at Four Loop*, [arXiv:1409.3089](#).
- [112] N. Arkani-Hamed, J. L. Bourjaily, F. Cachazo, A. Postnikov, and J. Trnka, *On-Shell Structures of MHV Amplitudes Beyond the Planar Limit*, *JHEP* **06** (2015) 179, [[arXiv:1412.8475](#)].
- [113] Z. Bern, J. Carrasco, and H. Johansson, *New Relations for Gauge-Theory Amplitudes*, *Phys.Rev.* **D78** (2008) 085011, [[arXiv:0805.3993](#)].
- [114] Z. Bern, J. J. M. Carrasco, and H. Johansson, *Perturbative Quantum Gravity as a Double Copy of Gauge Theory*, *Phys.Rev.Lett.* **105** (2010) 061602, [[arXiv:1004.0476](#)].
- [115] A. Kotikov, L. Lipatov, A. Onishchenko, and V. Velizhanin, *Three loop universal anomalous dimension of the Wilson operators in  $N=4$  SUSY Yang-Mills model*, *Phys.Lett.* **B595** (2004) 521–529, [[hep-th/0404092](#)].
- [116] S. G. Naculich, H. Nastase, and H. J. Schnitzer, *Two-loop graviton scattering relation and IR behavior in  $N=8$  supergravity*, *Nucl.Phys.* **B805** (2008) 40–58, [[arXiv:0805.2347](#)].
- [117] A. Brandhuber, P. Heslop, A. Nasti, B. Spence, and G. Travaglini, *Four-point Amplitudes in  $N=8$  Supergravity and Wilson Loops*, *Nucl.Phys.* **B807** (2009) 290–314, [[arXiv:0805.2763](#)].
- [118] T. Gehrmann, J. M. Henn, and T. Huber, *The three-loop form factor in  $N=4$  super Yang-Mills*, *JHEP* **1203** (2012) 101, [[arXiv:1112.4524](#)].
- [119] N. Arkani-Hamed, J. L. Bourjaily, F. Cachazo, and J. Trnka, *On the Singularity Structure of Maximally Supersymmetric Scattering Amplitudes*, [arXiv:1410.0354](#).
- [120] Z. Bern, J. Rozowsky, and B. Yan, *Two loop four gluon amplitudes in  $N=4$  superYang-Mills*, *Phys.Lett.* **B401** (1997) 273–282, [[hep-ph/9702424](#)].
- [121] J. L. Bourjaily, A. DiRe, A. Shaikh, M. Spradlin, and A. Volovich, *The Soft-Collinear Bootstrap:  $N=4$  Yang-Mills Amplitudes at Six and Seven Loops*, *JHEP* **1203** (2012) 032, [[arXiv:1112.6432](#)].
- [122] Z. Bern, J. Carrasco, L. J. Dixon, H. Johansson, D. Kosower, and R. Roiban, *Three-Loop Superfiniteness of  $N=8$  Supergravity*, *Phys.Rev.Lett.* **98** (2007) 161303, [[hep-th/0702112](#)].

- [123] J. M. Henn, *Multiloop integrals in dimensional regularization made simple*, *Phys.Rev.Lett.* **110** (2013), no. 25 251601, [[arXiv:1304.1806](#)].
- [124] J. M. Henn, A. V. Smirnov, and V. A. Smirnov, *Analytic results for planar three-loop four-point integrals from a Knizhnik-Zamolodchikov equation*, *JHEP* **1307** (2013) 128, [[arXiv:1306.2799](#)].
- [125] J. M. Henn, A. V. Smirnov, and V. A. Smirnov, *Evaluating single-scale and/or non-planar diagrams by differential equations*, *JHEP* **1403** (2014) 088, [[arXiv:1312.2588](#)].
- [126] J. M. Henn, *Lectures on differential equations for Feynman integrals*, [arXiv:1412.2296](#).
- [127] Z. Bern, L. J. Dixon, D. Dunbar, M. Perelstein, and J. Rozowsky, *On the relationship between Yang-Mills theory and gravity and its implication for ultraviolet divergences*, *Nucl.Phys.* **B530** (1998) 401–456, [[hep-th/9802162](#)].
- [128] Z. Bern, J. Carrasco, L. J. Dixon, H. Johansson, and R. Roiban, *Manifest Ultraviolet Behavior for the Three-Loop Four-Point Amplitude of  $N=8$  Supergravity*, *Phys.Rev.* **D78** (2008) 105019, [[arXiv:0808.4112](#)].
- [129] Z. Bern, J. Carrasco, L. Dixon, H. Johansson, and R. Roiban, *Simplifying Multiloop Integrands and Ultraviolet Divergences of Gauge Theory and Gravity Amplitudes*, *Phys.Rev.* **D85** (2012) 105014, [[arXiv:1201.5366](#)].
- [130] G. Passarino and M. Veltman, *One Loop Corrections for  $e^+e^-$  Annihilation Into  $\mu^+\mu^-$  in the Weinberg Model*, *Nucl.Phys.* **B160** (1979) 151.
- [131] Z. Bern, L. J. Dixon, and D. A. Kosower, *Dimensionally regulated pentagon integrals*, *Nucl.Phys.* **B412** (1994) 751–816, [[hep-ph/9306240](#)].
- [132] Z. Bern, J. J. Carrasco, T. Dennen, Y.-t. Huang, and H. Ita, *Generalized Unitarity and Six-Dimensional Helicity*, *Phys.Rev.* **D83** (2011) 085022, [[arXiv:1010.0494](#)].
- [133] Z. Bern, J. Carrasco, L. J. Dixon, H. Johansson, and R. Roiban, *The Complete Four-Loop Four-Point Amplitude in  $N=4$  Super-Yang-Mills Theory*, *Phys.Rev.* **D82** (2010) 125040, [[arXiv:1008.3327](#)].
- [134] F. Cachazo, *Sharpening The Leading Singularity*, [arXiv:0803.1988](#).
- [135] G. 't Hooft and M. Veltman, *Regularization and Renormalization of Gauge Fields*, *Nucl.Phys.* **B44** (1972) 189–213.
- [136] Z. Bern and G. Chalmers, *Factorization in one loop gauge theory*, *Nucl.Phys.* **B447** (1995) 465–518, [[hep-ph/9503236](#)].
- [137] C. Anastasiou, Z. Bern, L. J. Dixon, and D. Kosower, *Planar amplitudes in*

- maximally supersymmetric Yang-Mills theory*, *Phys.Rev.Lett.* **91** (2003) 251602, [[hep-th/0309040](#)].
- [138] Z. Bern, J. Carrasco, H. Johansson, and D. Kosower, *Maximally supersymmetric planar Yang-Mills amplitudes at five loops*, *Phys.Rev.* **D76** (2007) 125020, [[arXiv:0705.1864](#)].
- [139] N. Bjerrum-Bohr and P. Vanhove, *Absence of Triangles in Maximal Supergravity Amplitudes*, *JHEP* **0810** (2008) 006, [[arXiv:0805.3682](#)].
- [140] N. Arkani-Hamed, F. Cachazo, and J. Kaplan, *What is the Simplest Quantum Field Theory?*, *JHEP* **1009** (2010) 016, [[arXiv:0808.1446](#)].
- [141] Z. Bern, J. Carrasco, H. Johansson, and R. Roiban, *The Five-Loop Four-Point Amplitude of  $N=4$  super-Yang-Mills Theory*, *Phys.Rev.Lett.* **109** (2012) 241602, [[arXiv:1207.6666](#)].
- [142] Z. Bern, M. Czakon, L. J. Dixon, D. A. Kosower, and V. A. Smirnov, *The Four-Loop Planar Amplitude and Cusp Anomalous Dimension in Maximally Supersymmetric Yang-Mills Theory*, *Phys.Rev.* **D75** (2007) 085010, [[hep-th/0610248](#)].
- [143] F. Cachazo and D. Skinner, *On the structure of scattering amplitudes in  $N=4$  super Yang-Mills and  $N=8$  supergravity*, [arXiv:0801.4574](#).
- [144] B. Eden, P. Heslop, G. P. Korchemsky, and E. Sokatchev, *Constructing the correlation function of four stress-tensor multiplets and the four-particle amplitude in  $N=4$  SYM*, *Nucl.Phys.* **B862** (2012) 450–503, [[arXiv:1201.5329](#)].
- [145] Z. Bern, J. J. Carrasco, L. J. Dixon, M. R. Douglas, M. von Hippel, et al.,  *$D = 5$  maximally supersymmetric Yang-Mills theory diverges at six loops*, *Phys.Rev.* **D87** (2013) 025018, [[arXiv:1210.7709](#)].
- [146] N. Arkani-Hamed, J. L. Bourjaily, F. Cachazo, and J. Trnka, *Local Integrals for Planar Scattering Amplitudes*, *JHEP* **1206** (2012) 125, [[arXiv:1012.6032](#)].
- [147] J. J. M. Carrasco and H. Johansson, *Generic multiloop methods and application to  $N=4$  super-Yang-Mills*, *J.Phys.* **A44** (2011) 454004, [[arXiv:1103.3298](#)].
- [148] H. Elvang, D. Z. Freedman, and M. Kiermaier, *Recursion Relations, Generating Functions, and Unitarity Sums in  $N=4$  SYM Theory*, *JHEP* **0904** (2009) 009, [[arXiv:0808.1720](#)].
- [149] Z. Bern, J. Carrasco, H. Ita, H. Johansson, and R. Roiban, *On the Structure of Supersymmetric Sums in Multi-Loop Unitarity Cuts*, *Phys.Rev.* **D80** (2009) 065029, [[arXiv:0903.5348](#)].
- [150] Z. Bern, S. Davies, T. Dennen, and Y.-t. Huang, *Absence of Three-Loop Four-Point Divergences in  $N = 4$  Supergravity*, *Phys.Rev.Lett.* **108** (2012) 201301, [[arXiv:1202.3423](#)].

- [151] F. Tkachov, *A Theorem on Analytical Calculability of Four Loop Renormalization Group Functions*, *Phys.Lett.* **B100** (1981) 65–68.
- [152] K. Chetyrkin and F. Tkachov, *Integration by Parts: The Algorithm to Calculate Beta Functions in 4 Loops*, *Nucl.Phys.* **B192** (1981) 159–204.
- [153] M. L. Mangano, S. J. Parke, and Z. Xu, *Duality and Multi - Gluon Scattering*, *Nucl. Phys.* **B298** (1988) 653.
- [154] N. Arkani-Hamed, A. Hodges, and J. Trnka, *Positive Amplitudes In The Amplituhedron*, *JHEP* **08** (2015) 030, [[arXiv:1412.8478](https://arxiv.org/abs/1412.8478)].
- [155] J. J. M. Carrasco and H. Johansson, *Five-Point Amplitudes in  $N=4$  Super-Yang-Mills Theory and  $N = 8$  Supergravity*, *Phys. Rev.* **D85** (2012) 025006, [[arXiv:1106.4711](https://arxiv.org/abs/1106.4711)].
- [156] Z. Bern, L. Dixon, D. Kosower, R. Roiban, M. Spradlin, et al., *The Two-Loop Six-Gluon MHV Amplitude in Maximally Supersymmetric Yang-Mills Theory*, *Phys.Rev.* **D78** (2008) 045007, [[arXiv:0803.1465](https://arxiv.org/abs/0803.1465)].
- [157] Z. Bern, L. J. Dixon, D. C. Dunbar, and D. A. Kosower, *Fusing gauge theory tree amplitudes into loop amplitudes*, *Nucl.Phys.* **B435** (1995) 59–101, [[hep-ph/9409265](https://arxiv.org/abs/hep-ph/9409265)].
- [158] J. M. Drummond, J. Henn, G. P. Korchemsky, and E. Sokatchev, *The hexagon Wilson loop and the BDS ansatz for the six-gluon amplitude*, *Phys. Lett.* **B662** (2008) 456–460, [[arXiv:0712.4138](https://arxiv.org/abs/0712.4138)].
- [159] J. L. Bourjaily, S. Caron-Huot, and J. Trnka, *Dual-Conformal Regularization of Infrared Loop Divergences and the Chiral Box Expansion*, *JHEP* **01** (2015) 001, [[arXiv:1303.4734](https://arxiv.org/abs/1303.4734)].
- [160] J. L. Bourjaily and J. Trnka, *Local Integrand Representations of All Two-Loop Amplitudes in Planar SYM*, *JHEP* **08** (2015) 119, [[arXiv:1505.0588](https://arxiv.org/abs/1505.0588)].
- [161] R. Kleiss and H. Kuijf, *Multi - Gluon Cross-sections and Five Jet Production at Hadron Colliders*, *Nucl. Phys.* **B312** (1989) 616.
- [162] M. L. Mangano and S. J. Parke, *Multiparton amplitudes in gauge theories*, *Phys. Rept.* **200** (1991) 301–367, [[hep-th/0509223](https://arxiv.org/abs/hep-th/0509223)].
- [163] S. Franco, D. Galloni, B. Penante, and C. Wen, *Non-Planar On-Shell Diagrams*, *JHEP* **06** (2015) 199, [[arXiv:1502.0203](https://arxiv.org/abs/1502.0203)].
- [164] Z. Bern, L. J. Dixon, D. C. Dunbar, and D. A. Kosower, *One loop selfdual and  $N=4$  superYang-Mills*, *Phys. Lett.* **B394** (1997) 105–115, [[hep-th/9611127](https://arxiv.org/abs/hep-th/9611127)].
- [165] Z. Bern, L. J. Dixon, M. Perelstein, and J. S. Rozowsky, *Multileg one loop gravity amplitudes from gauge theory*, *Nucl. Phys.* **B546** (1999) 423–479, [[hep-th/9811140](https://arxiv.org/abs/hep-th/9811140)].
- [166] G. Mogull and D. O’Connell, *Overcoming Obstacles to Colour-Kinematics Duality at Two Loops*, [[arXiv:1511.0665](https://arxiv.org/abs/1511.0665)].

- [167] S. Caron-Huot and J. M. Henn, *Iterative structure of finite loop integrals*, *JHEP* **06** (2014) 114, [[arXiv:1404.2922](#)].
- [168] T. Gehrmann, J. M. Henn, and N. A. Lo Presti, *Analytic form of the two-loop planar five-gluon all-plus-helicity amplitude in QCD*, [arXiv:1511.0540](#).
- [169] R. Britto, F. Cachazo, and B. Feng, *Generalized unitarity and one-loop amplitudes in  $N=4$  super-Yang-Mills*, *Nucl.Phys.* **B725** (2005) 275–305, [[hep-th/0412103](#)].
- [170] S. Caron-Huot, *Loops and trees*, *JHEP* **05** (2011) 080, [[arXiv:1007.3224](#)].
- [171] R. E. Cutkosky, *Singularities and discontinuities of Feynman amplitudes*, *J. Math. Phys.* **1** (1960) 429–433.
- [172] S. Mandelstam, *Determination of the pion - nucleon scattering amplitude from dispersion relations and unitarity. General theory*, *Phys. Rev.* **112** (1958) 1344–1360.
- [173] P. Benincasa and F. Cachazo, *Consistency Conditions on the S-Matrix of Massless Particles*, [arXiv:0705.4305](#).
- [174] Z. Xu, D.-H. Zhang, and L. Chang, *Helicity Amplitudes for Multiple Bremsstrahlung in Massless Nonabelian Gauge Theories*, *Nucl. Phys.* **B291** (1987) 392.
- [175] J. Broedel and L. J. Dixon, *Color-kinematics duality and double-copy construction for amplitudes from higher-dimension operators*, *JHEP* **10** (2012) 091, [[arXiv:1208.0876](#)].
- [176] V. P. Nair, *A Current Algebra for Some Gauge Theory Amplitudes*, *Phys. Lett.* **B214** (1988) 215.
- [177] A. P. Hodges, *Twistor diagrams for all tree amplitudes in gauge theory: A Helicity-independent formalism*, [hep-th/0512336](#).
- [178] R. Frassek and D. Meidinger, *Yangian-type symmetries of non-planar leading singularities*, *JHEP* **05** (2016) 110, [[arXiv:1603.0008](#)].
- [179] S. Weinberg, *Photons and Gravitons in s Matrix Theory: Derivation of Charge Conservation and Equality of Gravitational and Inertial Mass*, *Phys. Rev.* **135** (1964) B1049–B1056.
- [180] S. Weinberg, *Photons and gravitons in perturbation theory: Derivation of Maxwell's and Einstein's equations*, *Phys. Rev.* **138** (1965) B988–B1002.
- [181] P. Benincasa, *On-shell diagrammatics and the perturbative structure of planar gauge theories*, [arXiv:1510.0364](#).
- [182] H. Kawai, D. Lewellen, and S. Tye, *A Relation Between Tree Amplitudes of Closed and Open Strings*, *Nucl.Phys.* **B269** (1986) 1.
- [183] H. Johansson and A. Ochirov, *Color-Kinematics Duality for QCD Amplitudes*, *JHEP* **01** (2016) 170, [[arXiv:1507.0033](#)].



- [184] G. Chen and Y.-J. Du, *Amplitude Relations in Non-linear Sigma Model*, *JHEP* **01** (2014) 061, [[arXiv:1311.1133](#)].
- [185] Z. Bern, L. J. Dixon, and R. Roiban, *Is  $N = 8$  supergravity ultraviolet finite?*, *Phys. Lett.* **B644** (2007) 265–271, [[hep-th/0611086](#)].
- [186] Z. Bern, L. J. Dixon, M. Perelstein, and J. S. Rozowsky, *One loop  $n$  point helicity amplitudes in (selfdual) gravity*, *Phys. Lett.* **B444** (1998) 273–283, [[hep-th/9809160](#)].
- [187] N. E. J. Bjerrum-Bohr, D. C. Dunbar, and H. Ita, *Six-point one-loop  $N=8$  supergravity NMHV amplitudes and their IR-behaviour*, *Phys. Lett.* **B621** (2005) 183–194, [[hep-th/0503102](#)].
- [188] P. Heslop and A. E. Lipstein, *On-Shell Diagrams for  $N = 8$  Supergravity Amplitudes*, [arXiv:1604.0304](#).